THE SYNTHESIS OF CELLULOSE GRAFT COPOLYMERS USING CU(0)-MEDIATED POLYMERIZATION

by

Jason L. Donaldson

A thesis submitted to the Department of Chemical Engineering

in conformity with the requirements for

the degree of Master of Applied Science.

Queen's University

Kingston, Ontario, Canada

May, 2013

Abstract

Cellulose is the most abundant renewable polymer on the planet and there is great interest in expanding its use beyond its traditional applications. However, its hydrophilicity and insolubility in most common solvent systems are obstacles to its widespread use in advanced materials. One way to counteract this is to attach hydrophobic polymer chains to cellulose: this allows the properties of the copolymer to be tailored by the molecular weight, density, and physical properties of the grafts. Two methods were used here to synthesize the graft copolymers: a 'grafting-from' approach, where synthetic chains were grown outward from bromoester moieties on cellulose (Cell-BiB) via Cu(0)-mediated polymerization; and a 'grafting-to' approach, where fully formed synthetic chains with terminal sulfide functionality were added to cellulose acetate with methacrylate functionality (CA-MAA) via thiol-ene Michael addition.

The Cell-BiB was synthesized in the ionic liquid 1-butyl-3-methylimidazolium chloride and had a degree of substitution of 1.13. Polymerization from Cell-BiB proceeded at similar but slightly slower rate than an analogous non-polymeric initiator (EBiB). The average graft density of poly(methyl acrylate) chains was 0.71 chains/ring, with a maximum of 1.0 obtained. The graft density when grafting poly(methyl methacrylate) was only 0.15, and this appeared to be due to the slow initiation of BiB groups. Using EBiB to model the reaction and improve the design should allow this to be overcome. Chain extension experiments demonstrated the living behaviour of the polymer.

The CA-MAA was synthesized by esterification with methacrylic acid. Reactions of CA-MAA with thiophenol and dodecanethiol resulted in quantitative addition of the thiol to the alkene. The grafts were synthesized by Cu(0)-mediated polymerization from a bifunctional initiator containing a disulfide bond, followed by reduction to sulfides. The synthetic polymers were successfully grafted to CA-MAA but the grafting yield was limited by the low sulfide functionality. Better retention of sulfide functionality is necessary for more efficient grafting.

Co-Authorship

This research was conducted independently by the author, under the supervision of Dr. Michael Cunningham and Dr. Pascale Champagne, both of whom reviewed this thesis.

Acknowledgements

I would like to thank first and foremost my parents, for their support, financial and otherwise, during my seven years of post-secondary education and all the time before that. They have left me on a firm footing for life and left me with a breadth of knowledge of which I am always appreciative.

I would also like to thank my thesis supervisors, Dr. Michael Cunningham and Dr. Pascale Champagne, for their guidance in this research, and especially for giving me the opportunity to travel and present my research and our group's research to the academic world.

I would like to thank all of my coworkers for providing their expertise the laboratory and their opinions during research presentations: the value in forcing people to exit their focussed bubble of expertise and engage with bright people of different research interests should never be dismissed. In addition, I would like to thank Dr. Hai-Dong Wang and Mr. Ryan Roeder for their assistance in critiquing my literature review, and I would like to especially thank Ryan for being a sounding-board for my ideas and suggesting solutions to my roadblocks.

Calista, my favourite part of our Canada Day weekend was when you, Lydia, Jenn, and I got lost on the way to Barrie; I believe it is enlightening for a person to not always know where they are. I would have thanked you, Jenn, for being an excellent roommate except that you went to The Netherlands instead. Nonetheless, I still enjoyed the time spent in Kingston with you, Calista, Kevin (thank you for delivering my thesis!), Eric, and all the other people too numerous to mention. I especially enjoyed the times where food was involved, which was most of the time.

And Bry, I thank you for your entertaining supply of inappropriate web-comics, as well as the excellent music which you have introduced to me. This has saved me hours of reading album reviews on Wikipedia, and I always look forward to your next suggestion.

"Education is a progressive discovery of our own ignorance."

~Will Durant, quoted in "Books: The Great Gadfly", *Time* magazine, 8 October 1965

Remarks Upon Notation Used

A brief description of the notation used in this thesis is provided here. A wide variety of cellulose derivatives were synthesized in this research and it is necessary to distinguish amongst them in a straight forward and easy to understand way. Firstly, the starting cellulose material: derivatives synthesized using commercially obtained microcrystalline cellulose (Avicel© PH-101) are abbreviated using the prefix 'Cell-', while those using commercially obtained cellulose acetate (Sigma-Aldrich) are abbreviated using the prefix 'CA-'. Secondly, the suffix attached to this describes the functional group that has been added: 'Cell-BiB' represents Avicel© cellulose functionalized with bromoisobutyrate groups, while 'CA-MAA' represents commercially obtained cellulose acetate functionalized with methacrylate groups using the monomer methacrylic acid (MAA). The notation 'Cell-AcO' would represent cellulose acetate synthesized in the lab and should not be confused with the commercially obtained material. Subscripts may also be used to denote the degree of substitution of the functional group (Cell-$BiB_{1.75}$, for example), and multiple suffixes may be used to denote multiple functional groups (Cell-$AcO_{2.79}$-$GMA_{0.09}$). Graft copolymers are designated with the backbone polymer first followed by '-g-'and the grafted polymer: 'Cell-g-PMA' would describe cellulose grafted with poly(methyl acrylate).

List of Abbreviations

ACN	Acetonitrile
AcO	Acetate
AGU	Anhydroglucose unit; sugar rings in cellulose
AMIM	1-allyl-3-methylimidazolium
ATRP	Atom transfer radical polymerization
BA	Butyl acrylate
BHEDS	bis(2-hydroxyethyl) disulfide
BiB	α-bromoisobutyrate groups
BMIM	1-butyl-3-methylimidazolium
BPY	2,2'-bipyridine
BrBiB	α-bromoisobutyryl bromide
Cell	Cellulose
CA	Cellulose acetate obtained from Sigma-Aldrich
CRP	Controlled radical polymerization
DCC	N,N'-dicyclohexylcarbodiimide
DMAam	N,N-dimethylacrylamide
DMAEMA	N,N-dimethylamino-2-ethyl methacrylate
DMAP	4-dimethylaminopyridine
DMF	N,N-Dimethyl formamide
DMSO	Dimethyl sulfoxide
DP	Degree of polymerization
DS	Degree of substitution
DTT	DL-dithiotheitol
EBiB	Ethyl α-bromoisobutyrate
EGDMA	Ethylene glycol dimethacrylate
EMIM	1-ethyl-3-methylimidazolium
GMA	Glycidyl methacrylate
GPC	Gel permeation chromatography
HA	Hexylamine
HEMA	2-Hydroxy ethyl methacrylate
HSQC	Heteronuclear single quantum coherence
HMTETA	1,4,7,10,10,-hexamethyl triethylenetetramine
HPC	Hydroxy propyl cellulose
IE	Initiator efficiency
LRP	Living radical polymerization
MA	Methyl acrylate
MAA	Methacrylic acid
MAC	Methacryloyl chloride
MCC	Microcrystalline cellulose
MDGMA	Methyl diethylene glycol methacrylate
ME	Mercaptoethanol
MeOH	Methanol
Me_6TREN	Tris[2-(dimethylamino)ethyl]amine
NIPAAm	N-isopropylacrylamide
MMA	Methyl methacrylate
NMP	Nitroxide mediated polymerization
NMR	Nuclear magnetic resonance
PDI	Polydispersity index, M_w/M_n

PEO	Poly(ethylene oxide)
PMA	Poly(methyl acrylate)
PMDETA	N,N,N',N",N"-pentamethyldiethylenetetramine
PMMA	Poly(methyl methacrylate)
RAFT	Reversible addition-fragmentation (chain) transfer
SET (-LRP)	Single electron transfer (living radical) polymerization
TEA	Triethylamine
TEMPO	2,2,6,6-Tetramethylpiperidyl-1-oxyl
THF	Tetrahydrofuran
TREN	Tris[2-(dimethylamino)ethyl]amine

List of Symbols

α	Mark-Houwink parameter
δ	Chemical shift, NMR
$[\eta]$	Intrinsic viscosity
[Br]	Concentration of bromine (ATRP initiating sites)
[Cu(II)]	Concentration of Cu(II)
K	Mark-Houwink parameter
k_{act}	Activation rate constant
k_{app}	Initial apparent polymerization rate constant
K_{ATRP}	ATRP equilibrium constant; ratio of k_{act}/k_{deact}
k_{deact}	Deactivation rate constant
k_p	Propagation rate constant
k_t	Termination rate constant
[L]	Concentration of ligand
[M]	Monomer concentration
M_n	Number average molecular weight
M_p	Peak molecular weight
M/P	Ratio of measured M_n to predicted M_n
M_w	Weight average molecular weight
MW	Molecular Weight
M_V	Viscosity average molecular weight
T_g	Glass transition temperature
Vr	Retention volume (GPC)
Vr_p	Peak retention volume (GPC)

Table of Contents

List of Figures

Chapter 1:

Chapter 2:

Chapter 3:

Chapter 4:

Chapter 5:

List of Tables

Chapter 1

Introduction

1.1 Research objective

This thesis investigates the chemical modification of cellulose as a means to tailor its properties: specifically, by grafting synthetic polymer chains to the cellulose backbone to form a copolymer with comb architecture. The determination and fine-tuning of the physical properties of the copolymer is a field of research in its own right, and so this thesis limits itself to the development of versatile and robust methods of synthesizing these copolymers. The nature of the copolymer requires these reactions to be carried out in a homogeneous medium, which presents additional challenges when working with cellulose.

1.2 Background information on cellulose and motivation for research

Cellulose is the most abundant renewable polymer on the planet, accounting for 50% of the bound carbon, and with about 10^{11} tons being regenerated yearly by plants, algae, bacteria, and even some animals [1]. Some typical cellulose contents from various sources are provided in Table 1.1. Biomass from plant sources has three main polymeric components: lignin, hemicellulose, and cellulose [2]. Lignin is a highly amorphous polymer that serves as the intercellular material that 'glues' together the fibres of the plant. It is a three-dimensional, highly branched polymer consisting of a random arrangement of phenyl groups with propyl linkages. Hemicellulose is a polymer of a variety of hexoses (glucose, mannose, galactose, et cetera) and pentoses (xylose, arabinose, et cetera). The type and proportion of these sugars are dependent on the biomass source. Because of the irregular nature of the repeat units, hemicellulose is less crystalline and more easily dissolved than cellulose [2]. Cellulose is a linear polymer consisting

of cellobiose units (a pair of glucopyranose units joined by a β-D-(1 → 4) linkage and therefore rotated 180^{O} to each other) repeating in a highly ordered fashion. Cellulose also has substantial inter- and intramolecular bonding from the pendant hydroxyl functional groups [1, 3]. The cellulose chains lay together in a single direction to form long fibres, and the highly ordered structure and regular hydrogen bonding pattern creates a polymer with a high degree of crystallinity. These fibres also contain amorphous regions where the chains do not properly overlap; these amorphous regions are more easily penetrated by solvents than the crystalline regions [2]. Cellulose chains have what is termed a 'reducing end', where the alcohol on the terminal group of the chain is in equilibrium with an open-ring aldehyde [1, 3]. New glucose molecules are added to the non-reducing end of cellulose during chain elongation [3]. Figure 1.1 illustrates the structure of cellulose, including inter- and intramolecular hydrogen bonding patterns and the reducing end.

Cellulose can exist in six different crystalline polymorphs: Cellulose I, II, III_I, III_{II}, IV_I, and IV_{II} [3]. Of these, only cellulose I and cellulose II are found in nature, with the remainder obtained through artificial means. In cellulose I, the O6'-H – O3' hydrogen bonding pattern is dominant (see Figure 1.1), while in cellulose II O6'-H – O2' is dominant.

Table 1.1: Typical cellulose content from various fibre sources [1].

Fibre Source	Cellulose Content (%)
Softwood	33-42
Hardwood	38-51
Cotton	83-95
Flax (unretted)	63
Flax (retted)	71
Hemp	70-74
Jute	61-72
Ramie	69-76
Sisal	67-78

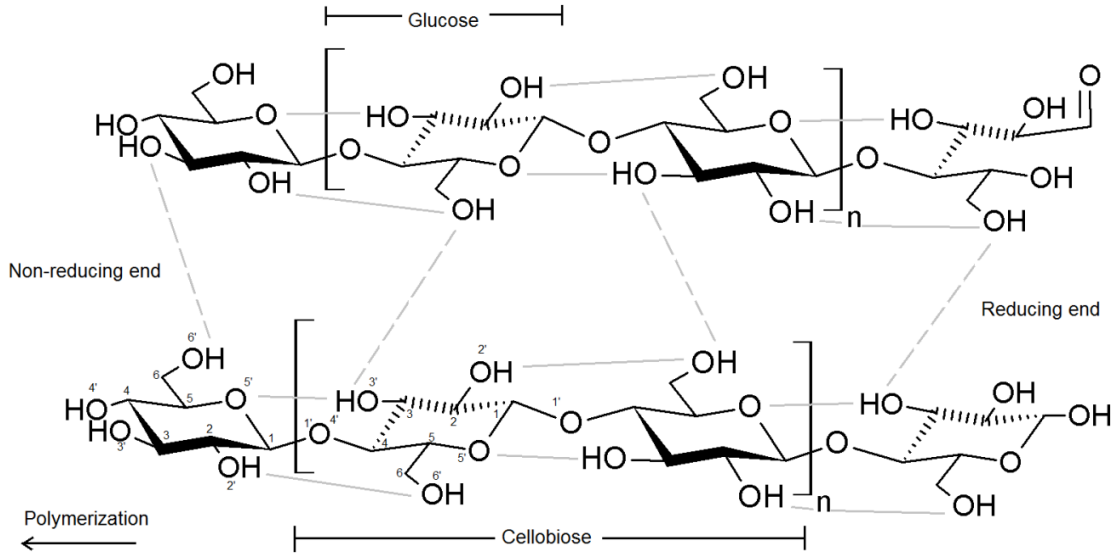

Figure 1.1: Structure of cellulose, showing intermolecular (dashed grey lines) and intramolecular (solid grey lines) hydrogen bonding patterns for cellulose I. Modified from Festucci-Buselli et al. [3].

The poor solubility and hygroscopic nature of cellulose in common solvents present challenges to its widespread use. Consequently, cellulose is often modified in order to tailor its properties: to increase its hydrophobicity; make it more amenable to dissolution; or to blend or increase its compatibility with other polymers. The most common modification (resulting in a wide range of commercially available products) involves the synthesis of cellulose derivatives, where some or all of the hydroxyl groups have been replaced with other functional groups: 0.9 million tons of cellulose acetate and 3.2 million tons of cellulose xanthate are produced annually [4]. Of more recent interest are cellulose copolymers with unique architectures, consisting of synthetic/renewable polymer hybrids. Such architectures include: cellulose chains with a synthetic polymer block [5, 6]; graft copolymers with a cellulose backbone and synthetic polymer branches [7, 8]; gels and interpenetrating networks of polymers [9-11]; and grafting of polymers from solid cellulose surfaces, including particles, fibres, and sheets [7, 8, 12, 13]. Surface modification of solid cellulose is a common research area as it avoids the need for dissolution of

the cellulose, but a homogeneous medium is required to synthesize other architectures, such as graft copolymers and block copolymers.

In the synthesis of cellulose graft copolymers there are two main approaches, known as 'grafting-from' and 'grafting-to', with the 'grafting-from' approach being more commonly applied [8]. In the 'grafting-from' approach, initiation sites are formed on the cellulose backbone and polymer chains are grown outward from these; the polymerizations are accomplished using both conventional [14, 15] and controlled radical mechanisms [7], including Reversible Addition-Fragmentation Chain Transfer (RAFT), Atom Transfer Radical Polymerization (ATRP), and Nitroxide Mediated Polymerization (NMP.) In theory, a controlled 'grafting-from' mechanism should allow for a well-tailored, controlled growth of polymer and high density of grafted chains, but in practice problems have been encountered with radical combination of the cellulose molecules due to bimolecular termination of growing chains [16-20], poor initiation efficiency [16, 21], and difficulties in characterizing the side chains and final copolymer [18, 19].

With the 'grafting-to' approach, fully formed (and characterized) chains with selected end-group functionalities are attached to the backbone polymer. This should allow for easier characterization of the copolymer and avoid intermolecular combination of the combs, although if grafting is incomplete the separation of the homopolymer can be problematic. One of the reasons that a 'grafting-to' approach receives less attention is that it is thought to have a lower possible graft density due to steric hindrance [7]; however, if the goal is to have a high cellulose content in the final copolymer this may not be an issue, and in fact may be considered a positive effect. In addition, there is a well-established body of literature on various controlled polymerization techniques, and growing the grafts separately from the backbone would allow this knowledge to be directly applied under optimal polymerization conditions (i.e. conditions that might not be possible for a 'grafting-from' polymerization due to restrictions imposed by the

macroinitiator such as solubility and initiator concentration). To date, there have been papers detailing the synthesis of graft copolymers with a cellulose acetate backbone and polystyrene arms [22, 23] and with a synthetic backbone and cellulose acetate arms [24] using a 'grafting-to' approach.

Both the 'grafting-from' and 'grafting-to' methods will be used in this thesis to synthesize copolymers with a cellulose backbone and synthetic branches. In both cases, Cu(0)-mediated polymerization will be used to synthesize the polymer branches. There are reports of Cu(0)-mediated polymerization being used to graft from cellulose, and so this has been established as a synthesis technique. However, as the literature review in Chapter 2 will discuss, characterization of these copolymers has been incomplete and it is unclear how differently the graft copolymerization behaves compared to linear homopolymerization. That question will be addressed here. As the 'grafting-to' approach has received a much more limited treatment in the literature, the objective here is to design a versatile method for grafting polymers to cellulose using thiol-ene chemistry.

1.3 Organization of thesis

Chapter 2 of this thesis consists of a literature review that summarizes the functionalization of cellulose in homogeneous media (with a strong focus on imidazolium-based ionic liquids), the growing of polymer chains from the backbone ('grafting-from') via Atom Transfer Radical Polymerization (ATRP) and Single Electron Transfer (SET), and the attachment of fully formed polymer chains to the cellulose backbone ('grafting-to'). Chapter 3 discusses the synthesis of cellulose derivatives that were used in the grafting reactions in Chapters 4 and 5. Chapter 4 details a 'grafting-from' approach using Cu(0)-mediated polymerization. Cellulose was dissolved in 1-butyl-3-methylimidazolium chloride (BMIM Cl) and then functionalized with

bromoester groups to give it ATRP functionality, and acrylic monomers were polymerized outward. The graft polymerization from cellulose was compared to a common ATRP initiator of similar structure in order to determine if the polymerization was similar in terms of rate and control. In Chapter 5, a 'grafting-to' approach was used. Here, cellulose acetate was imparted with methacrylate functionality along its backbone by esterification with methacrylic acid. Fully formed synthetic chains containing terminal sulfide functionality were attached to the cellulose acetate via thiol-ene Michael addition. The polymers with sulfide functionality were produced using a bifunctional ATRP initiator containing an internal disulfide linkage; after polymerization, the disulfide was reduced to form sulfide-terminated chains. Chapter 6 summarizes the conclusions presented in the thesis, and gives recommendations as to areas of further investigation.

1.4 References

[1] E. Sjoholm, "Size exclusion chromatography of cellulose and cellulose derivatives," in *Handbook of Size Exclusion Chromatography and Related Techniques*, New York, Marcel Dekker, 1995, pp. 311-354.

[2] G. A. Smook, Handbook For Pulp & Paper Technologists 3rd Ed., Vancouver: Angus Wilde Publications Inc., 2002.

[3] R. A. Festucci-Buselli, W. C. Otoni and C. P. Joshi, "Structure, organization, and functions of cellulose synthase complexes in higher plants," *Brazilian Journal of Plant Physiology*, vol. 19, no. 1, pp. 1-13, 2007.

[4] T. Heinze and T. Liebert, "Unconventional methods in cellulose functionaliztion," *Progress in Polymer Science*, vol. 26, no. 9, pp. 1689-1762, 2001.

[5] H. Kamitakahara and F. Nakatsubo, "Synthesis of diblock copolymers with cellulose derivatives. 1. Model study with azidoalkyl carboxylic acid and cellobiosylamine derivative," *Cellulose*, vol. 12, no. 2, pp. 209-219, 2005.

[6] H. Kamitakahara, Y. Enomoto, C. Hasegawa and F. Nakatsubo, "Synthesis of diblock copolymers with cellulose derivatives. 2. Characterization and thermal properties of cellulose triacetate-block-oligoamide," *Cellulose*, vol. 12, no. 5, pp. 527-541, 2005.

[7] M. Tizzotti, A. Charlot, E. Fleury, M. Stenzel and J. Bernard, "Modification of polysaccharides through controlled/living radical polymerization grafting - towards the generation of high performace hybrids," *Macromolecular Rapid Communications,* vol. 31, no. 20, pp. 1751-1772, 2010.

[8] D. Roy, M. Semsarilar, J. T. Guthrie and S. Perrier, "Cellulose modification by polymer grafting: a review," *Chemical Society Reviews,* vol. 38, no. 7, pp. 2046-2064, 2008.

[9] O. Fichet, F. Vidal, J. Laskar and D. Teyssie, "Polydimethylsiloxane-cellulose acetate butyrate interpenetrating polymer networks synthesis and kinetic study. Part 1," *Polymer,* vol. 46, no. 1, pp. 37-47, 2005.

[10] F. Vidal, O. Fichet, J. Laskar and D. Teyssie, "Polysiloxane-cellulose acetate butyrate cellulose interpenetrating polymers networks close to true IPNs on a large composition range. Part II," *Polymer,* vol. 47, no. 11, pp. 3747-3753, 2006.

[11] D. Aoki, Y. Teramoto and Y. Nishio, "SH-containing cellulose acetate derivatives: preapration and charachterization as a shape memory-recovery material," *Biomacromolecules,* vol. 8, no. 12, pp. 3749-3757, 2007.

[12] E. Malmstrom and A. Carlmark, "Controlled grafting of cellulose fibres - an outlook beyond paper and cardboard," *Polyme Chemistry,* vol. 3, no. 7, pp. 1702-1713, 2012.

[13] Y. Habibi, L. A. Lucia and O. J. Rojas, "Cellulose nanocrystals: chemistry, self-assembly, and applications," *Chemical Reviews,* vol. 110, no. 6, pp. 3479-3500, 2010.

[14] E. Bianchi, E. Marsano, L. Ricco and S. Russo, "Free radical grafting onto cellulose in homogeneous conditions 1. Modified cellulose-acrylonitrile system," *Carbohydrate Polymers,* vol. 36, no. 4, pp. 313-318, 1998.

[15] Y. A. Aggour and E. Abdel-Razik, "Graft copolymerization of end allenoxy polyoxyethylene macromonomer onto ethyl cellulose in a homogeneous system," *European Polymer Journal,* vol. 35, no. 12, pp. 2225-2228, 1999.

[16] V. Raus, M. Stepanek, M. Uchman, M. Slouf, P. Latalova, E. Cadova, M. Netopilik, J. Kriz, J. Dybal and P. Vleck, "Cellulose-based graft copolymers with controlled architecture prepared in a homogeneous phase," *Polymer Chemistry,* vol. 49, no. 20, pp. 4353-4367, 2011.

[17] P. Vlcek, M. Janata, P. Latalova, J. Kriz, E. Cadova and L. Toman, "Controlled grafting of cellulose diacetate," *Polymer,* vol. 47, no. 8, pp. 2587-2595, 2006.

[18] E. Ostmark, S. Harrisson, K. L. Wooley and E. E. Malmstrom, "Comb polymers prepared by ATRP from hydroxypropyl cellulose," *Biomacromolecules,* vol. 8, no. 4, pp. 1138-1148, 2007.

[19] X. Sui, J. Yuan, M. Zhou, J. Zhang, H. Yang, W. Yuan, Y. Wei and C. Pan, "Synthesis of cellulose-graft-poly(N,N-dimethylamino-2-ethyl methacryalte copolymers via homogeneous ATRP and their aggregates in homogeneous media," *Biomacromolecules,* vol. 9, no. 10, pp. 2615-2620, 2008.

[20] M. Hiltunen, J. Siirila and S. L. M. Maunu, "Effect of catalyst systems and reaction conditions on the synthesis of cellulose-g-PDMAam copolymers by controlled radical polymerization," *Polymer Chemistry*, pp. 3067-3076, 2012.

[21] M. S. Hiltunen, J. Raula and S. L. Maunu, "Tailoring of water-soluble cellulose-g-copolymers in homogeneous medium using single-electron-transfer living radical polymerization," *Polymer International* vol. 60, no. 9, pp. 1370-1379, 2011.

[22] P. Mansson and L. Westfelt, "Grafting of monodisperse low-molecular-molecular weight polystyrene onto cellulose acetate," *Journal of Polymer Science: Polymer Chemistry Edition*, vol. 19, no. 6, pp. 1509-1515, 1981.

[23] C. J. Biermann, J. B. Chung and R. Narayan, "Grafting of polystyrene onto cellulose acetate by nucleophilic displacement of mesylate groups using the polystyrylcarboxylate anion," *Macromolecules*, no. 20, pp. 954-957, 1987.

[24] Y. Enomoto-Rogers, H. Kamitakahara, A. Yoshinaga and T. Takano, "Comb-shaped graft copolymers with cellulose side-chains prepared via click chemistry," *Carbohydrate Polymers*, vol. 87, no. 3, pp. 2237-2245, 2012.

Chapter 2

Literature Review: Modification and Graft Copolymerization of Cellulose in Homogeneous Media

2.1 Introduction

The study of cellulose is a diverse field with many areas of research interest, including the structure and biosynthesis of cellulose [1], fractionation of lignocellulosic material [2], depolymerization of cellulose [3, 4], functionalization and derivatization of cellulose [4-7], and polymeric grafting from both dissolved cellulose [8, 9] and cellulose surfaces [8-10]. For grafting of polymers, controlled radical polymerization (CRP) techniques are commonly used in order to control the molecular weight of the grafts and minimize termination. Atom Transfer Radical Polymerization (ATRP) (with the related Single Electron Transfer (SET)) and Reversible Addition-Fragmentation Chain Transfer (RAFT) are two of the most commonly studied CRP techniques studied, with Nitroxide-Mediated Polymerization (NMP) receiving less attention [9]. This literature review is focussed on three main areas:

1) *The use of ionic liquids for cellulose dissolution and subsequent modification.* The lack of effective, non-derivatizing, and easy-to use solvents has limited the use of cellulose in homogeneous systems, and thereby limited the types of architectures and cellulose products that can be obtained. The proper choice of solvent is therefore very important for designing reactions, and ionic liquids are one potential solution.

2) *The synthesis of cellulose graft copolymers using ATRP or SET and a 'grafting-from' approach.* The discovery in the last decade of new cellulose solvents coupled with the wide and growing body of ATRP literature has made this an increasingly popular research topic.

3) *The synthesis of cellulose graft copolymers using a 'grafting-to' approach.* This has received very limited attention in the literature, but the emergence of fast and quantitative 'click' reactions makes this an attractive alternative to the 'grafting-from' approach that is more commonly used.

As much as possible, this review focusses on work conducted with cellulose and the synthesis of cellulose graft copolymers. However, where little is published in the literature this document will expand to other polysaccharides and polymer architectures.

2.2 Ionic liquids as solvents for cellulose modification

2.2.1 Solvent systems for cellulose

Cellulose is a highly crystalline polymer with very strong and repetitive hydrogen bonding. As a result, cellulose is incapable of being dissolved in most common solvents. Cellulose, however, does dissolve in certain molten salts and aqueous salt solutions. Isogai and Atalla [11] presented a method to dissolve cellulose in aqueous NaOH by first swelling, then freezing, and then diluting the mixture. They found that crystalline cellulose samples of DP up to 200 were completely soluble, but at a low concentration of 2 wt%. The solvent systems dimethylacetamide (DMAc)/LiCl [12-19] and N-methyl-2-pyrrolidone/LiCl [12] have also been

used to dissolve cellulose, as well as dimethylsulfoxide (DMSO)/tetrabutylammonium fluoride trihydrate [7, 20]. The solvent systems capable of dissolving cellulose are typically very hygroscopic; the presence of water in the solvent system both lowers the solubility of the cellulose and can hinder moisture-sensitive reactions. Swatloski et al. [21] described the ability of ionic liquids to dissolve cellulose pulp. They found that 1-butyl-3-methylimidazolium chloride (BMIM Cl) could dissolve 10 wt% cellulose under conventional heating at 100^{O}C, and 25 wt% under microwave heating. Remsing et al. [22] demonstrated that cellulose in BMIM Cl exhibited stoichiometric bonding of the protons on the hydroxyls to the chloride anions, which supported the dissolution model they proposed whereby the hydroxyls of cellulose can act as electron donor/acceptor sites. As such, the effectiveness of solvents in dissolving cellulose is dependent on their ability to bond to cellulose's hydroxyl groups and disrupt the regular hydrogen bonding pattern.

A study by Kosan et al. [23] suggested that acetate was a better anion for dissolving cellulose than chloride, both for solvating strength and reduced solution viscosity. Vitz et al. [24] conducted an extensive dissolution study of cellulose in imidazolium-based ionic liquids and concluded that ionic liquids with chloride, acetate, or phosphate anions were suitable for dissolving cellulose, with other anions examined having little or no dissolving capability. They suggested using diethyl phosphate as the anion in order to minimize depolymerization of the cellulose. Fukaya et al. [25] also noted the ability of phosphate-based anions to dissolve cellulose. To date, cellulose dissolution and modification is commonly done with the ionic liquids BMIM Cl [3, 5, 26-30], 1-allyl-3-methylimidazolium chloride (AMIM Cl) [6, 31-35], and 1-ethyl-3-methylimidazolium acetate (EMIM AcO) [2, 36, 37]. The ionic liquid 3-methyl-N-butyl-pyridinium chloride has also been found to dissolve cellulose but with significant depolymerization [30]. In addition, variations on these cations using different length alkyl groups are capable of dissolving cellulose to various degrees [5, 24]. A more comprehensive review of

cellulose solvent systems by Liebert et al. can be referred to for more information [38]. See Figure 2.1 for structures of some common ionic liquids.

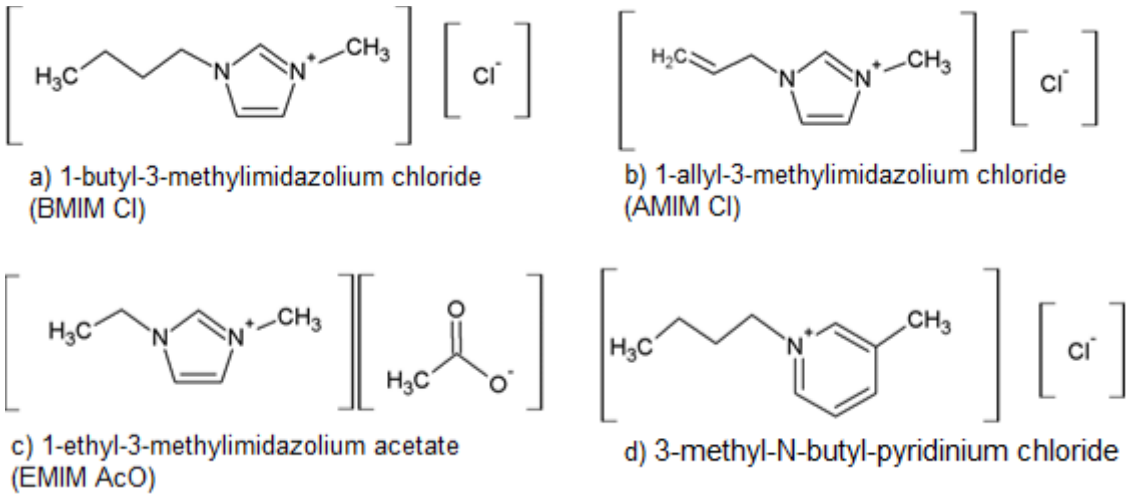

Figure 2.1: Structures of common imidazolium-based ionic liquids.

2.2.2 Viscosities of ionic liquid/cellulose solutions

The imidazolium-based ionic liquids are very viscous, and become substantially more so when cellulose is dissolved. Sescousse et al. [39] examined the viscosities of solutions of cellulose in EMIM AcO and BMIM Cl. They found that EMIM AcO (melting point <-20^{O}C) has a viscosity of about 0.01 Pa·s at 100^{O}C, but a 10 wt% solution of cellulose at the same temperature has a viscosity of 0.5 Pa·s. BMIM Cl (melting point 70^{O}C) is even more viscous with a viscosity of about 0.03 Pa·s at 100^{O}C, and a 10 wt% solution having a viscosity of about 6 Pa·s – *a 200 fold increase*. Figure 2.2 displays some of their experimental data. Kosan et al. [23] also reported on the lower viscosity of acetate anion when compared to chloride, which allows a greater amount of cellulose to be dissolved while still maintaining a manageable viscosity. Fukaya et al. [25] reported that EMIM methylphosphonate had a viscosity of 1 Pa·s at 25^{O}C, which was less than any imidazolium-based ionic liquid using a chloride anion. From Figure 2.2,

this is comparable to the viscosity of EMIM AcO at 0^{O}C. Tokuda et al. [40] examined the effect of variation in chain length in 1-alkyl-3-methylimidazolium cations on physical properties (they used bis(trifluoromethane sulfonyl)imide as the anion). They found that viscosity increased with alkyl length, while density and conductivity decreased. Huddleston et al. [41] also found similar effects of the alkyl length on physical properties.

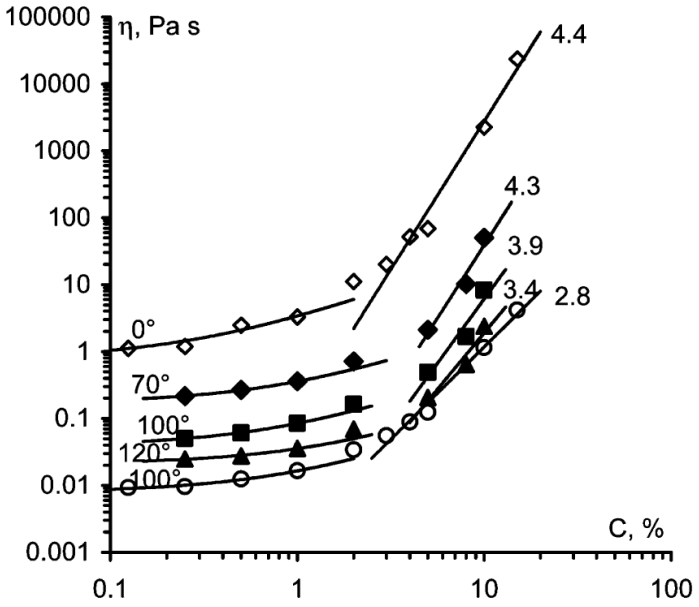

Figure 2.2: Viscosities of cellulose-ionic liquid solutions. This figure shows experimental data comparing viscosity of the solution with temperature and cellulose content. The open symbols are for EMIM AcO and the closed symbols are for BMIM Cl. The lines are linear approximations (in the dilute region) or power law approximations (in the semi-dilute region). Reprinted with permission from Sescousse et al. [39]. Copyright 2010, American Chemical Society.

2.2.3 Stability of ionic liquid/cellulose solutions

Ionic liquids have been reported to be stable and inert towards cellulose [21, 22]; however, new findings indicate that this is not necessarily the case. A study [42] on thermal aging of ionic liquids useful for cellulose dissolution (BMIM AcO, EMIM AcO, BMIM Cl, and

EMIM Cl) was conducted whereby the pure ionic liquids were heated at 200^{O}C for 24 h followed by analysis of the degradation products. It was found that in all cases yields of degradation products of less than 0.1% were obtained, consisting of imidazole in various states of alkylation and dimerization. Although these are low amounts, imidazole has a high boiling point (256^{O}C) and is unlikely to be removed by vacuum distillation. Thus, the impurities would increase in any recycling scheme that did not involve some other extraction technique for their removal. The acetate anion was found to be slightly less stable than the chloride anion. The authors also noted that imidazole is a relatively basic substance and can affect reactions taking place in solution, including the coupling of 1-alkyl-3-methylimidazolium cations with cellulose at its reducing end [44] and the formation of N-heterocyclic carbenes [44]. This would severely limit the potential for using ionic liquids as a solvent for reducing end reactions of cellulose (see Scheme 2.1). As well, technical grade EMIM AcO (>97%) was found to partially acetylate cellulose in the absence of any other reactants (DS of 0.017 after 20 minutes at 150^{O}C) [45], and in the presence of only 2-furoyl chloride, p-toluenesulfonyl chloride, or triphenylmethyl chloride could acetylate cellulose up to a degree of substitution (DS) of 1.86 [36]. Cellulose samples have also been found to depolymerize to a certain extent when dissolved in ionic liquids. Vitz et al. [24] found that the degree of polymerization (DP) of Avicel© cellulose decreased from 398 to 311 upon regeneration from BMIM Cl. Heinze et al. [30] did not observe any depolymerization when regenerated from BMIM Cl, but they reported that the DP of Avicel© cellulose decreased from 286 to 172 upon regeneration from 3-methyl-N-butyl-pyridinium chloride.

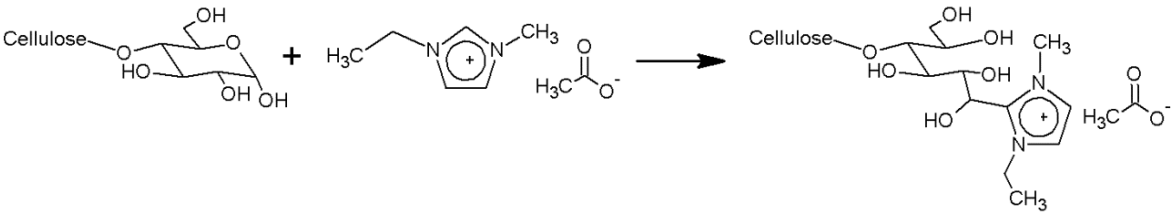

Scheme 2.1: Reaction of EMIM AcO with the reducing end of cellulose. Other imidazolium-based ionic liquids react similarly with cellulose.

2.3 Cellulose copolymers using a 'grafting-from' approach

Polymeric grafting from a solid cellulose surface, whether membranes, fibres, or crystals, has been an important research topic and has been extensively studied; it will not be discussed here, but the reader can find information in other reviews [8-10, 46]. The synthesis of cellulose graft copolymers in a homogeneous environment is a more recent area of study and is the focus of this review. ATRP and SET are the primary mechanisms considered, although other mechanisms will be discussed briefly to provide context.

Controlled radical polymerizations (CRP; sometimes called 'living' radical polymerizations, LRP) have the following characteristics: *control over molecular weight and architecture*, including high initiation efficiency (IE) and low intermolecular combination of growing chains; *suppression of radical termination*, as indicated by a constant radical concentration in the reaction and a narrow polydispersity (PDI less than 2 and approaching 1); and *functionally terminated polymer chains*, such that a majority may be re-initiated and continue polymerizing (living behaviour). IUPAC recommends using the term 'reversible-deactivation radical polymerization' as opposed to 'living' or 'controlled' [47]. They state that 'living' is inappropriate at all times, while 'controlled' is acceptable as long as the criteria for control is clearly defined.

2.3.1 Alternatives to ATRP

The earliest grafting experiments from dissolved cellulose used conventional radical polymerizations [48, 49]. The main drawback to this polymerization approach was termination that caused extensive crosslinking of the cellulose material making it insoluble or poorly soluble, as well as the generation of homopolymer that was not grafted to the cellulose [26, 27, 48-50]. This limited control over the architecture obtained.

Controlled radical polymerizations were attempted in an effort to exercise more control over the architecture. An early example of homogeneous cellulose grafting using a controlled radical mechanism was carried out by Daly et al. in 2001 [51]. In this case, they used carboxymethyl or hydroxypropyl cellulose as their backbone polymer functionalized with TEMPO groups. These TEMPO groups were used to graft styrene from the cellulose using NMP. Polydispersities of cleaved grafts ranged from 1.34 to 1.52, indicating a controlled polymerization. Stenzel et al. [52] used RAFT to graft styrene from hydroxypropyl cellulose. The RAFT agent (3-benzylsulfanylthiocarbonylsufanylpropionic acid) was attached to the cellulose via esterification. The reaction was not well controlled as polydispersities of cleaved chains ranged from 1.63 to 1.94. The authors also noted that the M_n of the grafts deviated significantly from the expected values due to termination reactions. Fleet et al. [53] also used RAFT to synthesize hydroxypropyl cellulose based copolymers, although in this case they grafted polyvinyl acetate instead of styrene. Depolymerization of the cellulose backbone was observed when attaching the RAFT agent to the cellulose. Homopolymer was formed in solution, and PDI (1.9, 1.6) and M_n (5000 g/mol, 4000 g/mol) values for the cleaved grafts were the same as for the homopolymer. RAFT was used by Lin et al. [54] to graft MMA from cellulose. An ATRP initiator (which they had used in an earlier study [29]) was first prepared by dissolving cellulose linter fibres in BMIM Cl and reacting with chloroacetyl chloride. This was precipitated and purified, and then reacted with bis(thiobenzoyl) disulfide to synthesize the cellulose with RAFT initiating sites (DS 0.96). The polymerization was conducted in BMIM Cl. The PDI of the cleaved chains was low, ranging from 1.28 to 1.46.

2.3.2 Cu(I)-mediated (ATRP) grafting from cellulose esters and ethers

Table 2.1 contains a sampling of results from the papers surveyed that employed ATRP as their polymerization mechanism. Generally, the 'best' or most informative results from each paper were included, judging from criteria such as high polymerization rate, low polydispersity, and high molecular weight, as well as the completeness of the data available. There is debate in the literature over whether SET has the same mechanism as ATRP [55, 56] or a different mechanism [57-59]. For the purposes of this thesis, reactions will be referred to as SET when Cu(0) is used as the catalyst and ATRP when Cu(I) is used as the catalyst. The ATRP mechanism is provided in Scheme 2.2.

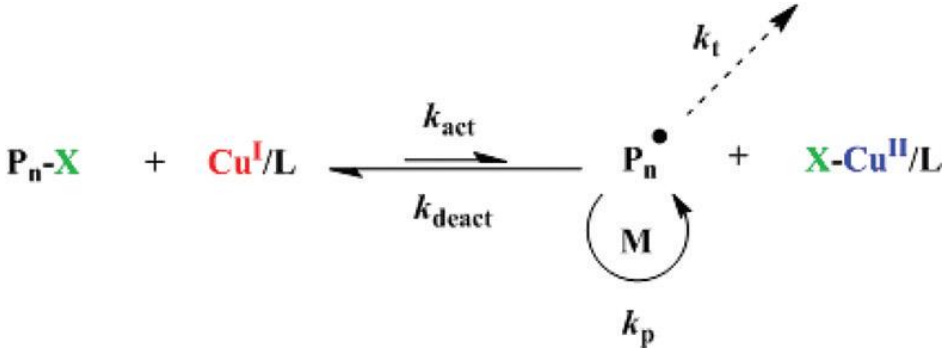

Scheme 2.2: Mechanism of ATRP. P_n-X is an alkyl halide (macro)initiator, Cu^I/L is the activator complex, $P_n^{\cdot}$ is a (macro)radical, and X-Cu^{II}/L is the deactivator complex. Reprinted with permission from Zhang et al. [55]. Copyright 2012, American Chemical Society.

Table 2.1: Sampling of ATRP polymerizations from dissolved cellulose**.**

Solvent	Catalyst	Monomer	Temp. (^{0}C)	Time (h)	Conv. (%)	DS	M_n (cellulose, g/mol)	M_n (copolymer, g/mol)	M_n (grafts, g/mol)	IE (%)	PDI (grafts)	Ref.
Toluene	CuBr/$CuBr_2$/ PMDETA	MMA	80	19	39	2.26	29,900*	83,700*	n.d.	n.d.	n.d.	[65]
Dioxane	CuBr/ PMDETA	MMA	70	8	5.4	0.43	n.d.	56,000*	3150*	n.d.	1.1	[60]
Dioxane	CuCl/ HMTETA	MMA	90	2.5	21	0.10	22,100	232,000*	n.d.	n.d.	n.d.	[62]
Dioxane	CuCl/ HMTETA	Styrene	90	12	14	0.12	19,500	104,500*	n.d.	n.d.	n.d.	[62]
Cyclo-pentanone	CuCl/ PMDETA	MDGMA	40	n.d.	16	0.02	n.d.	n.d.	5770*	n.d.	1.4	[63]
Toluene	CuBr/ PMDETA	Styrene	110	20	20	0.5	32,870*	50,995*	6500	96	1.3	[63]
Toluene	CuBr/ PMDETA	MMA	70	30	30	0.5	32,870*	64,702*	9000*	96	1.4	[61]
DMF	CuBr/ PMDETA	DMAEMA	60	1	35	0.70	156,000*	n.d.	n.d.	n.d.	n.d.	[36]
BMIM Cl	CuBr/BPY	MMA	60	4	15	1.87	n.d.	n.d.	31,000*	n.d.	1.6	[29]
Propanol/ water	CuBr/ HMTETA	DMAEMA	room	8	50	0.06	28,000*$^+$	89,000*	5800^{++}	n.d.	n.d.	[66]
DMF	CuCl/BPY	MMA	60	8	18.6	0.98	32,000$^+$	n.d.	96,000*	n.d.	1.3	[34]
Dioxane	CuCl/BPY	Styrene	110	2	14.1	0.98	32,000$^+$	n.d.	13,300	n.d.	1.5	[34]
DMSO	CuCl/ PMDETA	Acrylamide	80	3.5	9.2	2.0	n.d.	n.d.	2800*	20	1.1	[14]
DMSO	CuCl/ PMDETA	DMAam	50	3	17.2	0.44	n.d.	940,000*	1900^{++}	n.d.	1.4	[15]

*relative or not absolute molecular weight data, $^+$molecular weight of cellulose before addition of ATRP sites, $^{++}$estimated from NMR

The first grafting experiments performed on cellulose with an ATRP mechanism used cellulose derivatives (various esters and ethers of cellulose) with an incomplete degree of substitution [60-62]. The cellulose esters (or ethers, as the case may be) were soluble in various organic solvents and free hydroxyl groups were reacted to attach ATRP initiating sites. This was performed as early as 2004 by Shen and Huang [60] using cellulose diacetate and attaching α-bromoisobutyrate groups (DS 0.43). They grafted MMA from the cellulose: conversion was low (~5%), and combination of the cellulose backbones occurred. The side chains were hydrolyzed for GPC analysis. The polydispersity of the side chains measured was low (1.12), but molecular weight measurements were not absolute values due to the use of water as opposed to methanol for hydrolysis, and the lack of correction for the use of poly(styrene) standards. Vlcek also grafted from cellulose diacetate [62] using a variety of monomers. They prepared macroinitiators with 2-bromoisobutyryl and dichloroacetyl groups (DS ranged from 0.10 to 0.52). The styrene-grafted cellulose showed distinct bimodal behaviour with time and peak broadening from the GPC elution curves, indicating significant combination of the cellulose chains. The authors noted that conversion needed to be kept low to minimize combination. Block copolymerization was successfully performed, but no analysis of the grafts was conducted.

Methyl diethylene glycol methacrylate (MDGMA) was grafted from cellulose acetate sparsely functionalized with BiB groups (DS 0.02) by Billy et al. [63]. They first used a linear homopolymerization as a model in order to design their grafting reaction, but as the concentration of initiating sites for the homopolymerization was approximately 10^3 times greater than for homopolymerization the reactions are not directly comparable. Molecular weights of the copolymers were not reported, but the grafts were cleaved for GPC analysis, with polydispersities of 1.5 or less found. However, since NaOH in methanol was used as the agent for cleaving the grafts the ester groups on the polymer would have been cleaved as well. As such, the molecular weight measurements are not considered reliable.

Ethyl cellulose was used as the backbone polymer for grafting of MMA and styrene in a study by Shen et al. [61]. A high initiation efficiency (96%) was found, corresponding to one growing chain per two cellulose rings (DS 0.5). The side chains were hydrolyzed with 70% sulfuric acid and compared to polystyrene standards. The cleaved PMMA chains may not have been representative of the un-cleaved chains due to hydrolysis of the pendant methyl ester groups, thus affecting the calculated initiator efficiency. Dynamic light scattering analysis of the copolymer revealed a ratio of radius of gyration to hydrodynamic radius greater than 2, which indicates an extended, rod-like morphology. Liu et al. [64] examined the effect of graft density on the coil-to-rod transition of ethyl cellulose grafted with poly(acrylic acid). They made four polymer samples: two with a lower graft density (DS 0.3), and two with a higher graft density (DS 0.5). Each graft density had a sample with a long (DP of 43 or 53) and a sample with a short (DP of 21 or 28) side chain length. Using a combination of atomic force microscopy, dynamic light scattering and static light scattering, the authors found that the two samples with a lower graft density adopted a disc-like shape in a methanol solution with an extension ratio of 23% to 29%, indicating coiling of the backbone. The two samples with the higher graft density, however, adopted a rod-like structure with a much higher extension ratio of 77% to 78%, indicating almost complete extension. The width of the rods (25.5±2.2 nm) would indicate a near complete extension of the side chains (DP of 53) as well, as the authors predicted the length of the side chains to be 13 nm. The authors therefore concluded that the conformation of the copolymer could be varied by altering the graft density.

ATRP was performed on hydroxypropyl cellulose (HPC) by Ostmark et al. [65]. A number of the reactions gelled, and many of the others were poorly soluble and unsuitable for GPC analysis. The authors attributed this to significant coupling of the radicals growing on the combs. Attempts to cleave the grafts were unsuccessful, resulting in degradation of the synthetic chains before they were cleaved. A second block was grown from the first block, indicating the

retention of bromine functionality. Xu et al. [66] synthesized copolymers of hydroxypropyl cellulose by grafting with N,N-dimethylamino-2-ethyl methacrylate (DMAEMA) for the purpose of gene delivery. The HPC was modified by reacting with BrBiB in methylene chloride (DS 0.06), and ATRP was performed in a 20/1 isopropanol/water mixture with CuBr/HMTETA as the catalyst/ligand complex at room temperature. The average degree of polymerization from GPC was estimated to be 30, but this is relative to poly(styrene) standards. The DP from NMR was measured to be 37; this assumes complete initiation efficiency, which the authors did not measure. The authors stated that the reaction was controlled as the polydispersity of the cellulose did not broaden after the grafting. The authors demonstrated that their HPC-g-P(DMAEMA) could be bound to DNA for gene delivery, and had lower cytotoxicity than P(DMAEMA) homopolymer.

2.3.3 Cu(I)-mediated grafting from cellulose derivatized exclusively with ATRP sites

Research focus moved away from grafting using derivatized cellulose and towards grafting using underivatized cellulose. These macroinitiators are synthesized using unmodified cellulose as a starting material, which is then dissolved it an appropriate solvent (e.g. ionic liquid or DMAc/LiCl) and functionalized with initiation sites. These initiation sites also serve to disrupt the hydrogen bonding and often allow the macroinitiator to be dissolved in more common (but still polar) solvents for the polymerization. The use of unmodified cellulose as a starting material generally allows a higher density of ATRP initiating sites (due to the availability of all three hydroxyls on each glucose ring, although derivatives such as HPC retain hydroxyl functionality) and removes the intermediate step of obtaining a cellulose derivative [14, 29]. In 2008, Sui et al. [35] published a paper where wood pulp (95% cellulose) was dissolved in AMIM Cl and functionalized with α-bromopropionate groups (DS 0.70). The DMF-soluble macroinitiator was then used to initiate the polymerization of N,N-dimethylamino-2-ethyl

methacrylate (DMAEMA) using CuBr/PMDETA as catalyst. Several of the polymerizations gelled. The authors attempted GPC analysis but the molecular weights were too high for their equipment, which would suggest significant combination of the copolymer had occurred. Attempts to hydrolyze the side chains were unsuccessful, attributed to the very large grafted layer making the esters inaccessible. A subsequent article by Meng et al. [34] polymerized MMA and styrene from a cellulose macroinitiator in DMF, butanone, and 1,4-dioxane. In this case they were able to successfully hydrolyze the side chains and the PDI of the cleaved chains was found to be between 1.2 and 1.5, although the PMMA chains were likely degraded by this reaction as water was used as opposed to methanol (leading to hydrolysis of the pendant methyl ester groups and formation of poly(methacrylic acid)). Static and dynamic light scattering were used to study the morphology of the copolymer in DMF. The authors concluded that the polymer assumed sphere-like behaviour in solution.

Ionic liquids have also been used as the polymerization medium as well as the functionalization medium. A study by Chun-xiang et al. [29] polymerized MMA from cellulose functionalized with chloroacetyl groups (DS 1.87) in BMIM Cl. The grafts were cleaved from the cellulose using aqueous HCl and polydispersities were found in the range of 1.5-1.8; however, it is unknown the extent to which the cleaved grafts had been chemically modified by the hydrolysis (conversion of methyl methacrylate to methacrylic acid).

A paper by Hiltunen et al. [14] grafted poly(acrylamide) and poly(dimethylacrylamide) to cellulose to synthesize water soluble copolymers. They used softwood dissolving pulp as their starting material, dissolved it in DMAc/LiCl, and reacted it with BrBiB. They obtained very high degrees of substitution of up to 2.7. Stopping the reaction after 7 hours led to a lower degree of substitution (DS 0.3) when compared to leaving the same reaction for 24 hours (DS 0.5). The authors used dynamic light scattering to examine the behaviour of their macroinitiator in DMSO. The cellulose chains existed primarily as individual chains with an apparent hydrodynamic radius

of 18 nm, but a certain degree of intermolecular aggregation also occurred. The polymerizations were carried out with CuCl/PMDETA in DMSO; the authors refer to this as an SET reaction as opposed to ATRP, but since Cu(0) was not used as catalyst it is included here in the ATRP section. Hydrolysis of the chains revealed a low initiation efficiency (about 20%) but also a low polydispersity (PDI 1.1). They followed up on this with new experiments that used Cu(0) with Me_6TREN or PMDETA as the catalyst [15]. They attempted to graft dimethylacrylamide in DMSO from their macroinitiator (the same as used in [14]); however, they reported that under a variety of reaction conditions no polymerization occurred when Cu(0) was used. Reactions with Cu(I) were successful, although when Me_6TREN was used as the ligand the copolymers were not water-soluble; this was attributed to intermolecular combination. Reactions that used PMDETA as ligand resulted in water-soluble copolymers.

2.3.4 Cu(0)-mediated (SET) grafting from cellulose and related polysaccharides

Table 2.2 contains a summary of the SET reactions reviewed here. The mechanism that has been proposed for SET is provided in Scheme 2.3. One of the first examples of using a Cu(0)-mediated polymerization with cellulose in homogeneous medium used cellulose-acetate-butyrate as the backbone polymer functionalized with bromoisobutyryl or dicholoracetyl groups [67]. The functionality was low, with a DS range of 0.05 to 0.48. For the polymerizations, copper powder was used at or near to the stoichiometric amount of initiating sites. Reactions were generally slow, where MMA conversion of 38% in 5 hours at 60^{O}C was one of the faster reactions. The authors used a wide variety of reaction conditions but for the most part conclusions drawn from these should be treated with caution as the experiments were not duplicated and so the reproducibility is unknown. However, the reactions do appear to reach higher conversions when the temperature was raised from 30^{O}C to 60^{O}C. It should be noted that

SET using non-polymeric initiators proceeds rapidly at room temperature [57]. The side chains on two samples were successfully cleaved in MeOH/KOH, and initiation efficiencies of 30% and 70% were found (although the presence of hydroxide would have resulted in hydrolysis of the PMMA, affecting theinititator efficiency calculations). The PDI of the grafts for both samples was about 1.7. The authors noted that the elution curves of the copolymer samples were symmetrical up to about 45% conversion but became increasingly polymodal at higher conversions, suggesting intermolecular combination was occurring.

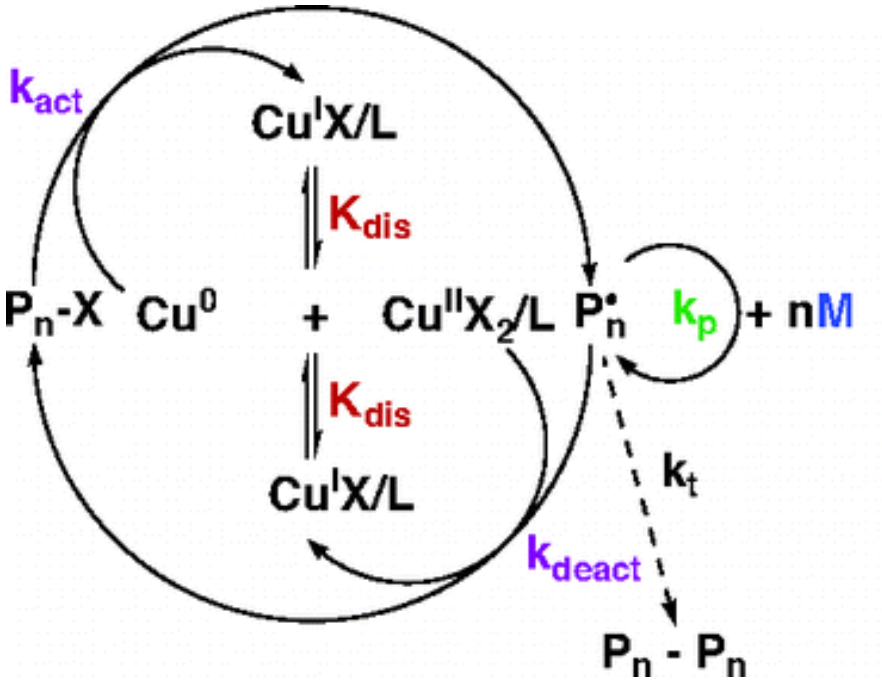

Scheme 2.3: Proposed mechanism of Cu(0)-mediated polymerization via SET. Cu^0 is oxidized to $Cu^{I}X/L$ during activation of the (macro)initiator. The $Cu^{I}X/L$ molecules disproportionate to form Cu^0 (the activator) and $Cu^{II}X_2/L$ (the deactivator). Reprinted with permission from Percec et al. [57]. Copyright 2006 American Chemical Society.

Table 2.2: Sampling of SET-LRP cellulose polymerizations

Solvent	Catalyst/ Ligand	Monomer	Temp. (^{0}C)	Time (h)	Conv. (%)	DS	M_n (cellulose, g/mol)	M_n (copolymer, g/mol)	M_n (grafts, g/mol)	IE (%)	PDI (grafts)	Ref.
DMSO	Cu(0)/ PMDETA	MMA	60	5.5	32	0.25	84,800*	n.d.	29,300	30	1.7	[67]
DMSO	Cu(0)/ Me_6TREN	BA	30	4	20	0.3	84,800*	n.d.	12,160^{++}	n.d.	n.d.	[67]
DMSO	Cu(0)/ Me_6TREN	MA	25	5	80	0.15	7000* (hemicellulose)	32,000*	n.d.	n.d.	n.d.	[68]
DMSO	Cu(0)/ Me_6TREN	MA	25	16.5	94	0.15	3540* (hemicellulose)	35,000*	n.d.	n.d.	n.d.	[69]
DMSO	CuCl/ PMDETA	Styrene	100	n.d.	19	1.04	30,000^{+}	n.d.	24,100	92	1.3	[13]
DMSO	Cu(0)/ PMDETA	Styrene	100	4	8	1.04	30,000^{+}	n.d.	47,700	7	1.9	[13]
DMSO	CuCl/ PMDETA	MMA	Room	n.d.	24	1.04	30,000^{+}	n.d.	73,500	26	1.4	[13]
DMSO	Cu(0)/ Me_6TREN	MMA	25	24	9	1.04	30,000^{+}	n.d.	136,200	3	1.6	[13]

*relative or not absolute molecular weight data; $^{+}$molecular weight of cellulose before addition of ATRP sites; $^{++}$estimated from NMR

Raus et al. [13] used cellulose functionalized only with bromoisobutyryl groups as their macroinitiator. They examined how activation of the cellulose prior to dissolution affected the acylation efficiency. The authors stated that activation was believed to make changes to the supramolecular structure of the cellulose. They activated their cellulose (microcrystalline Avicel© PH-101) by solvent exchange to DMAc or dioxane, or by thermal activation under reduced pressure. The activated cellulose samples were then acylated using BrBiB in DMAc/LiCl. The authors found that cellulose activated by solvent exchange to dioxane or thermally activated yielded a degree of substitution almost on par with the molar ratio of BrBiB:AGU used, whereas cellulose activated by DMAc showed a DS substantially lower than the molar ratio. This occurred when using both DMAc-swollen cellulose (potentially contaminated with water) and oven-dried cellulose. The authors stated that reactions using DMAc-activated cellulose were also poorly reproducible when compared to dioxane or thermal activation. They then polymerized MMA and styrene from their macroinitiator, using Cu(I) or Cu(0), primarily in the solvents DMAc and DMSO. When using Cu(I) as the activating agent, the reactions were well controlled (PDI<1.4); conversions were kept below ~25% to minimize crosslinking. The initiation efficiencies with styrene approached 100%, while those for MMA were substantially lower (26% to 59%). Adding three equivalents of EBiB, the authors found that initiation efficiency for MMA was substantially improved (75%-81%) while the graft chains were the same molecular weight as the sacrificial chains. Interestingly, when Cu(0) was used as the catalyst substantially different results were obtained. For both styrene and MMA the reaction was poorly controlled (PDI>1.8) and initiation efficiencies were extremely low (<10%). Conversions were also very low, with reactions left 24 h having less than 10% conversion. When DMAc at 70^{O}C was used as the solvent MMA conversion was higher (43% in 24 h) but initiation efficiencies and polydispersities were not improved. Molecular weights obtained for two samples

by light scattering were approximately three times higher than expected, suggesting significant combination of the cellulose copolymers.

Another early example of SET grafting is by Percec et al. [68], although they used hemicellulose that had been partially acetylated as their macroinitiator (M_n ~7000 g/mol) as opposed to cellulose. Their reactions were relatively fast, as after 5 hours most experiments reached between 60% and 90% conversion. Duplicate experiments were not done, so it is difficult to draw conclusions about the effects of changing reaction conditions. Edlund and Albertsson [69] also used hemicellulose as a macroinitiator; in this case, they utilized a variety of hemicellulose sources in order to determine the versatility of the SET grafting. The hemicellulose that was studied came from beech, birch, spruce, and Saccharomyces cerevisiae (a variety of yeast), and molecular weights varied from 3180 g/mol to 15,610 g/mol. The samples contained varying amounts of lignin (up to 8%). Esterification of bromoisobutyric acid was used to synthesize the macroinitiator; however, this caused significant degradation of the hemicellulose as the molecular weights decreased by about half. Methyl acrylate was used to polymerize from the macroinitiators; all reactions proceeded in a similar manner, regardless of source or lignin content, and the reaction could be done without degassing and without a decrease in rate if a reducing agent (hydrazine hydrate) was used. The molecular weights of the copolymers became significantly higher than the predicted values as the conversion increased. The authors used this difference in measured and predicted molecular weight of the copolymer to calculate the initiator efficiency; however, this is not likely to be correct as the M_n of the copolymer should be independent of the initiation efficiency (since a polymeric initiator was used). The increase in M_n over the predicted value was likely caused by combination of the hemicellulose copolymers.

2.4 Cellulose copolymers using ‘click’ chemistry and a ‘grafting-to’ approach

2.4.1 Cellulose graft copolymers prepared using non-‘click’ approaches

Substantially less work has been done investigating ‘grafting-to’ chemistry as compared to ‘grafting-from’, especially in homogeneous media. One of the earliest examples is by Mansson and Wesfelt in 1981 [70]. They synthesized well-defined (PDI 1.1), low molecular weight (2,500, 12,100, and 17,100 g/mol) poly(styrene) via anionic polymerization. The carbanion end group was converted to a carboxylic acid which was then activated with N,N’-dicyclohexylcarbodiimide, trifluoroacetic anhydride, or by conversion to acyl chloride: the acyl chloride was the only successful method of grafting. The activated polystyrene was attached to the cellulose acetate via esterification with the free backbone hydroxyls. They achieved a grafting density of up 21.8 branches per cellulose acetate chain (DS 0.078) with the lowest (2,500 g/mole) molecular weight polystyrene, although the grafting density decreased to 3.6 branches (DS 0.013) when the highest (17,100 g/mole) molecular weight polystyrene was used.

In a similar vein, Biermann et al. in 1987 [71] grafted polystyrene prepared by anionic polymerization onto cellulose acetate by forming an ester linkage. The carbanion at the end of the polystyrene chain was converted to a carboxylate by reacting with carbon dioxide. The hydroxyls of cellulose acetate (DS 2.5) were converted to methanesulfonyl groups which acted as the grafting sites. Using polystyrene of molecular weights of 6,200 or 10,900 g/mol gave a range of 0.13 to 0.18 branches per anhydroglucose unit (DS range of 0.043 to 0.060).

2.4.2 The azide/alkyne ‘click’ reaction

‘Click’ reactions are gaining attention for use with biopolymers due to their mild reaction conditions and high yields. According to Sharpless et al. [72], a ‘click’ reaction meets the following stringent guidelines: be modular in nature; obtain very high yields; generate inoffensive byproducts (if any); be stereospecific; and have simple conditions (insensitive to water and

oxygen) with benign solvents. The Huigsen cycloaddition of an azide to a terminal alkyne is used for 'click' applications [73]. Some of the more relevant uses of this reaction with homogeneous cellulose systems, especially pertaining to grafting of polymers onto cellulose, are discussed in this text. To date, though, no examples are available of graft copolymers with a cellulose backbone having been prepared using this reaction. A 2011 review of its use with polysaccharide chemistry can be referred to for more information [74].

Liebert et al. in 2005 [75] released a communication that they claimed was the first use of the Huisgen azide/alkyne click reaction with cellulose. Avicel cellulose was modified with p-toluenesulfonates in DMAc/LiCl (DS 0.92); these groups were then displaced by azide groups (DS 0.88). They did not click on polymer chains but clicked on a series of terminal-alkyne containing molecules, obtaining conversions in the range of 75% to 98%. This was followed [18] by synthesizing dendronized cellulose in EMIM AcO. The azide functionalized cellulose was prepared as discussed previously [75] and then dissolved in EMIM AcO. Polyamidoamine dendrons (with 1, 2, or 3 repetitions) with an alkyne moiety at the focal point were introduced. Despite the low molecular weights, the highest DS obtained through the click reaction was 0.60 in 48 hours (out of an original celluose azide functionality of DS 0.75), and the authors noted that reactivity decreased with increasing dendron size. It is not clear why EMIM AcO was used as the reaction solvent, as the cellulose derivative is soluble in more common solvents (according to their own paper), other than as a proof that it could be done and because "the recycling of these solvents is comparably easy". This group did this reaction again [76] except that the cellulose derivative was synthesized by heterogeneous carboxymethylation in isopropanol/aqueous NaOH. A study on chain conformation observed little effect of dendronization on the chain stiffness. Another study by this group [77] made hydrogels from cellulose. Water-soluble samples of carboxymethyl cellulose were functionalized with propargyl and azido groups and then crosslinked using $CuSO_4$/ascorbic acid. The native cellulose was degraded during the

functionalization steps, with the DP changing from an initial value of 600 to a range of between 43 and 200.

A study by Zhang et al. [19] used the azide/alkyne click reaction to make thermosensitive hydrogels from cellulose and P(NIPAAm-co-HEMA). Avicel© cellulose was modified with p-toluenesulfonates in DMAc/LiCl; some of these groups were then displaced with azide groups. The P(NIPAAm-co-HEMA) was functionalized with alkyne groups via an esterification reaction with 4-oxo-4-(prop-2-ynyloxy) butanoic acid. The two polymers were then clicked together in the presence of CuBr/PMDETA to form a crosslinked gel.

Another instance of the azide/alkyne click reaction with cellulose is in a study by Neigishi et al. [17]. Lactose and maltose end-functionalized with a propargyl group were clicked onto cellulose functionalized with azide groups. The azide-functionalized cellulose was prepared in DMAc/LiCl by activating the hydroxyls with triphenylphosphine, followed by bromination with carbon tetrabromide, and then displacing with sodium azide in DMAc/DMSO. The authors note that the azide-functionalized cellulose had near-perfect structural homogeneity, with all primary hydroxyls reacted and very few of the secondary hydroxyls. Lactose and maltose, respectively, were then clicked onto the cellulose quantitatively (DS 1.03) at room temperature (reaction time 12 hours, with $CuBr_2$/ascorbic acid). They then used a similar reaction scheme to functionalize cellulose with thymidine and/or trimethylammonium groups, which they used to disperse single-walled carbon nanotubes in water [78].

In addition to azide-functionalized cellulose, the same click reaction can be used with propargyl-functionalized cellulose. Faugeras et al. [79] used a Williamson ether synthesis reaction to couple propargyl bromide to cellulose in aqueous sodium hydroxide, assisted by microwave irradiation. Degrees of substitution up to 1.88 were obtained. This reaction scheme has the benefit of not requiring the synthesis of a cellulose intermediate, although the limitations of aqueous NaOH as a cellulose solvent have been discussed previously [11].

Gruskiene et al. [80] attempted to make graft copolymers with a chitosan backbone and poly(ethylene glycol) (M_n 2,000 g/mole) arms using the azide/alkyne click reaction. This was done using both propargyl-functionalized chitosan and azide-functionalized chitosan. Grafting yield was essentially quantitative for both reaction schemes; however, the authors noted that the intrinsic viscosity was low which indicated degradation of the chitosan backbone. Yuan et al. made amphiphilic copolymers with a chitosan backbone by functionalizing the chitosan with propargyl groups [81-83] and found coupling efficiencies above 80%.

An interesting twist on grafting chemistry was undertaken by Enomoto-Rogers et al. in 2012 [85]. Following the work of their earlier papers [85, 86] on functionalizing the reducing end of cellulose, they end-functionalized cellulose triacetate oligomers (DP = 2, 13) with azide and clicked them onto poly(2-propyn-1-yl methacrylate). They then removed the acetate protecting groups to regenerate the cellulose, thus making a graft copolymer with a synthetic backbone and cellulose grafts. Despite the low degree of polymerization of the cellulose, the reaction was not quantitative with a higher grafting efficiency (72% compared to 43%) noted for the lower molecular (DP = 2) weight grafts, although this is still a relatively high grafting density.

2.4.3 Thiol-ene reactions: photo-click and Michael addition

Substantially less work has been done on thiol-ene chemistry with polysaccharides as compared to the azide/alkyne reaction [87-89]. A publication by Tingaut et al. [90] detailed the functionalization of cellulose films with thiol-ene chemistry. The cellulose was suspended in $EtOH/H_2O$ and then reacted with commercially obtained 3-mercaptopropyl-trimethoxysilane or vinyl-trimethoxysilane in acidic media. The cellulose was dried and the silylated cellulose was soxhlet extracted and dried again to form films. They then clicked small molecules with thiol or alkene functionality to the cellulose film under UV irradiation; the grafting of polymers was not attempted. The reaction worked well for the alkene-functionalized cellulose but yields were low

for the sulfide-functionalized cellulose. The authors attributed this to partial oxidation of the sulfide groups to disulfide or sulfonic acid groups.

Thiol-ene chemistry has been used to make interpenetrating networks of cellulose-acetate-butyrate and polydimethylsiloxane [91, 92]. In this case, cellulose-acetate-butyrate and divinyl-poly(dimethylsiloxane) were dissolved in chloroform. Trimethyloylpropane tris(3-mercaptopropionate) was used as the crosslinking agent for the divinyl-poly(dimethylsiloxane) and Desmodur© was used as the crosslinking agent for the cellulose. All the ingredients were mixed to form an interpenetrating network. They also made networks where one of the polymers was not crosslinked. The thiol-ene reaction has also been used to make interpenetrating networks of cellulose acetate and PMMA [93]. Cellulose acetate was functionalized with sulfide groups by esterification with mercaptoacetic acid, and then polymerized with MMA using UV irradiation and a photoinitiator. A combination of thiol-ene links and disulfide links were formed. This follows their earlier work on making cellulose acetate gels using reversible disulfide linkages [94]. They used DMSO or O_2 as the oxidant, and 2-mercaptoethanol as the reductant.

Krasznai et al. [95] synthesized block copolymers that resembled the architecture of a core cross-linked micelle. The core of the molecule was created via catalytic chain transfer copolymerization of MMA and ethylene glycol dimethacrylate to make a hyperbranched core with alkene end-group functionality. Thiol-ene Michael addition was then used to attach cysteamine hydrochloride, and the resulting amines were used as sites for attaching dextran via reductive amination to yield a polysaccharide shell.

2.5 Conclusions

Ionic liquids are useful as solvents due to their ease of use and ability to dissolve cellulose from a wide range of sources under mild conditions. A wide range of functionalization and polymerization reactions can be carried out in homogenous ionic liquid solutions. However,

reports of their inert behaviour towards cellulose and reactions in general have been over-stated, with ionic liquids being observed to depolymerize cellulose, react with its reducing end, and acylate it, as well as catalyze and generally play a non-inert role in many reactions. They are also often highly hygroscopic and highly viscous (although this is common to most cellulose solvents), and their lack of a vapour pressure makes them impossible to remove by evaporation.

Controlled radical polymerizations, especially ATRP, have been widely used to synthesize graft copolymers from cellulose. SET is now becoming a research focus as well, but has received much less attention to date than ATRP. However, combination of the cellulose molecules has been problematic, in some cases leading to gelling or exceptionally high molecular weights. In addition, the reactions are poorly understood, with few attempts to compare the polymerization behaviour to linear homopolymerization. As such, it is not known exactly what effect the cellulose has on the polymerization kinetics, if any, and if the negative results obtained are due to the grafting reaction or the polymerization design. Characterization remains an issue, with very few groups reporting the amount of branching actually achieved (as opposed to theoretically achieved), and attempts at cleaving the grafts generally do not attempt to avoid hydrolyzing ester groups on acrylic polymers. Accurate characterization of the grafts is necessary for calculation of initiation efficiency, an important aspect of establishing control over the polymer architecture. Polymerizations using Cu(0) as catalyst appeared to have much worse initiation efficiencies than those where Cu(I) was used, and in some cases did not polymerize at all. This is in contrast to the excellent results obtained with SET and non-polymeric initiators.

Cellulose graft copolymers using a ‘grafting-to’ approach are almost unknown in the literature, and use non-‘click’ reactions that yield very low grafting densities. The use of ‘click’ reactions with cellulose in other applications is also very low but increasing; this type of chemistry has a large, mostly unexplored potential for cellulose grafting.

2.6 Acknowledgements

I would like to sincerely thank Mr. Ryan Roeder and Dr. Hai-Dong Wang for their assistance in editing this chapter. Their input was extremely valuable and very much appreciated.

2.7 References

[1] R. A. Festucci-Buselli, W. C. Otoni and C. P. Joshi, "Structure, organization, and functions of cellulose synthase complexes in higher plants," *Brazilian Journal of Plant Physiology,* vol. 19, no. 1, pp. 1-13, 2007.

[2] K. Shill, S. Padmanabhan, Q. Xin, J. M. Prausnitz, D. S. Clark and H. W. Blanch, "Ionic liquid pretreatment of cellulosic biomass: enzymatic hydrolysis and ionic liquid recycle," *Biotechnology and Bioengineering,* vol. 108, no. 3, pp. 511-520, 2011.

[3] R. Rinaldi, R. Palkovits and F. Schuth, "Depolymerization of cellulose using solid catalysts in ionic liquids," *Angewandte Chemie International Edition,* vol. 47, no. 42, pp. 8047-8050, 2008.

[4] M. Rose and R. Palkovits, "Cellulose-based sustainable polymers: state of the art and future trends," *Macromolecualr Rapid Communications,* vol. 32, no. 17, pp. 1299-1311, 2011.

[5] S. Barthel and T. Heinze, "Acylation and carbanilation of cellulose in ionic liquids," *Green Chemistry,* vol. 8, no. 3 pp. 301-306, 2006.

[6] Y. Cao, J. Zhang, J. He, H. Li and Y. Zhang, "Homogeneous acetylation of cellulose at relatively high concentrations in an ionic liquid," *Chinese Journal of Chemical Engineering,* vol. 18, no. 3, pp. 515-522, 2010.

[7] T. Heinze, R. Dicke, A. Koschella, A. H. Kull, E.-A. Klohr and W. Koch, "Effective preparation of cellulose derivatives in a new simple cellulose solvent," *Macromolecular Chemistry and Physics,* vol. 201, no. 6, pp. 627-631, 2000.

[8] D. Roy, M. Semsarilar, J. T. Guthrie and S. Perrier, "Cellulose modification by polymer grafting: a review," *Chemical Society Reviews,* vol. 38, no. 7, pp. 2046-2064, 2009.

[9] M. Tizzotti, A. Charlot, E. Fleury, M. Stenzel and J. Bernard, "Modification of polysaccharides through controlled/living radical polymerization grafting - towards the generation of high performance hybrids," *Macromolecular Rapid Communications,* vol. 31, no. 20, pp. 1751-1772, 2010.

[10] E. Malmstrom and A. Carlmark, "Controlled grafting of cellulose fibres - an outlook beyond paper and cardboard," *Polymer Chemistry,* vol. 3, no. 7, pp. 1702-1713, 2012.

[11] A. Isogai and R. Atalla, "Dissolution of cellulose in aqueous NaOH solutions," *Cellulose,* vol. 5, no. 4, pp. 309-319, 1998.

[12] A. El-Kafrawy, "Investigation of the cellulose/LiCl/dimethylacetamide and cellulose/LiCl/N-methyl-2-pyrrolidinone solutions by 13-C NMR spectroscopy," *Journal of Applied Polymer Science,* vol. 27, no. 7, pp. 2435-2443, 1982.

[13] V. Raus, M. Stepanek, M. Uchman, M. Slouf, P. Latalova, E. Cadova, M. Netopilik, J. Kriz, J. Dybal and P. Vleck, "Cellulose-based graft copolymers with controlled architecture prepared in a homogeneous phase," *Polymer Chemistry,* vol 49, no. 20, pp. 4353-4367, 2011.

[14] M. S. Hiltunen, J. Raula and S. L. Maunu, "Tailoring of water-soluble cellulose-g-copolymers in homogeneous medium using single-electron-transfer living radical polymerization," *Polymer International,* vol. 60, no. 9, pp. 1370-1379, 2011.

[15] M. Hiltunen, J. Siirila and S. L. M. Maunu, "Effect of catalyst systems and reaction conditions on the synthesis of cellulose-g-PDMAam copolymers by controlled radical polymerization," *Polymer Chemistry,* vol. 50, no. 15, pp. 3067-3076, 2012.

[16] B. Tosh, C. N. Saikia and N. N. Dass, "Homogeneous esterification of cellulose in the lithium chloride - N,N-dimethylacetamide solvent system: effect of temperature and catalyst," *Carbohydrate Research,* vol. 327, no. 3, pp. 345-352, 200.

[17] K. Negishi, Y. Mashiko, E. Yamashita, A. Otsuka and T. Hasegawa, "Cellulose chemistry meets click chemistry: syntheses and properties of cellulose-based glycocluster with high structural homogeneity," *Polymers,* vol. 3, no. 1, pp. 489-508, 2011.

[18] T. Heinze, M. Schobitz, M. Pohl and F. Meister, "Interactions of ionic liquids with polysaccharides. IV. Dendronization of 6-azido-6-deoxy cellulose," *Journal of Polymer Science: Part A: Polymer Chemistry,* vol. 46, no. 11 pp. 3853-3859, 2008.

[19] J. Zhang, X.-D. Xu, D.-Q. Wu, X.-Z. Zhang and R.-X. Zhuo, "Synthesis of thermosensitive P(NIPAAam-co-HEMA)/cellulose hydrogels via 'click' chemistry," *Carbohydrate Polymers,* vol. 77, no. 3, pp. 583-589, 2009.

[20] S. Kohler and T. Heinze, "New solvents for cellulose: dimethyl sulfoxide/ammonium fluorides," *Macromolecular Bioscience,* vol. 7, no. 3, pp. 307-314, 2007.

[21] R. P. Swatloski, S. K. Speak, J. D. Holbrey and R. D. Rogers, "Dissolution of cellulose with ionic liquids," *Journal of the American Chemical Society,* vol. 124, pp. 4974-4975, 2002.

[22] R. C. Remsing, R. P. Swatloski, R. D. Rogers and G. Moyna, "Mechanism of cellulose dissolution in the ionic liquid 1-n-butyl-3-methylimidazolium chloride: a 13-C and 35/37-Cl NMR relaxation study on model systems," *Chemical Communications,* vol. 48, no. 12, pp. 1271-1273, 2006.

[23] B. Kosan, C. Michels and F. Meister, "Dissolution and forming of cellulose with ionic liquids," *Cellulose,* vol. 15, no. 1, pp. 59-66, 2008.

[24] J. Vitz, T. Erdmenger, C. Haensch and U. S. Schubert, "Extended dissolution studies of cellulose in imidazolium based ionic liquids," *Green Chemistry,* vol. 11, no. 3, pp. 417-424, 2009.

[25] Y. Fukaya, K. Hayashi, M. Wada and H. Ohno, "Cellulose dissolution with polar ionic liquids under mild conditions: required factors for anions," *Green Chemistry,* vol. 10, no. 1, pp. 44-46, 2008.

[26] C.-x. Lin, H.-y. Zhan, M.-h. Liu, S.-y. Fu and L.-h. Huang, "Rapid homogeneous preparation of cellulose graft copolymer in BMIMCL under microwave irradiation," *Journal of Applied Polymer Science,* vol. 118, no. 1, pp. 399-404, 2010.

[27] Y. Hao, J. Peng, J. Li, M. Zhai and G. Wei, "An ionic liquid as reaction media for radiation-induced grafting of thermosensitive poly (N-isopopylacrylamide) onto microcrsytalline cellulose," *Carbohydrate Polymers,* vol. 77, no. 4, pp. 779-784, 2009.

[28] C.-x. Lin, H.-y. Zhan, M.-h. Liu, S.-y. Fu and L. A. Lucia, "Novel preparation and charachterization of cellulose microparticles functionalized in ionic liquid," *Langmuir,* vol. 25, no. 17, pp. 10116-10120, 2009.

[29] L. Chun-xiang, Z. Huai-yu, L. Ming-hua, F. Shi-yu and Z. Jia-jun, "Preparation of cellulose graft poly(methyl methacrylate) copolymers by atom transfer radical polymerization in an ionic liquid," *Carbohydrate Polymers,* vol. 78, no. 3, pp. 432-438, 2009.

[30] T. Heinze, K. Schwikal and S. Barthel, "Ionic liquids as reaction medium in cellulose functionalization," *Macromolecular Bioscience ,* vol. 5, no. 6, pp. 520-525, 2005.

[31] J. Wu, J. Zhang, H. Zhang, J. He, Q. Ren and M. Guo, "Homogeneous acetylation of cellulose in a new ionic liquid," *Biomacromolecules,* no. 5, pp. 266-268, 2004.

[32] Y. Cao, J. Wu, T. Meng, J. Zhang, J. He, H. Li and Y. Zhang, "Acetone-soluble cellulose acetates prepared by one-step homogeneous acetylation of cornhusk cellulose in an ionic liquid 1-allyl-3-methylimidazolium chloride (AmimCl)," *Carbohydrate Polymers,* vol. 69, no. 4, pp. 665-672, 2007.

[33] C. Yan, J. Zhang, Y. Lv, J. Yu, J. Wu, J. Zhang and J. He, "Thermoplastic cellulose-graft-poly(L-lactide) copolymers homogeneously synthesized in an ionic liquid with 4-dimethylaminopyridine catalyst," *Biomacromolecules,* vol. 10, no. 8, pp. 2013-2018, 2009.

[34] T. Meng, X. Gao, J. Zhang, J. Yuan, Y. Zhang and J. He, "Graft copoloymers prepared by atom transfer radical polymerization (ATRP) from cellulose," *Polymer,* vol. 50, no. 2, pp. 447-454, 2009.

[35] X. Sui, J. Yuan, M. Zhou, J. Zhang, H. Yang, W. Yuan, Y. Wei and C. Pan, "Synthesis of cellulose-graft-poly(N,N-dimethylamino-2-ethyl methacryalte copolymers via homogeneous ATRP and their aggregates in homogeneous media," *Biomacromolecules,* vol. 9, no. 10, pp. 2615-2620, 2008.

[36] S. Kohler, T. Liebert, M. Schobitz, J. Schaller, F. Meister, W. Gunther and T. Heinze, "Interactions of ionic liquids with polysaccharides 1. Unexpected acetylation of cellulose with 1-ethyl-3-methylimidazolium acetate," *Macromolecular Rapid Communications,* vol. 28, no. 24, pp. 2311-2317, 2007.

[37] D. C. Dibble, C. Li, L. Sun, A. George, A. Cheng, O. P. Cetinkol, P. Benke, B. M. Holmes, S. Singh and B. A. Simmons, "A facile method for the recovery of ionic liquid and lignin from biomass pretreatment," *Green Chemistry,* vol. 13, no. 11, pp. 3255-3264, 2011.

[38] T. F. Liebert, T. J. Heinze and K. J. Edgar, ACS Symposium Series 1033: Cellulose Solvents: For analysis, Shaping and Chemical Modification, New Orleans: Oxford University Press, 2010.

[39] R. Sescousse, K. A. Le, M. E. Ries and T. Budtova, "Viscosity of cellulose - imidazolium-based ionic liquid solutions," *Journal of Physical Chemistry B,* vol. 114, no. 21, pp. 7222-7228, 2010.

[40] H. Tokuda, K. Hayamizu, K. Ishii, M. A. B. H. Susan and M. Watanabe, "Physiochemical Properites and Structures of Room Temperature Ionic Liquids 2. Variation of Alkyl Chain Length in Imidazolium Cation," *Journal of Physical Chemistry B,* vol. 109, no. 13, pp. 6103-6110, 2005.

[41] J. G. Huddleston, A. E. Visser, W. M. Reichert, H. D. Willauer, G. A. Broker and R. D. Rogers, "Charachterization and comparison of hydrophilic and hydrophobic room temperature ionic liquids incorporating the imidazolium cation," *Green Chemistry,* vol. 3, no. 4, pp. 156-164, 2001.

[42] F. Liebner, I. Patel, G. Ebner, E. Becker, M. Horix, A. Potthast and T. Rosenau, "Thermal aging of 1-alkyl-3-methylimidazolium ionic liquids and its effect on dissolved cellulose," *Holzforschung,* vol. 64, no. 2, pp. 161-166, 2010.

[43] G. Ebner, S. Schiehser, A. Potthast and T. Rosenau, "Side reactions of cellulose with common 1-alkyl-3-methylimidazolium-based ionic liquids," *Tetrahedron Leters,* vol. 49, no. 51, pp. 7322-7324, 2008.

[44] S. Chowdhury, R. S. Mohan and L. J. Scott, "Reactivity of ionic liquids," *Tetrahedron,* vol. 63, no. 11, pp. 2362-2389, 2007.

[45] S. K. Karatzos, L. A. Edye and R. M. Wellard, "The undesirable acetylation of cellulose by the acetate ion of 1-ethyl-3-methylimidazolium acetate," *Cellulose,* vol. 19, no. 1, pp. 307-312, 2012.

[46] Y. Habibi, L. A. Lucia and O. J. Rojas, "Cellulose nanocrystals: chemistry, self-assembly, and applications," *Chemical Reviews,* vol. 110, no. 6, pp. 3479-3500, 2010.

[47] A. D. Jenkins, R. G. Jones and G. Moad, "Terminology for reversible-deactivation radical polymerization previously called 'controlled' radical or 'living' radical polymerization (IUPAC Recommendations 2010)," *Pure Applied Chemistry,* vol. 82, no. 2, pp. 483-491, 2010.

[48] E. Bianchi, E. Marsano, L. Ricco and S. Russo, "Free radical grafting onto cellulose in homogeneous conditions 1. Modified cellulose-acrylonitrile system," *Carbohydrate Polymers,* vol. 36, no. 4, pp. 313-318, 1998.

[49] Y. A. Aggour and E. Abdel-Razik, "Graft copolymerization of end allenoxy polyoxyethylene macromonomer onto ethyl cellulose in a homogeneous system," *European Polymer Journal,* vol. 35, no. 12, pp. 2225-2228, 1999.

[50] E. Bianchi, A. Bonazza, E. Marsano and S. Russo, "Free radical grafting onto cellulose in homogeneous conditions 2. Modified cellulose-methyl methacrylate system," *Carbohydrate Polymers,* vol. 41, no. 1, pp. 47-53, 2000.

[51] W. H. Daly, T. S. Evenson, S. T. Iacono and R. W. Jones, "Recent developments in cellulose grafting chemistry utilizing barton ester intermediates and nitroxide mediation," *Macromolecular Symposia,* no. 174, pp. 155-163, 2001.

[52] M. H. Stenzel, T. P. Davis and A. G. Fane, "Honeycomb structured porous fims prepared from carbohydrate based polymers synthesized via the RAFT process," *Journal of Materials Chemistry,* vol. 13, no. 9, pp. 2090-2097, 2003.

[53] R. Fleet, J. McLeary, V. Grumel, W. Weber, H. Matahwa and R. Sanderson, "RAFT mediated polysaccharide copolymers," *European Polymer Journal,* vol. 44, no. 9, pp. 2899-2911, 2008.

[54] C. Lin, H. Zhan, M. Liu, Y. Habibi, S. Fu and L. A. Lucia, "RAFT synthesis of cellulose-g-polymethylmethacrylate copolymer in an ionic liquid," *Journal of Applied Polymer Science,* vol. 127, no. *6*, pp. 4840-4849, 2012.

[55] Y. Zhang, Y. Wang, C.-h. Peng, M. Zhong, W. Zhu, D. Konkolewicz and K. Matyjaszewski, "Copper-Mediated CRP of Methyl Acrylate in the Presence of Metallic Copper: Effect of Ligand Structure on Reaction Kinetics," *Macromolecules,* vol. 45, no.1, pp. 78-86, 2012.

[56] K. Matyjaszewski, "Atom Transfer Radical Polymerization: from mechanisms to applications," *Israel Journal of Chemistry,* vol. 52, no. 3-4, pp. 206-220, 2012.

[57] V. Percec, T. Guliashvili, J. S. Ladislaw, A. Wistrand, A. Stjerndahl, M. J. Siekowska, M. J. Monteiro and S. Sahoo, "Ultrafast synthesis of ultrahigh molar mass polymers by metal-catalyzed living radical polymerization of acrylates, methacrylates, and vinyl chloride mediated by SET at 25^{O}C," *Journal of the American Chemical Society,* vol. 128, no. 43, pp. 14156-14165, 2006.

[58] G. Lligadas, B. M. Rosen, M. J. Monteiro and V. Percec, "Solvent choice differentiates SET-LRP and Cu-mediated radical polymerization with non-first order kinetics," *Macromolecules,* vol. 41, no. 22, pp. 8360-8364, 2008.

[59] N. H. Nguyen and V. Percec, "Disproportionating versus nondisproportionating solvent effect in the SET-LRP of methyl acrylate during catalysis with nonactivated and activated Cu(0) wire," *Journal of Polymer Science Part A: Polymer Chemistry,* vol. 49, no. 19, pp. 4227-4240, 2011.

[60] D. Shen and Y. Huang, "The synthesis of CDA-g-PMMA copolymers through atom transfer radical polymerization," *Polymer,* vol. 45, no. 21, pp. 7091-7097, 2004.

[61] D. Shen, H. Yu and Y. Huang, "Densely grafting copolymers of ethyl cellulose through atom transfer radical polymerization," *Journal of Polymer Science Part A: Polymer Chemistry,* vol. 43, no. 18, pp. 4099-4108, 2005.

[62] P. Vlcek, M. Janata, P. Latalova, J. Kriz, E. Cadova and L. Toman, "Controlled grafting of cellulose diacetate," *Polymer,* vol. 47, no. 8, pp. 2587-2595, 2006.

[63] M. Billy, A. Ranzani Da Costa, P. Lochon, R. Clement, M. Dresch, S. Etienne, J. Hiver, L. David and A. Jonquieres, "Cellulose acetate graft copolymers with nano-structured architectures," *European Polymer Journal,* vol. 46, no. 5, pp. 944-957, 2010.

[64] W. Liu, Y. Liu, G. Zeng, R. Liu and T. Huang, "Coil-to-rod conformational transition and single chain structure of graft copolymer by tuning the graft density," *Polymer,* vol. 53, no. 4, pp. 1005-1014, 2012.

[65] E. Ostmark, S. Harrisson, K. L. Wooley and E. E. Malmstrom, "Comb polymers prepared by ATRP from hydroxypropyl cellulose," *Biomacromolecules,* vol. 8, no. 4, pp. 1138-1148, 2007.

[66] F. J. Xu, Y. Ping, J. Ma, G. P. Tang , J. Li, E. T. Kang and K. G. Neoh, "Comb-shaped copolymers composed of hydroxypropyl cellulose backbones and cationic poly((2-dimethyl amino)ethyl methacrylate) side chains for gene delivery," *Bioconjugate Chemistry,* vol. 20, no. 8, pp. 1449-1458, 2009.

[67] P. Vlcek, V. Raus, M. Janata, J. Kriz and A. Sikora, "Controlled grafting of cellulose esters using SET-LRP process," *Journal of Polymer Science: Part A: Polymer Chemistry,* vol. 49, no. 1, pp. 164-173, 2010.

[68] J. Voepel, U. Edlund, A.-C. Albertsson and V. Percec, "Hemicellulose-based multifunctional macroinitiator for single-electron-transfer mediated living radical polymerization," *Biomacromolecules,* vol. 12, no. 1, pp. 253-259, 2011.

[69] U. Edlund and A.-C. Albertsson, "SET-LRP goes "green": various hemicellulose initiating systems under non-inert conditions," *Polymer Chemistry,* vol. 50, no. 13, pp. 2650-2658, 2012.

[70] P. Mansson and L. Westfelt, "Grafting of monodisperse low-molecular-molecular weight polystyrene onto cellulose acetate," *Journal of Polymer Science: Polymer Chemistry Edition,* vol. 19, no. 6, pp. 1509-1515, 1981.

[71] C. J. Biermann, J. B. Chung and R. Narayan, "Grafting of polystyrene onto cellulose acetate by nucleophilic displacement of mesylate groups usinf the polystyrycarboxylate anion," *Macromolecules,* vol. 20, no. 5, pp. 954-957, 1987.

[72] H. C. Kolb, M. Finn and K. B. Sharpless, "Click chemistry: diverse chemical function from a few good reactions," *Angewandte Chemie Internation Edition,* vol. 40, no. 11, pp. 2004-2021, 2001.

[73] V. V. Rostovtsev, L. G. Green, V. V. Fokin and K. B. Sharpless, "A stepwise Huigsen cycloaddition process: Copper(I)-catalyzed regioselective 'ligation' of azides and terminal alkynes," *Zuschriften,* vol. 114, no. 14, pp. 2708-2711, 2002.

[74] P.-H. Elchinger, P.-A. Faugeras, B. Boens, F. Brouillette, D. Montplaisir, R. Zerrouki and R. Lucas, "Polysaccharides: the 'click' chemistry impact," *Polymer,* vol. 3, no. 4, pp. 1607-1651, 2011.

[75] T. Liebert, C. Hansch and T. Heinze, "Click chemistry with polysaccharides," *Macromolecular rapid communications ,* vol. 27, no. 3, pp. 208-213, 2005.

[76] M. Pohl, G. A. Morris, S. E. Harding and T. Heinze, "Studies on the molecular flexibility of novel dendronized carboxymethyl cellulose derivatives," *European Polymer Journal,* vol. 45, no. 4, pp. 1098-1110, 2009.

[77] A. Koschella, M. Hartlieb and T. Heinze, "A 'click-chemistry' approach to cellulose-based hydrogels," *Carbohydrate Polymers,* vol. 86, no. 1, pp. 154-161, 2011.

[78] N. Kawagoe, Y. Kasori and T. Hasegawa, "Highly C6-selective and quantitative modification of cellulose: nucleoside-appended celluloses to solublilize single walled carbon nanotubes," *Cellulose,* vol. 18, no. 1, pp. 83-93, 2011.

[79] P.-A. Faugeras, P.-H. Elchinger, F. Brouillette and R. Zerrouki, "Advances in cellulose chemistry - microwave assisted synthesis of propargylcellulose in aqueous medium," *Green Chemistry,* vol. 14, no. 3, pp. 598-600, 2012.

[80] R. Gruskiene, G. Ciuta and R. Makuska, "Grafting of poly(ethylyene glycol) to chitosan at C(6) position of glucosamine units via 'click chemistry' reactions," *Chemija,* vol. 20, no. 4, pp. 241-249, 2009.

[81] X. Li, W. Yuan, S. Gu and J. Ren, "Synthesis and self-assembly of tunable thermosensitive chitosan amphiphilic copolymers by click chemistry," *Materials Letters,* vol. 64, no. 24, pp. 2663-2666, 2010.

[82] W. Yuan, X. Li, S. Gu, A. Cao and J. Ren, "Amphiphilic chitosan graft copolymer via combination of ROP, ATRP and click chemistry: synthesis, self-assembly, thermosensitivity, fluorescence, and controlled drug release," *Polymer,* vol. 52, no.3, pp. 658-666, 2011.

[83] W. Yuan, Z. Zhao, S. Gu and J. Ren, "Synthesis, characterization, and properties of amphiphilic chitosan copolymers with mixed side chains by click chemistry," *Journal of Polymer Science: Part A: Polymer Chemistry,* vol. 48, no. 15, pp. 3476-3486, 2010.

[84] Y. Enomoto-Rogers, H. Kamitakahara, A. Yoshinaga and T. Takano, "Comb-shaped graft copolymers with cellulose side-chains prepared via click chemistry," *Carbohydrate Polymers,* vol. 87, no. 3, pp. 2237-2245, 2012.

[85] H. Kamitakahara and F. Nakatsubo, "Synthesis of diblock copolymers with cellulose derivatives. 1. Model study with azidoalkyl carboxylic acid and cellobiosylamine derivative," *Cellulose,* vol. 12, no. 2, pp. 209-219, 2005.

[86] H. Kamitakahara, Y. Enomoto, C. Hasegawa and F. Nakatsubo, "Synthesis of diblock copolymers with cellulose derivatives. 2. Charachterization and thermal properties of cellulose triacetate-block-oligoamide-15," *Cellulose,* vol. 12, no. 5, pp. 527-541, 2005.

[87] A. Dondoni and A. Marra, "Recent applications of thiol-ene coupling as a click process for glycoconjugation," *Chemical Society Review,* vol. 41, no. 2, pp. 573-586, 2012.

[88] C. E. Hoyle and C. N. Bowman, "Thiol-ene click chemistry," *Angewandte Chemie International Edition,* vol. 49, no. 9, pp. 1540-1573, 2010.

[89] A. B. Lowe, "Thiol-ene 'click' reactions and recent applications in polymer and materials synthesis," *Polymer Chemistry,* vol. 1, no. 1, pp. 17-36, 2010.

[90] P. Tingaut, R. Hauert and T. Zimmermann, "Highly efficient and straighforward functionalization of cellulose films with thiol-ene click chemistry," *Journal of Materials Chemistry,* vol. 21, no. 40, pp. 16066-16076, 2011.

[91] O. Fichet, F. Vidal, J. Laskar and D. Teyssie, "Polydimethylsiloxane-cellulose acetate butyrate interpenetrating polymer networks synthesis and kinetic study. Part 1," *Polymer,* vol. 46, no. 1, pp. 37-47, 2005.

[92] F. Vidal, O. Fichet, J. Laskar and D. Teyssie, "Polysiloxane-cellulose acetate butyrate cellulose interpenetrating polymers networks close to true IPNs on a large composition range. Part II," *Polymer,* vol. 47, no. 11, pp. 3747-3753, 2006.

[93] D. Aoki, Y. Teramoto and Y. Nishio, "Cellulose acetate/poly(methyl methacryalte) interpenetrating networks: synthesis and estimation of thermal and mechanical properties," *Cellulose,* vol. 18, no. 6, pp. 1441-1454, 2011.

[94] D. Aoki, Y. Teramoto and Y. Nishio, "SH-containing cellulose acetate derivatives: preapration and charachterization as a shape memory-recovery material," *Biomacromolecules,* vol. 8, no. 12, pp. 3749-3757, 2007.

[95] D. J. Krasznai, T. F. L. McKenna, M. F. Cunningham, P. Champagne and N. M. B. Smeets, "Polysaccharide-stabilized core cross-linked polymer micelle analogues," *Polymers,* vol. 3, no. 4, pp. 992-1001, 2012.

Chapter 3

Functionalization of Cellulose in Homogeneous Media: Synthesizing Precursors for Graft Copolymerization

Abstract

Reactions involving cellulose are limited by the solubility of the polysaccharide. Cellulose derivatives are typically formed as intermediate products so that the cellulose can be dissolved in common solvents; cellulose acetate is one of the most common derivatives. Recently, a number of solvent systems capable of dissolving cellulose directly have been developed. These allow for direct control over the degree of substitution of the functional groups and avoid having to form intermediate products. Cellulose acetate and microcrystalline cellulose were used as starting materials for the synthesis of cellulose with functional groups required for graft copolymerizations, with imidazolium-based ionic liquids being used to dissolve the microcrystalline cellulose. The cellulose was functionalized with bromoester groups to allow controlled radical polymerization from the backbone, and with methacrylate groups for thiol-ene addition of grafts.

The ionic liquid 1-ethyl-3-methylimidazolium acetate (EMIM AcO) could readily dissolve cellulose at room temperature, but was found to interact with cellulose during acylation reactions to produce cellulose triacetate rather than the desired product. Using 1-butyl-3-methylimidazolium (BMIM Cl) as the solvent instead of EMIM AcO resulted in successful synthesis of cellulose with bromoisobutyrate groups (Cell-BiB), but the elevated temperatures required for BMIM Cl degraded the cellulose and caused side reactions of the functional groups. Ring-opening of glycidyl methacrylate in tetrahydrofuran or (1,4)-dioxane to impart methacrylate functionality on cellulose acetate was not found to be successful, with poor control over the reaction being exhibited. Steglich esterification of cellulose acetate with methacrylic acid was

found to be an easy method to control the reaction that did not harm the integrity of the cellulose acetate chains or result in side reactions occurring.

3.1 Introduction

The limited availability of solvents capable of dissolving cellulose is a major disadvantage for the chemical modification of cellulose: this limits the type of reactions that can be used, as well as the polymeric architecture obtainable. Consequently, cellulose derivatives that are soluble in common solvents are often synthesized as intermediates and are widely available commercially [1], with cellulose acetate being one of the most important derivatives. Industrial production of cellulose acetate is now primarily done using the "Acetic Acid Process", whereby the cellulose fibres are activated and swollen in acetic acid/sulfuric acid, and then reacted with acetic anhydride in a heterogeneous process [2]. The formed cellulose triacetate dissolves in the acetic acid. The primary difficulties associated with this are degradation of the cellulose backbone and the lack of control over the degree of substitution (DS) of the cellulose. This process primarily forms cellulose triacetate, which then needs to be de-acetylated by hydrolysis to the desired DS in order to regenerate hydroxyl groups for further modification.

Recently, attention has been directed to utilizing more exotic solvent systems in order to dissolve virgin cellulose and functionalize it directly. This has the benefit of not requiring the formation of intermediate products in order to solubilize the cellulose and allows greater control over the DS of the functional groups. Examples of such systems include dimethylacetamide (DMAc)/LiCl [3-10], N-methyl-2-pyrrolidone/LiCl [3], dimethyl sulfoxide (DMSO)/tetrabutylammonium fluoride trihydrate [11, 12], as well as ionic liquids 1-butyl-3-methylimidazolium chloride (BMIM Cl) [13-19], 1-allyl-3-methylimidazolium chloride (AMIM Cl) [20-25], and 1-ethyl-3-methylimidazolium acetate (EMIM AcO) [26-28].

An objective of this thesis is to graft synthetic chains onto cellulose in order to tailor its properties. To achieve this, the cellulose must be modified to give it functionality that allows the grafting to occur. The synthesis of cellulose derivatives that are useful precursors as the backbone polymer in graft copolymerization is discussed here. Both cellulose acetate and microcrystalline Avicel© cellulose were used as starting materials for these reactions, and the cellulose derivatives synthesized here were used as starting materials for the research discussed in Chapters 4 and 5: graft copolymerization using a 'grafting-from' and 'grafting-to' approach, respectively.

3.2 Experimental

3.2.1 Materials

Avicel© PH-101 microcrystalline cellulose (MCC, ~50 μm), cellulose acetate (CA, DS_{AcO} = 2.77 by NMR, M_n ~ 30,000 g/mol), 1-ethyl-3-methylimidazolium acetate (EMIM AcO, ≥90%, 1857±35 ppm water by Karl-Fischer titration), 1-butyl-3-methylimidazolium chloride (BMIM Cl, ≥98%, 5690±50 ppm water by Karl-Fischer titration), methacrylic acid (MAA, 99%), methacryloyl chloride (MAC, ≥97%), α-bromoisobutyryl bromide (BrBiB, 98%), N,N'-dicyclohexylcarbodiimide (DCC, 99%), 4-(dimethylamino) pyridine (DMAP, 99%), glycidyl methacrylate (GMA, 97%), triethylamine (TEA, 99%), and acetic anhydride (99%) were obtained from Sigma-Aldrich and used without modification. (1,4)-Dioxane was dried with magnesium sulfate, and tetrahydrofuran (THF) was distilled and then dried with magnesium sulfate prior to use. All other solvents and materials were used as received.

3.2.2 Modification of MCC in ionic liquids

3.2.2.1 Synthesis of Cell-AcO-BiB in EMIM AcO

In a typical procedure, MCC (0.50 g, 1 eq. of hydroxyl groups) was allowed to dissolve in EMIM AcO (15 g, 3.2 wt% cellulose) for at least one hour at room temperature under a nitrogen blanket. Upon formation of a transparent solution, the flask was submersed in an ice/water bath and BrBiB (2.3 mL, 2 eq.) was added drop-wise over 5 minutes in order to allow the exothermic reaction to dissipate heat. For some reactions, TEA (2.6 mL, 2 eq., used to neutralize the hydrobromic acid produced) was added as well during this time. The mixture was allowed to warm to room temperature while stirring. After 24 hours, the viscous, heterogeneous mixture was poured into a 4:1 water/methanol solution to precipitate the cellulose macroinitiator. The product was recovered by filtration and washed until the filtrate remained colourless before being dried in a vacuum oven overnight at 40^{O}C. The Cell-AcO-BiB was analyzed using proton and HSQC NMR in acetone-d_6. ^{1}H peak assignment: δ = 2.8 – 5.7 ppm (AGU); 1.85, 1.92, 1.96 ppm (-CH_3, acetate groups, bromoisobutyryl groups); 2.05 ppm (acetone); 2.85 ppm (water). In ^{13}C: δ = 63 – 131 ppm (AGU); 20 ppm (-CH_3, acetate groups); 29 ppm (-CH_3, bromoisobutyryl groups, acetone). The functionality could not be determined from NMR as the acetate and bromoester signals overlapped.

3.2.2.2 Synthesis of Cell-BiB in BMIM Cl

In a typical procedure (modified from Chun-xiang et al.[16]), MCC (0.50 g, 1 eq. of hydroxyl groups) was dissolved in BMIM Cl (20 g, 2.4 wt% cellulose) for 24 hours at 80^{O}C under a nitrogen blanket. Upon formation of a transparent solution, the flask was cooled to 50^{O}C and TEA (2.6 mL, 2 eq., used to neutralize the hydrobromic acid produced) and BrBiB (2.3 mL, 2 eq.) were added drop-wise over 10 minutes to allow the exothermic reaction to dissipate heat. A heterogeneous mixture formed. After 45 minutes a gel formed and water was used to extract the

solvent. The Cell-BiB was recovered by filtration and washed with water until the filtrate remained colourless before being dried in a vacuum oven overnight at 40^{O}C. The Cell-BiB was analyzed using ^{1}H and HSQC NMR in acetone-d6. ^{1}H peak assignment: δ = 2.8 – 5.7 ppm (AGU); 1.81 (-CH_3, bromoisobutyryl groups); 2.05 ppm (acetone); 2.85 ppm (water). ^{13}C peak assignment: δ = 63 – 131 ppm (AGU); 29 ppm (-CH_3, bromoisobutyryl groups, acetone). DS_{BiB}: 1.75 (from NMR). Yield: 0.90 g (69%).

3.2.2.3 Synthesis of Cell-AcO in EMIM AcO

In a typical procedure, MCC (2.0 g, 1 eq. hydroxyl groups) was allowed to dissolve in EMIM AcO (50 g, 3.8 wt% cellulose) overnight at 70^{O}C. Acetic anhydride (6.3 g, 1.7 eq) was added drop-wise over an hour and the reaction was continued for an additional 5 hours. The solution was then precipitated in excess water. The precipitate was filtered and washed with water until the filtrate remained colourless. The samples were dried and then the cellulose triacetate (DS_{AcO} ~ 3) was extracted with chloroform from the cellulose acetate (DS_{AcO} = 2.79). ^{1}H peak assignment in acetone-d_6: δ = 2.8 – 5.7 ppm (AGU); 1.85, 1.92, 1.96 ppm (-CH_3, acetate groups); 2.05 ppm (acetone); 2.85 ppm (water). ^{13}C peak assignment: δ = 63 – 131 ppm (AGU); 20 ppm (-CH_3, acetate groups); 29 ppm (-CH_3, acetone). Yield: 3.12 g (98%) total, 3.01 g of Cell-$AcO_{2.79}$.

3.2.2.4 Synthesis of cellulose with methacrylate functionality via ring-opening of GMA in EMIM AcO

MCC (0.2 g, 1 eq. of hydroxyls) was dissolved in 5 mL of EMIM AcO (3.8 wt%) at room temperature. After one hour, 0.6 mL of GMA (1.2 eq.) was added and the solution was allowed to stir. After 2.6 hours the transparent, red solution was poured into ACN to precipitate the cellulose. The product (Cell-GMA) was washed with ACN, dissolved in water, and re-

precipitated in ACN to yield the final product. ^{1}H peak assignment in D_2O: δ = 7.3 ppm (=CH_2); 3.0-5.5 ppm (AGU); δ = 3.1, 3.7, 4.1 ppm (propyl group); δ = 1.3 ppm (-CH_3 adjacent to alkene). DS_{alkene}: 0.54 (from NMR). Yield: 0.21 g, 71%.

3.2.3 Modification of cellulose acetate in cyclic ethers

3.2.3.1 Synthesis of cellulose acetate with methacrylate functionality via ring-opening of GMA

Cell-$AcO_{2.79}$ (0.50 g, 1 eq. of hydroxyls) was dissolved in 15 mL of THF (3.3 wt/vol%) in a 30^{O}C oil bath. Next, 0.05 mL of sulfuric acid (0.06 M) was added followed by 0.37 mL of GMA (6 eq.). The solution was stirred for 22 hours and then precipitated in water and washed with methanol. The recovered product (Cell-AcO-GMA) was dissolved in dioxane, re-precipitated in water, and washed with methanol until the alkene signal in the NMR spectra showed no change. ^{1}H peak assignment in acetone-d_6: δ = 5.5, 6.0 ppm (=CH_2); 3.0-5.3 ppm (AGU); δ = 3.6, 4.0, 4.1 ppm (propyl group); δ = 1.8 ppm (-CH_3 adjacent to alkene; signal overlaps acetate signal); 2.05 ppm (acetone); 2.85 ppm (water). DS_{alkene}: 0.09 (from NMR).

3.2.3.2 Synthesis of cellulose acetate with methacrylate functionality via esterification of MAA

$CA_{2.77}$ (2.4 g, 1 eq. of hydroxyls) was dissolved in 30 mL of THF (8 wt/vol%) at room temperature and 1.14 mL of MAA (6.8 eq.) was added. DCC (2.8 g, 6.8 eq.) was dissolved in 20 mL of THF and added to the reaction vessel, followed by DMAP (0.05 g). The resulting heterogeneous mixture was stirred overnight and then filtered to remove the precipitated dicyclohexylurea. The precipitate was washed with dioxane to recover the cellulose acetate. The product (CA-MAA) dissolved in THF/dioxane was precipitated in water, washed with methanol, re-dissolved in dioxane and precipitated with water, washed repeatedly with methanol, and then dried in a vacuum oven at 40^{O}C. The purification steps were repeated until the alkene signal in

the NMR spectra showed no change. ^{1}H peak assignment in acetone-d_6: δ = 5.6, 6.1 ppm (=CH_2); 3.0-5.3 ppm (AGU); δ = 1.8 ppm (-CH_3 adjacent to alkene; signal overlaps acetate signal). DS_{alkene}: 0.29 (from NMR). Yield: 1.20 g, 47%.

3.2.4 Characterization

Bromine analysis was carried out by Guelph Chemical Laboratories, Ltd. in Guelph, Ontario using ion chromatography. All other characterizations were carried out by the author.

3.2.4.1 Nuclear Magnetic Resonance (NMR)

^{1}H and Heteronuclear Single Quantum Correlation (HSQC) NMR spectroscopy were used to identify the samples, and to predict conversion and degree of substitution. Spectra were obtained on a 400 MHz Bruker Avance instrument. Degree of substitution (DS) of the functionalized cellulose was obtained by comparing the relative areas of the cellulose backbone protons and the attached functional group in ^{1}H NMR (64 scans). Spectra were assigned using information from [29], [30], and [31].

3.2.4.2 Gel permeation chromatography (GPC)

THF-soluble polymer samples were analyzed using a Viscotek GPCmax VE-2001 with a model VE 3580 refractive index (RI) detector, and a model 270 dual detector [light scattering (low angle light scattering and right angle light scattering), and viscosity (IV)]. Three PolyAnalytik columns (2 x PAS-106 with an exclusion molecular weight of 20 x 10^6 g/mol and guard) were used in series at a temperature of 40^{O}C. Distilled THF was used as the eluent at 1.0 mL/min. The triple detection system was calibrated using a narrow poly(styrene) sample of 93 x 10^3 g/mol, with refractive index 0.185 mL/g and intrinsic viscosity 0.465 dL/g. The molecular

weight analyses were performed using the Viscotek OmniSEC software. It is important that the concentration of these samples be accurately known for the molecular weight calculations.

Water-soluble polymer samples were analyzed on a Viscotek GPCmax VE-2001 with a Viscotek TDA 302 refractive index detector. Four PolyAnalytik columns (PAA-204, PAA-203, PAA-202.5, guard) with an exclusion limit of 1 x 10^6 g/mol were used in series at a temperature of 40^{O}C. Water with 0.02 M sodium azide was used as the eluent at 1.0 mL/min. The columns were calibrated with poly(ethylene oxide) (PEO) standards in the range 600 to 1 x 10^6 g/mol.

3.3 Results and discussion

3.3.1 Modification of microcrystalline cellulose in ionic liquids

3.3.1.1 Undesired acetylation of cellulose in EMIM AcO

The synthesis of Cell-BiB (cellulose functionalized with bromoisobutyrate groups that act as ATRP initiation sites) was first attempted in EMIM AcO. EMIM AcO seemed to be a promising ionic liquid for cellulose modification: its low melting point (<-20^{O}C) allows a wider range of reaction temperatures than ionic liquids that are solid at room temperature, as well as lower viscosity [32], and while it cannot dissolve as much cellulose as BMIM Cl [33] these lower temperatures and viscosities yield a more useful solution. EMIM AcO has been studied for use in lignocellulosic fractionation [34] and enzymatic hydrolysis [27]. The acylation reaction of cellulose with BrBiB is given in Scheme 3.1.

Scheme 3.1: Acylation of cellulose with BrBiB in EMIM AcO. Similar reactions were undertaken in BMIM Cl with TEA and BrBiB or MAC.

The reaction of cellulose dissolved in EMIM AcO with BrBiB led to an organic-soluble product with the ^{1}H NMR spectrum shown in Figure 3.1. The peak distribution in the obtained spectrum matched the predicted proton spectrum, and the three peaks between $\delta = 1.8 - 2.1$ ppm were assigned to be bromoisobutyrate groups distributed approximately equally on the three hydroxyl sites on the anhydroglucose unit (AGU). The DS was calculated to be 1.67. However attempts to use this material as an ATRP macroinitiator lead to unsatisfactory results; while polymerization using MA resulted in a living system, the polymerization rate was substantially slower than the expected rate at this concentration of initiation sites (see Chapter 4 for more detail). Numerous conditions were tried in an attempt to improve the rate, without success.

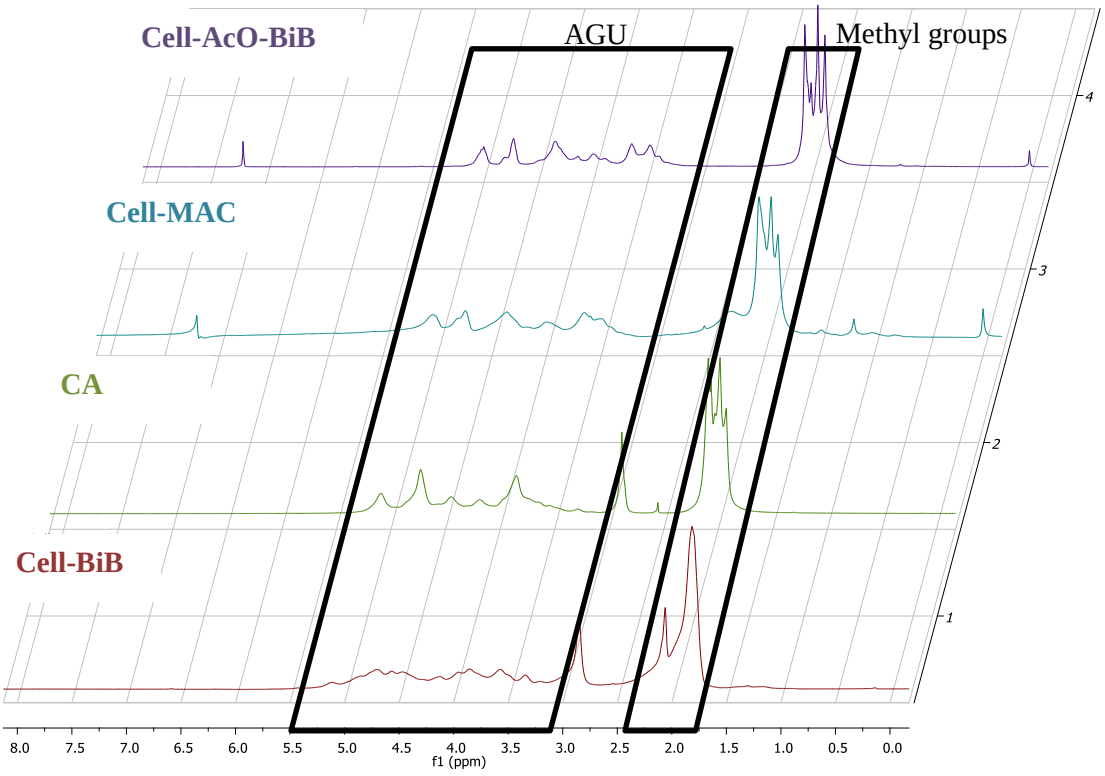

Figure 3.1: ^{1}H NMR spectra of cellulose samples prepared by acylation: Cell-AcO-BiB and Cell-MAC synthesized in EMIM AcO, unmodified cellulose acetate obtained from Sigma-Aldrich. and Cell-BiB synthesized in BMIM Cl. Acetone signal at 2.05 ppm (water 2.84 ppm); chloroform signal at 7.26 ppm.

The same reaction conditions were then used in an attempt to make cellulose functionalized with methacrylate groups (Cell-MAC) using methacryloyl chloride instead of BrBiB. Unexpectedly, a nearly identical ^{1}H NMR spectrum (Figure 3.1) was obtained as to that when using BrBiB, with no alkene presence in the region $\delta = 5.5 – 6.5$ ppm, and with a similar area of functional-group peak to AGU peak. It was observed that the spectrum of commercially obtained cellulose acetate appeared similar to the other two spectra, which would suggest that the samples were being acetylated by the solvent rather than having the desired acylation reaction occur. If the functional group appearing in the NMR spectrum for the sample of Cell-BiB synthesized in EMIM AcO was acetate rather than bromoisobutyrate, then the DS_{AcO} was calculated to be 2.97: essentially complete acetylation had occurred. To compare, Cell-BiB ($DS_{BiB} = 1.75$) was instead synthesized using BMIM Cl as the solvent (spectrum shown in Figure 3.1). The functional group appeared at the same chemical shift as those for the samples prepared in EMIM AcO but was qualitatively different, with the signal consisting of only one large peak rather than three peaks; this would indicate that the compounds prepared in the two solvents were not the same. To verify this, the HSQC spectra were examined. The spectra for the Cell-BiB synthesized in EMIM AcO (Figure 3.2-a) and the Sigma-Aldrich cellulose acetate (Figure 3.2-b) appeared identical. When comparing these to the spectrum of Cell-BiB prepared in BMIM Cl (Figure 3.2-c), the methyl groups for the BMIM Cl sample were in the same location on the proton axis as for the other two samples but appeared in a different location on the carbon axis: 29 ppm instead of 20 ppm. This would further support the conclusion that primarily acetylation was occurring in EMIM AcO rather than the desired acylation reaction.

Bromine analysis of the samples revealed that the macroinitiator synthesized in EMIM AcO had a bromine content of only 2.38±0.16 wt%, compared to 23.04±0.20 wt% for the macroinitiator synthesized in BMIM Cl: this corresponds to a DS_{BiB} of 0.0887 (assuming all other hydroxyls have been replaced by acetate groups) and 0.819 (assuming complete bromine

functionality on the bromoester groups), respectively. In an effort to improve the bromine content of the macroinitiator synthesized in EMIM AcO, TEA was added to the reaction in order to more effectively neutralize the acid produced. This led to a moderate increase of bromine content to 4.55±0.17 wt% (DS_{BiB} of 0.175).

The DS measured by bromine analysis was less than half that as measured by NMR for the Cell-BiB synthesized in BMIM Cl. The large difference should be well outside the margin of error for the measurement methods, suggesting that not all functional groups had bromine. NMR measured the methyl groups on the bromoisobutyrate rather than the bromine directly; since the bromine is labile, it is possible that it was being partially reacted during the synthesis, especially as elevated temperatures were used, and thus led to some of the functional groups not having bromine. The missing bromine groups were assumed to have been substituted by water (hydrolysis), and solving for DS_{Br} under this assumption obtained a value of 1.13 with a molecular weight of the repeating unit of 393 g/mol. These values were used for the calculation of degree of polymerization (DP) and the concentration of initiating sites.

A more extensive review of the literature in this area reveals reports of acetylation occurring in place of acylation in EMIM AcO [26, 35, 36]; this occurs by formation of an acetic anhydride or mixed anhydride intermediate (see Scheme 3.2). The excess of acetate as well as its greater reactivity in the anhydride species ensures it is dominant in the subsequent esterification. Acylation is clearly not possible in EMIM AcO and all further acylation reactions were conducted in BMIM Cl. The macroinitiator synthesized in EMIM AcO still had some bromine functionality and so will be referred to as Cell-AcO-BiB to differentiate it from the macroinitiator made in BMIM Cl which had no acetate groups and higher bromine functionality.

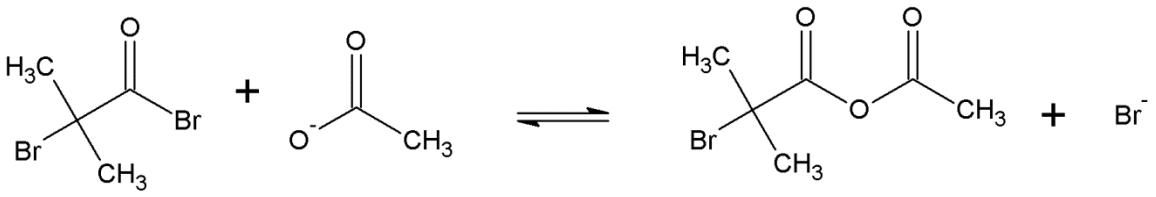

Scheme 3.2: Formation of mixed anhydride in presence of acetate.

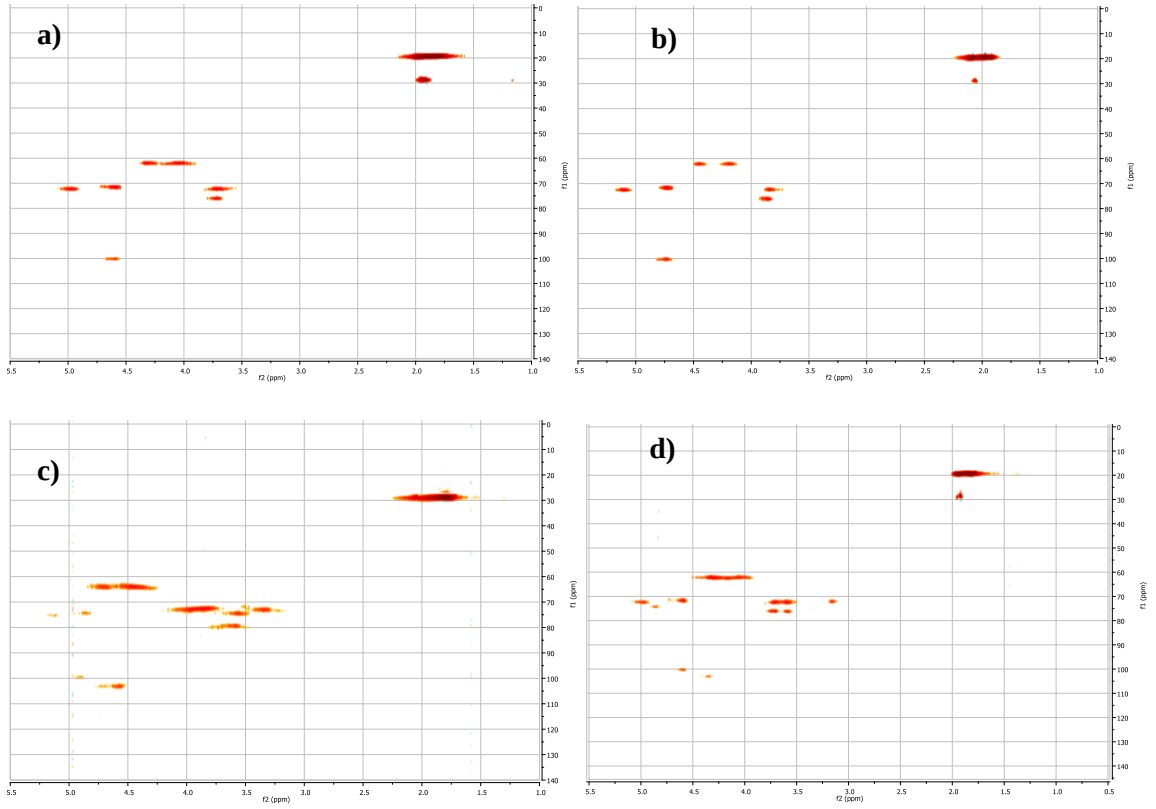

Figure 3.2: HSQC spectra of cellulose derivatives recorded in acetone-d_6: a) Cell-$AcO_{2.99}$-$BiB_{0.09}$ synthesized in EMIM AcO; b) cellulose acetate (DS_{AcO} = 2.77) obtained from Sigma-Aldrich; c) Cell-$BiB_{1.13}$ synthesized in BMIM Cl; d) Cell-$AcO_{2.79}$ synthesized in EMIM AcO.

3.3.1.2 Synthesis of Cell-BiB in BMIM Cl

Sui et al. [24] used a 4 wt% solution of cellulose in AMIM Cl and then diluted it with 29 wt% dimethyl formamide (DMF) as their solvent system to synthesize Cell-BiB. The cellulose was then reacted with 2-bromopropionyl bromide in an ice water bath. Meng et al. [23] also used

AMIM Cl diluted with DMF. A reaction scheme similar to this was first attempted using a 3.2 wt% solution of cellulose in BMIM Cl (0.5 g/15 g), which was then diluted by the addition of 24 wt% DMF (5.0 g), but with TEA used to neutralize the liberated hydrobromic acid. The undiluted solution was extremely viscous and did not allow for adequate stirring, but stirring was reinitiated upon the addition of DMF. The mixture appeared homogeneous with the addition of the DMF. The mixture was cooled in an ice bath and then TEA and BrBiB were added drop-wise; unfortunately, the mixture immediately gelled upon addition of the liquid reactants and stirring rapidly stopped. After purification, 0.60 g of solid was recovered. The recovered solid could not be re-dissolved in any common organic solvent, including DMSO, DMF, dioxane, or acetone. From the lack of solubility and the low mass recovered it was concluded that little or no functionalization had occurred, likely due to the cellulose not remaining in solution during the reaction.

Next, a procedure modified from Chun-xiang et al. [16] was used. The authors had used the same ionic liquid (BMIM Cl) as their solvent as that used in this work but did not add base to neutralize the hydrobromic acid. Triethylamine was used here in order to minimize any potential degradation to the cellulose that would occur from the acid. A 2.4 wt% solution of cellulose in BMIM Cl (0.5g /20 g) was prepared at 50^{O}C and then the liquid reactants were added. The mixture became heterogeneous but stirring was still possible unlike with the previously discussed method. After 45 minutes, stirring had ceased due to gelation and so the reaction was stopped by addition of water. After purification, 0.90 g of solid was recovered (69% yield) which could readily dissolve in DMSO, DMF, dioxane, and acetone, and was sparingly soluble in THF. From NMR analysis in acetone-d_6, the DS of BiB groups was calculated to be 1.75 (spectra given in Figure 3.1 and Figure 3.2). However, bromine analysis by ion chromatography gave a much lower DS of 1.13, and the discrepancy was believed to be caused by the labile bromine atom being removed from the BiB groups. The higher temperature (50^{O}C) of the reaction may have

contributed to this, especially as the reaction was exothermic and could have caused the reactor to overheat. However, this method gave better results than when EMIM AcO was used and was therefore chosen for future acylation reactions of microcrystalline cellulose. The use of Cell-BiB as a macroinitiator for ATRP will be discussed in detail in Chapter 4.

3.3.1.3 Synthesis of Cell-AcO with acetic anhydride in EMIM AcO

Cellulose acetate was synthesized in EMIM AcO to make a cellulose derivative with more favourable solubility characteristics which could then be further modified to impart the desired functionality. The cellulose solvents DMAc/LiCl [7], DMSO/tetrabutylammonium fluoride trihydrate [37], AMIM Cl [20, 25, 32], and BMIM Cl [19] have been used to acetylate cellulose in homogeneous medium. A method modified from Wu et al. [20] and Cao et al. [35, 32] using EMIM AcO and acetic anhydride was used here. The product was recovered in high yield (98%) and showed no impurities in NMR analysis (HSQC spectrum given in Figure 3.2-d). Chloroform was used to extract the cellulose triacetate fraction, and the remaining cellulose acetate (DS = 2.79) was used for further reactions. Considering the results for acylation reactions in EMIM AcO found previously in this work and in other published reports [26, 35, 36], it is probable that the solvent itself was primarily responsible for the acetylation that occurred in this reaction rather than the added acetic anhydride.

The molecular weight distributions of the derivatives of microcrystalline cellulose were measured on a Viscotek GPC in THF using a triple detection setup and are displayed in Figure 3.3 with the molecular weight data presented in Table 3.1. The molecular weight distribution of the virgin cellulose was not available and the degree of polymerization was not specified by the supplier so it was not known to what extent the cellulose had been degraded by the reactions. A paper by Mormann [38] reported a DP of 220 for Avicel© PH-101 by conversion to cellulose tricarbanilate, but there could be significant variation in DP between different batches of

cellulose. Degree of polymerization is the best metric to compare between the samples as the different functional groups change the molecular weight of the repeat units. The Cell-$AcO_{2.99}$-$BiB_{0.09}$ had the highest DP with a value of 142, while Cell-$BiB_{1.13}$ had a significantly lower value of 77. The Cell-$AcO_{2.79}$ had the lowest DP with a value of only 62. The degradation of the cellulose may be temperature related, as the highest DP sample (Cell-AcO-BiB) was dissolved at room temperature and synthesized in an ice bath. The other two samples were both dissolved at elevated temperatures (70 – 80^{O}C); the Cell-BiB synthesis then took place over 45 minutes in a 50^{O}C reactor, while the much more degraded Cell-AcO was synthesized over 6 hours at 70^{O}C. Solid cellulose has a decomposition temperature of 266^{O}C [39], but will likely exhibit signs of degradation at much lower temperatures. The acidic character of the solutions may also promote the degradation when temperatures are elevated. In addition, the columns for the chromatographic system have poor resolution in the low molecular weight region (<10^4 g/mol) and it was not clear if the low molecular weight shoulder had returned to baseline. This could lead to overestimation of M_n.

Table 3.1: Molecular weight data for cellulose derivatives.

Sample	M_n (g/mol)	PDI	DP	[η] (dL/g)	dn/dc (mL/g)	α
Cell-$BiB_{1.13}$	30,400	2.52	77	0.723	0.0922	0.806
Cell-$AcO_{2.91}BiB_{0.089}$	36,700	2.47	142	0.661	0.0517	0.783
Cell-$AcO_{2.79}$	15,600	2.26	62	1.24	0.0887	1.05

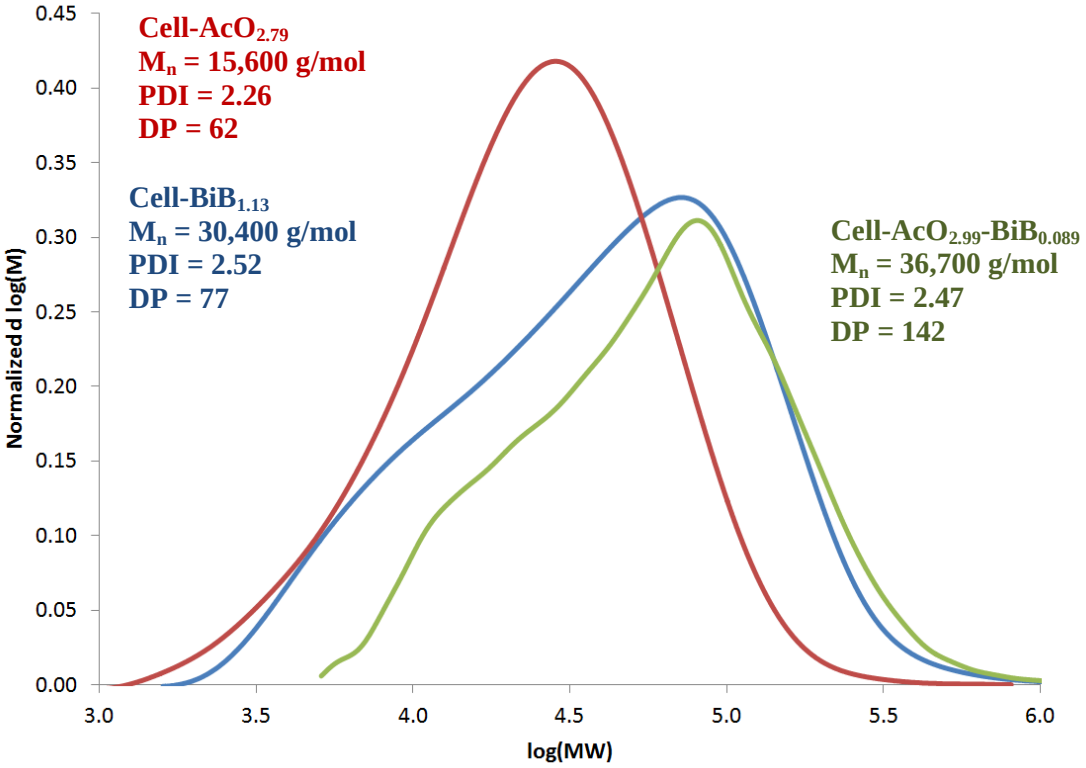

Figure 3.3: Molecular weight distributions of microcrystalline cellulose derivatives. The large range of DP values obtained suggests degradation of the cellulose is occurring. The molecular weights were obtained using the triple detection system.

3.3.1.4 Synthesis of Cell-MAC in BMIM Cl

Cellulose was reacted with methacryloyl chloride in order to give it methacrylate functionality along its backbone. The methacrylate groups function as sites for attaching other groups via thiol-ene photo-click or Michael addition. In the literature there are reports of cellulose dissolved in DMAc/LiCl reacted with acryloyl chloride to yield a DS of 2.36 [40] and methacryloyl chloride to yield a DS of up to 1.34 [41]. The reaction was undertaken here in a similar manner as for the synthesis of Cell-BiB and the product was precipitated in water. It first appeared that water was a good anti-solvent for the product, but during the subsequent washing and filtration steps it became evident that the product was being washed away as well; a similar

result was observed with acetone and methanol, with these being able to swell and partially dissolve the product. By the time a reasonably pure sample was obtained there was almost no product left for analysis. The NMR spectrum is given in Figure 3.4 and is quite dilute due to the small amount of product isolated; the peaks attributed to the methacrylate are nonetheless clearly visible, with the alkene peaks at δ = 5.7, 6.1 ppm and the methyl adjacent to the alkene at 1.9 ppm. An unknown peak also appears at 1.2 ppm. This may indicate a loss of alkene functionality, causing the methyl group signal to shift. DMSO and DMF were able to fully dissolve the product. Dichloromethane and chloroform were observed to be excellent anti-solvents for the Cell-MAC. Since these are both miscible with BMIM Cl, it is recommended that they be used as anti-solvents.

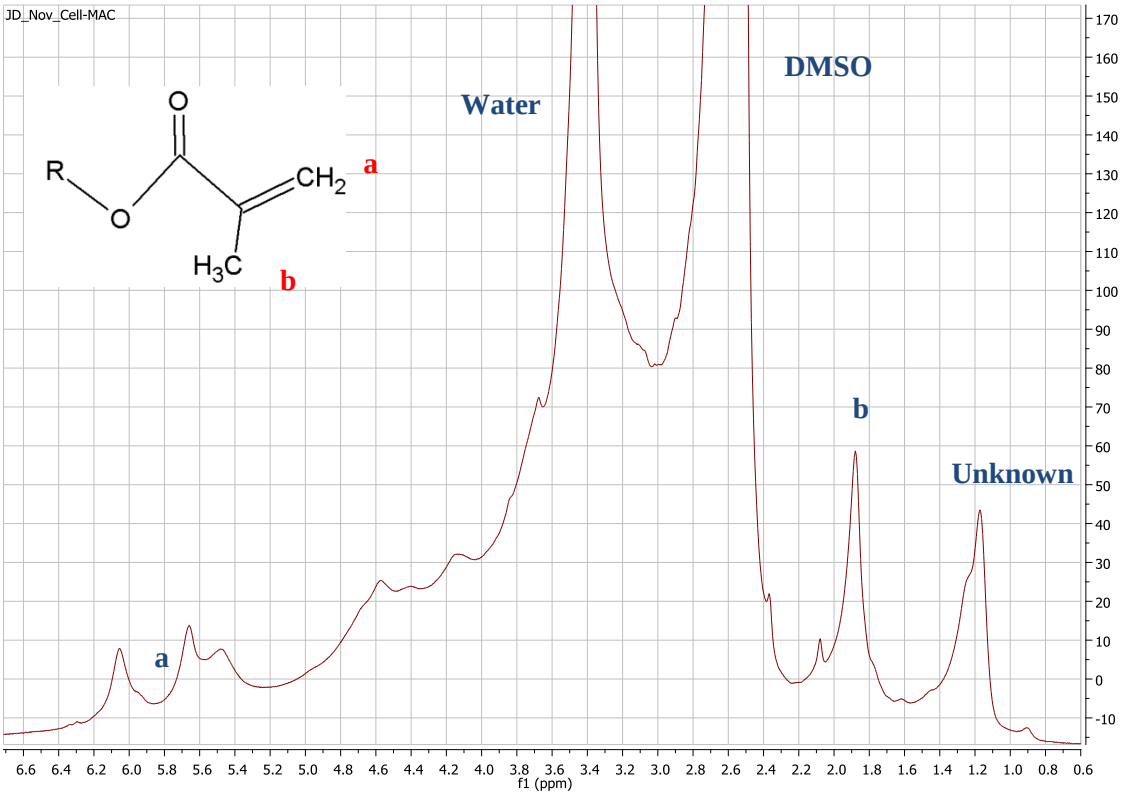

Figure 3.4: ^{1}H NMR spectrum of Cell-MAC. The sample was dilute but methacrylate peaks are clearly visible. Spectrum recorded in DMSO-d_6.

With this solvent information now available, the reaction was repeated in an attempt to improve the purification procedure. However, a different result was obtained this time with the product being highly insoluble in water as well as most other solvents. It would swell but not dissolve in DMSO. This was attributed to the BMIM Cl having become too wet by this point. All reactions were performed using the same container of BMIM Cl without access to a glove-box. As the BMIM Cl is an extremely hygroscopic solid, it is reasonable to assume that moisture content increased each time the container was opened. The final moisture content of the BMIM Cl was measured to be 5690±50 ppm by Karl-Fischer titration: for these reaction conditions, this corresponds to 0.11 g of water, or 0.69 equivalents, and does not include the bound moisture that is inevitably present in the cellulose itself. This is enough water to severely hamper the reaction. As a further verification of this conclusion, the BMIM Cl was then used in an attempt to make the Cell-BiB discussed earlier, with unsatisfactory results. Considering the results of the first reaction with methacryloyl chloride, as well as the literature reports for DMAc/LiCl [40, 41], it is expected that this reaction can be done successfully provided the solvent is kept dry and the cellulose remains adequately solvated.

3.3.1.5 Etherification of cellulose with glycidyl methacrylate in EMIM AcO

Epoxides have been used to react with cellulose under heterogeneous conditions via ring-opening [42], and glycidyl methacrylate has been used to react with chitosan dissolved in aqueous acid [43] and dextran dissolved in DMSO [54] to impart methacrylate functionality, although in the dextran/DMSO case the authors concluded that transesterification was occurring rather than opening of the epoxide. EMIM AcO has also been used to prepare hydroxyl propyl cellulose without the addition of catalyst using propylene oxide [45]; the authors found that ionic liquids with acetate anion catalyzed the etherification but not ionic liquids with chloride anion. In addition, NMR studies of the reactions in EMIM AcO showed side reactions occurring and the

authors note that "detailed analyses" were necessary to interpret the spectra [45]. The reaction of GMA with cellulose is shown in Scheme 3.3. Note that multiple isomers can form: as EMIM AcO has a pH less than 7, the second isomer is expected to be the most prevalent.

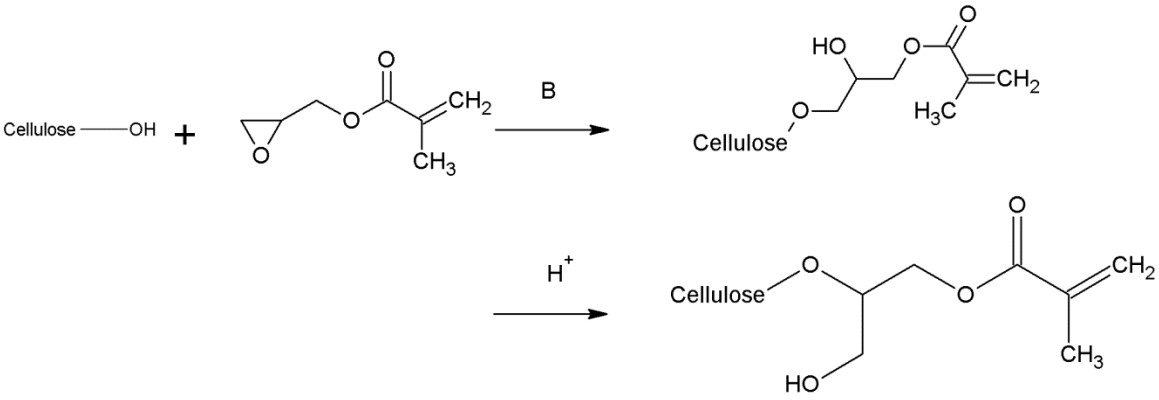

Scheme 3.3: Reaction of cellulose with GMA and formation of favoured isomers under acidic and basic conditions.

The etherification reaction was first attempted using GMA and un-derivatized cellulose dissolved in EMIM AcO in an attempt to obtain cellulose with methacrylate functionality and without any other functional groups (Cell-GMA) using a method similar to that by Kohler et al. [45]. The Cell-GMA was to be used as the starting material for the work in Chapter 5 and so it was required that it be soluble in organic solvents, with DMF being one of the more desirable solvents. The results of these reactions are summarized in Table 3.2. In the first two reactions (samples GMA1E and GMA2E), 6.0 GMA monomer units were added per cellulose hydroxyl. In the first 45 minutes of stirring at room temperature, no observable change was noticed. After 50 minutes, the solution quickly became very hot and began changing in colour from a golden brown to a dark red. After 80 minutes stirring had ceased due to the increased viscosity and the reaction was stopped. It was found that precipitation in water, methanol, or acetone was impossible but the use of acetonitrile or chloroform resulted in excellent precipitation provided a large excess was used (~10 times by volume). Once separated, the product could only be re-dissolved in

water. Due to the observed high reactivity and exothermic behaviour of the reaction, the ratio of GMA used in subsequent reactions was decreased which helped mitigate rapid increases in temperature.

Table 3.2: Summary of reaction conditions for synthesis of Cell-GMA in EMIM AcO.

Sample	GMA:OH	Mass Cellulose (g)	Temp.	Reaction time (h)	Result
GMA1E	6.0	0.20	Ambient	2	DS = 0.85
GMA2E	6.0	0.20	Ambient	1.3	DS = 1.80
GMA3E	1.2	0.20	Ambient	2.6	DS = 0.54
GMA4E	0.5	0.75	Ambient	20.5	DS = 1.52
GMA5E	0.5	0.60	Ambient	18	DS = 1.05
GMA6E	1.0	0.50	Ice bath	20	DS = 1.24

Analysis through HSQC NMR of sample GMA5E (Figure 3.5) revealed the desired methacrylate presence, as well as the propyl group that linked it to the cellulose, but also showed peaks that did not correspond to the desired functionality. The signal marked ‘a’ in Figure 3.5 is attributed to the alkene protons. However, this is substantially downfield of the values obtained of samples of other cellulose-methacrylate materials in acetone (see Figure 3.8 and Figure 3.12), and it is uncertain whether D_2O would cause the signal to shift this much. The equivalent unsaturated protons of the imidazolium ring would appear in this approximate region and this could possibly be contaminating the sample; the inequivalent unsaturated proton on the imidazolium ring should then appear at ~9-10 ppm in the proton spectrum, but no signals appear above 7.5 ppm. The circle directly above the AGU protons contains the protons attributed to the propyl group in glycidyl methacrylate after the epoxide has opened; the presence of more peaks than the expected three may be due to isomerization. The methyl group appears at ‘b’. The signals that appear in the circle labeled ‘f’ do not correspond to any groups in the desired product.

The signal that appears at {2.1, 20 ppm} may be due to acetate groups; it has been seen previously in this chapter (section 3.3.1.1) that the acetate anions of EMIM AcO can attach to cellulose under certain conditions. However, the major source of this signal is speculated to be methylene groups formed by polymerization of methacrylate groups. The spectrum is complicated, though, and other side reactions should not be ruled out.

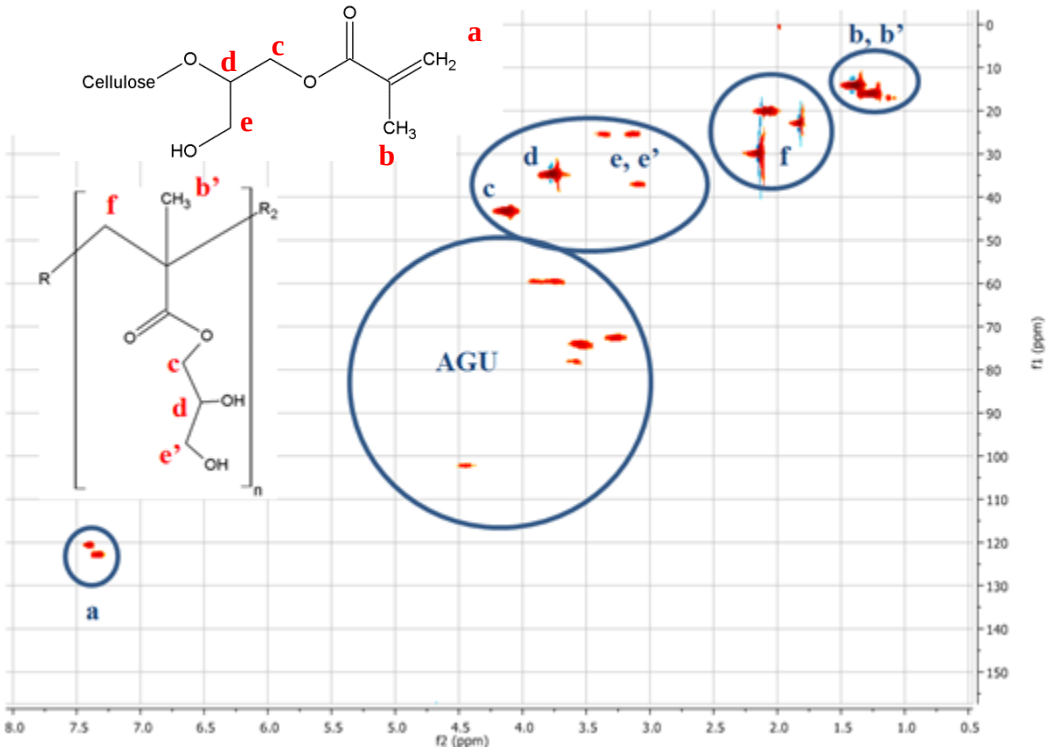

Figure 3.5: HSQC Spectrum of Cell-GMA (sample GMA5E) recorded in D_2O. It appears that some autopolymerization of the monomer may have occurred.

^{1}H NMR spectra of the samples are presented in Figure 3.6. These spectra show the same general peak patterns, but the region 1.75 – 2.25 ppm in each spectrum (where no peaks are expected to be in the desired product) show different peaks and peak intensities among samples. The rest of the regions are similar amongst the spectra. This suggests that side reactions were

taking place, and that they were not necessarily happening in the same way or to the same extent in each sample.

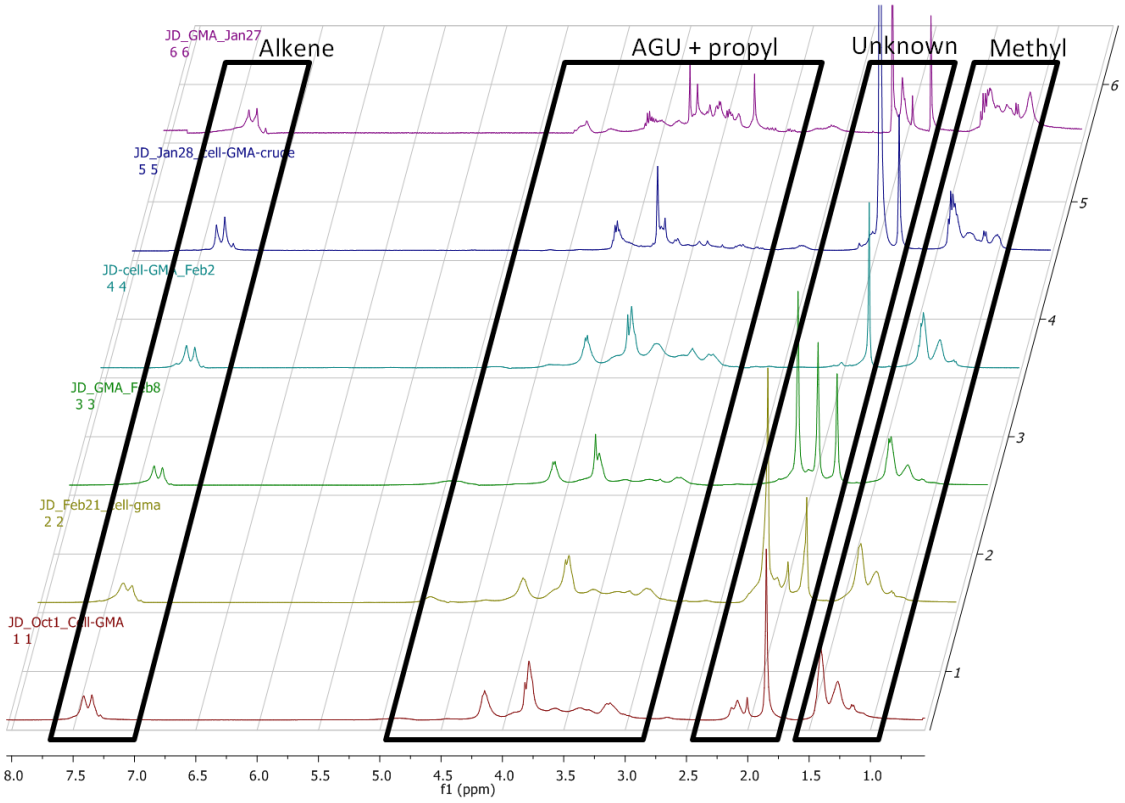

Figure 3.6: ^{1}H NMR spectra of Cell-GMA samples recorded in D_2O.

Molecular weight distributions for samples GMA5E and GMA6E were obtained on an aqueous Viscotek GPC (Figure 3.7). In both distributions, a sharp peak appears at 1,100 g/mol with a broader peak appearing at higher molecular weight. The higher molecular weight peak corresponds to the main cellulose chain. It is not clear whether the low molecular weight peak is a degradation product, homopolymer of GMA, or something else. Since this peak is identical in molecular weight and distribution for each sample it is unlikely to be homopolymer. When comparing the distributions to that of Cell-BiB prepared previously in this chapter (Figure 3.3), the molecular weights of the Cell-GMA samples are substantially lower; Cell-BiB has an M_p of

100,000 g/mol, while GMA5E has an M_p of only 16,000 g/mol and GMA6E has an even lower M_p of 3,200 g/mol. The molecular weights measured for GMA5E and GMA6E are only relative to PEO and are not absolute values, but the difference when compared to Cell-BiB and even between the two samples is stark enough that it can be concluded that the cellulose was being severely degraded during the reaction.

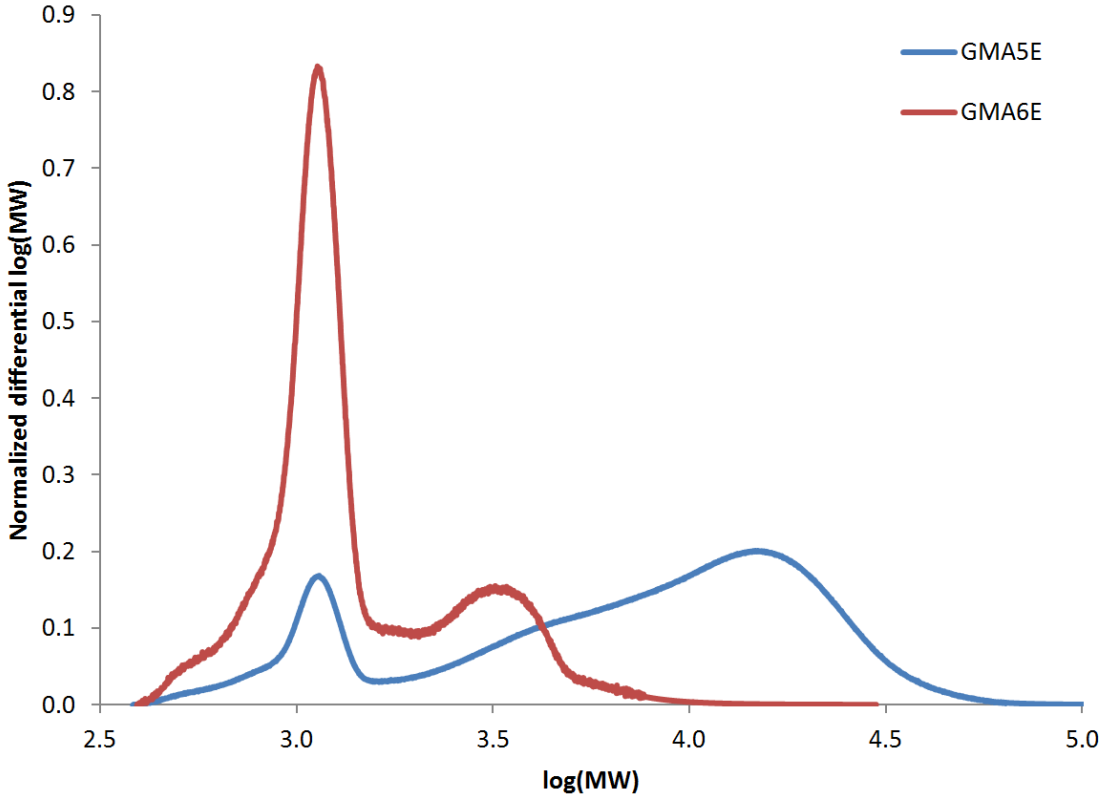

Figure 3.7: Molecular weight distributions of Cell-GMA (relative to PEO standards).

It is apparent that while the reaction proceeded readily and imparted methacrylate functionality, it also had problems of side reactions taking place which decrease the efficiency of the reaction and impart non-functional material to the cellulose. In addition, GPC traces show that the cellulose was experiencing significant degradation during the reaction. There may be

ways to mitigate these difficulties, but it was not deemed fruitful to further pursue this reaction route as the Cell-GMA produced was water-soluble rather than organic-soluble.

3.3.2 Modification of cellulose acetate in cyclic ethers

3.3.2.1 Etherification of cellulose acetate with glycidyl methacrylate

In order to ensure a hydrophobic product with good solubility in organic solvents, cellulose acetate with a DS of about 2.8 was used as the starting material. A variety of reaction conditions were attempted in the solvents THF and (1,4)-dioxane which are summarized in Table 3.3. The reaction was first attempted using Cell-$AcO_{2.79}$ in THF at $30^{O}C$ (entry GMA1T in Table 3.3). This was successful, with an alkene signal clearly present in ^{1}H NMR (Figure 3.9; assignment in acetone-d_6: δ = 5.5, 6.0 ppm, alkene; δ = 3.6, 4.0, 4.1 ppm, propyl; δ = 1.8 ppm, methyl signal hidden behind acetate signal) although the degree of substitution was only 0.09 (out of a theoretical 0.21). In an attempt to increase the DS, the temperature and stoichiometry of the reaction were increased (GMA2T, Figure 3.9) and the reaction was allowed to proceed for a longer period of time. This resulted in a DS of 0.98, which was substantially higher than the theoretical 0.21. While it is possible that there may have been some unreacted monomer still bound to the cellulose after purification, this value of DS was too large for that to be the primary cause as unreacted monomer would have to be about 40% of the mass of the solid. Instead, it is hypothesized that transesterification was occurring between the acetate groups on the cellulose and the methacrylate groups on the GMA. It has been noted in the literature that GMA can react with dextran in DMSO via a transesterification reaction rather than the expected ring-opening of the epoxide [44]. For both GMA1T and GMA2T, the obtained Cell-AcO-GMA exhibited a greatly reduced solubility in THF as compared to the starting Cell-AcO, with solid and gel material being observed in the reactor prior to stopping the reaction.

The HSQC spectrum for GMA2T is given in Figure 3.8 and aids in assignment of the proton spectrum. The spectrum is complicated which makes identification of each individual peak difficult but the general peak patterns are identified. The characteristic circular patterns of the AGU protons of cellulose acetate are clearly visible in the centre of the spectrum, as are the acetate protons at {1.8 ppm, 20 ppm}. The propyl group of GMA once its ring has opened consists of methylene and methine groups bonded to oxygen atoms similar to the AGU groups, and so the signals from these protons overlap the signals from the AGU protons. The alkene functionality is clearly seen by a pair of peaks located at a carbon shift of 125 ppm. The corresponding methyl signal almost overlaps the acetate signal but has a slightly lower carbon shift of 17 ppm. The low proton-shift signals (<1.0 ppm) are suspected to be methyl groups shifting upfield due to loss of alkene functionality.

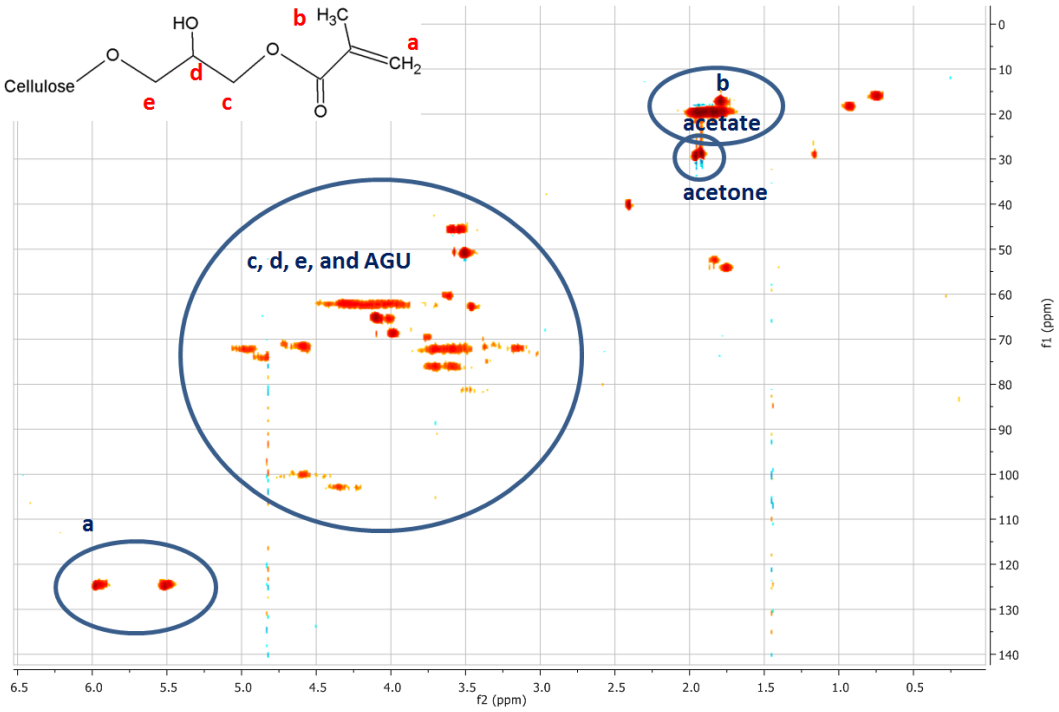

Figure 3.8: HSQC spectrum of GMA2T in acetone-d_6.

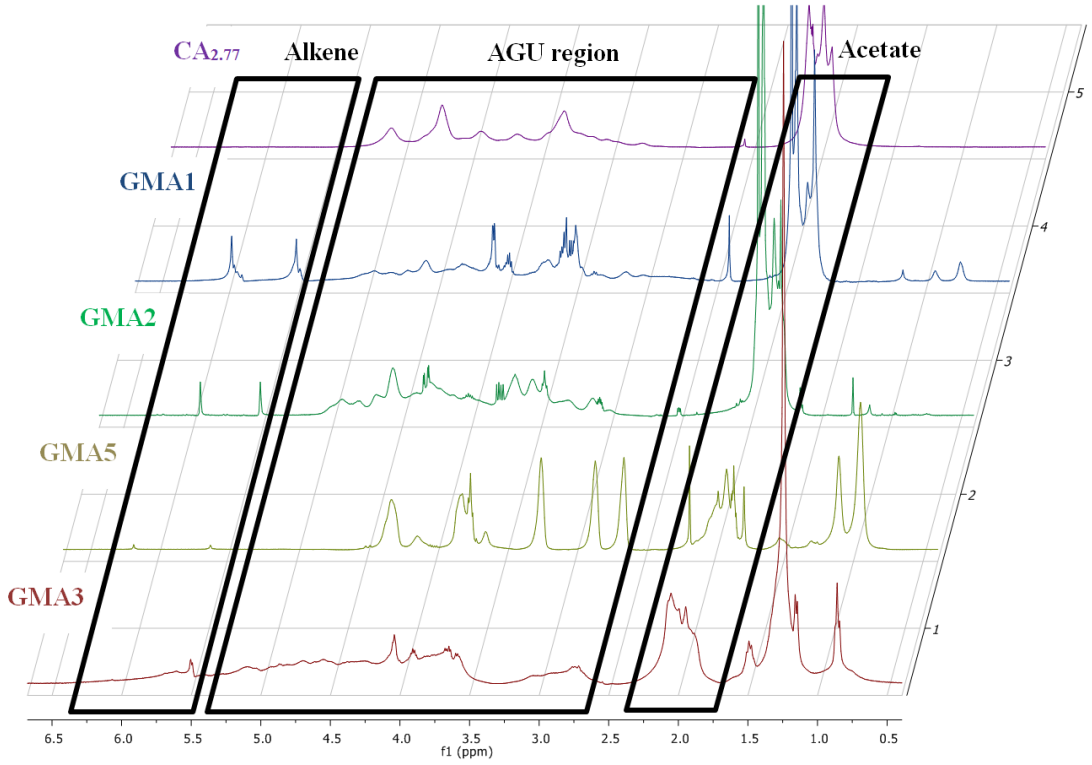

Figure 3.9: ^{1}H NMR Spectra of GMA reactions carried out in THF. GMA3T recorded in DMSO-d_6 (solvent signal 2.50 ppm, water 3.33 ppm; both signals suppressed); GMA5T recorded in $CDCl_3$; all others recorded in acetone-d_6 (solvent signal 2.05 ppm, water 2.84 ppm; water signal suppressed).

Subsequent reactions in THF experienced the problem of autopolymerization of the monomer occurring, even at the relatively mild temperature of 50^{O}C. This was observed by excessive mass of polymer, changes in solubility, lack of alkene functionality, and methyl peaks shifting upfield in the proton NMR spectra (Figure 3.9). The reaction was exothermic which may have caused uncontrolled temperature rises in the reactor and subsequent polymerization even though the monomer was inhibited. The reactions were first performed using Cell-$AcO_{2.79}$ synthesized in the laboratory, but concerns over batch-to-batch variability in this material led to commercially obtained $CA_{2.77}$ being used instead. However, while two of the reactions with Cell-$AcO_{2.79}$ were successful (GMA1T and GMA2T), both of the reactions using $CA_{2.77}$ (GMA4T and GMA5T) led to autopolymerization of the monomer, as well as a third reaction with Cell-$AcO_{2.79}$

(GMA3T). Autopolymerization was confirmed for GMA3T and GMA5T through NMR, with minimal alkene signal being observed and the methyl signal shifting to the 0.8 – 1.5 ppm; the polymer peaks were significantly more pronounced for GMA5T than GMA3T due to the higher ratio of GMA to cellulose used. In the case of GMA4T, attempts to precipitate it in water were unsuccessful and the polymer was not recovered. As Cell-AcO-GMA was insoluble in water, the solubility in this case was attributed to the polymerization of GMA and followed by the hydrolysis of the epoxide, making a water-soluble polymer. In addition, THF is susceptible to ring-opening polymerization in acidic conditions and could have copolymerized with the epoxide functionality of the GMA, contributing to the poor reproducibility in the experiments [46]. The DS of alkene groups would be altered depending upon the type of polymerization that could occur: whether radical polymerization of the methacrylate groups or ring-opening of the epoxide.

Table 3.3: Reaction conditions for etherification of cellulose acetate with glycidyl methacrylate.

ID	GMA:OH	Mass CA (g)	Solvent	T (^{O}C)	Reaction time (h)	Result
GMA1T	6	0.50^{+}	THF	30	22	DS = 0.09
GMA2T	100	0.24^{+}	THF	50	23, 46	DS = 0.74, 0.98
GMA3T	4	0.30^{+}	THF	50	22	Autopolymerization
GMA4T	4	0.1	THF	50	24	Autopolymerization
GMA5T	120	0.1	THF	50	24	Autopolymerization
GMA1D	27	1.5	Dioxane	30	35	DS = 0.01
GMA2D	4	1.15^{+}	Dioxane	40	4	DS = 0.02
GMA3D	4	2.5	Dioxane	40	19	No reaction
GMA4D	4	2.5	Dioxane	50	22	No reaction
GMA5D	4	0.73^{+}	Dioxane*	50	20	No reaction

(*uses TEA as base catalyst rather than HCl; +uses Cell-$AcO_{2.79}$ rather than $CA_{2.77}$)

(1-4)-Dioxane was tried as the solvent for the reaction as it is a cyclic ether similar to THF, but unlike THF will readily dissolve both Cell-AcO and Cell-AcO-GMA (in general, dioxane was found to dissolve a much wider range of the cellulose derivatives discussed in this chapter than THF could), but under a variety of reaction conditions little or no change was

observed. For samples GMA1D and GMA2D a low alkene functionality (DS = 0.01, 0.02; Table 3.3) was found, but for all other reactions no change was observed in the NMR spectra (see Figure 3.10 for examples of the spectra). However, even the low degree of substitution obtained with GMA1D and GMA2D led to the samples being poorly soluble in THF, making analysis on a THF GPC unfeasible. It is not known why the reaction in dioxane was less reactive than in THF.

Concerns with the difficulties encountered in controlling the etherification reaction and the degree of substitution of methacrylate groups led to esterification reactions being considered instead.

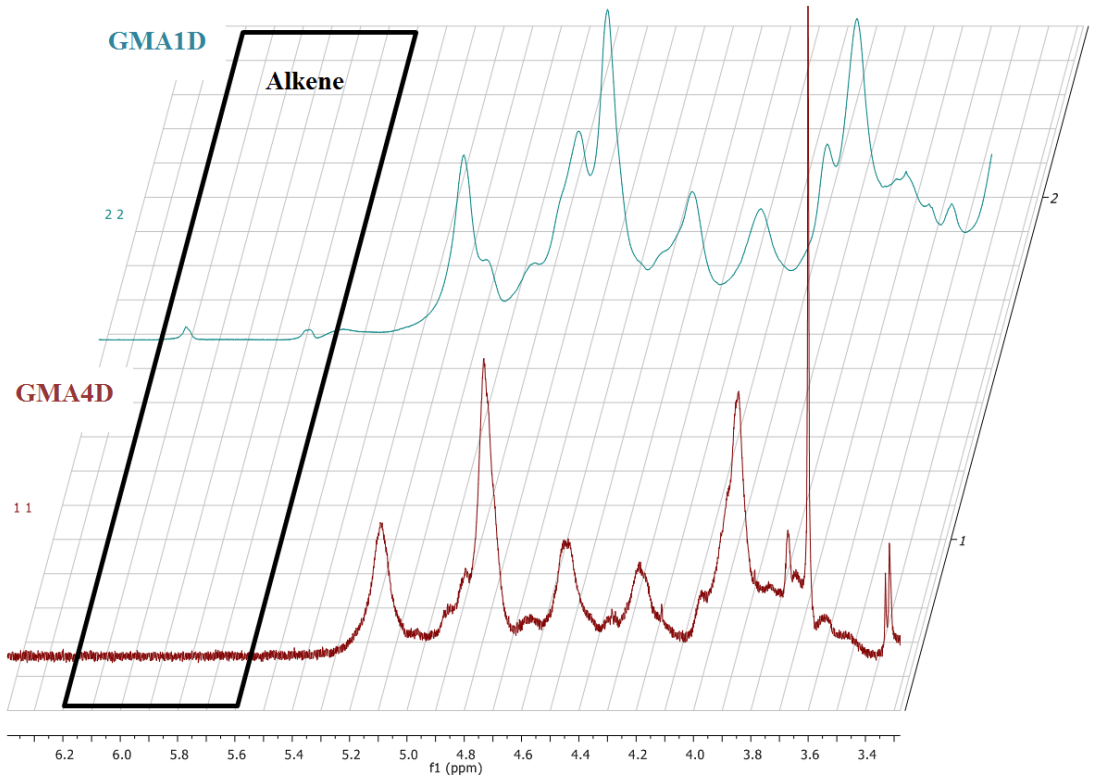

Figure 3.10: ^{1}H NMR spectra of CA-GMA samples prepared in (1,4)-dioxane and recorded in acetone-d_6. Minimal alkene functionality is observed.

3.3.2.2 Steglich esterification of cellulose acetate with methacrylic acid

Steglich esterification was examined as an alternative route to give cellulose methacrylate functionality with the reactions summarized in Table 3.4. The use of DCC with 3-10 mol%

DMAP allows the esterification of carboxylic acids in high yields, including sterically demanding esters, at mild conditions while limiting side reactions [47]. Mild conditions are desirable in order to prevent the autopolymerization of methacrylate observed when using GMA, as well as to prevent degradation of the cellulose. The reaction is presented in Scheme 3.4. The reaction was first attempted using a small stoichiometric excess of reagents in an ice bath but only limited esterification was observed (DS = 0.02, MAA1T) and the mixture remained in a single phase throughout the reaction. The ice bath was used because the reaction was exothermic and there was concern about the vessel overheating. However, the diluteness of the cellulose solution and the low concentration of hydroxyls present should prevent an excessive amount of heat being released. In addition, esterification reactions are sensitive to water and the hygroscopic cellulose solvents are difficult to keep dry, which can hamper high yields when stoichiometric proportions of reactants are used. Subsequently, the reaction was performed successfully at room temperature using a larger (6.8 fold) excess of MAA and DCC, with a precipitate being immediately formed and the reaction vessel becoming moderately warmer than ambient. The CA-MAA possessed similar solubility properties to the unmodified cellulose acetate, being readily soluble in acetone, THF, dioxane, DMSO, and DMF.

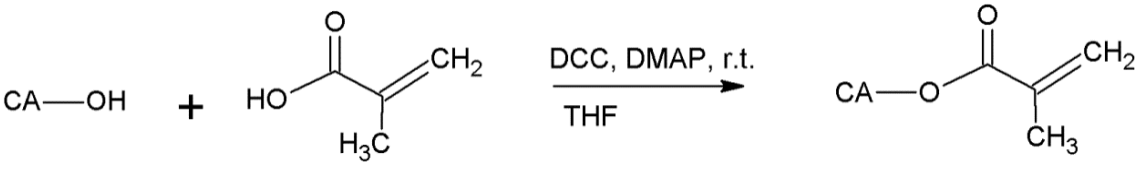

Scheme 3.4: Steglich esterification of cellulose acetate with methacrylic acid.

Table 3.4: Summary of reaction conditions for esterification of $CA_{2.77}$ with MAA.

Sample	MAA:OH	Mass $CA_{2.77}$ (g)	Solvent	Temperature	Result
MAA1T^{+}	1.8	2.5	THF	Ice bath	DS=0.02
MAA2T^{+}	6.8	1.25	THF	Ambient	DS=0.29
MAA3T^{++}	6.9	0.50	THF	Ambient, increase to 50^{0}C	DS=0.13
MAA4T^{+}	6.8	2.4	THF	Ambient	DS=0.28

(+ uses 4.8 wt/vol% cellulose/THF; ++ uses 8.3 wt/vol% cellulose/THF)

NMR spectra were recorded in acetone-d_6; the HSQC spectrum for sample MAA4T is given in Figure 3.11. In contrast to the other methods that were attempted in order to provide methacrylate functionality, this method yielded a relatively clean and easy to identify spectrum. The alkene and AGU protons can both be seen clearly separated from each other. The methyl signals from the acetate and methacrylate groups overlap on the proton axis, but are separated from each other on the carbon axis, allowing both groups to be visible in the HSQC spectrum, but not the proton spectrum (Figure 3.12).

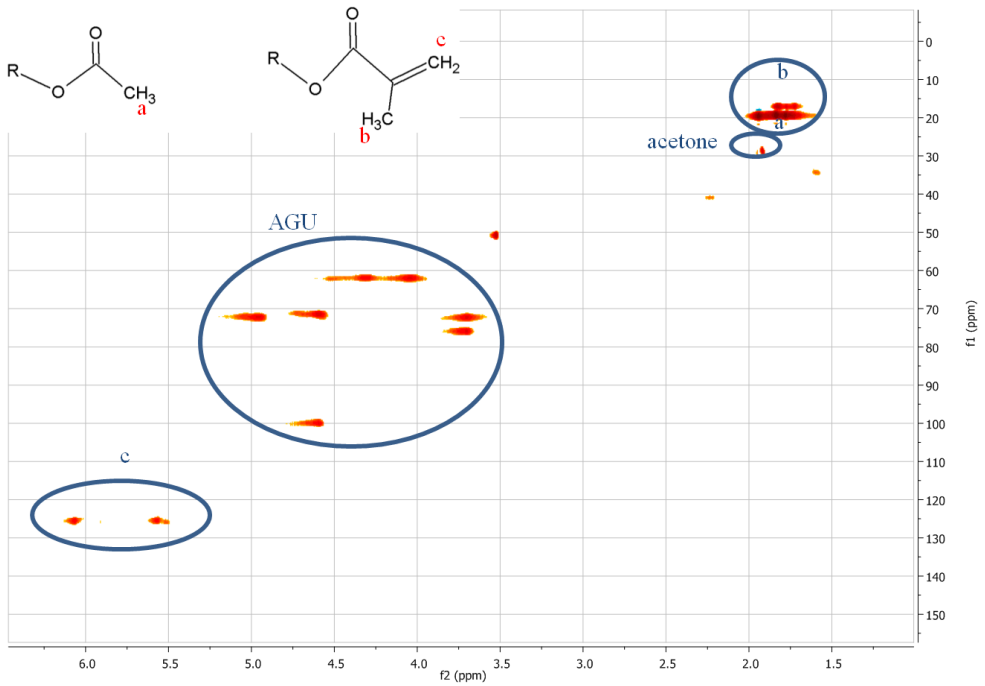

Figure 3.11: HSQC spectrum of MAA4T (CA-$MAA_{0.28}$) recorded in acetone-d_6.

Both samples MAA2T and MAA4T had degrees of substitution higher than the theoretical value of 0.21. When observing the ^{1}H NMR spectra for these samples (Figure 3.12), as well as MAA3T, it can be seen that the alkene peaks are not present as a clean pair, but that there appears to be smaller peaks doubling the main peaks. This would indicate that there are alkene groups present that are chemically dissimilar, and that there may remain unreacted methacrylic acid bound to the product despite the vigorous washings undertaken. The presence of bound monomer could limit the yields of grafting reactions if a sub-stoichiometric amount of thiol is used.

The standard reaction conditions used a 4.8 wt/v% solution of cellulose in THF and allowed a DS_{alkene} of 0.29 to be reached; using a more concentrated 8.3% solution resulted in a much more viscous solution and a final DS_{alkene} of only 0.13. When using the more concentrated solution, the temperature was increased to 50^{O}C after mixing the reactants in order to decrease the viscosity and improve mixing. The intermediate compound formed between the methacrylic acid and the DCC is temperature sensitive, and Steglich esterification is typically carried out below ambient temperature in order to avoid unwanted products [47]. It is likely that the elevated temperature reduced the yield of the reaction for this sample.

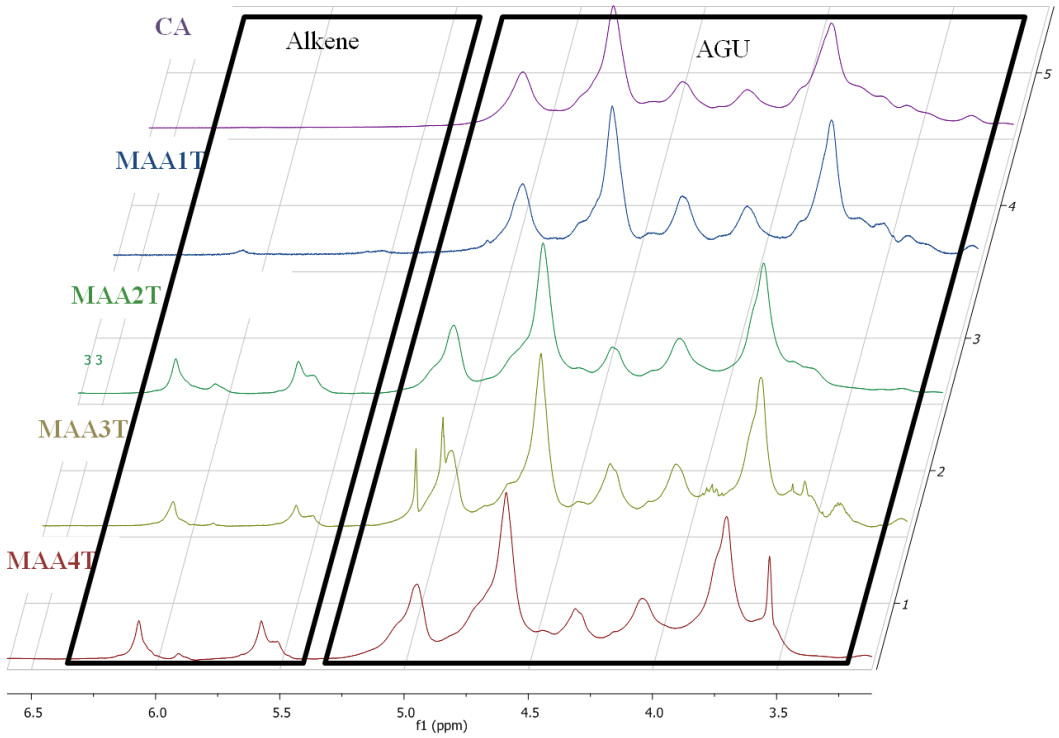

Figure 3.12: ^{1}H NMR spectra of CA-MAA samples. Substantial alkene functionality is observed.

GPC was used in order to compare the elution profiles of the samples MAA3T and MAA4T before and after esterification. Since the amount of methacrylate functionality imparted was low, CA-MAA was expected to have a similar molecular weight distribution to CA. If the molecular weight increased substantially it would likely be due to crosslinking of the methacrylate groups (particularly if the distribution broadens), while a decrease in molecular weight would indicate degradation of the cellulose chain. The molecular weight distributions were recorded on the Viscotek GPC with triple detection and are displayed in Figure 3.13. The curves for unmodified cellulose acetate and sample MAA3T were very similar, with only a small change in M_n and M_P observed. The triple detection system has a greater error associated with molecular weight measurements than using a calibration curve, but it allows for analysis of samples with unknown Mark-Houwink parameters and unknown dn/dc. In particular, the

columns had poorer resolution in the low molecular weight region (<10^4 g/mol), and so the differences observed were not considered significant. Sample MAA4T had a higher M_n and a slightly higher M_P than the cellulose acetate. Since the high molecular weight shoulder did not change, this may be due to lower molecular weight polymer being washed out during the purification procedures (yields of these reactions were low, suggesting polymer was lost during purification). An M_N of 24,000 g/mol was measured for the unmodified cellulose acetate: Sigma-Aldrich specifies that it should be about 30,000 g/mol.

The lack of increase in either high or low molecular weight tailings indicated that the integrity of the cellulose acetate was being preserved throughout the reaction. As such, these samples (MAA3T and MAA4T) were used for the grafting reactions in Chapter 5.

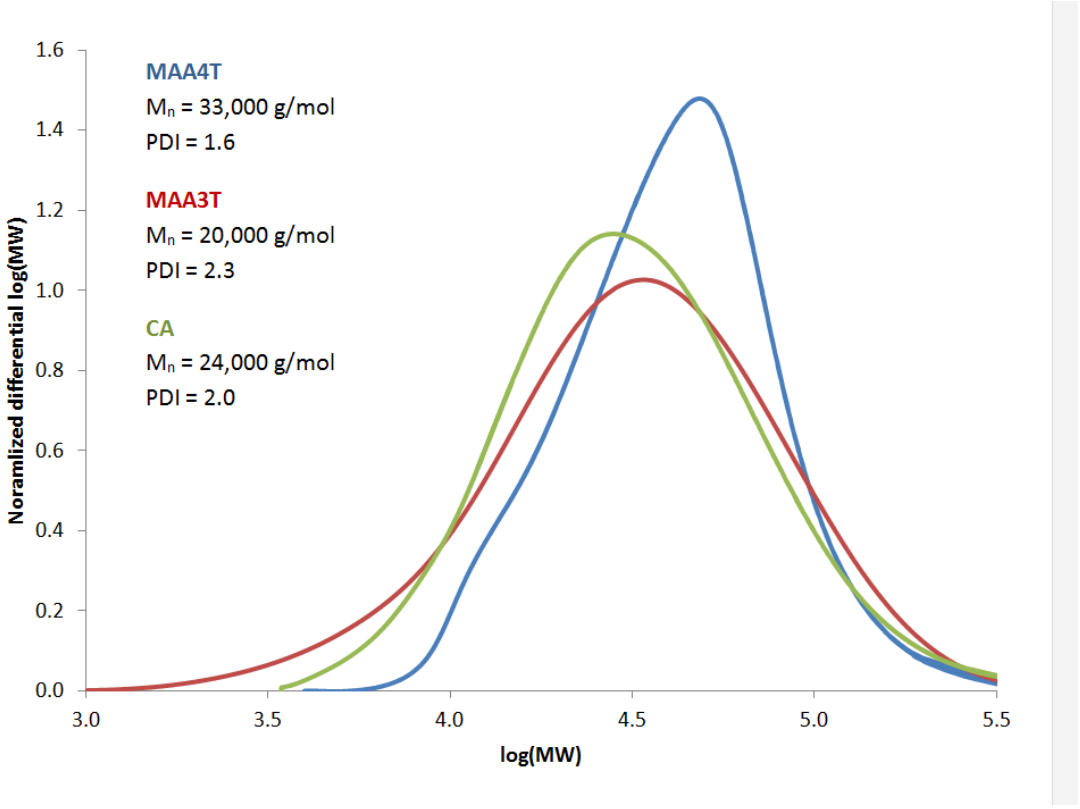

Figure 3.13: Molecular weight distributions of CA and CA-MAA (MAA3T and MAA4T) recorded in THF using a triple detection system**.** Sigma-Aldrich specifies an M_n of about 30,000 g/mol for the CA.

3.4 Conclusions and recommendations

3.4.1 Conclusions

It was found that EMIM AcO was unsuitable for esterification reactions due to the acetate anions of the solvent attaching to the cellulose. Reactions with acyl halides resulted in the formation of cellulose triacetate rather than the desired cellulose ester. Carrying out the reactions in BMIM Cl instead resulted in the formation of the desired product, such as the Cell-$BiB_{1.13}$ that was used in Chapter 4. The reactions using methacryloyl chloride had mixed results; this was attributed to the high moisture content of the solvent. It is expected that the reaction would be successful if the solvent was drier. BMIM Cl may not be an appropriate solvent, however, as the elevated temperatures may promote polymerization of the methacrylate groups. When attempting to attach gylcidyl methacrylate to cellulose in EMIM AcO, polymerization of the monomer was observed through NMR and significant degradation of the cellulose was observed through GPC. This was likely due to the exothermic reaction that caused uncontrolled temperature increases in the reactor, and the high viscosity of the solution which hindered heat transfer. Since the product was soluble in water rather than organic solvents the reaction was not pursued.

The reactions of cellulose acetate and glycidyl methacrylate in tetrahydrofuran were difficult to control: autopolymerization was a major problem. In (1-4)-dioxane, however, very little reaction was observed resulting in extremely low alkene functionality. Esterification of cellulose acetate with methacrylic acid using DCC resulted in a highly functional product with favourable solubility characteristics without degradation or side reactions occurring. This Cell-MAA was used extensively in Chapter 5.

3.4.2 Recommendations and future work

- The use of non-ionic liquid solvent systems such as DMAc/LiCl should be examined. The difficulties encountered here by both EMIM AcO and BMIM Cl suggests that other solvents would be more effective.

- Cellulose acetate with a lower degree of substitution should be examined in order to allow greater numbers of functional groups to be attached (due to the greater availability of free hydroxyl sites).

3.5 Acknowledgements

The author would like to thank the financial support provided by the Ontario Ministry of Environment (Best in Science Program), by the Ontario Ministry of Research Innovation (Early Researcher Award Program, Dr. Pascale Champagne), by the Government of Ontario (Ontario Research Chair in Green Chemistry and Engineering, Dr. Michael F. Cunningham), and by Queen's University. The author also thanks Ms. Oxana Zaskoka for performing GPC analysis on some of the samples and for preparing samples to be mailed to Guelph Chemical Laboratories.

3.6 References

[1] T. Heinze and T. Liebert, "Unconventional methods in cellulose functionalization," *Progress in Polymer Science*, vol. 26, no. 9, pp. 1689-1762, 2001.

[2] H. Steinmeier, "3. Acetate Manufacturing, Process and Technology 3.1 Chemistry of Cellulose Acetylation," *Macromolecular Symposia*, vol. 208, no. 1, pp. 49-60, 2004.

[3] A. El-Kafrawy, "Investigation of the cellulose/LiCl/dimethylacetamide and cellulose/LiCl/N-methyl-2-pyrrolidinone solutions by 13-C NMR spectroscopy," *Journal of Applied Polymer Science*, vol. 27, no. 7, pp. 2435-2443, 1982.

[4] V. Raus, M. Stepanek, M. Uchman, M. Slouf, P. Latalova, E. Cadova, M. Netopilik, J. Kriz, J. Dybal and P. Vleck, "Cellulose-based graft copolymers with controlled architecture prepared in a homogeneous phase," *Polymer Chemistry*, vol. 49, no. 20, pp. 4353-4367, 2011.

[5] M. S. Hiltunen, J. Raula and S. L. Maunu, "Tailoring of water-soluble cellulose-g-copolymers in homogeneous medium using single-electron-transfer living radical polymerization," *Polymer International*, vol. 60, no. 9, pp. 1370-1379, 2011.

[6] M. Hiltunen, J. Siirila and S. L. M. Maunu, "Effect of catalyst systems and reaction conditions on the synthesis of cellulose-g-PDMAam copolymers by controlled radical polymerization," *Polymer Chemistry*, vol. 50 no. 15, pp. 3067-3076, 2012.

[7] B. Tosh, C. N. Saikia and N. N. Dass, "Homogeneous esterification of cellulose in the lithium chloride - N,N-dimethylacetamide solvent system: effect of temperature and catalyst," *Carbohydrate Research,* vol. 327, no. 3, pp. 345-352, 200.

[8] K. Negishi, Y. Mashiko, E. Yamashita, A. Otsuka and T. Hasegawa, "Cellulose chemistry meets click chemistry: syntheses and properties of cellulose-based glycocluster with high structural homogeneity," *Polymers,* vol. 3, no. 1, pp. 489-508, 2011.

[9] T. Heinze, M. Schobitz, M. Pohl and F. Meister, "Interactions of ionic liquids with polysaccharides. IV. Dendronization of 6-azido-6-deoxy cellulose," *Journal of Polymer Science: Part A: Polymer Chemistry,* vol. 46, no. 11, pp. 3853-3859, 2008.

[10] J. Zhang, X.-D. Xu, D.-Q. Wu, X.-Z. Zhang and R.-X. Zhuo, "Synthesis of thermosensitive P(NIPAAam-co-HEMA)/cellulose hydrogels via 'click' chemistry," *Carbohydrate Polymers,* vol. 77, no. 11, pp. 583-589, 2009.

[11] T. Heinze, R. Dicke, A. Koschella, A. H. Kull, E.-A. Klohr and W. Koch, "Effective preparation of cellulose derivatives in a new simple cellulose solvent," *Macromolecular Chemistry and Physics,* vol. 201, no. 6, pp. 627-631, 2000.

[12] S. Kohler and T. Heinze, "New solvents for cellulose: dimethyl sulfoxide/ammonium fluorides," *Macromolecular Bioscience,* vol. 7, no. 3, pp. 307-314, 2007.

[13] C.-x. Lin, H.-y. Zhan, M.-h. Liu, S.-y. Fu and L.-h. Huang, "Rapid homogeneous preparation of cellulose graft copolymer in BMIMCL under microwave irradiation," *Journal of Applied Polymer Science,* vol. 118, no. 1, pp. 399-404, 2010.

[14] Y. Hao, J. Peng, J. Li, M. Zhai and G. Wei, "An ionic liquid as reaction media for eadiation-induced grafting of thermosensitive poly (N-isopopylacrylamide) onto microcrsytalline cellulose," *Carbohydrate Polymers,* vol. 77, no. 4, pp. 779-784, 2009.

[15] C.-x. Lin, H.-y. Zhan, M.-h. Liu, S.-y. Fu and L. A. Lucia, "Novel preparation and characterization of cellulose microparticles functionalized in ionic liquid," *Langmuir,* vol. 25, no. 17, pp. 10116-10120, 2009.

[16] L. Chun-xiang, Z. Huai-yu, L. Ming-hua, F. Shi-yu and Z. Jia-jun, "Preparation of cellulose graft poly(methyl methacrylate) copolymers by atom transfer radical polymerization in an ionic liquid," *Carbohydrate Polymers,* vol. 78, no. 3, pp. 432-438, 2009.

[17] R. Rinaldi, R. Palkovits and F. Schuth, "Depolymerization of cellulose using solid catalysts in ionic liquids," *Angewandte Chemie International Edition,* vol. 47, no. 42, pp. 8047-8050, 2008.

[18] T. Heinze, K. Schwikal and S. Barthel, "Ionic liquids as reaction medium in cellulose functionalization," *Macromolecular Bioscience,* vol. 5, no. 6, pp. 520-525, 2005.

[19] S. Barthel and T. Heinze, "Acylation and carbanilation of cellulose in ionic liquids," *Green Chemistry,* vol. 8, no. 3, pp. 301-306, 2006.

[20] J. Wu, J. Zhang, H. Zhang, J. He, Q. Ren and M. Guo, "Homogeneous acetylation of cellulose in a new ionic liquid," *Biomacromolecules,* vol. 5, no. 2, pp. 266-268, 2004.

[21] Y. Cao, J. Wu, T. Meng, J. Zhang, J. He, H. Li and Y. Zhang, "Acetone-soluble cellulose acetates prepared by one-step homogeneous acetylation of cornhusk cellulose in an ionic liquid 1-allyl-3-methylimidazolium chloride (AmimCl)," *Carbohydrate Polymers,* vol. 69, no. 4, pp. 665-672, 2007.

[22] C. Yan, J. Zhang, Y. Lv, J. Yu, J. Wu, J. Zhang and J. He, "Thermoplastic cellulose-graft-poly(L-lactide) copolymers homogeneously synthesized in an ionic liquid with 4-dimethylaminopyridine catalyst," *Biomacromolecules,* vol. 10, no. 8, pp. 2013-2018, 2009.

[23] T. Meng, X. Gao, J. Zhang, J. Yuan, Y. Zhang and J. He, "Graft copoloymers prepared by atom transfer radical polymerization (ATRP) from cellulose," *Polymer,* vol. 50, no. 2, pp. 447-454, 2009.

[24] X. Sui, J. Yuan, M. Zhou, J. Zhang, H. Yang, W. Yuan, Y. Wei and C. Pan, "Synthesis of cellulose-graft-poly(N,N-dimethylamino-2-ethyl methacryalte copolymers via homogeneous ATRP and their aggregates in homogeneous media," *Biomacromolecules,* vol. 9, no. 10, pp. 2615-2620, 2008.

[25] Y. Cao, J. Zhang, J. He, H. Li and Y. Zhang, "Homogeneous acetylation of cellulose at relatively high concentrations in an ionic liquid," *Chinese Journal of Chemical Engineering,* vol. 18, no. 3, pp. 515-522, 2010.

[26] S. Kohler, T. Liebert, M. Schobitz, J. Schaller, F. Meister, W. Gunther and T. Heinze, "Interactions of ionic liquids with polysaccharides 1. Unexpected acetylation of cellulose with 1-ethyl-3-methylimidazolium acetate," *Macromolecular Rapid Communications,* vol. 28, no. 24, pp. 2311-2317, 2007.

[27] K. Shill, S. Padmanabhan, Q. Xin, J. M. Prausnitz, D. S. Clark and H. W. Blanch, "Ionic liquid pretreatment of cellulosic biomass: enzymatic hydrolysis and ionic liquid recycle," *Biotechnology and Bioengineering,* vol. 108, no. 3, pp. 511-520, 2011.

[28] D. C. Dibble, C. Li, L. Sun, A. George, A. Cheng, O. P. Cetinkol, P. Benke, B. M. Holmes, S. Singh and B. A. Simmons, "A facile method for the recovery of ionic liquid and lignin from biomass pretreatment," *Green Chemistry,* vol. 13, no. 11, pp. 3255-3264, 2011.

[29] P. Y. Bruice, Organic Chemistry, 5th ed., Toronto: Pearson Education Canada, Inc., 2007.

[30] R. M. Silverstein, F. X. Webster and D. J. Kiemle, Spectrometric Identification of Organic Compounds, 7th ed., Hoboken, NJ: John Wiley & Sons, Inc., 2005.

[31] L. Patiny, "nmrdb.org: Database of NMR Spectra," Ecole Polytechnique Fédérale de Lausanne, [Online]. Available: http://www.nmrdb.org/. [Accessed January 2013].

[32] R. Sescousse, K. A. Le, M. E. Ries and T. Budtova, "Viscosity of cellulose - imidazolium-based ionic liquid solutions," *Journal of Physical Chemistry B,* vol. 114, no. 21, pp. 7222-7228, 2010.

[33] J. Vitz, T. Erdmenger, C. Haensch and U. S. Schubert, "Extended dissolution studies of cellulose in imidazolium based ionic liquids," *Green Chemistry,* vol. 11, no. 3, pp. 417-424, 2009.

[34] D. Fu, G. Mazza and Y. Tamaki, "Lignin extraction from straw by ionic liquids and enzymatic hydrolysis of the cellulosic residues," *Journal of Agricultural and Food Chemistry,* vol. 58, no. 4, pp. 2915-2922, 2010.

[35] M. Shobitz, F. Meister and T. Heinze, "Unconventional reactivity of cellulose dissolved in ionic liquids," *Macromolecular Symposia,* vol. 280, no. 1, pp. 102-111, 2009.

[36] T. Liebert and T. Heinze, "Interaction of ionic liquids with polysaccharides 5. Solvents and reaction media for the modification of cellulose," *Bioresources,* vol. 3, no. 2, pp. 576-601, 2008.

[37] B. A. P. Ass, E. Frollini and T. Heinze, "Studies on the homogeneous acetylation of cellulose in the novel solvent dimethyl sulfoxide/tetrabutylammonium fluoride trihydrate," *Macromolecular Bioscience,* vol. 4, no. 11, pp. 1008-1013, 2004.

[38] W. Mormann, "Silyation of cellulose with hexamethyldisilazane in ammonia - activation, catalysis, mechanism, properties," *Cellulose,* vol. 10, no. 3, pp. 271-281, 2003.

[39] A. Nada and M. L. Hassan, "Thermal behavior of cellulose and some cellulose derivatives," *Polymer Degradation and Stability,* vol. 67, no. 1, pp. 111-115, 2000.

[40] S. Zhao, W. Zhang, F. Zhang and B. Li, "Determination of Hansen solubility parameters for cellulose acrylate by inverse gas chromatography," *Polymer Bulletin,* vol. 61, no. 1m pp. 189-196, 2008.

[41] E. Marsano, L. De Paz, E. Tambuscio and E. Bianchi, "Cellulose methacrylate: synthesis and liquid crystalline behaviour of solutions and gels," *Polymer,* vol. 39, no. 18, pp. 4289-4294, 1998.

[42] R. Steele, "The reactivity of some epoxides toward cellulose," *Textile Research Journal,* pp. 257-262, 1961.

[43] N. Flores-Ramirez, E. Elizalde-Pena, S. R. Vasquez-Garcia, J. Gonzalez-Hernandez, A. Martinez-Ruvalcaba, I. C. Sanchez, G. Luna-Barcenas and R. B. Gupta, "Characterization and degradation of functionalized chitosan with glycidyl methacrylate," *Journal of Biomaterials Science, Polymer Edition,* vol. 16, no. 4, pp. 473-488, 2005.

[44] W. van Dijk-Wolthius, J. Kettenes-van den Bosch, A. van der Kerk-van Hoof and W. Hennink, "Reaction of dextran with glycidyl methacrylate: an unexpected transesterification," *Macromolecules,* vol. 30, no. 11, pp. 3411-3413, 1997.

[45] S. Kohler, T. Liebert, T. Heinze , A. Vollmer, P. Mischinck, E. Mollmann and W. Becker, "Interactions of ionic liquids with polysaccharides 9. Hydroxyalkylation of cellulose without additional inorganic bases," *Cellulose,* vol. 17, no. 2, pp. 437-448, 2010.

[46] B.A. Rosenburg, E.B. Ludvig, A.R. Gantmahker, and S.S. Medvedev, "The mechanism of polymerization of tetrahydrofuran," *Journal of Polymer Science: Part C,* vol. 16, no. 4, pp. 1917-1929, 1967.

[47] B. Neises and W. Steglich, "Simple method for the esterification of carboxylic acids," *Angewandte Chemie International Edition,* vol. 17, no. 7 pp. 522-524, 1978.

Chapter 4

Synthesis of Cellulose Graft Copolymers Using Cu(0)-Mediated Polymerization and a 'Grafting-From' Approach

Abstract

The 'grafting-from' approach has been utilized for the synthesis of cellulose graft copolymers, often in conjunction with controlled radical polymerization techniques. Atom Transfer Radical Polymerization (ATRP) with Cu(I) as catalyst is one of the most common methods, but as the cellulose derivatives tend to be soluble in highly polar solvents the use of Single Electron Transfer (SET) with Cu(0) is increasing in frequency. However, little effort has been made to compare the kinetics of the grafting polymerization to that of homopolymerization. Understanding this behaviour would allow better reaction design through the use of easier to characterize homopolymers as models.

The grafting of poly(methyl acrylate) (PMA) and poly(methyl methacrylate) (PMMA) was undertaken using Cu(0)-mediated polymerization with a cellulose macroinitiator (Cell-BiB) in DMSO. The polymerization rate of PMA from Cell-BiB was about 60% to 70% that obtained using a standard ATRP initiator (EBiB) under similar conditions. An average graft density of 0.71 grafts per glucose ring was obtained; this may have been limited due to steric reasons as the initiation efficiency for Cell-BiB was lower than EBiB. The rate using MMA was initially similar between the two initiators but increased with time for EBiB but not Cell-BiB. This appears to have been caused by slow initiation of the BiB groups, which limited the graft density for Cell-g-PMMA to 0.15 grafts per glucose ring. The grafted chains were cleaved from the cellulose using acid-catalyzed transesterification with methanol. The reaction was very sensitive to the solvent conditions used, and using basic conditions resulted in degradation due to irreversible hydrolysis.

4.1 Introduction

In the synthesis of cellulose graft copolymers using a 'grafting-from' approach, initiation sites are formed on the cellulose backbone and polymer chains are grown outward from these sites. Polymerizations have been reported using both conventional free radical [1, 2] and controlled radical polymerization mechanisms [3]. In theory, using a controlled 'grafting-from' mechanism should allow for a well-tailored, controlled growth of polymer and high density of grafted chains, but in practice problems have been encountered with bimolecular termination of growing chains on different cellulose molecules [4-8], poor initiation efficiency [4, 9], and difficulties in characterizing the side chains and final copolymer [6, 7].

It has been discovered that the use of Cu(0) as a catalyst in highly polar solvents with acrylic monomers results in a well-controlled and very fast polymerization [10]. The authors called this 'Single Electron Transfer Living Radical Polymerization' (SET-LRP), but there is debate in the literature over whether SET-LRP has the same mechanism as ATRP [11, 12] or a different mechanism [10, 13, 14]. In any case, as the cellulose macroinitiators are highly polar and soluble in polar solvents such as DMSO and DMF, Cu(0)-mediated polymerization was seen as a suitable choice for the 'grafting-from' reaction with acrylic monomers, and beginning in 2010 it began to be used for the grafting reaction from cellulose [4, 8, 15], as well as the related biopolymers hemicellulose [16, 17] and dextran [18].

Raus et al. [4] experienced poorer rates and initiation efficiencies when using an SET type reaction (Cu(0) as catalyst) as opposed to ATRP (Cu(I) as catalyst), while Hiltunen et al. [8] successfully polymerized N,N-dimethylacrylamide from cellulose using Cu(I) as catalyst but were unsuccessful when using Cu(0). However, it is not clear to what extent these results were due to the grafting reaction itself as opposed to the conditions used for polymerization; it would clearly be beneficial in designing reactions to know whether the graft copolymerization will behave in a similar fashion to a linear (i.e. non-branched) homopolymerization in terms of kinetics and degree of control, and whether the homopolymerization is capable of successful

results under the conditions used. Furthermore, it would be desirable to first design a successful reaction using inexpensive and ubiquitous commercial initiators prior to attempting the grafting. This is especially pertinent as the cellulose macroinitiators typically have limited solubility, restricting the choice of solvents and the concentration of initiating sites to conditions that have not necessarily been previously examined for the polymerization technique utilized. While grafting from cellulose using a controlled radical polymerization has been widely reported, few papers provide a comparison between the graft copolymerization and homopolymerization using an analogous non-polymeric initiator. Billy et al. [19] used a linear homopolymerization as a model in order to design a successful reaction for ATRP grafting of methyl diethylene glycol methacrylate from cellulose acetate in their desired solvent, cyclopentanone; however, the concentration of initiating sites used for the model homopolymerization was approximately 10^3 times greater for the homopolymerization than for the grafting and so the reactions are not directly comparable. Dupayage et al. [18] studied ATRP grafting of methyl methacrylate from dextran in DMSO and found that while the dextran macroinitiator protected with acetate groups behaved similarly to EBiB during polymerizations, unprotected dextran had a much faster polymerization rate and problems with gelation.

This research was conducted in order to investigate whether the cellulose macroinitiator (Cell-BiB) behaves in a similar fashion during Cu(0)-mediated polymerization as an analogous non-polymeric initiator (EBiB) in terms of rate, initiation efficiency, and molecular weight control, or whether the presence of the cellulose and the graft architecture has a retarding effect on the reaction rate and control.

4.2 Experimental

4.2.1 Materials

Avicel© microcrystalline cellulose (MCC, ~50 μm), Copper (II) bromide (98%), α-bromoisobutyryl bromide (BrBiB, 98%), 1-ethyl-3-methylimidazolium acetate (EMIM AcO, ≥90%), ethyl α-bromoisobutyrate (EBiB, 98%), tris[2-(dimethylamino)ethyl]amine (Me_6TREN), and anhydrous dimethylsulfoxide (DMSO, 99.8%) were purchased from Sigma-Aldrich and used without further modification. Copper electrical wiring (14 gauge) was stripped of insulation, submerged in sulfuric acid, and rinsed with acetone prior to immediate use. Tetrahydrofuran (THF) was distilled and dried with magnesium sulfate prior to use. Methyl methacrylate (MMA) and methyl acrylate (MA) were obtained from Sigma-Aldrich, passed through a column to remove inhibitor, and stored in the refrigerator prior to use. All other solvents were used as received. The cellulose macroinitiators Cell-$AcO_{2.99}$-$BiB_{0.089}$ and Cell-$BiB_{1,13}$ were synthesized as described in Chapter 3.

4.2.2 Experimental procedure

4.2.2.1 Polymerization of MMA from Cell-$AcO_{2.91}$-$BiB_{0.089}$ in EMIM AcO

To 5 mL of EMIM AcO was added 0.153 g of Cell-$AcO_{2.91}$-$BiB_{0.089}$ (46 μmol of bromine, 1 eq.). A stirring magnet wrapped with 10 cm of copper wire was introduced and the mixture was stirred at 70^{O}C for 27 hours, at which point the temperature was reduced to 50^{O}C and the solution sparged with nitrogen. After 30 minutes, 60 μL (4.9 eq.) of Me_6TREN was added followed by 5 mL of MMA (1020 eq.). The reaction was left overnight and the mixture solidified. The polymer was separated from the EMIM AcO by dissolving the mixture in THF and precipitating in water three times. The polymer was then dissolved in THF again and passed through a column of basic aluminum oxide. Solvent was evaporated under air and the polymer

sample was dried in a vacuum oven for 24 hours (70^{O}C, -20 inHg) prior to analysis by GPC and NMR.

4.2.2.2 Polymerization from EBiB and Cell-BiB$_{1.13}$ in DMSO

In a typical polymerization, 10 cm of copper wire (cut into four pieces) was added to a round-bottom flask along with a stirring magnet. The flask was placed in a 50^{O}C oil bath and purged with nitrogen for at least 15 minutes to remove oxygen. Simultaneously, bottles of DMSO, MA, and a stock solution of EBiB in DMSO (12 µL/mL) or Cell-BiB$_{1.13}$ in DMSO (21.1 mg/mL) were degassed by sparging with nitrogen for at least 45 minutes. A stock solution of $CuBr_2$ in acetonitrile (ACN) was prepared in advance (60.7 mg/mL). If $CuBr_2$ was used in the reaction (as an added deactivator to improve livingness) it was injected into the flask during the degassing step (38 µL, 2.3 mg $CuBr_2$, 0.05 eq.). Following the degassing, 2.5 mL of MA (134 eq.) along with 11 µL of Me_6TREN (0.2 eq.) were injected into the flask. The reaction was started by injecting 2.5 mL of the EBiB/DMSO solution (30 µL EBiB, 200 µmol, 1 eq) or 2.4 mL of the Cell-BiB solution (0.051 mg Cell-BiB, 250 µmol of Br, 0.71 eq). Samples were withdrawn at periodic intervals and diluted with chloroform-d, shaken to dissolve oxygen, and stored in the freezer (-20^{O}C) prior to NMR analysis for conversion. Similar procedures were used for polymerization of MMA.

4.2.2.3 Chain extension of Cell-g-PMA

The Cell-g-PMA (sample G-PMA-1B, 50 mg, estimated 5.1 µmol of Br, 1 eq.) was dissolved in 5 mL DMSO, 5 cm of copper wire (cut into two pieces) was added, and the flask was sparged with nitrogen for 45 minutes in a 30^{O}C oil bath. To start the reaction, 50 µL of Me_6TREN/DMSO stock solution (0.27 µL Me_6TREN, 0.2 eq.) and 0.58 mL of degassed MA (1285 eq.) were injected into the reactor. Samples were withdrawn at periodic intervals and

diluted with chloroform-d, shaken to dissolve oxygen, and stored in the freezer (-20^{O}C) prior to NMR analysis for conversion.

4.2.2.4 Cleaving of grafted chains by selective transesterification

In a typical procedure, 50 mg of copolymer was dissolved in 5 mL of dry THF and sparged with nitrogen for 15 minutes. After degassing, 0.5 mL of a 2 N sulfuric acid/methanol solution was added (for a final concentration of 0.2 N sulfuric acid) and the reactor was placed in a 60^{O}C oil bath. After 6 hours a sample was withdrawn, filtered through basic aluminum oxide, and diluted with THF prior to GPC analysis.

4.2.3 Characterization

4.2.3.1 Nuclear Magnetic Resonance (NMR)

^{1}H NMR spectroscopy (64 scans) was used to identify the samples and to predict conversion. Spectra were obtained on a 400 MHz Bruker Avance instrument. Conversion was determined by comparing the area of the alkene protons of the monomer (approximately 5.0 ppm and 5.5 ppm) to the area of the methoxy protons belonging to the monomer and polymer (approximately 2.9 ppm and 2.8 ppm) Spectra were assigned using information from [21], [22], and [23].

4.2.3.2 Gel Permeation Chromatography (GPC)

The NMR samples used for conversion analysis were diluted with acetone, passed through basic aluminum oxide to remove the dissolved copper, and evaporated to dryness. The samples were then stored in a vacuum oven (50^{O}C, -20 inHg) for 24 hours in order to further remove solvent. The dry samples were dissolved in distilled THF to a concentration of

approximately 5-10 mg/mL. After dissolution the samples were passed through 0.2 μm (for homopolymer) or 0.45 μm (graft copolymer) nylon syringe filters into sample vials.

The homopolymer samples of PMA and PMMA were analyzed on a Waters 2695 separations module using a model 410 differential refractometer as detector. Five Waters Styragel HR columns (guard, HR 4.0, HR 3.0, HR 1.0, HR 0.5) were used in series at a temperature of 40 ^{0}C. Distilled THF was used as the eluent at a flow rate of 1.0 mL/min. The system was calibrated using poly(styrene) standards with narrow molecular weights ranging from 374 to 400 x 10^3 g/mol. The molecular weights obtained using the poly(styrene) calibration were corrected using the Mark-Houwink parameters summarized in Table 4.1. The correction can be made through the use of the Mark-Houwink equation (Equation 4-1).

$$[\eta] = K(MW)^{\alpha} \qquad \textbf{Equation 4-1}$$

Table 4.1: Summary of Mark-Houwink parameters.

Polymer	T (^{0}C)	Molecular Weight for Measurements (g/mole)	K/10^{-3} (mL/g)	α	Ref.
PS	30	-	11.4	0.716	[30]
PMA	30	<20,000	6.11	0.799	[31]
PMMA	30	100,000	9.44	0.719	[32]

The copolymers were analyzed using a Viscotek GPCmax VE-2001 with a model VE 3580 refractive index (RI) detector, and a model 270 dual detector [light scattering (low angle light scattering, LALS, and right angle light scattering, RALS), and viscosity (IV)]. Three PolyAnalytik columns (2 x PAS-106, guard) with an exclusion molecular weight of 20 x 10^6 g/mol were used in series at a temperature of 40 ^{0}C. Distilled THF was used as the eluent at 1.0 mL/min. The triple detection system was calibrated using a narrow poly(styrene) sample of 93 x 10^3 g/mol, with refractive index increment (dn/dc) of 0.185 mL/g and intrinsic viscosity ([η]) of 0.465 dL/g. The molecular weight analysis was performed using the Viscotek OmniSEC

software which estimated the molecular weight, refractive index increment, Mark-Houwink parameters, and the intrinsic viscosity of the polymer samples. It is important that the concentration of these samples be accurately known for these calculations.

4.3 Results and discussion

4.3.1 Polymerization of MMA from Cell-$AcO_{2.91}$-$BiB_{0.089}$ in EMIM AcO

Ionic liquids have been used for copper catalyzed controlled radical polymerizations: the ionic liquid 1-butyl-3-methylimidazolium hexafluorophosphate has been found to improve the rate and livingness of the Cu_2O/2,2'-bipyridine catalyst system with MMA [26], and in general ionic liquids have been found to increase propagation rate while decreasing termination rate for radical polymerizations [27]. In addition, the high polarity of ionic liquids allow excellent disproportionation of Cu(I) species to Cu(0) and Cu(II) for SET [10]. The grafting reaction was first attempted in the original solvent for the Cell-BiB synthesis, EMIM AcO. The reaction was conducted assuming a DS of bromine of 1.6 from NMR: this value was subsequently revised to 0.089 upon bromine analysis by ion chromatography for reasons discussed in Chapter 3, and the ratios of reactants reported here reflect this new value.

While cellulose dissolved readily in EMIM AcO at room temperature, the Cell-$AcO_{2.91}$-$BiB_{0.089}$ did not and elevated temperatures ($70^{O}C$) and long dissolution times (27 hours) were required in order to obtain a homogeneous solution. In addition to this, the MMA was immiscible in the EMIM AcO, and so the reaction was run overnight as a dispersed phase reaction. After 16 hours the mixture had solidified. Time samples to measure conversion could not be taken due to the phase separation: final conversion was calculated to be 78% by weighing the purified polymer. NMR analysis was undertaken for the final polymer and is displayed in Figure 4.1. Signals attributed to PMMA are clearly visible in the spectrum. There are some signals in the region 3.0 ppm – 5.0 ppm that may be from cellulose anhydroglucose units (AGU)

although it is difficult to be certain as they are broad and ill-defined. As the Cell-$AcO_{2.91}$-$BiB_{0.089}$ was only expected to be about 4% by mass of the final copolymer any signals that would be present would be very weak.

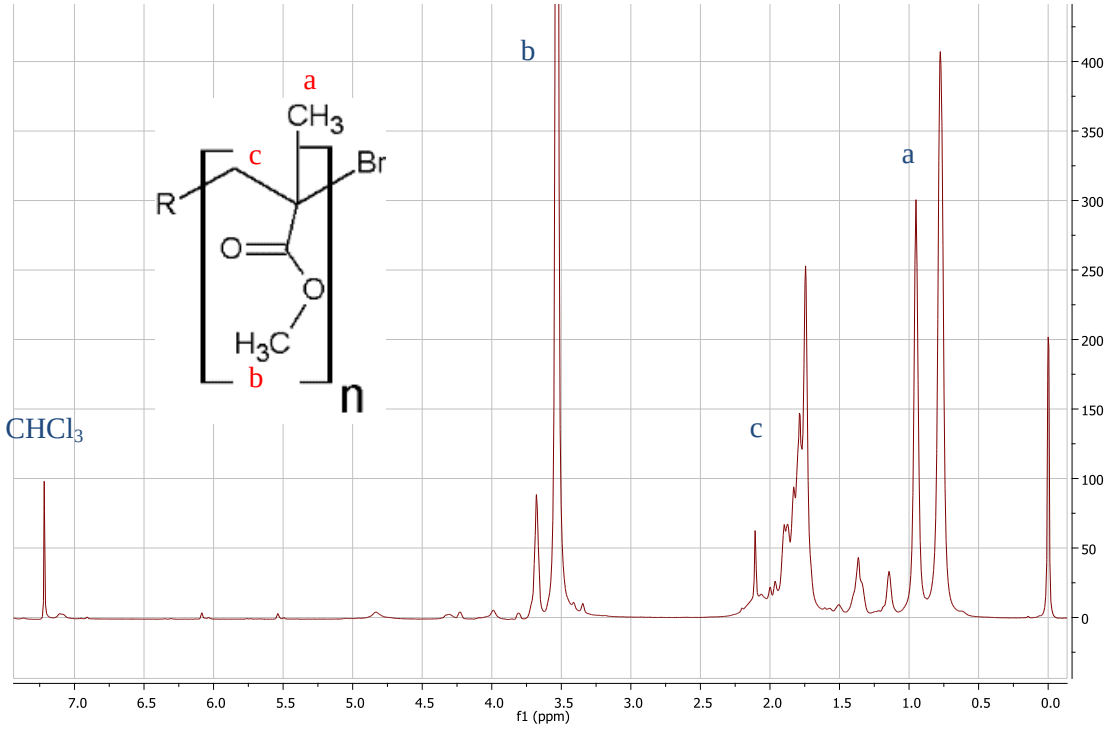

Figure 4.1: ^{1}H NMR spectrum of Cell-g-PMMA synthesized in EMIM AcO. The PMMA signals (a, b, and c) are clearly visible. The signals appearing in region 3.0 ppm – 5.0 ppm may be from cellulose AGU but it is not clear. Alkene signals at 5.5 ppm and 6.0 ppm indicates some residual monomer is present. Spectrum recorded in $CDCl_3$. Reaction conditions: [M]:[L]:[Cu(II)] = 1020 : 4.9 : 0; 50% EMIM AcO by volume; $50^{O}C$.

Molecular weight data was obtained for the copolymer; the data is summarized in Table 4.2 with the molecular weight distributions presented in Figure 4.2. The molecular weight distribution shifts to higher molecular weight after grafting, and the PDI narrows from 3.43 to 2.17. The measured molecular weight of the copolymer is only a little more than half of the predicted value; however, it is possible that the M_n of the Cell-BiB was overestimated due to poor resolution in the low molecular region (see Chapter 3) and this would lead to overestimation of the predicted copolymer molecular weight as well. From the molecular weight data obtained, as

well as the NMR spectrum, it was not clear whether the sample was in fact Cell-g-PMMA or only PMMA homopolymer (which could form if BiB groups were non-covalently bonded to the cellulose). However, intrinsic viscosity ([η]) measurements were also made for the polymer samples, and intrinsic viscosity is known to be substantially lower for branched polymers than linear polymers of the same molecular weight [28]. The Cell-g-PMMA had a measured intrinsic viscosity of 0.683 dL/g: linear homopolymer of PMMA at this value of [η] is calculated to have a viscosity-average molecular weight (M_v) of only 229,000 g/mol using Equation 4-1. This is substantially less than the measured molecular weight of the copolymer which indicates a highly branched polymer rather than linear; this would suggest that grafting had occurred. The polymerization was attempted using EBiB in EMIM AcO without success, which is believed to have been caused by the initiator migrating to the monomer phase rather than remaining in the solvent phase.

Table 4.2: Summary of molecular weight data for polymerization of MMA in EMIM AcO.

Sample	IV (dL/g)	dn/dc (mL/g)	Mark-Houwink α	M_N (kDa)	Predicted M_N (kDa)	PDI
Cell-$AcO_{2.91}$-$BiB_{0.089}$	0.404	0.0435	0.711	32.5	-	3.43
Cell-g-PMMA	0.683	0.0642	0.683	445	811	2.17

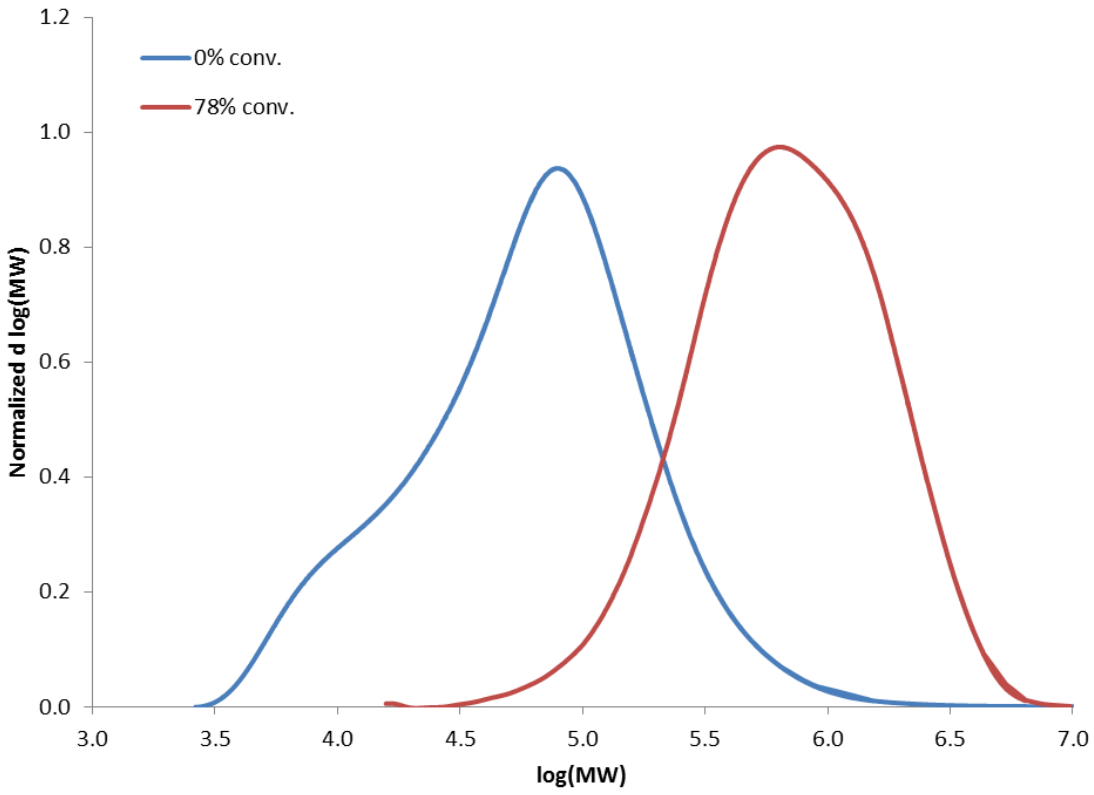

Figure 4.2: Molecular weight distributions of Cell-$AcO_{2.91}$-$BiB_{0.089}$ (**blue**) and Cell-g-PMMA (**red**) grown in EMIM AcO recorded using a triple detection system. Reaction conditions: [M]:[L]:[Cu(II)] = 1020 : 4.9 : 0; 50% EMIM AcO by volume; 50^{O}C.

4.3.2 Polymerization of MA from EBiB in DMSO

Polymerizations in DMSO were first attempted using EBiB in order to model the growth of the grafted polymer chains and optimize the conditions for the grafting, with the reactions summarized in Table 4.3. The graft polymerization was expected to result in a very viscous solution due to the high molecular weights, and there was concern about potential gelling occurring due to combination through intermolecular termination of the radicals. As there are many growing radicals on each cellulose chain, even a small proportion of them combining could cause detrimental crosslinking and gelling to occur. As such, the model homopolymerization was designed in order to mitigate these problems. While Cu(0)-mediated homopolymerizations are often carried out at a low solvent fraction (33%) [10, 14, 29, 30], much higher fractions (50% to

90%) were used here in order to prevent the viscosity from becoming too great. In addition, it has been reported that adding a small amount of Cu(II) at the beginning of a Cu(0)-mediated polymerization (0.05 eq.) allows for higher end-group fidelity of polymer chains than when Cu(0) is used alone [31], and this was also examined as a method to inhibit combination of the copolymers. Polymerization rates have been found to be dependent on the surface area of solid copper available [32], and have also been found to be higher when the solid copper has been activated by removing copper oxide from the surface [14].

Table 4.3: Summary of polymerizations of MA from EBiB in DMSO.

Sample	[M] (vol%)	T (^{O}C)	[M]:[L]:[Cu(II)]	Conv. (%)	K_{app} (min^{-1})	[I] (M)	Pred. M_N (kDa)	Meas. M_N (kDa)	PDI	IE (%)
F-PMA-1A	33	50	140:0.10:0.05	99	0.058	0.027	12.0	41.1	1.28	29
F-PMA-1B	33	50	140:0.10:0	100	0.050	0.027	12.0	36.8	1.33	33
F-PMA-2A	50	50	134:0.20:0	97	0.13	0.040	11.2	10.6	1.17	106
F-PMA-2B	50	50	134:0.20:0	94	0.096	0.040	10.9	12.1	1.15	90
F-PMA-3A	33	30	134:0.20:0.05	77	0.090	0.028	8.93	8.93	1.07	93
F-PMA-3B	33	30	134:0.20:0.05	84	0.098	0.028	9.75	10.3	1.12	95

Figure 4.3 displays the kinetic data of the model polymerizations with EBiB, with each set of conditions duplicated to demonstrate the degree to which they were reproducible. It was seen that only one pair of experiments exhibited significant deviation in rate between each other (red lines in Figure 4.3); it appears that the slow experiment in this pair may have had an induction period, indicating some oxygen was present at the start of the reaction and leading to the variation. Increasing the volume of solvent from 50% to 67% (blue to orange) led to a decrease in rate as expected, but decreasing the temperature from 50^{O}C to 30^{O}C (orange to red) had no significant effect on rate (taking into account that the one experiment was slower due to the induction period). The addition of 0.05 eq. of $CuBr_2$ had no discernible effect on rate (orange squares to orange triangles). The polymerizations were very fast, with even the slowest reaction

reaching 80% conversion after 45 minutes. Furthermore, after only 5 minutes the conversions for the reactions were typically around 40%. All reactions showed a decreasing slope (decreasing rate) up to around 45 minutes, indicating non-first order kinetics, but the two reactions that were allowed to continue to complete conversion displayed a constant slope beyond this point; these two reactions reached a final conversion of 99.2% and 99.5%, respectively.

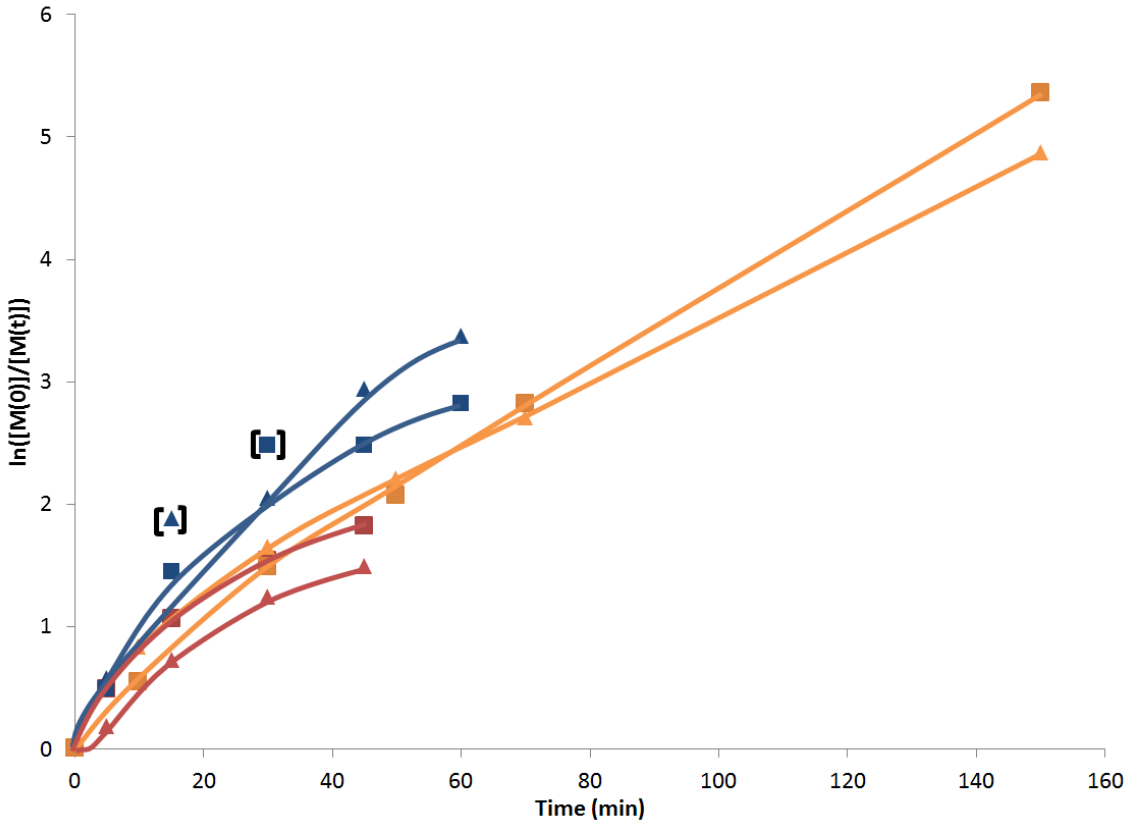

Figure 4.3: Kinetic data for polymerization of MA from EBiB. **Orange Triangles:** Sample F-PMA-1A [M]:[L]:[Cu(II)] = 140:0.1:0.05, 67 vol% DMSO, 50^{O}C; **Orange Squares:** Sample F-PMA-1B, [M]:[L]:[Cu(II)] = 140:0.1:0, 67 vol% DMSO, 50^{O}C; **Blue:** Samples F-PMA-2, [M]:[L]:[Cu(II)] = 134:0.2:0, 50 vol% DMSO, 50^{O}C; **Red:** Samples F-PMA-3, [M]:[L]:[Cu(II)] = 134:0.2:0.05, 67 vol% DMSO, 30^{O}C. No significant effect on rate was observed when increasing temperature from 30^{O}C to 50^{O}C (red to orange). The rate increased as solvent fraction decreased (orange to blue). Lines are drawn to guide the eye.

Since the cellulose macroinitiator was a solid it needed to be dissolved prior to the polymerization, and as it had poor solubility the concentration of the stock solution of Cell-BiB in DMSO was limited when compared to EBiB in DMSO. The initiator stock solutions were made to be about 20-30 mg/mL to ensure the Cell-BiB was well dissolved; this stock solution would then account for anywhere from a third to half of the total reaction volume. As such, a procedure modified from Voepel et al. [16] and Edlund et al. [17] was adopted whereby the Cell-BiB would be dissolved in DMSO, after which the monomer would be added and the contents degassed together by sparging with nitrogen at the reaction temperature. The reaction would be started by addition of the ligand followed by the catalyst. This was first conducted using EBiB instead of Cell-BiB (samples F-PMA-1) with the kinetics displayed in Figure 4.3 and the molecular weight data displayed in Figure 4.4 and Figure 4.5. The reaction was very fast with a narrow polydispersity (<1.3) but had poor initiation efficiency of 29% when $CuBr_2$ was used (Figure 4.4) and 33% when no $CuBr_2$ was used (Figure 4.5). Using $CuBr_2$ resulted in a lower PDI (<1.2) until around 95% conversion when polydispersity began to increase sharply. The obtained initiation efficiencies were substantially less than the >90% values expected according to the literature. It was not clear exactly what was causing the low initiation efficiency but it was suspected to be related to the initiator being in the presence of the monomer during degassing.

The procedure was modified so that the monomer and the initiator/DMSO stock solution would be degassed separately and that the reactor flask containing only the catalyst would be placed in the oil bath and also degassed. The reaction method was again conducted with EBiB, with the order of reagent addition being: monomer, extra DMSO (if needed), ligand, and finally the initiator/DMSO solution to start the reaction. This resulted in much more satisfactory results (F-PMA-2B, Figure 4.6; and F-PMA-3A, Figure 4.7), with initiator efficiencies greater than 90% obtained. In addition, the distributions were narrower without any sign of combination occurring in the distribution until 94% conversion when a high molecular weight hump appeared. All subsequent reactions used this degassing method, and reactions using EBiB obtained initiation

efficiencies in the range of 90% to 106%. From the molecular weight distributions of PMA initiated by EBiB, the polydispersities do not begin to broaden until around ~80% conversion, and so reactions with Cell-BiB were kept well below this conversion.

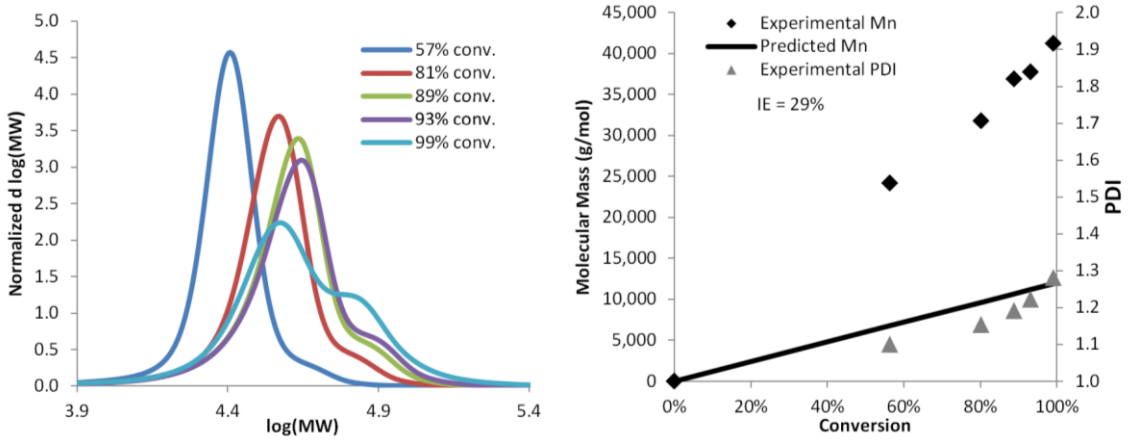

Figure 4.4: Molecular weight data for sample F-PMA-1A: [M]:[L]:[Cu(II)] = 140:0.1:0.05, 67 vol% DMSO, 50^{O}C. Reaction started by adding catalyst.

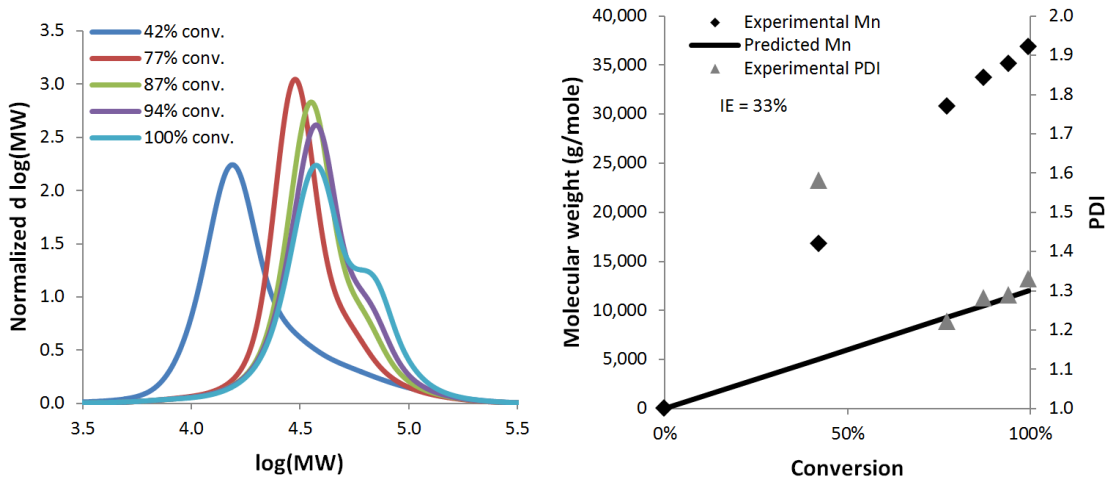

Figure 4.5: Molecular weight data for sample F-PMA-1B: [M]:[L]:[Cu(II)] = 140:0.1:0, 67 vol% DMSO, 50^{O}C. Reaction started by adding catalyst.

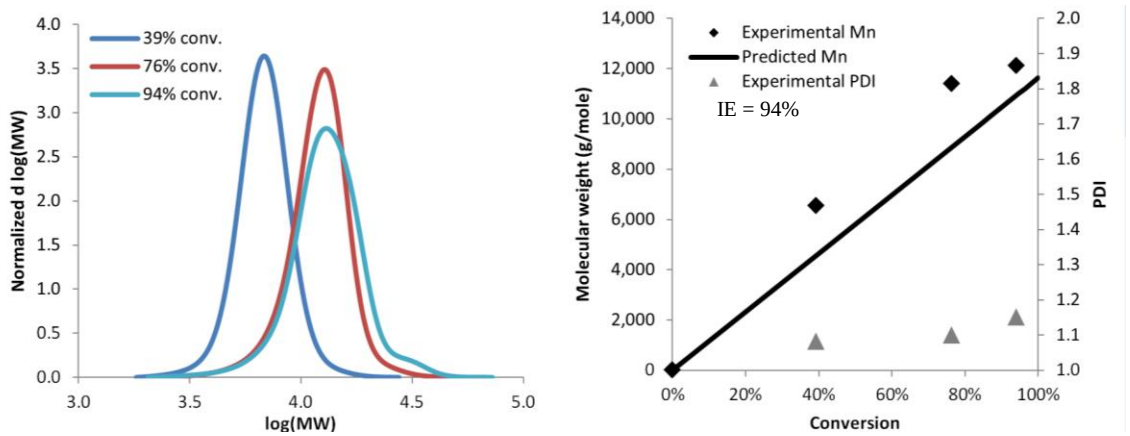

Figure 4.6: Molecular weight data for sample F-PMA-2B, [M]:[L]:[Cu(II)] = 134:0.2:0, 50 vol% DMSO, 50^{O}C. Reaction started by injecting EBiB stock solution.

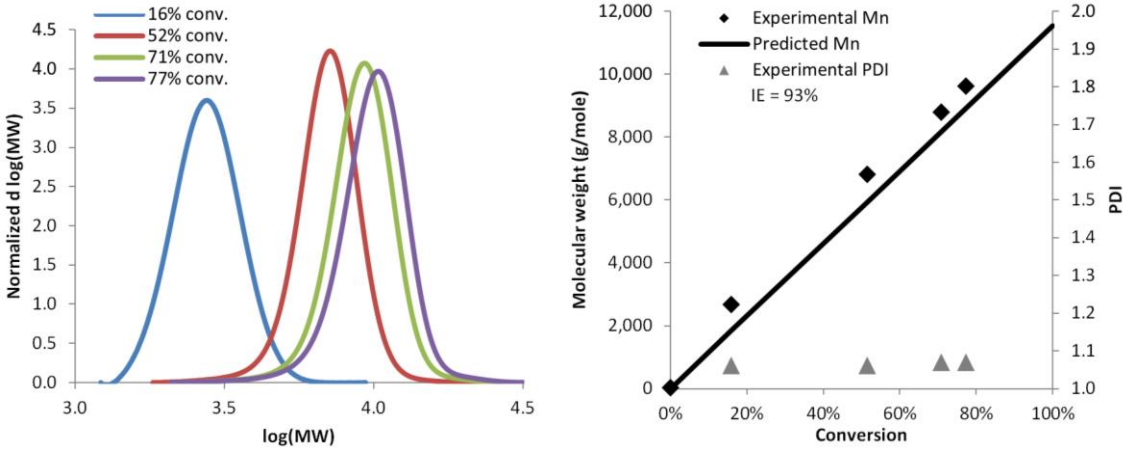

Figure 4.7: Molecular weight data for sample F-PMA-3A, [M]:[L]:[Cu(II)] = 134:0.2:0.05, 67 vol% DMSO, 30^{O}C. Reaction started by injecting EBiB stock solution.

4.3.3 Polymerization of MA from Cell-$AcO_{2.91}$-$BiB_{0.089}$ in DMSO

The graft polymerization from cellulose was first attempted using a macroinitiator synthesized in EMIM AcO (details in Chapter 3). From NMR, the DS_{BiB} was estimated to be 1.6, and so the reaction was attempted using conditions similar to those for F-PMA1. However, as seen in Figure 4.8, this had unsatisfactory results. While the system did result in polymerization, it was at an extremely slow rate. Varying the reaction temperature between 30^{O}C and 70^{O}C did not lead to an improvement. A more thorough analysis of the macroinitiator (discussed

previously in Chapter 3) revealed that the methyl groups identified in NMR were primarily acetate groups rather than the desired BiB groups, and that the DS of BiB groups measured by bromine analysis was only 0.089. This meant that the concentration of initiating sites used was only $1/13^{th}$ of the desired amount – 0.00205 M as opposed to 0.0267 M – and explained the slow rate of polymerization. This also meant that instead of the desired reaction conditions of [Br]:[M]:[L]:[Cu(II)] = 1:140:0.1:(0/0.05), the conditions were actually 1:1811:1.29:(0/0.65). While good results have been obtained using a wide range of ligand concentrations [10], of which 1.29 per initiating group fits comfortably into, the high ratio of Cu(II) to bromine (0.65) could hamper the polymerization due to the lack of a suitable reducing agent and explain the lack of polymerization when $CuBr_2$ was added. The copolymer obtained did not dissolve in DMF or THF so analysis by GPC was impossible, although it would swell substantially in these solvents. The copolymer was not crosslinked (it dissolved completely in chloroform) and therefore NMR was performed on the samples. The ^1H NMR spectrum for the Cell-g-PMA sample synthesized at 50^OC is displayed in Figure 4.9. As the conversion was only 6.8% the cellulose acetate peaks are clearly visible as well as peaks corresponding to PMA, showing that both polymers are present in the mixture. Polymerizations using MMA had no measurable conversion.

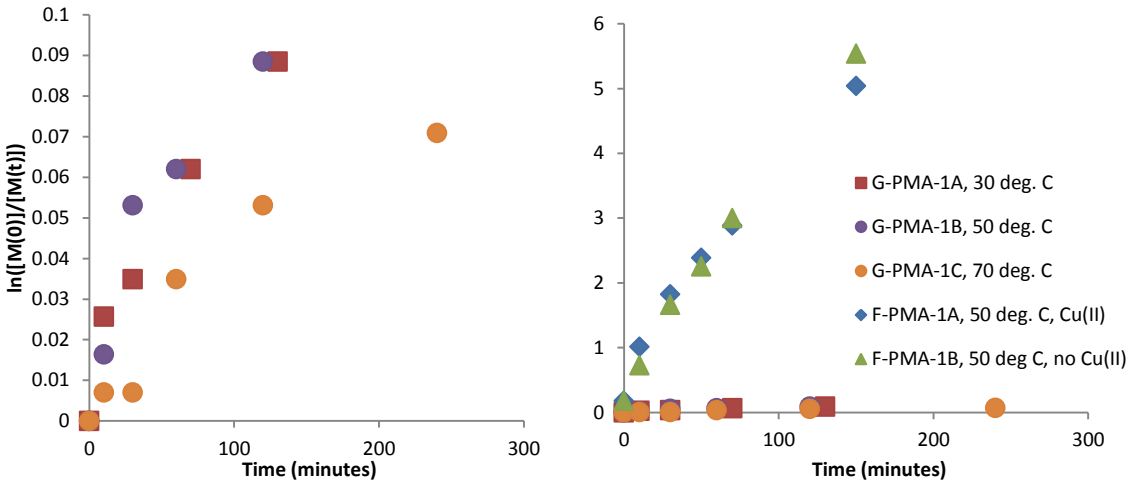

Figure 4.8: Comparing kinetics of polymerization of MA from Cell-$AcO_{2.91}$-$BiB_{0.089}$ and EBiB. Figure on left displays only polymerizations from Cell-$AcO_{2.91}$-$BiB_{0.089}$, while the figure on the right shows both Cell-$AcO_{2.91}$-$BiB_{0.089}$ and EBiB. Reactions using Cell-$AcO_{2.91}$-$BiB_{0.089}$ with added Cu(II) showed no evidence of polymerization and are not displayed here. Reaction conditions for EBiB: [M]:[L]:[Cu(II)] = 140:0.1:(0/0.05); 50% DMSO by volume; 50^{O}C. The reaction was carried out for Cell-$AcO_{2.91}$-$BiB_{0.089}$ under the same conditions as EBiB assuming DS_{BiB} was 1.6: revising these numbers to the new DS_{BiB} of 0.089 leads to conditions of 1560:1.29:(0/0.65).

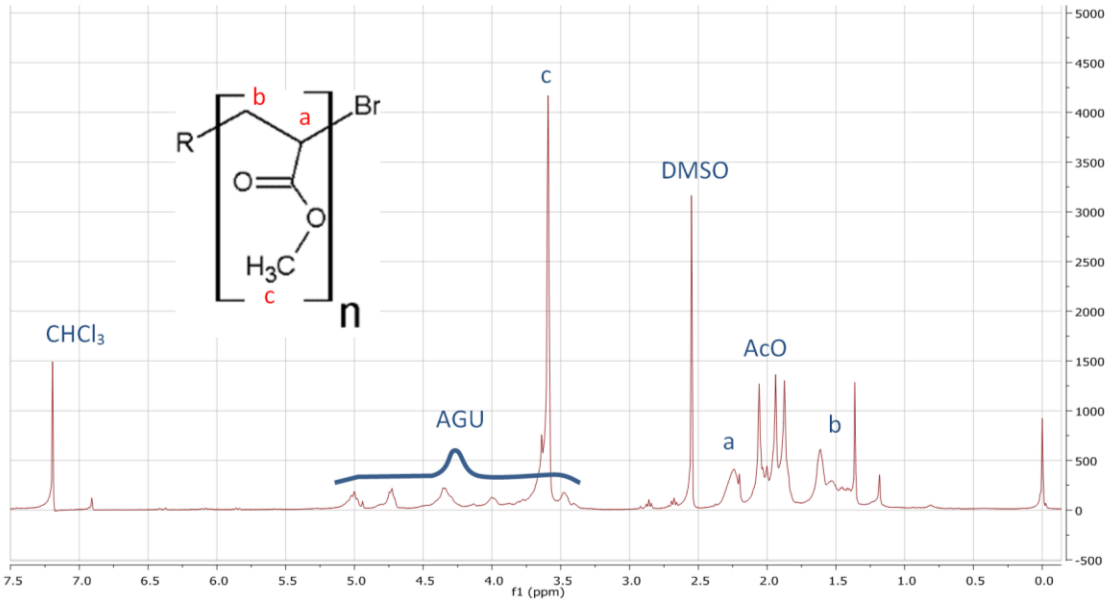

Figure 4.9: ^{1}H NMR spectrum of Cell-g-PMA sample synthesized in DMSO using Cell-$AcO_{2.91}$-$BiB_{0.089}$. Reaction conditions: [M]:[L]:[Cu(II)] = 1560:1.29:0; 50% DMSO by volume; 50^{O}C. As polymerization reached only 6.8% conversion, both cellulose acetate and PMMA peaks are clearly evident. Spectrum obtained in $CDCl_3$.

4.3.4 Polymerization of MA from Cell-$BiB_{1.13}$ in DMSO

Following the poor performance of the macroinitiator synthesized in EMIM AcO (Cell-$AcO_{2.91}$-$BiB_{0.089}$), the macroinitiator was instead synthesized from BMIM Cl with a DS_{BiB} measured by NMR to be 1.75 (subsequently adjusted to 1.13 following bromine analysis, Chapter 3). These reactions are summarized in Table 4.4. Polymerization with MA was fast with 58% conversion being obtained after 30 minutes (Figure 4.10). The reaction was stopped at this point as the solution had become extremely viscous and difficult to sample. Repeating the experiment twice more with more frequent sample taking resulted in a somewhat slower rate with only 40% conversion being reached after 30 minutes. The difference in rate appears to be due to differences in initiator efficiency (IE), as the first reaction had an IE of 71% (calculation of IE of graft copolymers to be discussed later) while the two repeat experiments had an IE of only 45% and 56%. It is not known the reason for the difference in initiator efficiencies, but this is clearly an item of interest. Though the rates were fast, they were nonetheless still much slower than the reactions with EBiB which had reached about 90% conversion in this time. Following the adjustment of the DS_{BiB} downward, the concentration of initiating sites of the Cell-$BiB_{1.13}$ was calculated to be 71% of that for the accompanying EBiB reactions (0.031 M compared to 0.040 M) and this would partly explain the slower rate. The average initial apparent rate constant (k_{app}, initial slope in Figure 4.10) for the Cell-$BiB_{1.13}$ was 0.024 min^{-1}, and 0.11 min^{-1} for EBiB. Using the initiation efficiencies of each reaction to calculate the average effective initiator concentration (concentration of growing chains) led to values of 0.017 M for Cell-$BiB_{1.13}$ and 0.042 M for EBiB. Finally, calculation of the ratio of rate constant to effective initiator concentration yields 1.7 min^{-1}/M for Cell-$BiB_{1.13}$ and 2.7 min^{-1}/M for EBiB: the ratio for Cell-$BiB_{1.13}$ is only 63% of the ratio for EBiB. This would suggest that while the two systems have similar rates, the polymerization with Cell-BiB is still slower even when taking into account the concentration of growing chains.

Table 4.4: Summary of polymerizations of MA from Cell-$BiB_{1.13}$

Sample	[M] (v%)	T (^{O}C)	[M]: [Me_6TREN]: [Cu(II)]	Conv. (%)	K_{app} (min^{-1})	[I] (M)	IV (dL/g)	Pred. M_n (kDa)	Meas. M_n (kDa)	PDI	Pred. Graft M_n(kDa)	Meas. Graft M_n (kDa)	Graft PDI	IE (%)	DS Graft
G-PMA-1A	50	50	188:0.28:0	58	0.040	0.029	0.160	880	1,210	4.28	9.49	13.3	1.11	71	0.80
G-PMA-1B	50	50	179:0.28:0	36	0.015	0.031	0.238	529	426	3.94	5.56	9.85	1.06	56	0.63
G-PMA-1C	50	50	188:0.28:0	50	0.016	0.031	0.247	751	546	3.98	8.05	17.7	1.04	45	0.51
G-PMA-2A	33	30	188:0.28:0.07	56	0.048	0.020	0.0883	842	1,040	3.84	9.07	9.84	1.06	92	1.0
G-PMA-2B	33	30	180:0.28:0.07	40	0.020	0.020	0.0671	608	468	4.01	6.45	12.4	1.06	52	0.59

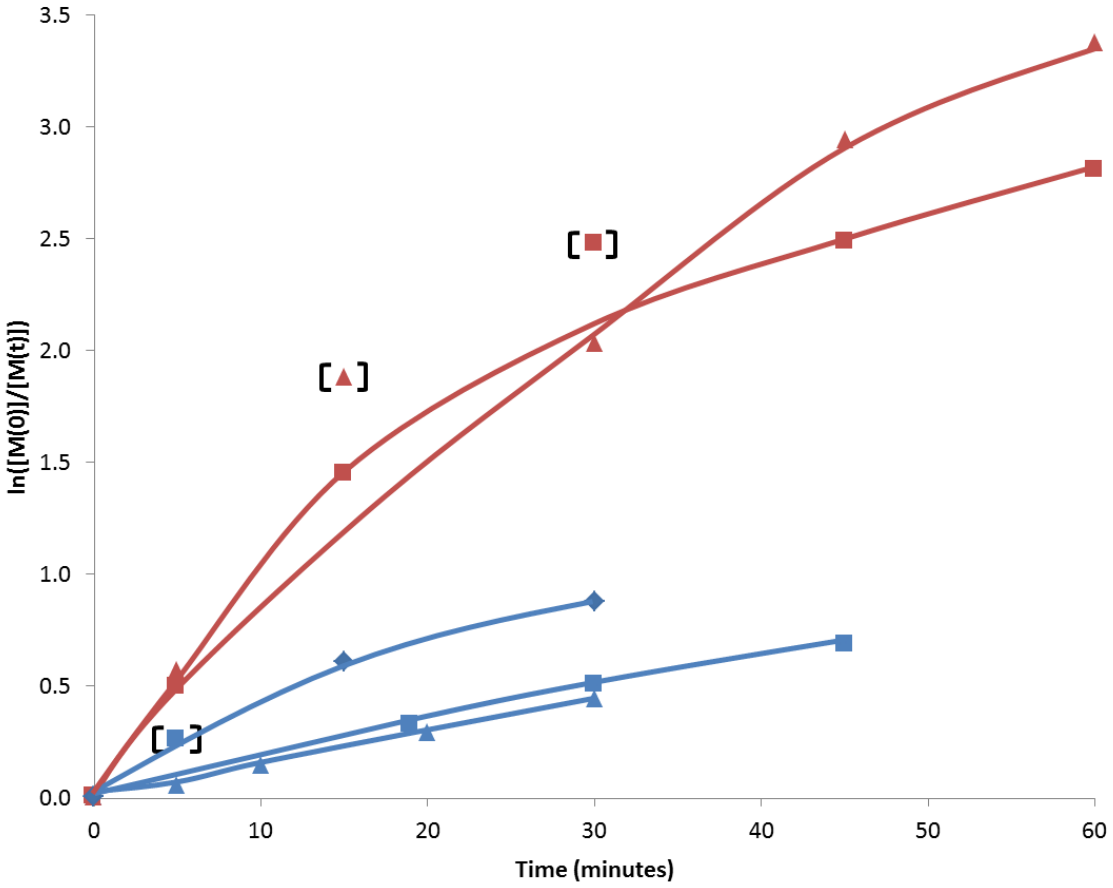

Figure 4.10: Kinetic data for polymerization of MA from Cell-$BiB_{1.13}$ compared to EBiB. Conditions for EBiB polymerization (**red**): [M]:[L]:[Cu(II)] = 134:0.2:0; 50% DMSO by volume; 50^{O}C. The polymerizations using Cell-$BiB_{1.13}$ (**blue**) was first conducted under the same conditions as EBiB using the DS_{BiB} of 1.75 calculated from NMR. Adjusting these numbers for the final bromine analysis obtains conditions of 188:0.28:0. The Cell-$BiB_{1.13}$ polymerizations were slower than the EBiB polymerizations but had constant slope in these plots, except for the faster reaction which had a decreasing slope. Lines are drawn to guide the eye.

The fraction of copolymer that was gel was determined by dissolving a mass of copolymer in a large volume of acetone (<10 mg/mL), a good solvent for both PMA and Cell-BiB, and then filtering to separate the insoluble fraction from the dissolved polymer. The gel fraction for sample G-PMA-1C was calculated to be 65% at 50% conversion. In an effort to decrease this value, new reaction conditions were attempted where the solvent fraction was increased to 67%, the temperature reduced to 30^{O}C, and $CuBr_2$ was added to improve end-group

fidelity. Figure 4.11 displays the plot of monomer consumption for these reactions. The EBiB reactions proceeded at the same rate as each other (although one appeared to have an induction period) but the Cell-$BiB_{1.13}$ reactions did not. Again, this seems attributable to initiation efficiency, as the faster reaction had an IE of 92% calculated, while the slower reaction had an IE of only 52%. Through the same type of calculations used previously, ratios of initial k_{app} to effective initiator concentration were determined to be 2.4 min^{-1}/M for Cell-$BiB_{1.13}$ and 3.5 min^{-1}/M for EBiB; the ratio for Cell-$BiB_{1.13}$ is 69% of the ratio for EBiB, which is comparable to that obtained previously. The rates for Cell-BiB and EBiB are expected to be similar in magnitude but not identical as the group attached to the BiB (ethyl or cellulose) is expected to affect the ATRP equilibrium constant [32], and these results appear to be consistent with this expectation and do not indicate any negative effects on rate attributable to grafting itself. The gel fraction for sample G-PMA-2B was calculated to be 52% at a conversion of 40% which is not a large improvement over the value obtained using more concentrated conditions and no Cu(II).

The average initiator efficiency for the reactions with Cell-BiB was only 63%, while those using EBiB under similar conditions had an average initiator efficiency of 96%. Furthermore, the variation was substantially greater with Cell-BiB (ranging from a low of 45% to a high of 92%) compared to EBiB (90% to 106%). One possibility is that the grafting was being limited directly by steric hindrance. The repeat structure of cellulose (cellobiose) has been reported to have a length of 1.03 nm [33]. The highest DS_{graft} of PMA obtained here was 1.0; this would correspond to one grafted chain every ~0.50 nm along the backbone. However, as each glucose unit is rotated 180^{O} to the adjacent units this allows the grafts to grow in opposite directions to each other and reduce the steric hindrance. Furthermore, this would not explain the large variation obtained in graft density. Another possibility is that the BiB groups were not initiating simultaneously; as the polymerization rate was very fast, any uninitiated BiB group would quickly become buried in the grafted polymer brush and rendered inaccessible. Attempting the grafting with Cell-BiB of a higher DS would reveal whether higher graft densities

could be achieved. Of the studies that reported a graft density for their obtained copolymer, only one has comparable levels of grafting to those reported here. Raus et al. [4] used Cell-$BiB_{1.04}$ as their macroinitiator and obtained a DS_{graft} of 1.0 for poly(styrene) chains and 0.70 for poly(methyl methacrylate) when using Cu(I) as catalyst. However, they obtained much lower maximum values of 0.32 and 0.094 when using Cu(0) as catalyst. Vlcek et al. [15] obtained a maximum value of DS_{graft} for poly(methyl methacrylate) of 0.18 using Cu(0) as catalyst in DMSO and cellulose acetate functionalized with dichloroacetyl groups as the macroinitiator.

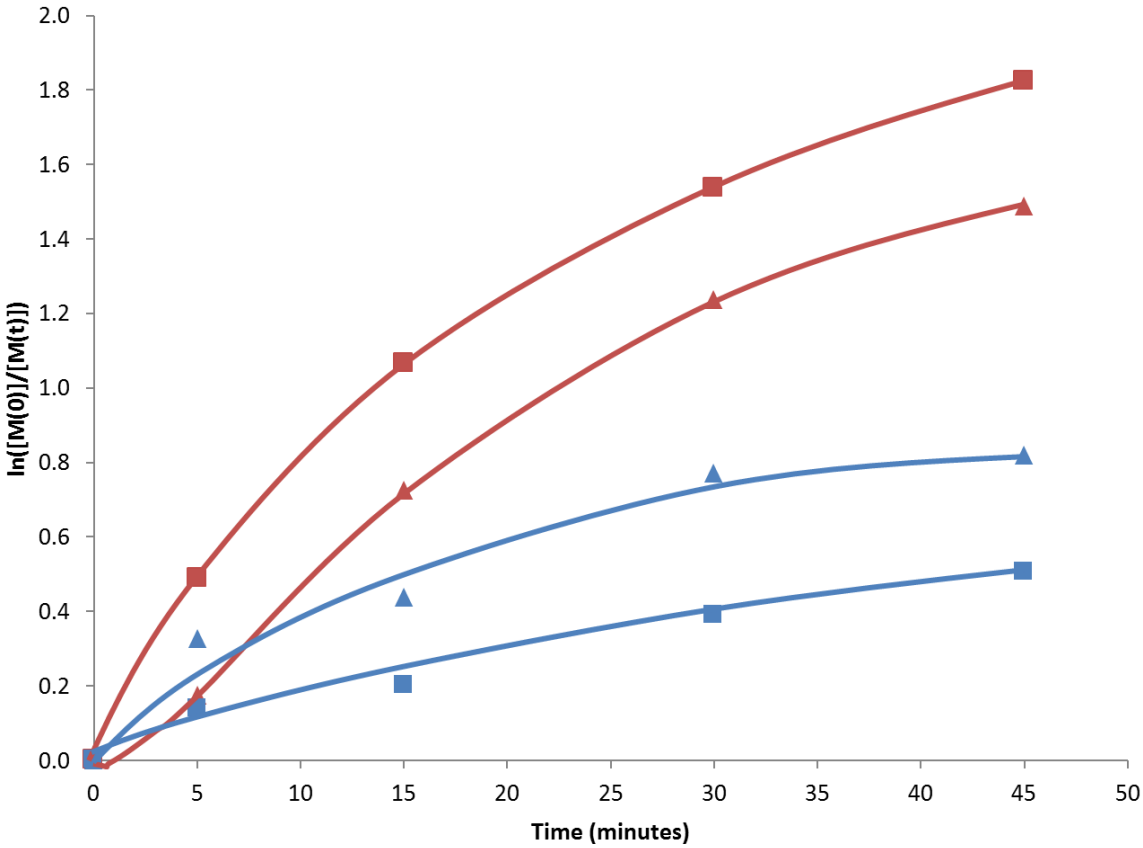

Figure 4.11: Kinetic data for polymerization of MA from Cell-$BiB_{1.13}$ using diluted conditions and added Cu(II). Conditions for EBiB polymerization (**red**): [M]:[L]:[Cu(II)] = 134:0.2:0.05; 67% DMSO by volume; 30^{O}C. The polymerizations using Cell-$BiB_{1.13}$ (**blue**) were first conducted under the same conditions as EBiB using the DS_{BiB} of 1.75 calculated from NMR. Adjusting these numbers for the final bromine analysis obtains conditions of 188:0.28:0.070. The Cell-$BiB_{1.13}$ polymerizations were slower than the EBiB polymerizations but also had dissimilar rates to each other as there was a large difference in IE between the two runs.

Molecular weight measurements were made for each of the final, non-gel fractions of the copolymers, and molecular weight distributions with time were obtained for one experiment each from the reaction set without Cu(II) (Figure 4.12, Table 4.5) and with Cu(II) (Figure 4.13, Table 4.6). In Figure 4.12, it is seen that the peak profiles evolved cleanly as the conversion increased with only small broadening of the peak from a polydispersity of 2.52 for the Cell-$BiB_{1.13}$ to 3.98 for the final copolymer. The measured molecular weights of the Cell-g-PMA samples were lower than the predicted values; it is important to note that the ratio of these values do not correspond to the initiation efficiency of the grafts, as the number of discrete polymer chains is fixed by the number of cellulose chains at the beginning of the reaction. Instead, if the measured-to-predicted ratio (M/P) is greater than unity this would indicate fewer discrete cellulose chains and thus combination of the molecules. A ratio less than unity indicates more chains than expected; this could be due do to the formation of homopolymer or scission of the copolymers, but in this case it was expected that the M_n of the Cell-BiB was overestimated due to poor resolution of the columns in the low molecular weight region, and thus the predicted copolymer values would also be overestimated. As such, from the low M/P ratio, the lack of major peak broadening, and the absence of high molecular weight shoulder formation the GPC analysis does not show evidence of combination through intermolecular termination occurring. However, the samples were diluted with acetone and filtered through basic aluminum oxide during which insoluble material was removed and this could have removed high molecular weight material. If this were the case, it would be expected that the M_n values would show a leveling off and the high molecular weight shoulder would stop growing, but instead the peaks shift cleanly and molecular weight increases linearly.

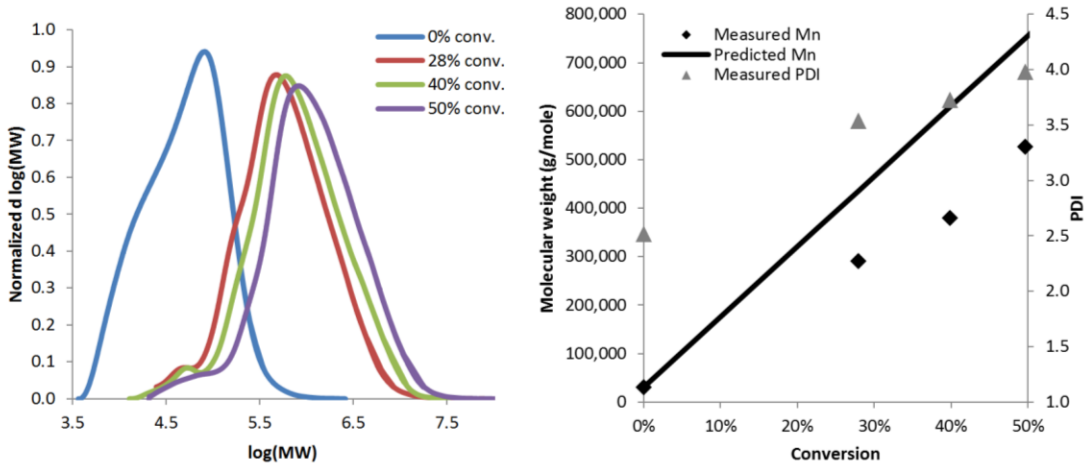

Figure 4.12: Molecular weight distributions for polymerization of sample G-PMA-1C. Reaction conditions: [M]:[L]:[Cu(II)] = 188:0.28:0; 50% DMSO by volume; 50^{O}C. The distributions evolve cleanly with some broadening of the peak with increasing conversion. The M_n of the Cell-BiB is thought to be overestimated which explains why the M_n of the copolymers is lower than predicted.

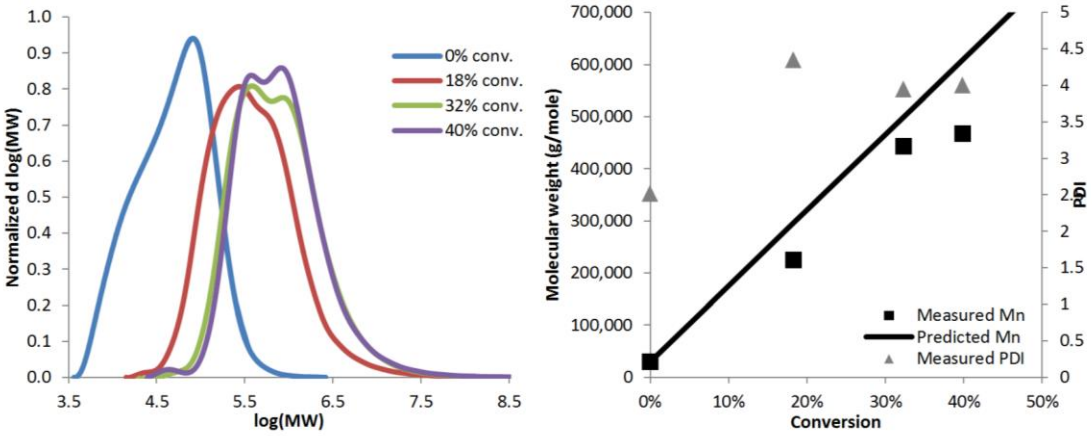

Figure 4.13: Molecular weight distributions for polymerization of sample G-PMA-2B. Reaction conditions: [M]:[L]:[Cu(II)] = 188:0.28:0.07; 67% DMSO by volume; 30^{O}C. These copolymer peaks appear bimodal and have a higher M/P ratio than those for sample G-PMA-1C (no added Cu(II)).

Molecular weight distributions for the samples with Cu(II) (Figure 4.13) show bimodal behaviour. It is not known why this would be as the distributions are not much broader than those in Figure 4.12 and the behaviour of the evolution does not suggest the presence of

homopolymer. The M_p of the higher peak in the pair is about 2 to 3 times that of the M_p of the lower peak amongst the distributions.

Table 4.5: Molecular weight data for sample G-PMA-1C.

Conversion (%)	Predicted M_N (kDa)	Measured M_N (kDa)	PDI	M/P	[η] (dL/g)	dn/dc (mL/g)	α
0	30.4	30.4	2.52	1	0.723	0.0922	0.806
28	435	290	3.54	0.67	0.322	0.0561	0.450
40	609	380	3.73	0.62	0.299	0.0541	0.437
50	751	526	3.98	0.70	0.247	0.0486	0.375

Table 4.6: Molecular weight data for sample G-PMA-2B.

Conversion (%)	Predicted M_N (kDa)	Measured M_N (kDa)	PDI	M/P	[η] (dL/g)	dn/dc (mL/g)	α
0	30.4	30.4	2.52	1	0.723	0.0922	0.806
18	296	226	4.35	0.76	0.103	0.0293	0.501
32	499	444	3.95	0.889	0.0885	0.0241	0.481
40	608	468	4.01	0.77	0.0671	0.0282	0.676

The solvent-polymer behaviour measured for the samples in Table 4.5 and Table 4.6 display some unusual results. In particular, the measured intrinsic viscosity of the samples consistently decreased as the reactions proceeded. This was highly unexpected. While graft copolymers have been reported to decrease in intrinsic viscosity below the value for their backbone depending on the solvent [34, 35], it was expected that the intrinsic viscosity should then increase as the graft length increased [36, 37]. Despite THF being a good solvent for PMA homopolymer (α=0.799 [24]), the Cell-g-PMA exhibited reduced solubility in acetone and THF, requiring more dilute conditions. In addition, the values of α found for the copolymer were generally <0.5 and decreased as the polymerization proceeded. A contraction of the chains due to decreased solvation would decrease the intrinsic viscosity, but this should be offset by the more than an order of magnitude increase in molecular weight. The samples of Cell-g-PMA appeared completely soluble but were difficult to filter through the 0.45 μm filters, and as such some

material may have been filtered out, reducing the concentration and affecting the measurements. The variability and unexpected behavior in the results suggests that this was occurring and that the molecular weight measurements of the copolymer (here and in the following sections) should therefore be treated with a great deal of caution. In the future, more suitable solvents should be found for the GPC that better solvate the copolymer and increase the refractive index increment of the copolymer in solution. Multiple injections should be made for each sample so that the measurements can be more easily accepted or dismissed.

4.3.5 Chain extension of Cell-g-PMA

In order to demonstrate the living behaviour of the polymer, chain extension experiments were undertaken. Sample G-PMA-1B was used as the starting macroinitiator with graft lengths measured to be 9,850 g/mole, and the experiment was conducted three times at the same conditions. 50 mg of the copolymer was dissolved in 5 mL of DMSO and polymerized with 0.58 mL of MA (1285 eq.). As seen in Figure 4.14, the reaction proceeded readily despite the low concentration of initiating sites (0.00091 M) and monomer (10 vol%, 1.2 M). Low concentration was required due to the poor solubility of G-PMA-1B and the high viscosity; despite the low monomer concentration, the reactions were very difficult to sample once about 40% conversion had been reached due to the viscosity. There was variation in the rates obtained but the two reactions with slower rates appeared to have induction periods, and slower propagation rates have been observed when residual oxygen causes induction periods [38].

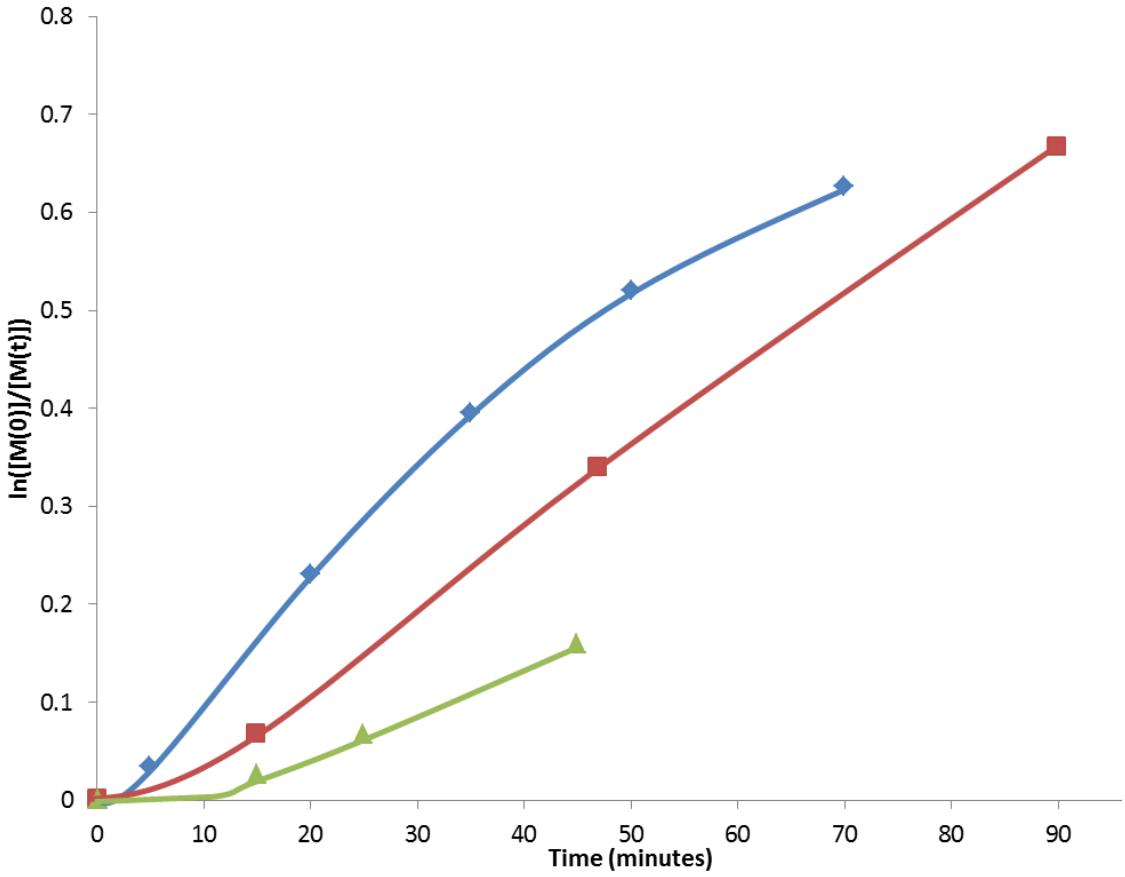

Figure 4.14: Kinetic plot of chain extension experiments from macroinitiator G-PMA-1B. Reaction conditions: [M]:[L]:[Cu(II)] = 1285:0.2:0; 90% DMSO by volume; 30^{O}C; MA as monomer. Lines are drawn to guide the eye.

Molecular weight measurements were made for the final graft copolymer samples from the three chain extension experiments and are displayed in Figure 4.15. The molecular weights are substantially higher for these samples than for the predicted values. This would suggest that the molecules were combining; however, the shape of the distributions does not show much change from the initial macroinitiator and the measured PDI actually decreases. As seen in Table 4.7, the intrinsic viscosity for these samples did not change substantially from the initial macroinitiator, while α decreased further to <0.3.

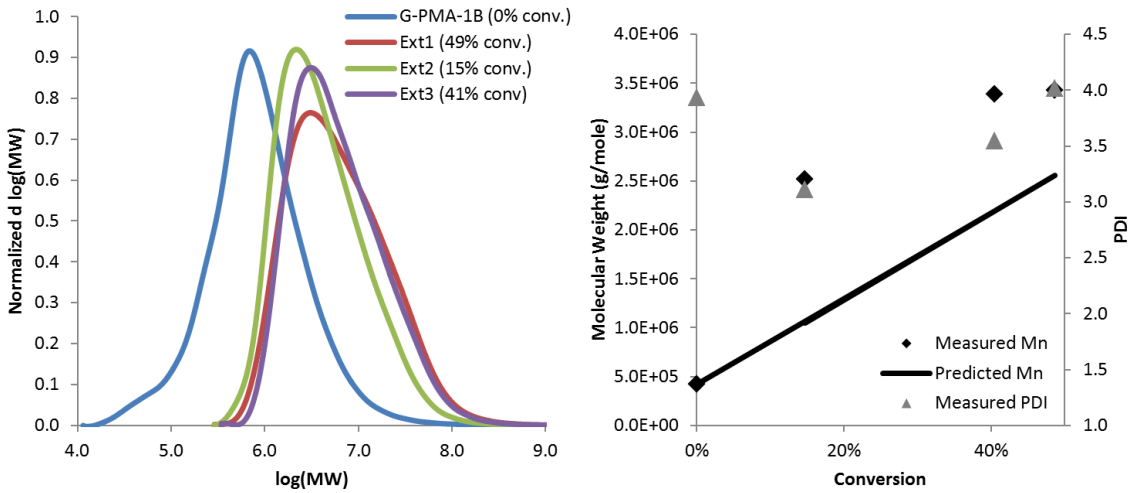

Figure 4.15: Molecular weight distributions for final copolymer samples from the three chain extension experiments. Reaction conditions: [M]:[L]:[Cu(II)] = 1285:0.2:0; 90% DMSO by volume; 30^{O}C; MA as monomer.

Table 4.7: Molecular weight data for chain extension experiments.

Sample	Conv. (%)	Pred. Graft M_N (kDa)	Pred. M_N (kDa)	Meas. M_N (kDa)	PDI	M/P	[η] (dL/g)	dn/dc (mL/g)	α
G-PMA-1B	0	9.85	426	426	3.94	1	0.238	0.0382	0.429
Ext1	49	63.7	2,550	3,430	4.02	1.3	0.293	0.0400	0.201
Ext2	15	26.1	1,050	2,520	3.12	2.4	0.201	0.0290	0.276
Ext3	41	61.3	2,190	3,390	3.55	1.5	0.241	0.0332	0.173

4.3.6 Polymerization of MMA in DMSO

Polymerization of MMA was attempted with added Cu(II) and the diluted conditions used previously with MA. The reaction was carried out three times using both EBiB and Cell-$BiB_{1.13}$. It was seen that while the reaction initially proceeded at a similar rate for both initiators, reactions with EBiB began to increase in rate while those with Cell-$BiB_{1.13}$ slowly decreased in rate (Figure 4.16). This appears to be attributable to slow initiation in the MMA system. As more EBiB molecules began to initiate, the rate increased. However, this could not happen for the Cell-BiB system as once polymerization began the uninitiated BiB groups were buried in the polymer brush and no further initiation could take place. Initiation efficiency could only be measured for one of the copolymer samples, but this value was found to be 16% at the end of the

reaction. In contrast, the EBiB initiated sample F-PMMA-3 had an IE of 13% (DS_{graft} 0.15) after the first sample point (4.4% conversion) but the efficiency continued to increase throughout the reaction, reaching a final value of 56% at 41% conversion. This increase in initiating efficiency is illustrated in Figure 4.17: the difference between measured and predicted molecular weight becomes steadily less, while a low molecular weight tail steadily increases in size in the molecular weight distributions leading to increases in the PDI. Thus, it would appear that in order to increase the graft density of the cellulose copolymer faster initiation needed to be achieved. Low initiation efficiency with MMA has been encountered before [10, 39] although in these papers the initiating efficiency appeared constant and not to increase with time.

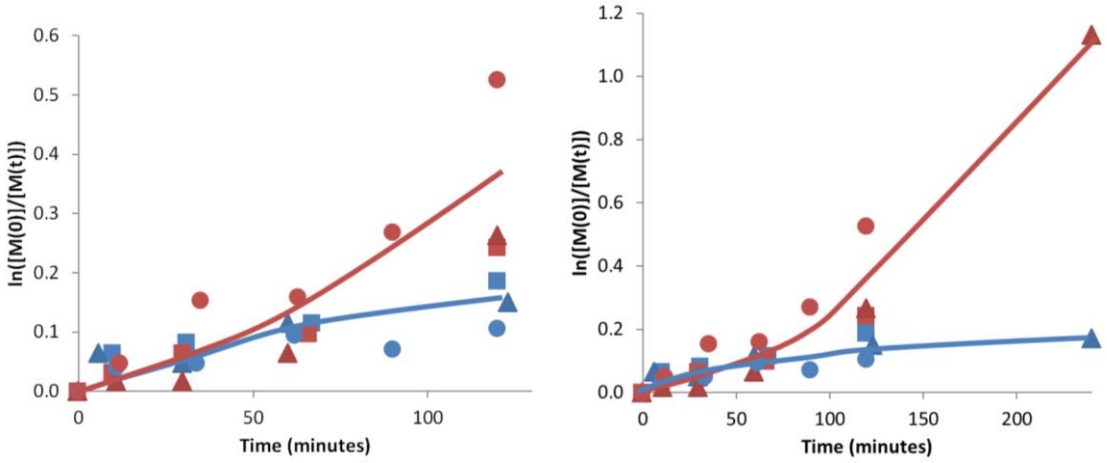

Figure 4.16: Kinetic plots for polymerization of MMA from EBiB and Cell-$BiB_{1.13}$. The experiments were conducted three times: two experiments for 120 minutes and one experiment for 240 minutes. The plot on the left highlights the region up to 120 minutes while the plot on the right shows the entire time scale. The data points for each experiment are noisy but taken together they show the trends of the reaction. Polymerization from each initiator appeared to proceed at a similar initial rate but began to increase for EBiB (**red**) as the reaction proceeded, indicating a slow initiation of EBiB. The reactions with Cell-BiB (**blue**) slowly decreased in rate as the reaction proceeded: the initiating sites on Cell-BiB would be buried in the polymer brush and thus unable to continue initiating once polymerization had started. Reaction conditions for EBiB: [M]:[L]:[Cu(II)] = 113:0.2:0.05; 67% DMSO by volume; 30^{O}C. Reaction conditions for Cell-$BiB_{1.13}$ were 158:0.28:0.07. Best-fit lines were drawn through each set of experiments to guide the eye.

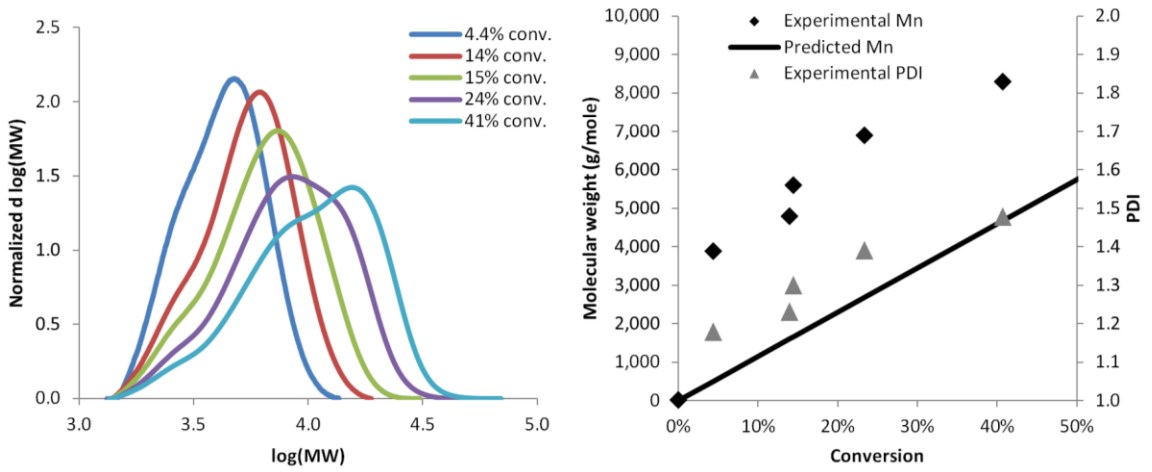

Figure 4.17: Molecular weight data of PMMA initiated by EBiB (sample F-PMMA-3). Reaction conditions: [M]:[L]:[Cu(II)] = 113:0.2:0.05; 67% DMSO by volume; 30^{O}C. The distributions show low molecular weight tailing as initiation efficiency increased throughout the polymerization.

GPC analysis was performed on Cell-g-PMMA samples; the molecular weight distributions with conversion are displayed in Figure 4.18 for the polymerization that was left for 4 hours (G-PMMA-1). It was observed that the peaks broadened quite severely over the course of the reactions with M_n increasing well above its predicted value, which would indicate that combination of the copolymer was occurring. This was not unexpected as the average gel fraction of these samples was measured to be 66%. As can be seen in Table 4.8, the intrinsic viscosity followed a pattern that agreed better with the literature, with intrinsic viscosity initially decreasing upon grafting and subsequently increasing as graft length increased. In addition, α remained above 0.5 for the samples, indicating less contraction of the Cell-g-PMMA in THF than Cell-g-PMA in THF. In contrast to the Cell-g-PMA, the partial insolubility of the Cell-g-PMMA appears to be due to combination and crosslinking. Figure 4.19 shows the final molecular weight distributions for the three grafting reactions with the molecular weight data summarized in Table 4.9. A very large high molecular weight shoulder is seen in each sample indicating that combination is occurring; furthermore, the shoulders appear to extend beyond the resolution

limits of the system, and so the actual broadness of the peaks could be quite larger than that measured here.

It is known that MMA experiences a larger proportion of termination by disproportionation as opposed to combination; however, studies report that the ratio of disproportionation to combination decreases as the temperature decreases [45]. The low temperature used here ($30^{O}C$) would allow a greater proportion of termination by combination. In addition, the structure of the copolymer (with multiple radical sites in each molecule) would mean that the molecular weight would change much more dramatically than with homopolymer (which has only one radical site per molecule) for the same amount of combination. This is observed through the GPC traces, with both the molecular weight distributions and the elution profiles broadening through high molecular weight tailing. The very narrow distributions of PMA homopolymer (Figures 4.4 - 4.7) indicate that termination was not occurring to an appreciable degree until high conversion (>80%) in the PMA system. The broadness of the PMMA homopolymer (Figure 4.17) was caused at least partially by slow initiation resulting in low-molecular weight tailing; termination could also have contributed to this, although it is difficult to determine just from the molecular weight distributions.

Table 4.8: Molecular weight data for G-PMMA-1.

Conv. (%)	Pred. M_N (kDa)	Meas. M_N (kDa)	PDI	M/P	[η] (dL/g)	dn/dc (mL/g)	α
0	30.4	30.4	2.52	1	0.723	0.0922	0.806
4.6	101	144	3.34	1.4	0.380	0.0701	0.718
10.8	195	139	4.35	0.71	0.342	0.0603	0.623
13.8	243	427	3.25	1.76	0.481	0.0735	0.732
15.4	266	527	6.42	1.98	0.648	0.0806	0.598

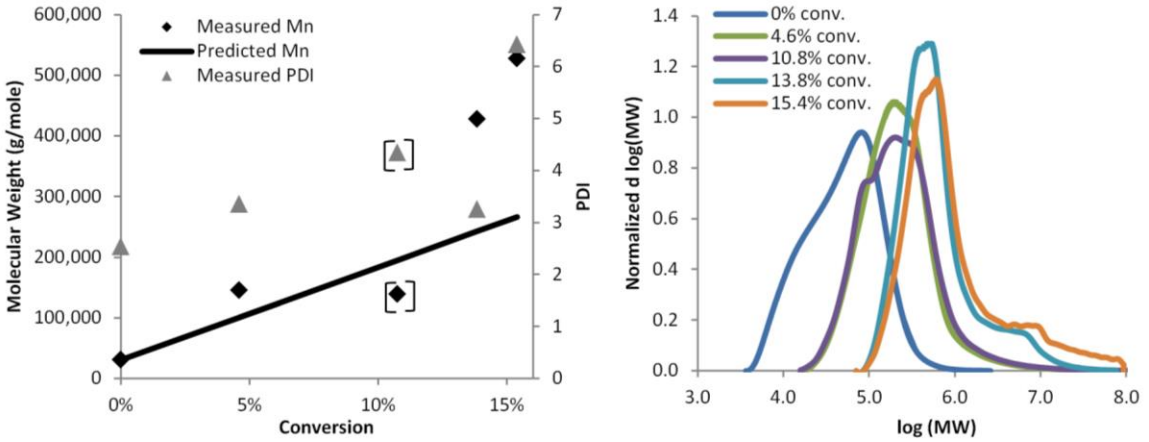

Figure 4.18: Molecular weight distributions of G-PMMA-1. The peaks show a very large amount of broadening, with the PDI increasing from 2.5 to 6.4 over the course of the reaction and a large high molecular weight shoulder forming: this would suggest combination of the copolymer occurring. Reaction conditions: [M]:[L]:[Cu(II)] = 158:0.28:0.07; 67% DMSO by volume; 30^{O}C.

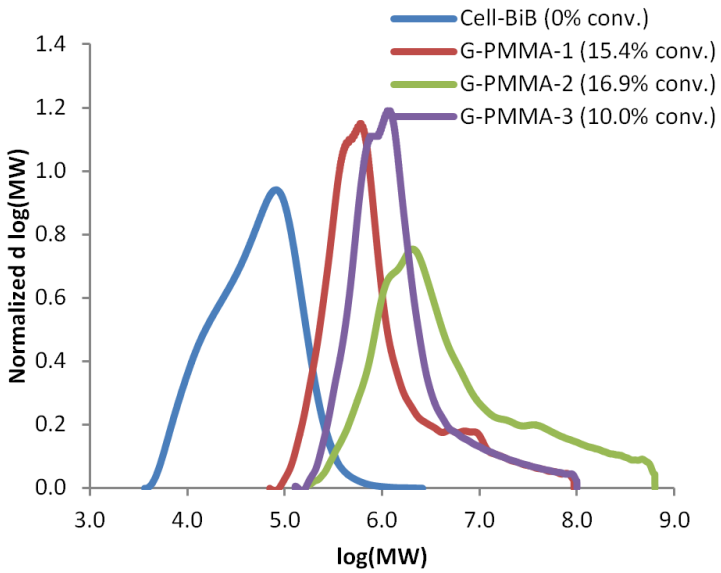

Figure 4.19: Molecular weight distributions of final Cell-g-PMMA samples. Combination is quite severe in the reactions and the high molecular weight shoulders appear to extend beyond the resolution limits of the columns. Reaction conditions: [M]:[L]:[Cu(II)] = 158:0.28:0.07; 67% DMSO by volume; 30^{O}C.

Table 4.9: Molecular weight data for polymerization of MMA from Cell-$BiB_{1.13}$.

Sample	Conv. (%)	Pred. M_N (kDa)	Meas. M_N (kDa)	PDI	M/P	[η] (dL/g)	dn/dc (mL/g)	α
Cell-$BiB_{1.13}$	0	30.4	30.4	2.52	1	0.723	0.0922	0.806
G-PMMA-1	15.4	266	527	6.42	2.0	0.648	0.0806	0.598
G-PMMA-2	16.9	264	1,856	16.9	7.0	0.279	0.0364	0.356
G-PMMA-3	10.0	169	925	4.14	5.5	0.27	0.0319	0.737

4.3.7 Cleavage of grafted chains through selective transesterification

Cleavage of polymer chains grafted to cellulose has been extensively reported [4, 9, 15, 19, 40-43]; however, these reports used a hydrolysis mechanism to cleave the chains, even in the case of acrylic polymers. Acrylic polymers contain ester groups and the ester group in these acrylic polymers would presumably have hydrolyzed as well, as no evidence was presented to contradict that assumption. In addition, there have been reports of an inability to successfully cleave the grafted polymer chains, despite using similar conditions reported by other groups; this was attributed to the graft density being too high and hindering access to the ester attached to cellulose [7], or because the conditions were found to degrade the grafts [6]. Scheme 4.1 summarizes the transesterification and hydrolysis reactions encountered in this research. These reactions will be used to discuss the results obtained here.

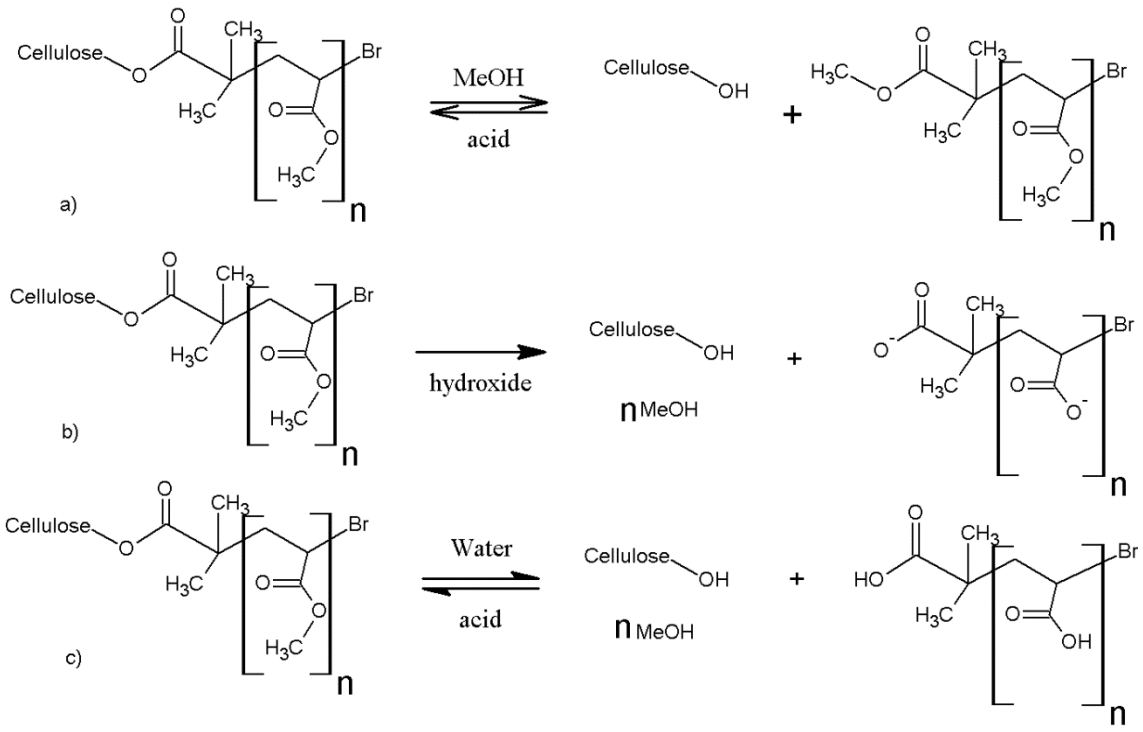

Scheme 4.1: Summary of transesterification and hydrolysis reactions of Cell-g-PMA. a) The use of methanol selectively breaks the desired ester with acid as catalyst. Using water breaks both ester groups. b) In the presence of hydroxide, hydrolysis of an ester is irreversible, regardless of the presence of an alcohol. Alkoxides can be used for transesterification reactions under anhydrous conditions. c) Under acidic conditions, hydrolysis is reversible. An excess of alcohol will minimize hydrolysis. Summarizing information from Bruice [20].

As shown in Scheme 4.1, methanol is the alcohol needed to break the ester attaching the synthetic chain to cellulose as it will not affect the methyl ester in PMA and PMMA. A hydrolysis reaction could be used instead with the goal of converting all the ester groups to their acidic form and obtaining poly(acrylic acid) or poly(methacrylic acid), but this presents several problems. The acid versions of the polymer are soluble in water but have limited solubility in organic solvents; thus, an aqueous GPC would be needed to analyze them. As well, the polymers would change solubility during the reaction and the product polymer may not be soluble in the reaction solvent. This change in solubility during the reaction would hinder complete conversion of the esters to acid. As such, the methanol transesterification reaction was chosen to use.

The cleavage reaction was first attempted by modifying methods reported in the literature that used methanol. These methods all used hydroxide to promote the reaction rather than an acid

catalyst: Billy et al. [19] used 20 g/mL of cellulose-g-poly(diethylene glycol methacrylate in 0.2 M NaOH/MeOH (heterogeneous reaction) and stirred at room temperature; Vlcek et al. [15] used 8 mg/mL of cellulose-g-PMMA dissolved in 0.3 M KOH/(2 parts THF/1 part MeOH) and stirred at room temperature for 3 days; and Raus et al. [4] used the same conditions as Vlcek et al.

Cell-g-PMA (G-PMA-1A) was dissolved in 19 mL of THF (5 mg/mL) and 1 mL of 2 M KOH/MeOH was injected to start the reaction (final concentration of KOH was 0.1 M). However, addition of the base solution caused the reaction mixture to turn heterogeneous as the polymer began to precipitate. This was instantaneous for the reaction done at 60^{O}C, and began occurring within minutes for the reaction at 30^{O}C. The copolymer itself was soluble at these solvent concentrations at a neutral pH, and so the insolubility was attributed to the presence of the base. After allowing the reactions to stir overnight, they were filtered to separate the THF-soluble fraction from the solid. The solid fraction was found to be water soluble. Figure 4.20 displays the molecular weight distributions of the THF soluble fractions compared to the original copolymer. The higher molecular weight portion of the distribution is cut-off due to the size-exclusion limits of the column, but the low molecular weight tail is the portion of the distribution that is of interest. It is seen that the original copolymer peak disappeared, to be replaced with a bimodal peak of lower molecular weight. The lower molecular weight peak in this bimodal distribution may be from the cleaved chains with the higher molecular weight peak being the copolymer residue, but it is not clear. In addition, a large series of signals appeared in the elution profile below the calibration limits of the column. This is not shown in the distribution here but does indicate that a very large fraction of the sample consisted of oligomeric or otherwise degraded material. The molecular weight distributions were not satisfactory for obtaining molecular weight data of the grafts. Similar results were obtained for attempts using other samples, other solvent concentrations, and using NaOH.

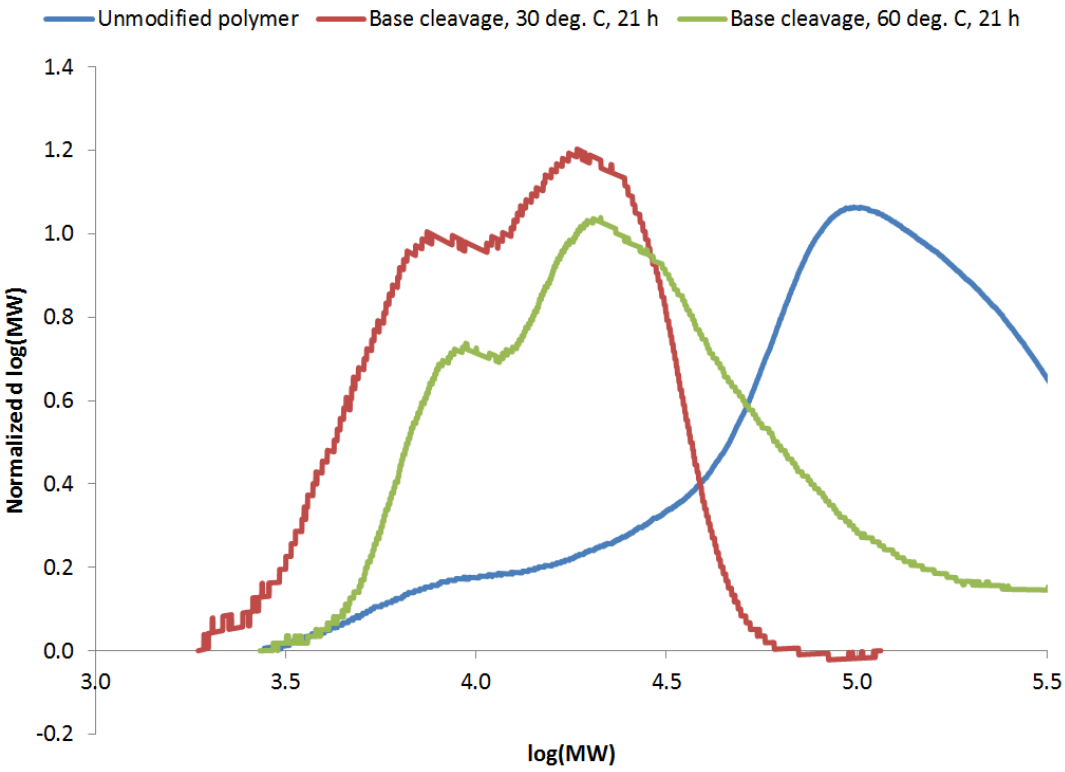

Figure 4.20: Molecular weight distributions of sample G-PMA-1A before and after base-promoted ester cleavage. The sample appeared highly degraded and it was not clear if the peak that formed was from the cleaved chains or other degradation products.

It was suspected that the methyl ester groups of PMA were being hydrolyzed during the reaction, and this was confirmed through NMR (spectra given in Figure 4.21). The expected ratio of signals of the methyl ester group to the PMA backbone was 1:1. The measured ratio was only 0.87:1 for the organic-soluble fraction, and decreased further to 0.38:1 for the water-soluble fraction. While the spectrum for the organic-soluble sample showed the presence of contaminants which could skew the integration (BHT being the largest one), the spectrum for the water-soluble sample was relatively clean and showed the larger disparity in the measured ratio. Thus, a majority of the methyl ester groups were being converted to carboxylate groups. This can be explained by the reactions in Scheme 4.1; hydroxide does not catalyze transesterification

reactions and instead results in irreversible hydrolysis. As such, no proportion of excess alcohol will prevent the hydrolysis from occurring.

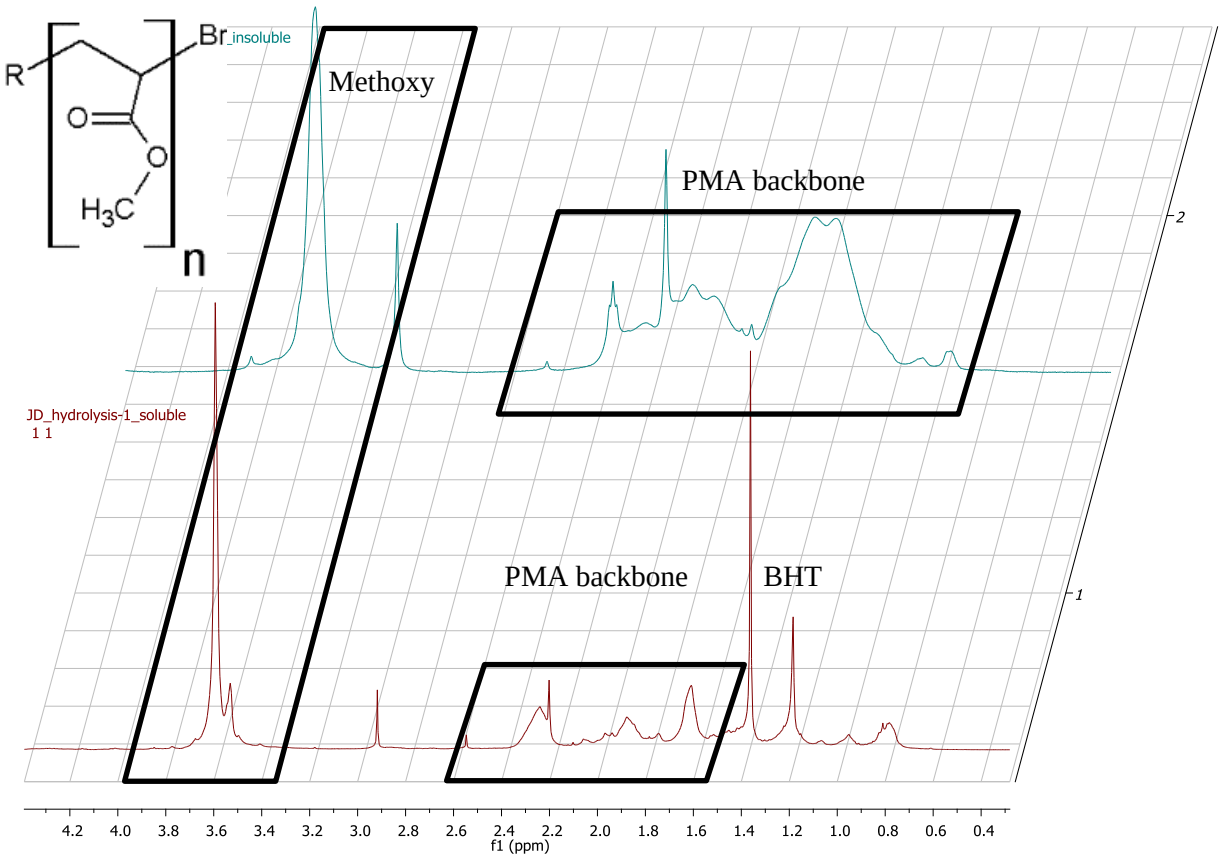

Figure 4.21: Spectra of sample G-PMA-1A after base-promoted ester-cleavage at 60^{O}C. A ratio of methyl ester to backbone signals of 1 was expected. The ratio was only 0.87 for the organic-soluble fraction (bottom, $CDCl_3$), and decreased further to 0.38 for the water-soluble fraction (top, D_2O). This indicated that most of the methyl-ester groups were being converted to carboxylates. The peaks upfield of ~1.45 ppm in the organic spectrum are not attributed to PMA: the largest peak is due to BHT (a preservative in the solvent THF) and the others are due to unknown contaminants. Integration of the PMA backbone was carried out between 1.45 and 4.5 ppm for this sample.

Hydrolysis is reversible under acidic conditions, as Scheme 4.1 illustrates. Provided that a large enough excess of methanol is provided, hydrolysis of the methyl ester groups should be minimized. The reaction was therefore attempted using sulfuric acid in place of the potassium hydroxide. Markedly different results were obtained. The reaction mixture remained in a single

phase upon addition of the acid, and the polymer remained completely dissolved throughout the reaction. The reaction was sampled at 6.5 hours and 23.5 hours. Analysis of the samples by GPC (Figure 4.22) showed that while the main copolymer peak did not change significantly, a new peak was clearly formed after the transesterification reaction. This new peak overlapped the low molecular weight tail of the original copolymer; however, since this tail was relatively flat it was treated as the baseline for the new peak, allowing integration to be performed. The peak obtained by this was very narrow and similar in appearance to homopolymer samples of PMA at this conversion (~40%). The measured PDI of 1.06 was extremely low; this polydispersity may be somewhat underestimated due to part of the cleaved peak's shoulders being obscured by the copolymer peak, but the obtained PDI was not substantially lower than expected as polydispersities of 1.08 were obtained with EBiB at this conversion (F-PMA-2B), and so this was deemed an acceptable approximation. There was no change observed when increasing the time from 6.5 hours to 23.5 hours.

Figure 4.22 also plots the macroinitiator. Although this peak did shift to higher molecular weight after the grafting, the extreme low molecular weight portion of the tail does not appear to shift very much, and the cleaved grafts appear at higher molecular weights than the copolymer tail. It was observed previously that the Cell-g-PMA copolymers had lower intrinsic viscosity than their backbone polymers, and it has been reported elsewhere that intrinsic viscosity can be lower for graft copolymers than their constituent polymers [36, 37]; this could explain why the copolymer appears at lower molecular weight than the cleaved polymer. In addition, in Chapter 3 it was found that bromine content measured by ion chromatography was lower than that predicted by NMR suggesting that some of the bromine groups had become substituted; this may have happened preferentially to the lower molecular weight material, thereby preventing grafting from occurring.

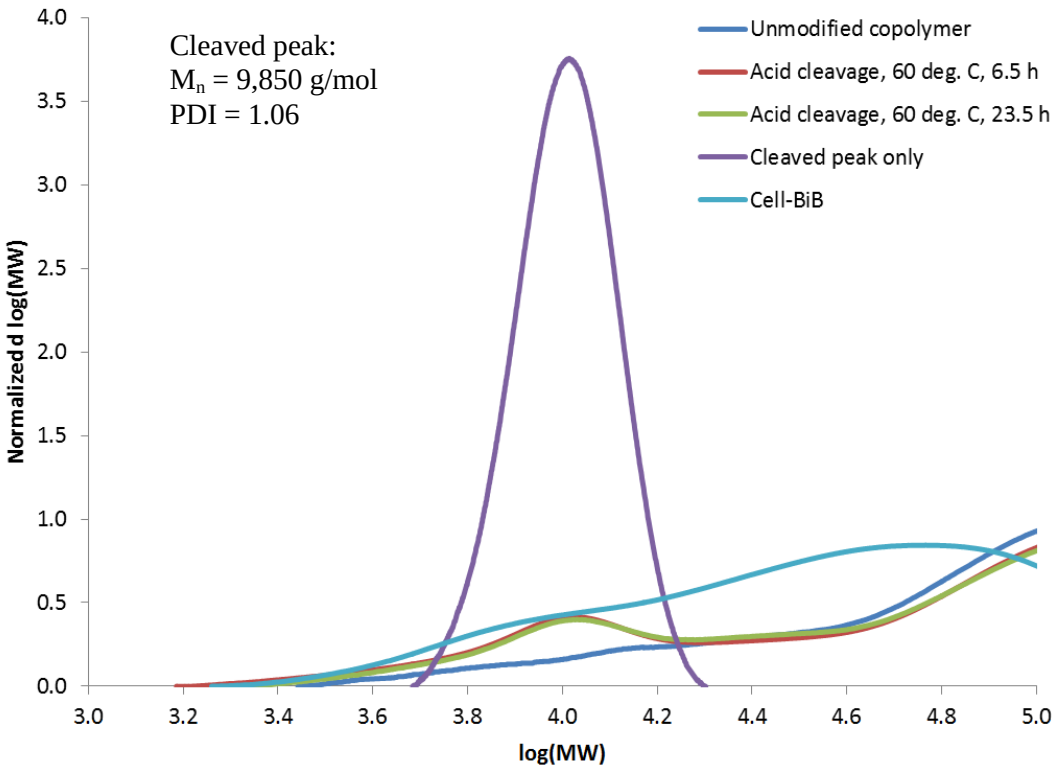

Figure 4.22: Molecular weight distributions of samples before and after acid-catalyzed transesterification of sample G-PMA-1B. A new peak appeared at M_p = 10,000 g/mol. There was no observable change when increasing the time from 6.5 hours to 23.5 hours. The cleaved peak was integrated using the copolymer tail as a baseline.

The NMR spectrum (Figure 4.23) of the sample with the transesterification carried out using an acid catalyst is similar in appearance to the organic-soluble polymer fraction from the base-promoted reaction, with a similar methyl ester to backbone ration of 0.83; however, there was a large degree of error associated with this as contaminants in the sample cause partial overlap of peaks. The large number of unidentified signals may indicate some chemical changes in the polymer occurring; the visual appearance of the polymer would support this, as the polymer changed from a relatively colourless solid before the reaction to a yellow-brown colour after the reaction. However, there was less discoloration than when a base was used, the entire polymer sample retained its original solubility characteristics, and the NMR spectrum showed a more

favourable ratio of methyl ester peaks to PMA backbone peaks. Thus, it was concluded that using an acid as catalyst was a more appropriate choice for the reaction.

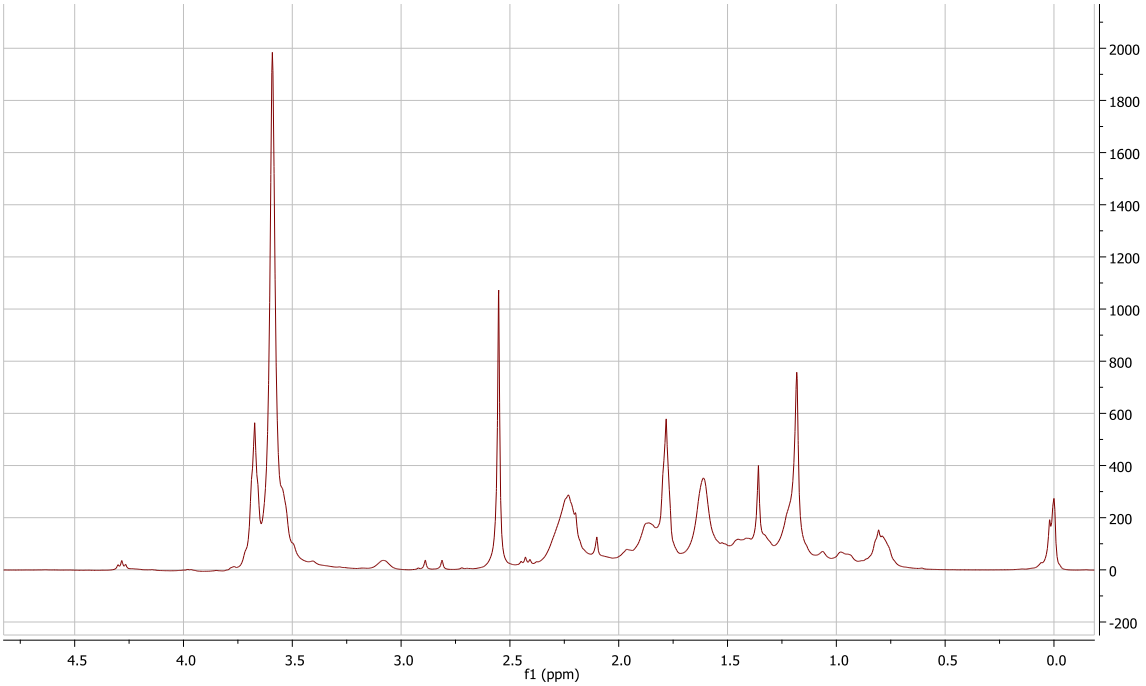

Figure 4.23: NMR spectrum of sample G-PMA-1B after acid-catalyzed transesterification. The peaks upfield of ~1.45 ppm are not attributed to PMA. BHT is the peak at 1.36 ppm, but the others may indicate chemical modification of the polymer or some unidentified contaminants. The ratio of methyl ester to PMA backbone was measured to be 0.83.

The conditions for the transesterification reaction were varied in order to determine if a greater quantity of grafts could be removed from the copolymer. The reaction was carried out by adding aliquots of a 2 N H_2SO_4/MeOH solution to 10 mg/mL solutions of copolymer dissolved in THF. It was hypothesized that increasing the volume of the H_2SO_4/MeOH solution used would result in greater chain cleavage due to the higher concentrations of methanol and acid. However, this was not what was observed. When samples G-PMA-1A, G-PMA-2A, and G-PMMA-1 were used, along with twice the methanol concentration as that used in Figure 4.22, only limited peak formation was observed after 5.5 h that left interpretation ambiguous. This was unexpected as the samples appeared completely dissolved throughout the reaction, and so this study was expanded

using sample G-PMA-1A at a variety of H_2SO_4/MeOH concentrations and leaving the reaction for 24 h. These results are summarized in Figure 4.24, and show that while at least limited peak formation was observed for all reactions, only the reaction carried out at 4.8 vol% MeOH/THF resulted in a sharp peak forming (the conditions used in Figure 4.22).

The acid and alcohol concentration changed in tandem throughout these reactions, but the acid (as a catalyst) was only expected to affect the rate of reaction. Since Figure 4.22 showed no change in the distributions when increasing the reaction time from 6.5 hours to 23.5 hours at 0.1 N H_2SO_4, it was expected that all reactions studied in Figure 4.24 would be complete after 24 hours and that therefore the acid concentration was not what was limiting the reaction. Instead, it was hypothesized that the methanol concentration was affecting the solvation of the copolymer. The ester that was the focus of the reaction was buried in the centre of a very large, hydrophobic molecule: for the ester to react, it required a hydrophilic molecule (methanol) to migrate to the centre of this hydrophobic molecule. A large enough concentration of methanol is required in order to create a strong gradient for migration, but too large of a methanol concentration could cause the grafted chains to retract and make the ester less accessible. This was not examined further, but what was clear from the reactions carried out was that the transesterification was very sensitive to the conditions used. Furthermore, it is expected that the optimal conditions will be different between graft copolymers of different structure (i.e. graft density, graft length, type of polymer). The solvation of the copolymer and its grafts needs to be understood better for a more efficient reaction.

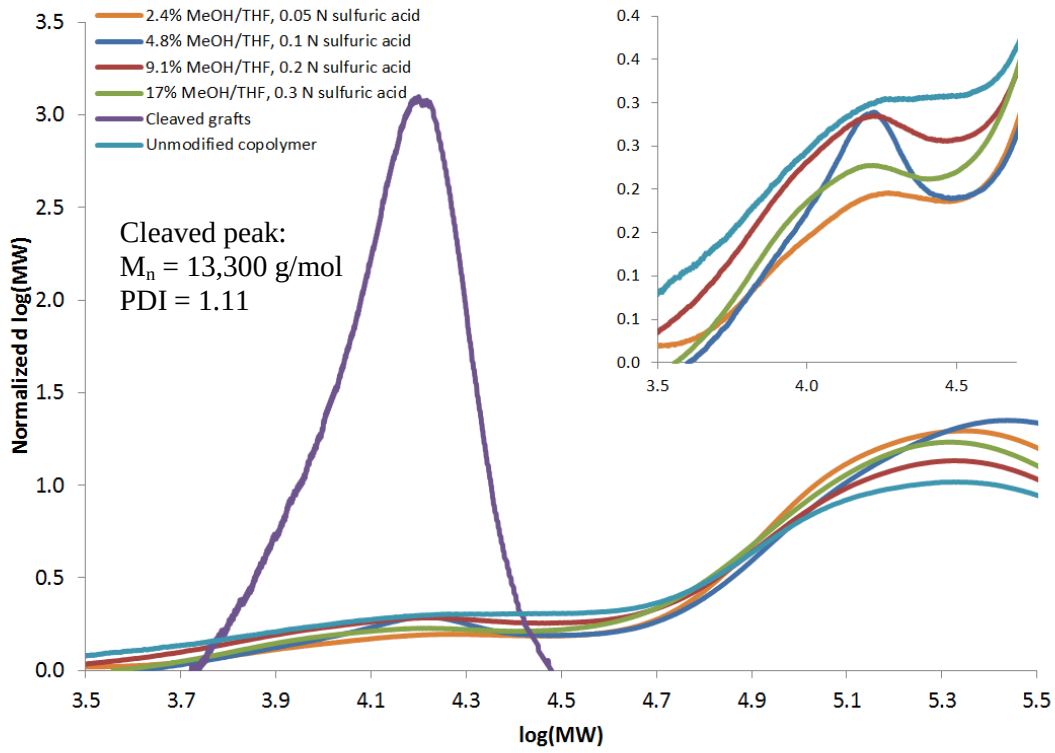

Figure 4.24: Identification of optimal conditions for the acid-catalyzed transesterification of G-PMA-1A. Main chart: distribution of cleaved grafts superimposed on distributions of entire samples. Inset: enlarged region of copolymer distribution where cleaved peak appears. While all reactions show some formation of a cleaved peak, only the 4.8% MeOH/THF solution shows a very clear peak forming.

The copolymer sample in Figure 4.24 had a hump in the shoulder that corresponded to the area where the cleaved peak appeared: this may indicate the presence of a small portion of un-grafted polymer, although that is not clear. The cleaved peak was not as symmetrical as the peak in Figure 4.22, but this is due to the fact that the copolymer shoulder for this sample was less linear and therefore skewed the integration more. The peak was still very narrow, with a polydispersity of 1.11 measured. All other transesterification reactions were conducted at these optimal conditions. However, only one sample grafted with PMMA (G-PMMA-1) resulted in the grafted chains being cleaved, and none of the chain extension samples resulted in successful

cleaving of the grafts; this was likely due to the very thick layer of PMA that the methanol would need to diffuse through.

4.4 Conclusions

Grafted chains of PMMA were grown from cellulose in EMIM AcO. However, the monomer was not miscible in the solvent leading to a dispersed phase reaction, and the macroinitiator was poorly soluble requiring long dissolution times. DMSO was used for the grafting instead due to the ease of use and reproducibility. The grafting of PMA from cellulose in DMSO appeared to proceed at a slower rate than EBiB; when scaling these values to the concentration of growing chains, the rate for Cell-BiB was about 60% to 70% of the rate for EBiB. This difference in rate is minor and appears to be consistent with the differences in ATRP equilibrium constant expected, and as such using EBiB to model the polymerization is an appropriate choice. Chain extension experiments from Cell-g-PMA demonstrated the living behaviour of the polymerization and the retention of bromine functionality. Graft density for the Cell-g-PMMA appeared to be limited by the slow initiation in the system (as demonstrated using EBiB), as once the chains began to grow they blocked any uninitiated BiB groups. The DS_{graft} obtained for PMMA grafting was 0.15 chains/ring. Graft density for the Cell-g-PMA may have been limited due to steric hindrance, as the average initiation efficiency for Cell-BiB was 63% (DS_{graft} 0.71), while that for EBiB was 96%. However, there was a large variation in efficiencies obtained (ranging from 45% to 92%) and it is possible that the efficiency was being limited for a similar reason as in the MMA system: not all BiB groups initiating simultaneously. While there was minimal evidence of intermolecular combination of cellulose occurring for the PMA grafting, it was prevalent for the PMMA grafting leading to very high molecular weight material of broad distribution being formed. Optimization of the system by using EBiB as a model initiator should allow these obstacles to be overcome.

Cleaving of chains grafted to cellulose was successfully accomplished via acid-catalyzed transesterification with methanol. However, only a small portion of the chains were cleaved, and there was a narrow window of solvent conditions were the reaction was successful, with 4.8 vol% MeOH/THF being the optimal point. This is thought to be due to the balancing of solvation of the polymer with adequate methanol concentration for the reaction. Using hydroxide to promote the reaction (as commonly done in the literature) was unsuccessful as this resulted in irreversible hydrolysis of the ester groups in PMA and PMMA.

4.5 Acknowledgements

The author would like to thank the financial support provided by the Ontario Ministry of Environment (Best in Science Program), by the Ontario Ministry of Research Innovation (Early Researcher Award Program, Dr. Pascale Champagne), by the Government of Ontario (Ontario Research Chair in Green Chemistry and Engineering, Dr. Michael F. Cunningham), and by Queen's University.

4.6 References

[1] E. Bianchi, E. Marsano, L. Ricco and S. Russo, "Free radical grafting onto cellulose in homogeneous conditions 1. Modified cellulose-acrylonitrile system," *Carbohydrate Polymers*, vol. 36, no. 4, pp. 313-318, 1998.

[2] Y. A. Aggour and E. Abdel-Razik, "Graft copolymerization of end allenoxy polyoxyethylene macromonomer onto ethyl cellulose in a homogeneous system," *European Polymer Journal*, vol. 35, no. 12, pp. 2225-2228, 1999.

[3] M. Tizzotti, A. Charlot, E. Fleury, M. Stenzel and J. Bernard, "Modification of polysaccharides through controlled/living radical polymerization grafting - towards the generation of high performace hybrids," *Macromolecular Rapid Communications*, vol. 31, no. 20, pp. 1751-1772, 2010.

[4] V. Raus, M. Stepanek, M. Uchman, M. Slouf, P. Latalova, E. Cadova, M. Netopilik, J. Kriz, J. Dybal and P. Vleck, "Cellulose-based graft copolymers with controlled architecture prepared in a homogeneous phase," *Polymer Chemistry*, vol. 49, no. 20, pp. 4353-4367, 2011.

[5] P. Vlcek, M. Janata, P. Latalova, J. Kriz, E. Cadova and L. Toman, "Controlled grafting of cellulose diacetate," *Polymer*, vol. 47, no. 8, pp. 2587-2595, 2006.

[6] E. Ostmark, S. Harrisson, K. L. Wooley and E. E. Malmstrom, "Comb polymers prepared by ATRP from hydroxypropyl cellulose," *Biomacromolecules,* vol. 8, no. 4, pp. 1138-1148, 2007.

[7] X. Sui, J. Yuan, M. Zhou, J. Zhang, H. Yang, W. Yuan, Y. Wei and C. Pan, "Synthesis of cellulose-graft-poly(N,N-dimethylamino-2-ethyl methacryalte copolymers via homogeneous ATRP and their aggregates in homogeneous media," *Biomacromolecules,* vol. 9, no. 10, pp. 2615-2620, 2008.

[8] M. Hiltunen, J. Siirila and S. L. M. Maunu, "Effect of catalyst systems and reaction conditions on the synthesis of cellulose-g-PDMAam copolymers by controlled radical polymerization," *Polymer Chemistry,* vol. 50, no. 15, pp. 3067-3076, 2012.

[9] M. S. Hiltunen, J. Raula and S. L. Maunu, "Tailoring of water-soluble cellulose-g-copolymers in homogeneous medium using single-electron-transfer living radical polymerization," *Polymer International,* vol. 60, no. 9,pp. 1370-1379, 2011.

[10] V. Percec, T. Guliashvili, J. S. Ladislaw, A. Wistrand, A. Stjerndahl, M. J. Sienkowska, M. J. Monteiro and S. Sahoo, "Ultrafast synthesis of ultrahigh molar mass polymers by metal-catalyzed living radical polymerization of acrylates, methacrylates, and vinyl chloride mediated by SET at 25^{O}C," *Journal of the American Chemical Society,* vol. 128, no. 43, pp. 14156-14165, 2006.

[11] Y. Zhang, Y. Wang, C.-h. Peng, M. Zhong, W. Zhu, D. Konkolewicz and K. Matyjaszewski, "Copper-Mediated CRP of Methyl Acrylate in the Presence of Metallic Copper: Effect of Ligand Structure on Reaction Kinetics," *Macromolecules,* vol. 45, no. 1, pp. 78-86, 2012.

[12] K. Matyjaszewski, "Atom Transfer Radical Polymerization: from mechanisms to applications," *Israel Journal of Chemistry,* vol. 52, no. 3-4, pp. 206-220, 2012.

[13] G. Lligadas, B. M. Rosen, M. J. Monteiro and V. Percec, "Solvent choice differentiates SET-LRP and Cu-mediated radical polymerization with non-first order kinetics," *Macromolecules,* vol. 41, no. 22, pp. 8360-8364, 2008.

[14] N. H. Nguyen and V. Percec, "Disproportionating versus nondisproportionating solvent effect in the SET-LRP of methyl acrylate during catalysis with nonactivated and activated Cu(0) wire," *Journal of Polymer Science Part A: Polymer Chemistry,* vol. 49, no. 19, pp. 4227-4240, 2011.

[15] P. Vlcek, V. Raus, M. Janata, J. Kriz and A. Sikora, "Controlled grafting of cellulose esters using SET-LRP process," *Journal of Polymer Science: Part A: Polymer Chemistry,* vol. 49, no. 1, pp. 164-173, 2010.

[16] J. Voepel, U. Edlund, A.-C. Albertsson and V. Percec, "Hemicellulose-based multifunctional macroinitiator for single-electron-transfer mediated living radical polymerization," *Biomacromolecules,* vol. 12, no. 1, pp. 253-259, 2011.

[17] U. Edlund and A.-C. Albertsson, "SET-LRP goes ‘green’: various hemicellulose initiating systems under non-inert conditions," *Polymer Chemistry,* vol. 50, no. 13, pp. 2650-2658, 2012.

[18] L. Dupayage, C. Nouvel and J.-L. Six, "Copper-mediated ATRP of MMA in DMSO from unprotected dextran macroinitiators," *Polymer Bulletins,* vol. 68, pp. 647-665, 2012.

[19] M. Billy, A. Ranzani Da Costa, P. Lochon, R. Clement, M. Dresch, S. Etienne, J. Hiver, L. David and A. Jonquieres, "Cellulose acetate graft copolymers with nano-structured architectures," *European Polymer Journal,* vol. 46, no. 3, pp. 944-957, 2010.

[20] P. Y. Bruice, Organic Chemistry, 5th ed., Toronto: Pearson Education Canada, Inc., 2007.

[21] R. M. Silverstein, F. X. Webster and D. J. Kiemle, Spectrometric Identification of Organic Compounds, 7th ed., Hoboken, NJ: John Wiley & Sons, Inc., 2005.

[22] L. Patiny, "nmrdb.org: Database of NMR Spectra," Ecole Polytechnique Fédérale de Lausanne, [Online]. Available: http://www.nmrdb.org/. [Accessed January 2013].

[23] S. Beuermann, D. Paquet, J. McMinn and R. Hutchinson, "Determination of free-radical propagation rate coefficients of butyl, 2-ethylhexyl, and dodecyl acrylates by pulsed-laser polymerization," *Macromolecules,* vol. 29, no. 12, pp. 4206-4215, 1996.

[24] T. Gruendling, T. Junkers, M. Guilhaus and C. Barner-Kowollik, "Mark-Houwink parameters for the universal calibration of acrylate, methacrylate, and vinyl acetate polymers determined by online size-exclusion chromatography - mass spectrometry," *Macromolecular Chemistry and Physics,* vol. 211, no. 5, pp. 520-528, 2010.

[25] R. A. Hutchinson, J. H. McMinn, D. A. J. Paquet, S. Beuermann and C. Jackson, "A pulsed-laser study of penultimate copolymerization propagation kinetics for methyl methacrylate/n-butyl acrylate," *Industrial & Engineering Chemistry Research,* vol. 36, no. 4, pp. 1103-1113, 1997.

[26] V. Percec and C. Grigoras, "Catalytic effect of ionic liquids in the Cu(I)O/2,2'-bipyridine catalyzed living radical polymerization of methyl methacrylate initiated with arenesulfonyl chlorides," *Journal of Polymer Science: Part A: Polymer Chemistry,* vol. 43, no. 11, pp. 5609-5619, 2005.

[27] P. Kubisa, "Ionic liquids as solvents for polymerization processes - Progress and challenges," *Progress in Polymer Science,* vol. 34, no. 12, pp. 1333-1347, 2009.

[28] B. H. Zimm and R. W. Kilb, "Dynamics of Branched Polymer Molecules in Dilute Solution," *Journal of Polymer Science,* vol. 37, no. 131, pp. 19-42, 1959.

[29] X. Jiang, B. M. Rosen and V. Percec, "Immortal SET-LRP mediated by Cu(0) wire," *Journal of Polymer Science: Part A: Polymer Chemistry,* vol. 48, no. 12, pp. 2716-2721, 2010.

[30] N. H. Nguyen, B. M. Rosen, G. Lligadas and V. Percec, "Surface-dependent kinetics of Cu(0)-wire-catalyzed Single-Electron Transfer Living Radical Polymerization of methyl acrylate in DMSO at 25^{O}C," *Macromolecules,* vol. 42, no. 7, pp. 2379-2386, 2009.

[31] F. Nystrom, A. H. Soeriyadi, C. Boyer, P. B. Zetterlund and M. R. Whittaker, "End-group fidelity of copper(0)-mediated radical polymerization at high monomer conversion: an ESI-MS investigation," *Journal of Polymer Science Part A: Polymer Chemistry,* vol. 49, no. 24, pp. 5313-53-21, 2011.

[32] W. Tang, Y. Kwak, W. Braunecker, N. V. Tsarevsky, M. L. Coote and K. Matyjaszewski, "Understanding atom transfer radical polymerization: effect of ligand and initiator structures on the equilibrium constants," *Journal of the American Chemical Society,* vol. 130, no. 32, pp. 10702-10713, 2008.

[33] B. Stone, "Cellulose: structure and distribution," *eLS,* 2005.

[34] A. Gosnell, D. Woods, J. Gervasi, J. Williams and V. Stannett, "The intrinsic viscosity of graft copolymers in mixed solvents," *Polymer,* vol. 9, pp. 561-565, 1968.

[35] J. Wellons, J. Williams and V. Stannett, "Preparation and characterization of some cellulose graft copolymers. Part IV. Some properties of isolated cellulose-acetate-stryrene graft copolymers," *Journal of Polymer Science Part: A,* vol. 5, no. 6, pp. 1341-1357, 1967.

[36] S. Krishnamoorthi, D. Mal and R. Singh, "Characterization of graft copolymer based on polyacrylamide and dextran," *Carbohydrate Polymers,* vol. 69, no. 2, pp. 371-377, 2007.

[37] D. Biswal and R. Singh, "Characterization of carboxymethyl cellulose and polyacrylamide graft copolymer," *Carbohydrate Polymers,* vol. 57, no. 4, pp. 379-387, 2004.

[38] S. Fleischmann, B. M. Rosen and V. Percec, "SET-LRP of acrylates in air," *Journal of Polymer Science: Part A: Polymer Chemistry,* vol. 48, no. 5, pp. 1190-1196, 2010.

[39] S. Fleischmann and V. Percec, "SET-LRP of methyl methacrylate initiated with sulfonyl halides," *Journal of Polymer Science: Part A: Polymer Chemistry,* vol. 48, no. 10, pp. 2236-2242, 2010.

[40] D. Shen and Y. Huang, "The synthesis of CDA-g-PMMA copolymers through atom transfer radical polymerization," *Polymer,* vol. 45, no. 21, pp. 7091-7097, 2004.

[41] D. Shen, H. Yu and Y. Huang, "Densely grafting copolymers of ethyl cellulose through atom transfer radical polymerization," *Journal of Polymer Science Part A: Polymer Chemistry,* vol. 43, no. 18, pp. 4099-4108, 2005.

[42] T. Meng, X. Gao, J. Zhang, J. Yuan, Y. Zhang and J. He, "Graft copoloymers prepared by atom transfer radical polymerization (ATRP) from cellulose," *Polymer,* vol. 50, no. 2, pp. 447-454, 2009.

[43] L. Chun-xiang, Z. Huai-yu, L. Ming-hua, F. Shi-yu and Z. Jia-jun, "Preparation of cellulose graft poly(methyl methacrylate) copolymers by atom transfer radical polymerization in an ionic liquid," *Carbohydrate Polymers,* vol. 78, no. 3, pp. 432-438, 2009.

[44] G. Moad and D. H. Solomon, The Chemistry of Radical Polymerization, 2nd Ed., Boston: Elsevier 2005.

Chapter 5

Synthesis of Cellulose Graft Copolymers Using Thiol-Ene Addition and a 'Grafting-to' Approach

Abstract

Cellulose is an abundant, renewable polymer, but it often requires modification in order to overcome barriers to its use. Graft copolymers that have a cellulose backbone and synthetic polymer arms are one way to tailor the properties of the cellulose. Research in this area has focused primarily on using a 'grafting-from' mechanism, whereby chains are polymerized outwards from the cellulose substrate. 'Grafting-to', where fully formed chains are attached to the cellulose, has received much less attention but has some potentially beneficial characteristics, including ease of characterizing side chains, reduced intermolecular termination between growing chains, and optimized polymerization conditions for the growth of the synthetic arms as the polymerization is not limited by the solubility of the cellulose macroinitiator.

Thiol-ene Michael addition is a robust, fast, and high yield reaction that was explored for the grafting step. An Atom Transfer Radical Polymerization (ATRP) initiator with a cleavable internal disulfide bond was chosen to give the synthetic polymer sulfide functionality. Cu(0)-mediated ATRP from this initiator yielded good control over poly(methyl acrylate) (PMA) molecular weights, but less control for poly(methyl methacrylate) (PMMA). Subsequent reduction of the disulfide and reaction with cellulose acetate (functionalized with methacrylate groups) yielded a graft copolymer with a cellulose acetate backbone and synthetic polymer arms. The efficiency of the grafting reaction was limited by the sulfide functionality of the polymers. The cellulose acetate/methacrylate could also react quantitatively with thiophenol and dodecanethiol, demonstrating the versatility of this reaction for attaching functional groups to cellulose.

5.1 Introduction

Cellulose is the most abundant renewable polymer on Earth, with about 100 billion tons produced every year [1]. Its relative abundance makes it an attractive alternative to petroleum-based feedstocks for polymers and synthetic materials. However, its poor solubility in common solvents and hygroscopic nature can be obstacles to widespread use. Consequently, cellulose is often modified in order to tailor its properties. The most common modification (resulting in a wide range of commercially available products) involves the synthesis of so-called cellulose derivatives, where some or all of the hydroxyl groups have been replaced with other functional groups: 0.9 million tons of cellulose acetate and 3.2 million tons of cellulose xanthate are produced annually [2]. Of more recent interest are cellulose copolymers with unique architectures, consisting of synthetic/renewable polymer hybrids. Such architectures include: cellulose chains with a synthetic polymer block [3, 4]; graft copolymers with a cellulose backbone and synthetic polymer branches [5, 6]; gels and interpenetrating networks of polymers [7-9]; and grafting of polymers from solid cellulose surfaces, including particles, fibres, and sheets [5, 6, 10, 11].

In the synthesis of cellulose graft copolymers there are two main approaches, known as 'grafting-from' and 'grafting-to', with the 'grafting-from' approach being more common [6]. With 'grafting-from', initiation sites are formed on the cellulose backbone and polymer chains are grown outwardly from these. The polymerizations are done using both conventional [12, 13] and controlled radical mechanisms [5], including Reversible Addition Fragmentation (Chain) Transfer (RAFT), Atom Transfer Radical Polymerization (ATRP), and Nitroxide Mediated Polymerization (NMP). In theory, a controlled 'grafting-from' mechanism should allow for a well-tailored, controlled growth of polymer and high density of grafted chains, but in practice problems are encountered with combination of the cellulose molecules due to bimolecular termination of growing chains on different cellulose molecules [14-18], poor initiation efficiency [14, 19], and difficulties in characterizing the side chains and final copolymer [17, 16].

With the ‘grafting-to’ approach, fully formed (and characterized) chains with appropriate end-group functionality are attached to the backbone polymer. This should allow for easier characterization of the copolymer and avoid intermolecular combination of the combs, although if grafting is incomplete the separation of the homopolymer can be problematic. Part of the reason that a ‘grafting-to’ approach receives less attention is that it is thought to have a lower possible graft density due to steric hindrance [5]; however, if the goal is to have a high cellulose content in the final copolymer this may not be a serious problem. In addition, there is well-established literature on various controlled polymerization techniques, and growing the grafts separately from the backbone would allow this knowledge to be directly applied under optimal polymerization conditions (i.e. conditions that might not be possible for a ‘grafting-from’ polymerization due to restrictions imposed by the macroinitiator, such as solubility and initiator concentration).

To date, there are a handful of papers detailing the synthesis of graft copolymers with a cellulose acetate backbone [20, 21] and with a synthetic backbone and cellulose acetate arms [22] using a ‘grafting-to’ approach. With cellulose acetate employed as the backbone polymer, poly(styrene) was prepared by anionic polymerization and then attached to the free hydroxyls of the cellulose acetate via esterification. The grafting densities were low (the highest had a degree of substitution (DS) of 0.078), and decreased with increasing molecular weight of the grafts [20, 21]. A polymer consisting of synthetic backbone with grafted cellulose acetate (oligomer) arms used the azide/alkyne ‘click’ reaction and reached a much higher grafting density of 0.44 cellulose acetate arms per synthetic repeat unit [22]. However, the cellulose acetate arms had a degree of polymerization (DP) of only 13.

In the work presented here, it was hypothesized that using a more reactive mechanism than esterification for the grafting reaction would allow higher graft densities. It was also desired to create a method that could be applicable to a wider range of controlled radical polymerization techniques, including ATRP, and that the reactive functionality be a part of the initiator in order to avoid post-polymerization end-modification of the polymer chains. An initiator with an

internal disulfide bond was chosen to allow for subsequent reduction to sulfide and use in thiol-ene addition reactions. Thiol-ene chemistry has been utilized for 'click' applications, including ultraviolet (UV)-induced 'click' [7, 8, 23] as well as Michael addition of activated alkenes [24, 25]. This mechanism is also useful for RAFT-made polymers, as the RAFT end group can be reduced to a sulfide; this has been used to make star polymers using thiol-ene Michael addition [24]. The thiol-ene reaction allows near quantitative yields under mild conditions, is extremely rapid, and is relatively insensitive to water and oxygen [26]; it was therefore seen as a promising reaction for cellulose modification and grafting.

5.2 Experimental

5.2.1 Materials

Copper (II) bromide (98%), bis(2-hydroxyethyl) disulfide (BHEDS, technical grade), N,N'-dicyclohexylcarbodiimide (DCC, 99%), 4-(dimethylamino) pyridine (DMAP, 99%), tris[2-(dimethylamino)ethyl]amine (Me_6TREN), Tris(2-aminoethyl)amine (TREN, 96%), 2-bromobutyric acid (97%), sodium borohydride ($NaBH_4$, 99.99%), DL-dithiotheitol (DTT, 99%), mercaptoethanol (ME, 99%), thiophenol (97%), dodecanethiol (98%), hexylamine (HA, 99%), and triethylamine (TEA, 99%) were purchased from Sigma-Aldrich and used without further modification. Copper electrical wire (14 gauge) was submerged in sulfuric acid and rinsed with acetone prior to immediate use. Methyl methacrylate (MMA, 99%) and methyl acrylate (MA, 99%) were obtained from Sigma-Aldrich, passed through a column to remove inhibitor, and stored in the refrigerator prior to use. Tetrahydrofuran (THF) was distilled and dried with magnesium sulfate prior to use. All other solvents were used as received. The syntheses of Cell-AcO-GMA, CA-GMA, and CA-MAA samples were discussed in Chapter 3.

5.2.2 Synthesis of sulfide-terminated polymers

5.2.2.1 Synthesis of bis[2-(2-bromobutyrate)ethyl] disulfide [$(BrBE)_2S_2$]

The bifunctional ATRP initiator containing an internal disulfide linkage was synthesized using a procedure modified from Tsarevsky and Matyjaszewski [27, 28]. BHEDS (4.9 g, 1 eq. of hydroxyls) was dissolved in 100 mL THF. This solution was then immersed in an ice/water bath and 2-bromobutyric acid (6.9 mL, 1 eq.) was added, followed by DCC (13.2 g, 1 eq.) dissolved in 50 mL of THF. A solution of DMAP (0.18 g, 0.05 eq.) in 5 mL of THF was added drop-wise. The resulting heterogeneous mixture was stirred for 18 h and then filtered to remove the precipitated dicyclohexylurea; the precipitate was washed with THF on the filter paper. Solvent was removed from the filtrate by rotary evaporation at 50^{O}C and the resultant turbid oil was filtered to remove crystallized impurities. The filtrate was kept under vacuum (-20 inHg) for three more days to further remove solvent and then stored in the refrigerator (4^{O}C) overnight and filtered again to yield the final product, a viscous, yellow liquid. Yield: 11.2 g (81%), 92% functional by nuclear magnetic resonance (NMR; 8% unreacted alcohols remaining). The specific gravity was measured to be 1.38 at 4^{O}C.

5.2.2.2 Polymerization from $(BrBE)_2S_2$

In a typical polymerization, 15 mL of MA (100 eq.) and 7.5 mL of anhydrous DMSO were added to a round-bottom flask along with 10 cm of copper wire (cut into 8 equal-sized pieces) and 18.6 mg of $CuBr_2$ dissolved in 0.29 mL of acetonitrile (0.05 eq.). The flask was placed in a 50^{O}C oil bath and sparged with nitrogen for at least 45 minutes. At this point, 44 µL of Me_6TREN (0.1 eq.) was added followed by 0.30 mL of $(BrBE)_2S_2$ (1 eq.) to start the reaction. Samples were withdrawn periodically from the reactor for 1 hour at which point the poly(methyl acrylate) (PMA) was precipitated and washed with water. The samples were injected into NMR tubes, diluted with chloroform-d, and stored in the freezer prior to conversion measurements by

NMR. The samples were then diluted with acetone, filtered through basic aluminum oxide, and the solvent was evaporated under air. The dried samples were dissolved in THF for analysis by gel permeation chromatography (GPC).

5.2.2.3 Substitution of bromine functional groups on polymer chain ends with thiophenol

Poly(methyl methacrylate) (PMMA) with M_n of 10,400 g/mole (6.9 g, 1 eq. bromine) was dissolved in 20 mL of DMF at 40^{O}C and sparged with nitrogen for 30 minutes, after which TEA (0.18 mL, 1 eq) and thiophenol (0.14 mL, 1 eq.) were added. The mixture was stirred for 2 hours followed by precipitation in water/methanol. The precipitate was filtered, washed with methanol (MeOH), and then dissolved in acetone and re-precipitated in water/MeOH followed by a final washing in MeOH. The final dried product had no remaining odour of thiol and was analyzed by NMR and GPC.

5.2.2.4 Redox of internal disulfide of polymer chains

PMA with M_n of 11,900 g/mol (11.9 g) was dissolved in 60 mL of DMF and sparged with nitrogen in a 60^{O}C oil bath. After 45 minutes of purging, $NaBH_4$ (0.69 g, 0.30 M solution) was added to start the reaction. After 2 h, the reactor contents were cooled in an ice bath and added slowly to cold, acidic water to precipitate. **Flammable decomposition gases evolve**. The polymer was washed with water (or MeOH in the case of PMMA), re-dissolved in THF, and then precipitated again. This cycle was repeated several times. For several samples the polymer was also dialyzed against THF in dialysis tubing with a molecular weight cut-off of 3,500 g/mol. The same reduction procedure was also used with DTT or mercaptoethanol as the reducing agent instead of $NaBH_4$, except that enough TEA to make a 0.1 M solution was added as well.

To oxidize the sulfides back to their original disulfide form, approximately 0.05 g of reduced and purified polymer was dissolved in an equal-volume mixture of THF and DMF (~2

mL). The solution was then heated at 60^{O}C for 24 hours, at which point the solvent was removed by drying under air. Redox reactions were characterized by GPC.

5.2.3 Modification of cellulose acetate with thiol-ene Michael addition

5.2.3.1 Model thiol-ene addition with methyl methacrylate and thiophenol

To 2.5 mL of DMF, 0.16 mL of MMA was added (1 eq.; 0.6 M solution). The catalyst hexylamine (0.20 mL, 0.6 M) or triethylamine (0.21 mL, 0.6 M) was then added and the solution placed in a 30^{O}C oil bath. After sparging with nitrogen for 30 minutes, 0.18 mL of thiophenol (1.2 eq) was added to start the reaction. Samples were withdrawn, diluted with chloroform-d, and cooled on ice. Conversion was determined by the ratio of phenyl to alkene signals in the NMR spectrum.

5.2.3.2 Model thiol-ene addition with $CA_{2.77}$-$MAA_{0.13}$ and thiophenol

To 6 mL of DMF, 0.10 g of $CA_{2.77}$-$MAA_{0.13}$ (1 eq.; sample MAA3T from Chapter 3) and 0.48 mL of hexylamine (0.6 M) were added. The reactor was placed in a 30^{O}C oil bath and sparged with nitrogen for 30 minutes. The reaction was begun by injecting 34 μL of thiophenol (1.2 eq.). After 24 hours, water was added to precipitate the product which was collected by filtration. The product was subsequently washed with methanol three times, followed by two washings with pentane to remove the hydrophobic thiophenol. The sample was analyzed by NMR and GPC.

5.2.3.3 Model thiol-ene addition with Cell-$AcO_{2.02}$-$GMA_{0.98}$ and dodecanethiol

To 10 ml of DMSO, 0.19 g of Cell-$AcO_{2.02}$-$GMA_{0.98}$ (1 eq. of alkene; sample GMA2T from Chapter 3) was added and allowed to dissolve at 50^{O}C. Upon formation of a transparent solution, 0.17 mL of TEA (0.12 M) and 0.15 mL of dodecanethiol (1.5 eq.) were added. The reaction was stopped after 24 hours by precipitation in water, followed by washing three times

with MeOH. The solvent was evaporated under air and the product was washed twice with pentane before being dried in a vacuum oven (40^{O}C, -20 inHg) for 24 hours. The sample was analyzed by NMR.

5.2.3.4 Grafting of synthetic chains onto $CA_{2.77}$-$MAA_{0.13}$

To 3 mL of DMF, 0.051 g of $CA_{2.77}$-$MAA_{0.13}$ (1 eq. of alkene; sample MAA3T from Chapter 3) and 0.24 mL of hexylamine (0.6 M) were added. The solution was sparged with nitrogen at 30^{O}C for 45 minutes at which time 0.10 g of reduced PMMA (0.11 eq. of sulfide) or PMA was added. The reaction was stirred for 24 hours and then a sample was withdrawn. The remainder of the solution was stirred for an additional 24 hours before the reaction was stopped. Solvent was evaporated under air and the samples were further dried in a vacuum oven (40^{O}C, -20 inHg) for 24 hours before analysis by GPC.

5.2.3.5 In-situ reduction and grafting of synthetic chains onto $CA_{2.77}$-$MAA_{0.13}$

To 3 mL of DMF, 0.050 g of $CA_{2.77}$-$MAA_{0.13}$ (1 eq. of alkene; sample MAA3T from Chapter 3), 0.24 mL of hexylamine (0.6 M) were added, followed by 0.10 g of PMA or PMMA. The solution was sparged with nitrogen at 60^{O}C for 45 minutes at which time 0.030 g of $NaBH_4$ (0.3 M) was added to start the reaction. After 45 minutes, water and then HCl were added to the mixture to precipitate the product and decompose the $NaBH_4$. The samples were washed with water, dried under air, and further dried in a vacuum oven (40^{O}C, -20 inHg) for 24 hours before analysis by GPC.

5.2.4 Characterization

5.2.4.1 Nuclear Magnetic Resonance (NMR)

^{1}H (64 scans) and Heteronuclear Single Quantum Correlation (HSQC; 12 scans) NMR spectroscopy were used to identify the samples, and to predict conversion and degree of substitution. Spectra were obtained on a 400 MHz Bruker Avance instrument. Degree of substitution (DS) of the functionalized cellulose was obtained by comparing the relative areas of the cellulose backbone (anhydroglucose units; AGU) protons and the attached functional group in ^{1}H NMR. Spectra were assigned using information from [29], [30], and [31].

5.2.4.2 Gel Permeation Chromatography (GPC)

The homopolymer samples of PMA and PMMA were analyzed on a Waters 2695 separations module using a model 410 differential refractometer as detector. Five Waters Styragel HR columns (guard, HR 4.0, HR 3.0, HR 1.0, HR 0.5) were used in series at a temperature of 40^{O}C. Distilled THF was used as the eluent at a flow rate of 1.0 mL/min. The system was calibrated using poly(styrene) (PS) standards with narrow molecular weights ranging from 374 to 400 x 10^{3} g/mol. The molecular weights obtained using the poly(styrene) calibration were corrected using the Mark-Houwink parameters summarized in Table 5.1. The correction can be made through the use of the Mark-Houwink equation (Equation 5-1)

$$[\eta] = K(MW)^{\alpha} \qquad \textbf{Equation 5-1}$$

Table 5.1: Summary of Mark-Houwink parameters.

Polymer	T (^{0}C)	Molecular Weight for Measurements (g/mole)	K/10^{-3} (mL/g)	α	Ref.
PS	30	-	11.4	0.716	[32]
PMA	30	<20,000	6.11	0.799	[33]
PMMA	30	100,000	9.44	0.719	[34]

The cellulose derivatives and copolymers were analyzed using a Viscotek GPCmax VE-2001 with a model VE 3580 refractive index (RI) detector, and a model 270 dual detector [light scattering (low angle light scattering, and right angle light scattering) and viscosity]. Three PolyAnalytik columns (2 x PAS-106, guard) with an exclusion molecular weight of 20 x 10^6 g/mol were used in series at a temperature of 40^{O}C. Distilled THF was used as the eluent at 1.0 mL/min. The triple detection system was calibrated using a narrow poly(styrene) sample of 93 x 10^3 g/mol, with refractive index increment (dn/dc) of 0.185 mL/g and intrinsic viscosity ([η]) of 0.465 dL/g. The molecular weight analysis was performed using the Viscotek OmniSEC software. It is important that the concentration of these samples be accurately known for the molecular weight calculations.

5.3 Results and discussion

5.3.1 Synthesis of sulfide-terminated synthetic polymers

5.3.1.1 Synthesis of $(BrBE)_2S_2$

Scheme 5.1 displays the reaction for the synthesis of $(BrBE)_2S_2$. The $(BrBE)_2S_2$ was analyzed using ^{1}H NMR with the spectrum recorded in methanol-d_4. From Figure 5.1, the functionality of the initiator was calculated to be 92% by comparing the areas of the CH_2S protons in the reacted and unreacted compounds: δ = 2.9 ppm (f) for the protons adjacent to the unreacted alcohol; and δ = 3.0 ppm (e) for the protons adjacent to the ester. All of the diol was assumed to have been consumed in the reaction, with the unreacted alcohol being located on mono-functional initiators. Some unidentified signals appear in the region δ = 1.2 – 2.0 ppm indicating some impurities were still present. The negligible signal at 3.71 ppm shows that THF has been fully removed.

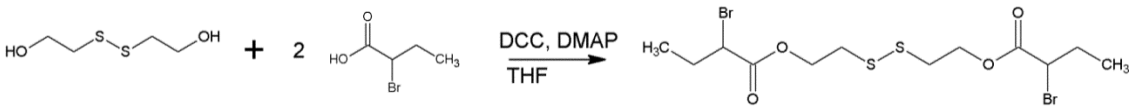

Scheme 5.1: Synthesis of $(BrBE)_2S_2$

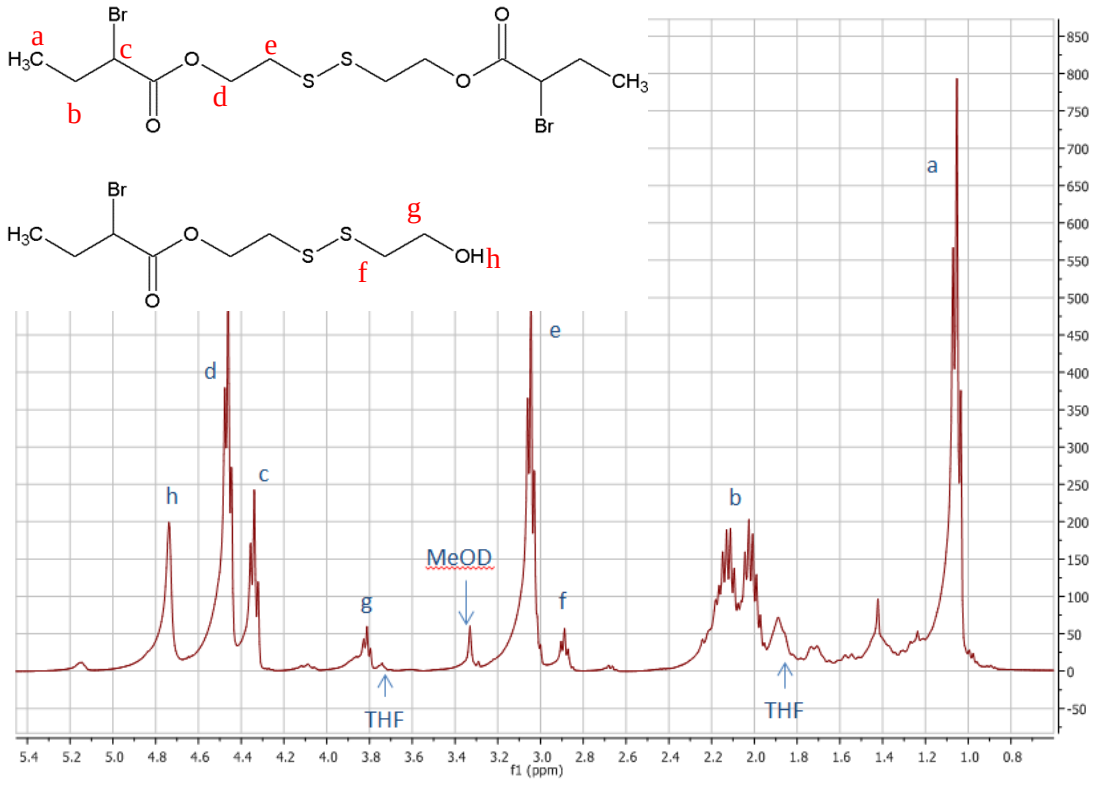

Figure 5.1: ^{1}H NMR spectrum of $(BrBE)_2S_2$ in methanol-d_4.

5.3.1.2 Polymerization of methyl acrylate and methyl methacrylate from $(BrBE)_2S_2$

The poly(methyl acrylate) had a targeted DP that varied from 100 to 200 (per sulfide, so length of disulfide containing chain would be approximately 200 to 400). It was expected that longer chains would result in less efficient grafting and lower graft density due to steric effects and so the DP of the chains was kept low. However, too low of a molecular weight made the polymer very difficult to separate and purify as it became more soluble in water and alcohols, particularly after the disulfide bond had been cleaved. The poly(methyl methacrylate) chains had a lower targeted DP of 20 to 100, reflecting the fact that this polymer was less soluble in water and methanol, and therefore easier to purify.

The polymerizations of methyl acrylate from $(BrBE)_2S_2$ are summarized in Table 5.2. Entry PMA8 (used for the grafting in section 5.3.2.4) is discussed in detail here to highlight the typical features and important observations of these polymerizations. The polymerization of PMA8 was fast with 82% conversion being reached after 60 minutes, but the time dependence of ln([M(0)]/[M(t)]) was non-linear and showed a decreasing radical concentration (decreasing slope, Figure 5.2). The measured molecular weight decreased steadily below the predicted value as conversion increased, which was a recurring observation in the polymerization of MA. The molecular weight distributions showed low molecular weight tailing that was attributed to monofunctional initiator species (see Figure 5.3); this low molecular weight tailing appeared to increase with intensity throughout the reaction, but nonetheless the PDI remained below 1.2 throughout. For some polymerizations (e.g. PMA6), the low molecular weight tailing became pronounced enough to show a distinct second peak due to mono-functional chains.

It should be noted that with the bifunctional initiators, the ratio of predicted-to-measured molecular weight does not correspond directly to the actual initiator efficiency (IE) as it would with monofunctional initiators. For example, if all the bifunctional initiators grew chains in only one direction (rather than both directions) the measured molecular weight would still be the same as the predicted molecular weight, despite the initiator efficiency being only 50%. If initiation is incomplete, it would be reasonable to expect a mixture of $(BrBE)_2S_2$ initiated on one side, both sides, and neither side, with more of the bi-initiated species at higher initiation efficiency and more of the non-initiated species existing at lower initiating efficiencies. Thus, molecular weights of the chains after scission of the disulfide bond should be used for initiator efficiency calculations. Redox reactions of the disulfide bond will be discussed later, but reduction of the bond for this sample (PMA8) allowed an initiation efficiency of 108% to be calculated; the reason for this being higher than 100% is expected to be due to the error involved in the reduction process. The average initiator efficiency for all PMA samples was 101% indicating all the bromine groups initiate in the MA polymerization within the margin of error.

Table 5.2: Summary of polymerizations with MA.

Sample	[M] (Vol%)	[M]:[L]:[Cu(II)]	Conv. (%)	Meas. M_n (g/mol)	Pred. M_n (g/mol)	PDI	Meas. M_n after reduction (g/mol)	Pred. M_n after reduction (g/mol)	PDI after reduction	IE (%)
PMA1	50	95:0.1:0.05	86	13,100	13,200	1.21	-	7,030	-	-
PMA2	50	160:0.1:0.05	84	16,300	21,700	1.21	-	11,600	-	-
PMA3	50	200:0.1:0.05	69	15,900	22,400	1.23	-	11,900	-	-
PMA4	67	120:0.1:0.05	85	13,400	16,600	1.20	8,890	8,760	1.17	99
PMA5	67	100:0.1:0.05	81	12,000	12,900	1.16	7,070	7,000	1.08	99
PMA6	67	100:0.1:0.05	87	11,900	13,700	1.13	7,020	7,470	1.07	106
PMA7	67	100:0.2:0.05	98	15,800	15,400	1.17	9,050	8,440	1.13	93
PMA8	73	200:0.1:0.05	82	21,700	26,700	1.13	13,100	14,100	1.10	108

Table 5.3: Summary of polymerizations with MMA.

Sample	[M] (Vol%)	[M]:[L]:[Cu(II)]	Conv. (%)	Meas. M_n (g/mol)	Pred. M_n (g/mol)	PDI	Meas. M_n after reduction (g/mol)	Pred. M_n after reduction (g/mol)	PDI after reduction	IE (%)
PMMA1	50	50:0.1:0.05	51	12,700	4,850	1.81	-	2,780	-	-
PMMA2	67	100:0.1:0.05	54	24,000	10,100	1.70	17,000	5,390	1.49	32
PMMA3	67	20:0.2:0.05[+]	59	10,400	2,160	1.83	12,300	1,180	1.79	9.6
PMMA4	67	50:0.2:0.05	68	15,400	6,210	1.64	14,200	3,380	1.49	24
PMMA6	73	50:0.1:0.05	43	17,900	4,050	1.59	14,300	2,030	1.61	14

[+]TREN as ligand

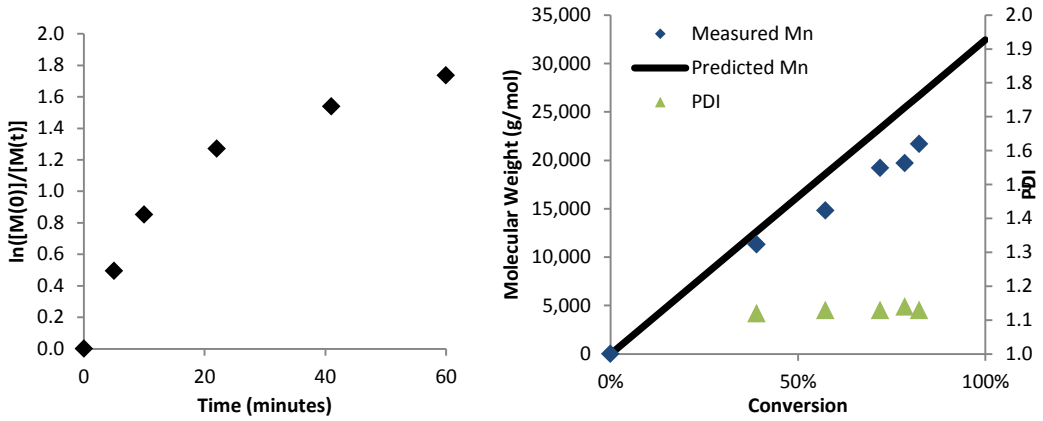

Figure 5.2: Kinetic plots for polymerization of PMA8. [MA]:[L]:[Cu(II)] = 200:0.1:0.05.

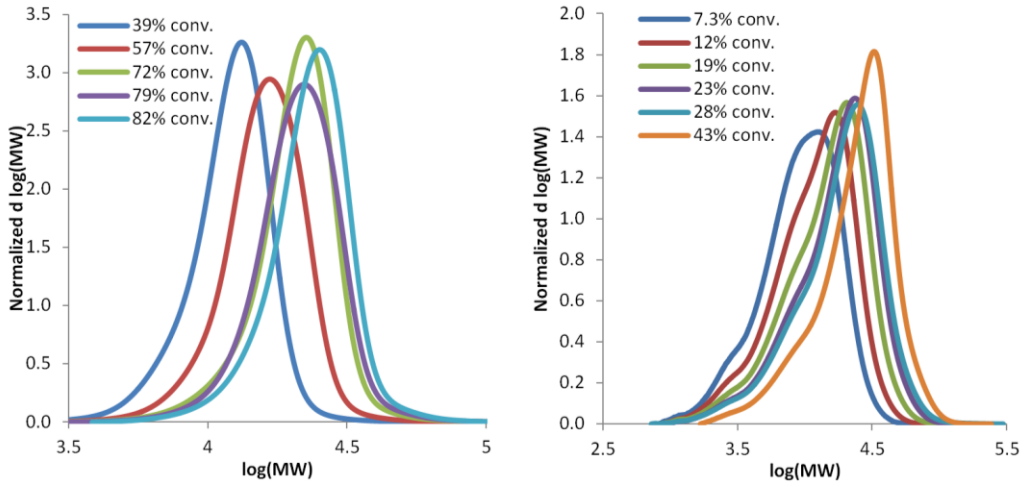

Figure 5.3: Molecular weight distributions of PMA8 (left) and PMMA6 (right).

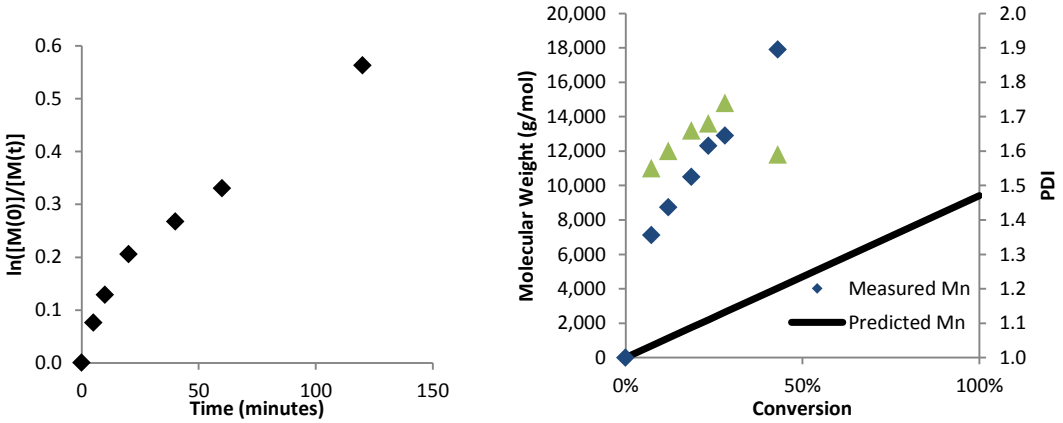

Figure 5.4: Kinetic plots for polymerization of PMMA6**.** [MMA]:[L]:[Cu(II)] = 50:0.1:0.05.

Table 5.3 summarizes the polymerizations of methyl methacrylate from $(BrBE)_2S_2$. When MMA was used as the monomer, polymerization was slower compared to MA. Sample PMMA6 (used for the grafting in section 5.3.2.4) is discussed here, and obtained a conversion of 43% conversion after 120 minutes (although with four times the initiator concentration as PMA6). The PMMA samples did not reach complete conversion under the conditions studied here as once the solutions reached between 60% and 80% (depending on the solvent concentration and targeted molecular weight) the solution would become highly viscous (too viscous to stir) and the reaction would be stopped. Note that gelling did not occur, as there was no crosslinking, loss of solubility, or severe increase in the PDI observed. The kinetic plot for PMMA6 showed a non-linear time dependence of ln([M(0)]/[M(t)]) (Figure 5.4); a decreasing radical concentration was commonly observed in the other MMA polymerizations, although some experiments (such as PMMA3) showed an increasing concentration. In contrast to the MA polymerizations, the molecular weights obtained using MMA were substantially higher than the predicted values, indicating low initiation efficiency. This may partially explain the broadness of the PMMA distributions (final PDI 1.59) as a mixture of bi- and mono-initiated chains would increase the bimodal nature of the distribution (see Figure 5.3 and Figure 5.11). Low initiation efficiencies with MMA in Cu(0)-mediated polymerization were observed in Chapter 4 and have been reported elsewhere [35, 36].

Initiation efficiency of sample PMMA6 was calculated to be 14% with an average for all reactions of 20%; this resulted in substantially higher molecular weights obtained than was desired. As shown in Figure 5.5, the initiation efficiency decreased as the targeted DP was decreased (i.e. as the initiator concentration was increased). In order to obtain low molecular weights, a high monomer-to-initiator ratio (high targeted DP) with low conversion should be targeted instead. A more detailed analysis is necessary to study the initiator efficiency issue with MMA.

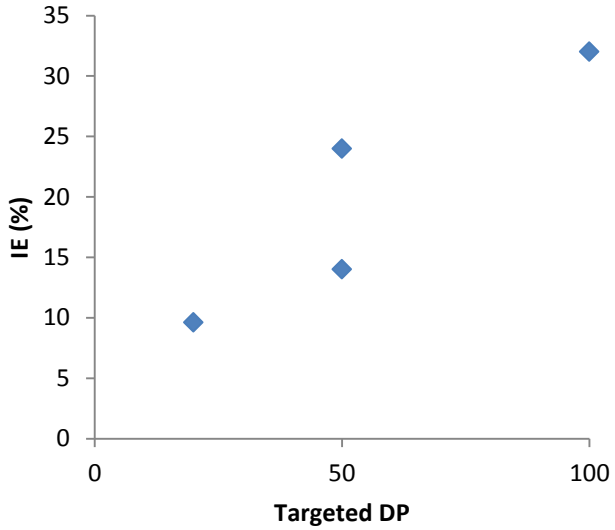

Figure 5.5: Initiation efficiency vs. targeted DP in MMA polymerizations from Table 5.3. Initiation efficiency is correlated with targeted DP. Polymerization conditions ([M]:[L]:[Cu(II)]): PMMA2, 100:0.1:0.05; PMMA3, 20:0.2:0.05; PMMA4, 50:0.2:0.05; PMMA6, 50:0.1:0.05.

As seen in Table 5.2, the initiator efficiencies calculated for the MA polymerizations were high, with an average of 101% for the five samples measured. However, as Figure 5.6 shows, the measured molecular weights of the unreduced samples were in almost all cases significantly less than the predicted values. M/P is defined here as the ratio of measured M_n to predicted M_n; an M/P less than unity means that there are more chains present than expected. An M/P less than unity was observed for the unreduced samples, but since the reduced chains had an M/P of ~1 there could not have been more chains initiating than there should have been. Instead, it appears that the disulfide bond was being partially reduced during the polymerization. As Cu(0)-mediated ATRP operates via a redox equilibrium with Cu(0) acting as a reducing agent assisted by a ligand, it should not be surprising to see the disulfide bond capable of being partially reduced under these conditions. Previous studies using Cu(I)-mediated polymerizations and a disulfide containing initiator [27, 28] did not report any interaction with the disulfide bond, but the catalyst/ligand/solvent systems used were not the same as those used here. The initiation

efficiency of the PMMA samples had an average of only 20%; thus, it was more difficult to observe whether the disulfide bonds were being reduced for these.

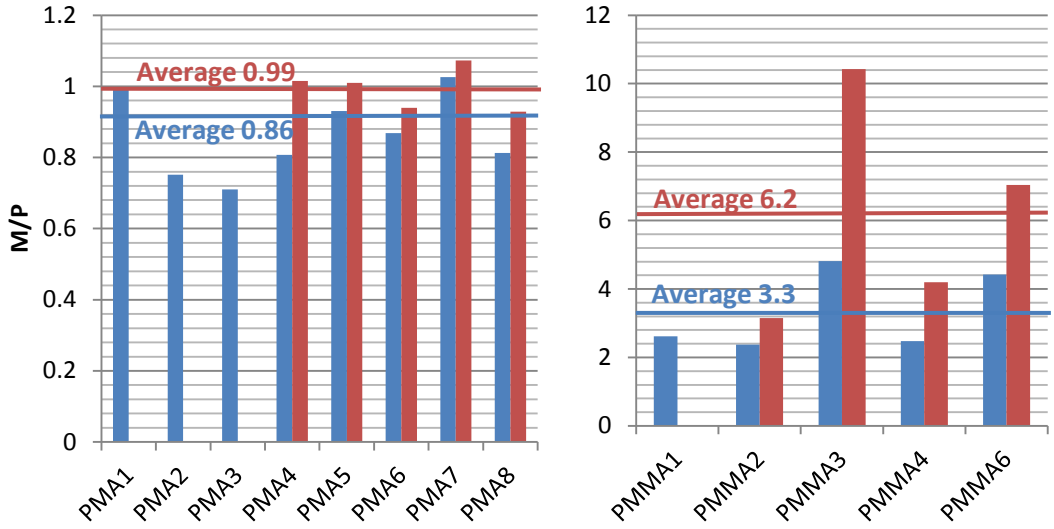

Figure 5.6: Ratio of measured molecular weight to predicted molecular weight for PMA samples (left) and PMMA samples (right). Unreduced samples are in blue; reduced samples are in red. The lower M/P ratio for unreduced samples than reduced samples suggests that the disulfide bond was being reduced during the polymerization.

When comparing sample PMA6 with PMA7 (a sample produced under the same conditions as PMA6 except with twice the ligand concentration) some interesting trends were observed in the kinetics. Overlaying the two plots shows that PMA7 proceeded at a faster rate (Figure 5.7), and that the value of M/P for PMA7 was about 1 while that for PMA6 was less than 0.9; this suggests that PMA7 was not being reduced, and proceeded at a faster rate than PMA6 which was being reduced. If the disulfide bond is not inert in the reaction but is instead being reduced by the catalyst, presumably this would affect the polymerization kinetics. A decrease in the amount of reduced catalyst relative to oxidized catalyst would decrease the ATRP equilibrium constant and thereby decrease the concentration of radicals as well as the rate. These are only two experiments, however, and so this remains a source of speculation. A more thorough series

of experiments would need to be designed in order to examine the interactions of the disulfide bond, catalyst, and polymerization kinetics.

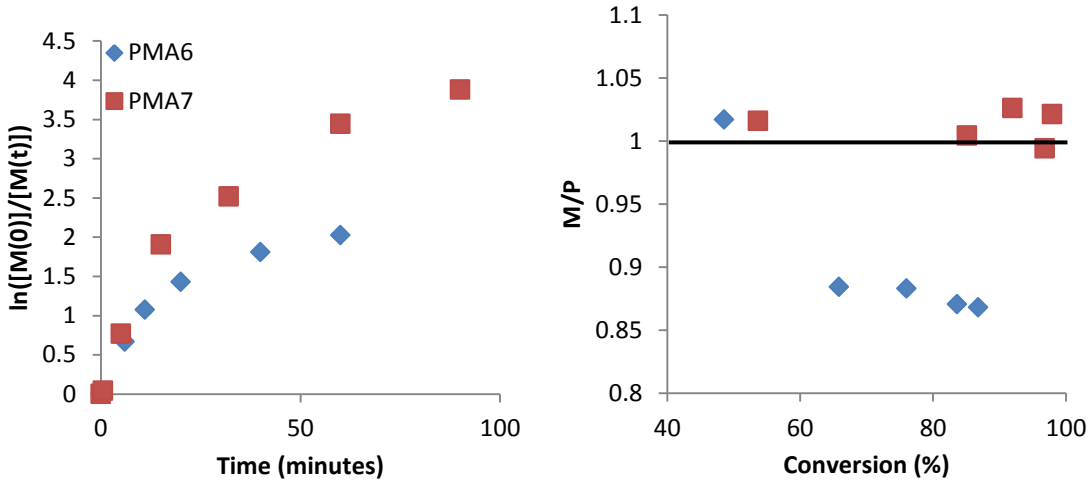

Figure 5.7: Comparing kinetics of PMA6 with PMA7. The sample with an M/P ratio closer to 1 proceeded at the faster rate. Polymerization conditions ([M] : [L] : [Cu(II)]): PMA6, 100 : 0.1 : 0.05; PMA7, 100 : 0.2 : 0.05.

5.3.1.3 Substitution of bromine groups with thiophenol

Bromine groups can be substituted by sulfide groups via an S_N2 reaction to form a thioether, particularly when the bromine is activated by being in proximity to an electron-withdrawing group such as the ester group in acrylic polymers, and under basic conditions such as those used for the thiol-ene Michael addition [37]. In order to prevent the sulfide groups of one polymer chain from reacting with the bromine group on another chain, the polymers were reacted with thiophenol in order to remove the bromine functionality prior to being reduced. An overview of the redox treatment of the polymers is presented in Scheme 5.2 along with the bromine substitution step.

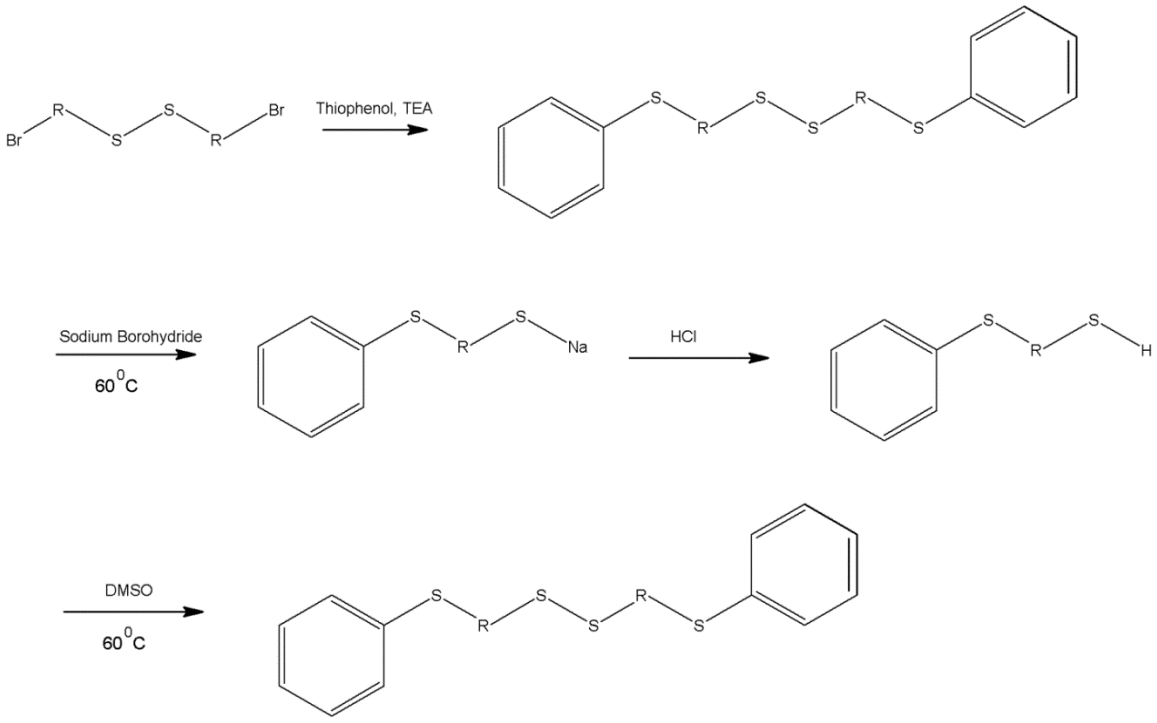

Scheme 5.2: Overview of redox treatment of polymers grown from $(BrBE)_2S_2$ (R = polymer chain).

The presence of the thiophenol in the polymers following substitution and purification was confirmed by ^1H NMR (Figure 5.8), and the molar amount of thiophenol was calculated by comparing the areas of the phenyl and methyl ester signals. The PMA was calculated to be 187% substituted, whereas the PMMA was calculated to be 79% substituted. Purification of the PMA was more difficult than the PMMA due to its lower T_g (10^OC for PMA as opposed to 105^OC for PMMA [38]). The low T_g created difficulties in removing all traces of non-covalently bound sulfides, as was evidenced by the unmistakeable odour that remained with the purified PMA but not the PMMA. As such, it was suspected that the PMA still had non-covalently bound thiophenol in the mixture. The reaction with PMA was first done using a four times excess of thiophenol, but this was reduced to a stoichiometric amount, or slight excess, in subsequent reactions in order to ease the purification.

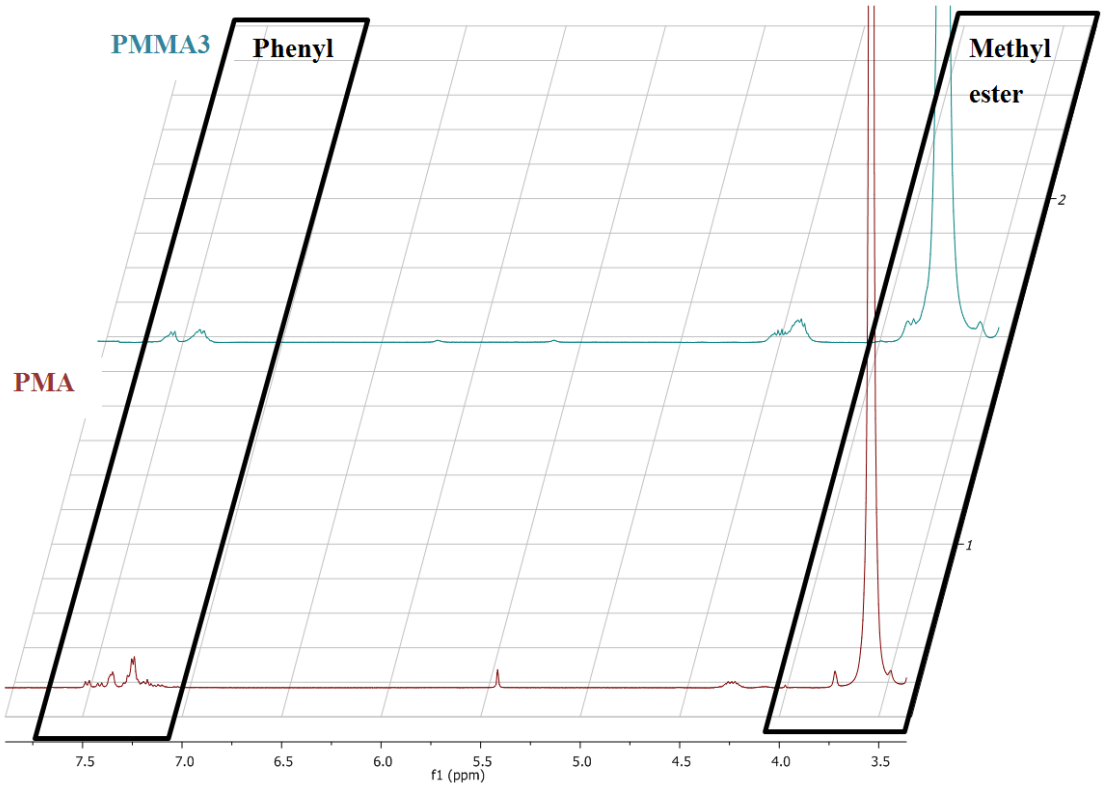

Figure 5.8: ^{1}H NMR spectra of polymer samples after thiophenol substitution. The amount of substitution that occurred was calculated by taking the ratio of the area of the phenyl groups (5 protons per group) to the area of the methyl ester groups (3 protons per group) and comparing this ratio to the one predicted according to the molecular weight of the polymer. Spectra recorded in acetone-d_6.

The measured molecular weights of the polymer samples showed drastic decreases after the substitution reaction, particularly the PMA samples, as shown in Table 5.4. As can be seen in Figure 5.9 for PMA5, the peak became strongly bimodal after the thiophenol reaction, with the two peaks lining up with the original polymer peak and the reduced polymer peak, respectively. It is clear that the excess thiophenol used in the reaction (four times excess) was cleaving a portion of the disulfide bonds in the polymer. This may also explain the extra phenyl presence in the NMR spectrum, as sulfides reduce disulfides by exchange. Without a large enough excess of the thiophenol it will only partially exchange positions with the polymer chains; that is, the polymer chains will be connected by a disulfide linkage to a thiophenol rather than to each other, but will not be reduced to the sulfide. In addition, thiolates at the end of the polymer chain are

generated during this exchange, and these can compete with the thiophenol molecules during the bromine substitution: in this case, the reduction step would appear non-quantitative due to this new bond formation that would increase the molecular weight. This was not observed, however, as the PMA could be reduced quantitatively. After these test reactions, the bromine substitution was done using a one-pot approach, where the polymer was mixed with thiophenol or mercaptoethanol first and allowed a sufficient time to react, and then the reducing agent was introduced in the same vessel without purifying the polymer.

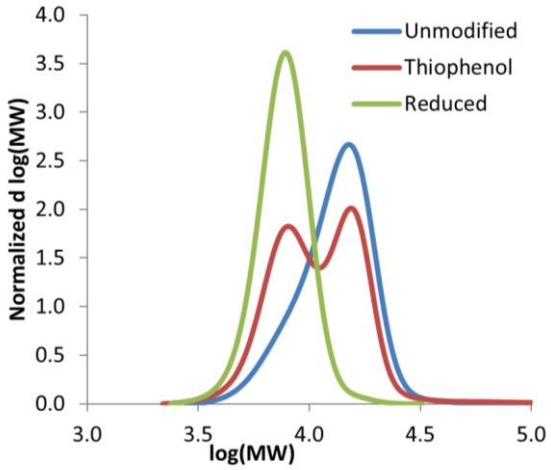

Figure 5.9: Molecular weight distributions of PMA5 before and after thiophenol substitution (4x excess thiophenol). The thiophenol reaction resulted in partial cleavage of the disulfide bond.

Table 5.4: Summary of molecular weight changes after thiophenol substitution.

Sample	M_n (g/mol)	PDI	M_n after substitution (g/mol)	PDI after substitution
PMA5	12,000	1.16	9,800	1.28
PMA6	11,900	1.13	8,420	1.20
PMMA2	24,000	1.70	18,000	1.64
PMMA3	10,400	1.83	11,200	1.74

5.3.1.4 Redox of synthetic polymers with internal disulfide linkage

The use of redox reactions to change molecular weight was seen as a good approach to measure sulfide functionality due to the ease and accuracy of molecular weight measurements of

the homopolymers on the Waters GPC. Since the DP of the polymer was typically around 100, this led to a concentration of sulfides being present which was undetectable by IR or NMR. Reduction of the disulfide was necessary in order to generate the sulfides required for the addition reaction, and so oxidation of the final polymer samples to their original disulfide form was a complementary method with an easily measureable effect. The reducing agents examined were sodium borohydride ($NaBH_4$), dithiothreitol (DTT), and mercaptoethanol (ME). DTT [27, 39, 40] and ME [9] are commonly used as reducing agents for disulfide bonds, while $NaBH_4$ has been used to analyze disulfide content [41]. DTT and ME are better reducing agents under basic conditions: DTT has a redox potential of -0.322 v at pH 7, but this increase to -0.366 v at pH 8.1 [39]. DMSO is capable of oxidizing sulfides to disulfides [9, 42] and was used for that purpose here due to its ability to be both solvent and oxidant for the reaction; the high concentration of DMSO aids in efficient oxidation, while the mild nature of its oxidation prevents side reactions from occurring. Redox reactions of PMA are summarized in Table 5.5, while those for PMMA are summarized in Table 5.6.

Sodium borohydride was first used as a reducing agent for the reduction of PMA at a concentration of ~0.3 M in DMF at 60^{O}C. Samples were taken with time (2.5 hours, 8.5 hours, and 24 hours) and precipitated in water. However, only the first sample precipitated well. The second sample formed an opaque mixture in water without properly precipitating, and the final sample formed a clear solution in water. It appears the polymer was being degraded, either from hydrolysis of the ester groups under the basic conditions in the solution or from reduction of the ester groups to alcohols. Thus the reaction was never left longer than 2 hours when $NaBH_4$ was used as the reducing agent in order to minimize degradation of the polymer; all reactions with PMA showed complete scission of the disulfide during this time period. Figure 5.9 is an example of a sample reduced with $NaBH_4$.

Table 5.5: Summary of redox reactions with PMA.

Sample	M_n (g/mol)	PDI	Reduction method	M_n after reduction (g/mol)	PDI after reduction	M_n after oxidation (g/mol)	PDI after oxidation	Sulfide (%)
PMA6-R1	11,900	1.13	0.30 M $NaBH_4$, DMF, 60^0C, 2 h	7,020	1.07	7,080	1.08	0.85
PMA7-R1	15,800	1.17	0.38 M DTT, THF, 0.1 M TEA, 60^0C, 2 h	9,150	1.11	10,900	1.39	19
PMA7-R2	15,800	1.17	1.4 M ME, THF, 0.1 M TEA, 60^0C, 2 h	9,430	1.15	9,970	1.17	5.7
PMA7-R3	15,800	1.17	0.16 M DTT, THF, 0.1 M TEA, 60^0C, 4 h	9,050	1.13	12,800	1.71	41
PMA8-R1	21,700	1.13	0.23 M DTT, DMF, 0.1 M TEA, 60^0C, 24 h	13,100	1.10	13,100	1.11	0.0
PMA8-R2	21,700	1.13	0.16 M $NaBH_4$, DMF, 0.1 M TEA, 60^0C, 2 h	n.d.	n.d.	11,940	1.12	(0)

Table 5.6: Summary of redox reactions with PMMA.

Sample	M_n (g/mol)	PDI	Reduction method	M_n after reduction (g/mol)	PDI after reduction	M_n after oxidation (g/mol)	PDI after oxidation	Sulfide (%)
PMMA3-R2	10,400	1.83	0.51 M $NaBH_4$, DMF, 60^0C, 2 h	12,300	1.74	15,500	1.52	26
PMMA3-R3	10,400	1.83	0.33 M $NaBH_4$, DMF, 60^0C, 2 h	11,700	1.74	12,200	1.69	4.3*
PMMA4-R1	15,600	1.55	0.38 M DTT, THF, 0.1 M TEA, 60^0C,28 h	14,400	1.51	25,400	1.51	76
PMMA4-R2	15,600	1.55	1.4 M ME, THF, 0.1 M TEA, 60^0C, 28 h	14,100	1.48	17,900	1.40	27
PMMA4-R3	15,600	1.55	1.2 M ME, THF, 0.1 M TEA, 60^0C, 48 h	13,900	1.44	19,200	1.59	38
PMMA4-R4	15,600	1.55	0.14 M DTT, THF, 0.1 M TEA, 60^0C, 4 h	14,200	1.48	22,900	1.46	61
PMMA6-R1	17,900	1.59	0.23 M DTT, DMF, 0.1 M TEA, 60^0C, 24 h	14,300	1.61	19,900	1.47	39
PMMA6-R2	17,900	1.59	0.19 M $NaBH_4$, DMF, 0.1 M TEA, 60^0C, 2 h	17,300	1.43	17,900	1.38	3.5

*purified with acetone

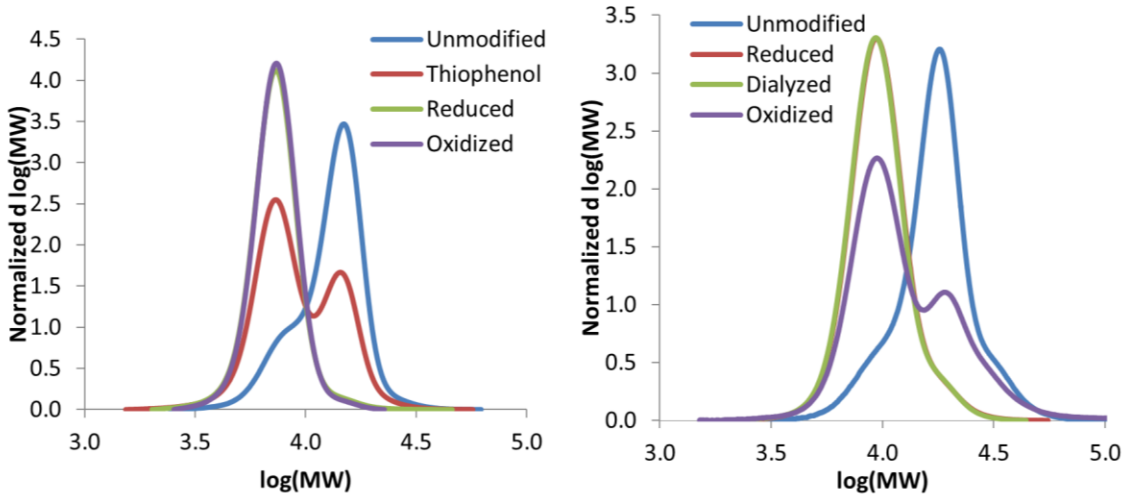

Figure 5.10: Redox reactions of PMA6-R1 (left) and PMA7-R3 (right). PMA6-R1 was reduced using $NaBH_4$ in THF. PMA7-R3 was reduced using DTT in THF. PMA6-R1 shows no sign of oxidation, while PMA7-R3 shows some oxidation has occurred.

Figure 5.10 contains the molecular weight distributions of the redox reactions of sample PMA6-R1. This sample was reduced with $NaBH_4$ in DMF. It can be seen here that the large hump in the low molecular weight shoulder that is present in the unmodified polymer completely disappears upon scission of the disulfide bond, leaving a monomodal peak with a very low polydispersity of 1.07. However, the sample showed no significant change in molecular weight after oxidation, with a negligible sulfide functionality of 0.85% calculated. This can be compared to PMA7-R3 in the same figure which was reduced using DTT in THF. While PMA7-R3 did not regain its original shape after oxidation, it did show oxidation occurring, with a sulfide functionality of 41% calculated. This plot also shows that no oxidation occurred after the reduced sample was dialyzed in non-degassed THF during the purification process, indicating the sample was stable in the presence of oxygen at room temperature.

In contrast to the reduction of PMA, reduction of PMMA resulted in only small changes in molecular weight, or in some cases no change. This was not unexpected as the initiator efficiency of the PMMA was low, and so many (or most) of the bifunctional initiators were

thought to have initiated on only one side and would not show a measureable change in molecular weight upon reduction. However, qualitative examination of the molecular weight distributions suggests that the PMMA samples were in some cases not being completely reduced, as they appeared to retain bimodal character after the reduction. Sample PMMA3-R2 was a good example of this; as can be seen in Figure 5.11, there was very little change in molecular weight after the reduction step (in fact, the measured molecular weight increased, likely due to oligomers being washed out during the purification steps) and the same hump in the low molecular weight shoulder remained. Upon oxidation, a symmetrical profile was obtained with a lower PDI of 1.52, and it was seen that the low molecular weight shoulder was shifted toward the main peak, while the main peak and high molecular weight shoulder remained stationary. This suggests that primarily chains that have disulfide group at the end (that is, mono-initiated) were being reduced, and that chains with the disulfide in the middle (that is, bi-initiated) were not. Since the PMA chains discussed previously did not oxidize fully, it would be fair to question whether the oxidation method utilized could form disulfides quantitatively; from the shape of the curve in this sample, it would appear that it could. The monomodal behaviour exhibited in this oxidized sample indicates there was not a problem with the oxidation step itself. This is a qualitative assessment; quantitatively, it can be calculated that the reduced PMMA chains of PMMA3-R2 had sulfide functionality of 26% based on the change in molecular weight.

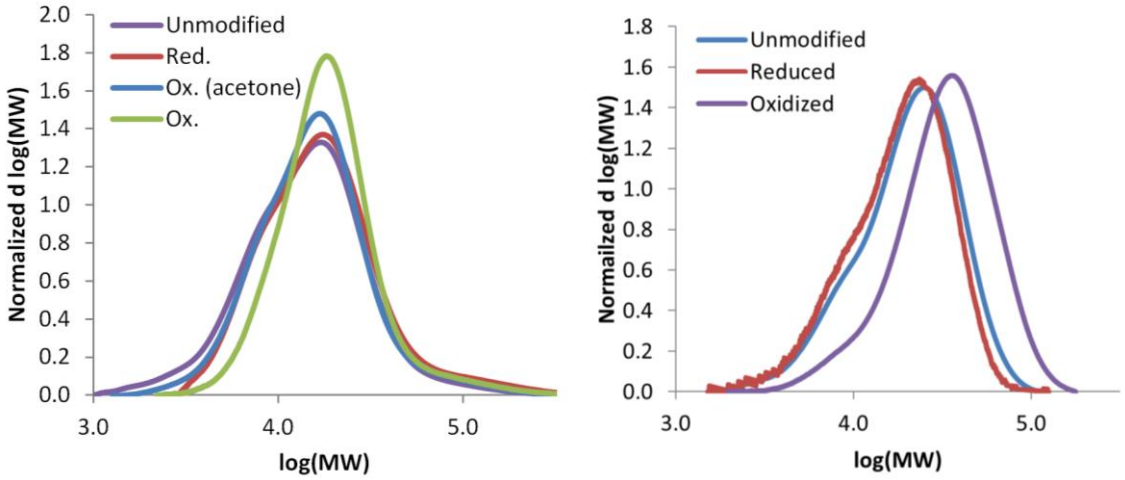

Figure 5.11: Redox reactions of PMMA3-R2 (left) and PMMA4-R1 (right). PMMA3-R2 was reduced using $NaBH_4$ in DMF. When acetone was used as a solvent for purification no oxidation was observed, likely due to the formation of thioketals. PMMA4-R1 was reduced using DTT in THF and showed the highest sulfide functionality (76%) of any sample.

The purification of sample PMMA3-R2 was first done by dialyzing against THF. Plotted on the same graph in Figure 5.11 is the molecular weight distribution of a sample that was purified by dialyzing against acetone instead of THF. When acetone was used, essentially no increase in molecular weight was observed upon oxidation. Sulfides can react with aldehydes and ketones in acidic conditions to form thioacetals and thioketals [29] and this was thought to be occurring here. The use of acetone was therefore avoided with the sulfide/disulfide containing polymers.

Also plotted in Figure 5.11 are the molecular weight distributions of sample PMMA4-R1. This sample had the highest measured sulfide content (76%). In this case, the entire distribution shifted after the oxidation reaction, indicating there were little or no un-cleaved disulfide bonds remaining after the reduction step. The narrow polydispersity, monomodal behaviour, and high sulfide functionality measured in this sample also supported the conclusion that the DMSO oxidation step was adequate.

Mono-functional initiation would mean that non-polymeric sulfides were generated during the reduction process. As the polymers are only end-functional, even a small quantity of these sulfides (or the ME, DTT, or thiophenol used during the reactions) remaining bound to the polymer throughout purification would significantly alter the total concentration of sulfides. Analytical techniques that measure sulfides directly [41] would tend to overestimate the polymer functionality in this case. In the case of the redox reactions used here, sulfide functionality is measured indirectly through molecular weight. Oxidation that results in bonding of the non-polymeric sulfides with the polymeric sulfides would show no measurable change in molecular weight, and thus would underestimate the sulfide functionality of the polymer. When considering competition of polymeric and non-polymeric sulfides in the thiol-ene addition reaction, however, this measurement technique may give a more accurate depiction of the effective sulfide functionality than measuring the total sulfide concentration. Since the PMA was more difficult to purify, this may explain why the sulfide functionalities measured for these samples were substantially lower than the PMMA samples.

Figure 5.12 compares the effect of reaction solvent and reducing agent on the sulfide functionality obtained, as well as the type of polymer sample used (PMA or PMMA). It is immediately obvious that PMMA samples had substantially higher sulfide functionality than PMA. It is not known why this would be, as the PMA samples were all easily and quantitatively reduced. PMA required more vigorous purification techniques that still did not completely clean the samples – as evidenced by the sulfide odour that remained – and it is possible that the sulfides were being reacted with something during the purification process (similar to the way they reacted with acetone), or the ester groups that attach the sulfide to the polymer chain could have been hydrolyzed. The polymeric sulfides may also have been forming disulfide bonds with other residual sulfides; these disulfide bonds would not show any change in molecular weight of the PMA chains.

DTT was the reducing agent that resulted in the highest sulfide functionality, followed by ME, and then $NaBH_4$. When the reduction step was done in THF it resulted in a much higher sulfide functionality than when performed in DMF. However, $NaBH_4$ was used only with DMF (due to its poor solubility in THF), while ME was used only in THF, and DTT was used in both. It is not immediately clear if these trends are reflective of the role of the solvent or the role of the reducing agent. Comparing reactions using DTT in the two solvents is more revealing. With PMA samples PMA7-R1 (DTT, THF, 2 h), PMA7-R3 (DTT, THF, 4 h), and PMA8-R1 (DTT, DMF, 24 h) it can be seen that while the samples reduced in THF showed sulfide functionality (19% and 41%, respectively), the sample reduced in DMF had no measurable functionality. In fact, no reduction of PMA conducted in DMF resulted in a successful subsequent oxidation. For PMMA, reductions in DMF did leave some sulfide functionality intact, but similar reactions done with DTT in THF showed that DMF was less successful. Comparing PMMA4-R1 reduced in THF to PMMA6-R1 reduced in DMF, the reaction performed in THF resulted in a 76% sulfide functionality while the functionality was only 39% when done in DMF.

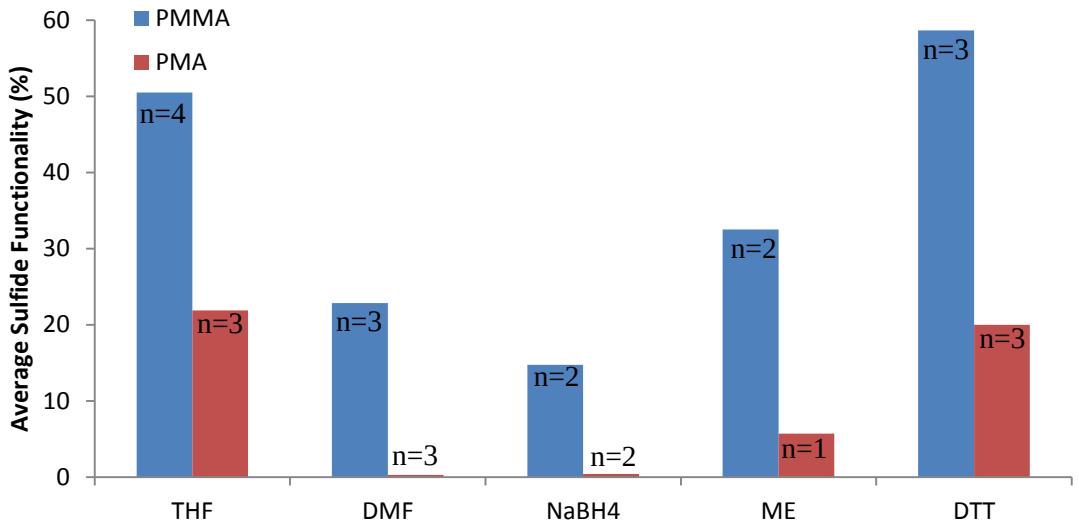

Figure 5.12: Comparing sulfide functionality amongst samples prepared using different reduction techniques. THF resulted in the highest sulfide functionality along with DTT. $NaBH_4$ and DMF resulted in lower measured functionalities. Summarizing data for all samples in Table 5.5 and Table 5.6.

5.3.2 Modification of cellulose acetate with thiol-ene Michael addition

5.3.2.1 Model thiol-ene reaction with methyl methacrylate to determine optimal addition conditions

The thiol-ene Michael addition reaction used here is given in Scheme 5.3. The sulfide is de-protonated by a base, and the resulting thiolate is added across an alkene activated by an electron withdrawing group (such as an ester, amide, or nitrile) [26]. To investigate the optimal catalyst type and temperature for the thiol-ene Michael addition, methyl methacrylate and thiophenol were reacted together in DMF. The MMA and thiophenol were used as models for the polymeric compounds, and DMF was used as the solvent as it is capable of dissolving a wide range of cellulose derivatives and synthetic polymers of interest. The results are summarized in Table 5.7. The reaction was first done at 60^{O}C using a stoichiometric amount of thiol and alkene. However, as can be seen for the hexylamine (HA) entry, the reaction plateaued at a conversion of less than 100%. This was attributed to the presence of disulfide bond impurities in the thiophenol reagent due to oxidation, resulting and less than complete sulfide functionality. When the reaction was repeated at 30^{O}C the stoichiometry was increased to 1.2 equivalents of sulfide in order to overcome this and ensure that all of the alkene would be consumed (see Figure 5.13 for NMR spectra). It can be seen that when hexylamine was used as catalyst the reaction essentially reached a maximum value within the first hour regardless of temperature, while triethylamine (TEA) did not reach maximum conversion in this time frame in either reaction. This was as expected, as primary amines like hexylamine were reported to be better catalysts for the reaction than tertiary amines like triethylamine [26]. It was also seen that the solvent, DMF, did not catalyze the reaction as none of the alkene reacted at 30^{O}C, although some alkene did react at 60^{O}C. From these results, hexylamine was chosen to be used as the catalyst for the grafting reactions and it was concluded that elevating the reaction temperature above ambient provided no benefit to the addition reaction.

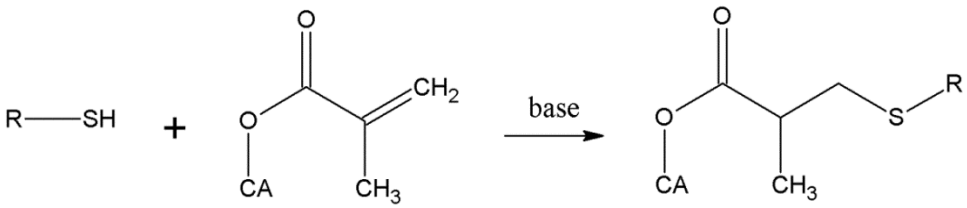

Scheme 5.3: Michael addition of sulfide to an activated alkene bonded to cellulose acetate.

Table 5.7: Optimization of thiol-ene addition conditions.

Catalyst	30^{O}C (1 hour)$^{+}$	60^{O}C (1 hour)*	60^{O}C (24 h)*
None	0%	25%	55%
Triethylamine (0.6 M)	81%	65%	78%
Hexylamine (0.6 M)	97%	80%	88%

*1 eq. of thiophenol; $^{+}$1.2 eq. of thiophenol

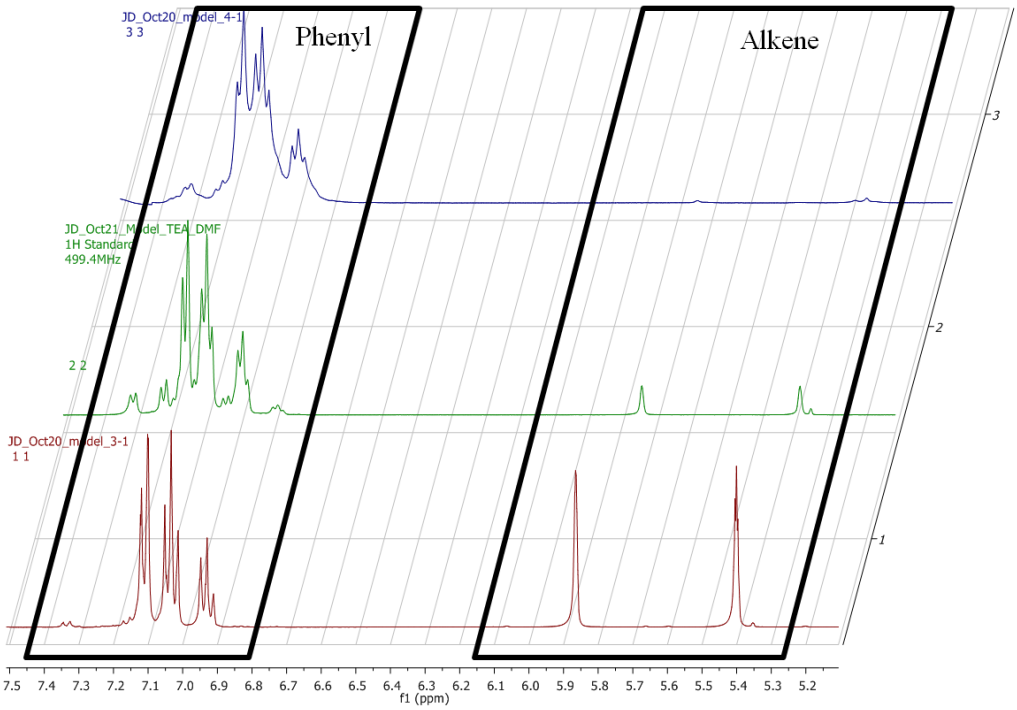

Figure 5.13: Reaction of MMA with thiophenol under different catalyst conditions in DMF at 30^{O}C: 0.6 M hexylamine (top), 0.6 M triethylamine (middle), and no catalyst (bottom**).** No reaction was observed when no catalyst is used, while the reaction using hexylamine has reached essentially complete conversion (97%). The reaction with triethylamine reached 81% conversion. Spectra recorded in chloroform-d.

5.3.2.2 Model thiol-ene addition with $CA_{2.77}$-$MAA_{0.13}$ and thiophenol

The reaction was modeled using $CA_{2.77}$-$MAA_{0.13}$ (sample MAA3T from Chapter 3) and thiophenol under the same (optimized) conditions as for the grafting reaction (30^{O}C, 0.6 M hexylamine in DMF). $CA_{2.77}$-$MAA_{0.13}$ without any source of thiol was used as a control. As seen in the NMR spectrum (Figure 5.14), the reaction with thiophenol resulted in almost complete suppression of the alkene peaks (δ=5.6, 6.1 ppm), as well as the addition of phenyl peaks (δ = 7.0-7.7 ppm). The alkene peaks in the control reaction were retained. This indicates the reaction proceeded readily in the presence of sulfide, and the alkenes were otherwise stable under these conditions.

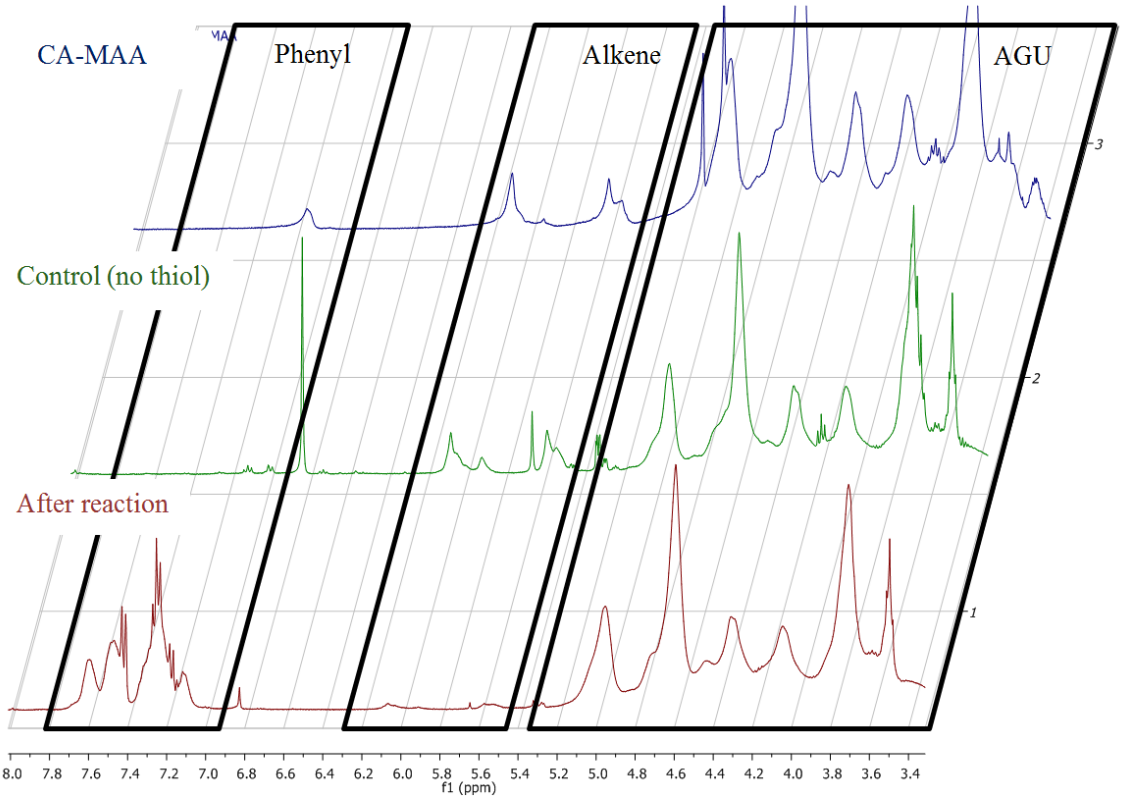

Figure 5.14: ^{1}H NMR spectra of model reaction with CA-MAA (MAA3T) and thiophenol in DMF with 0.6 M hexylamine as catalyst. The reaction with thiophenol results in almost complete suppression of the alkene peaks while the control shows minimal change. Spectra recorded in acetone-d_6.

GPC traces of the samples were obtained on the Viscotek GPC to ensure that there were no drastic changes in molecular weight occuring due to backbone degradation of the cellulose or combination of the methacrylate groups (Figure 5.15). The molecular weight measurements using the triple detection appararus are very sensitive to the measured concentration of the samples, and as such a larger error would be expected when compared to a sample measured against a calibration curve. The raw elution profiles are provided as well, as they are expected to show changes more accurately than the molecular weight distributions. The peak retention volume of the three samples showed no change, and only small changes in M_p were observed. The reaction conditions were therefore concluded not to affect the integrity of the cellulose samples.

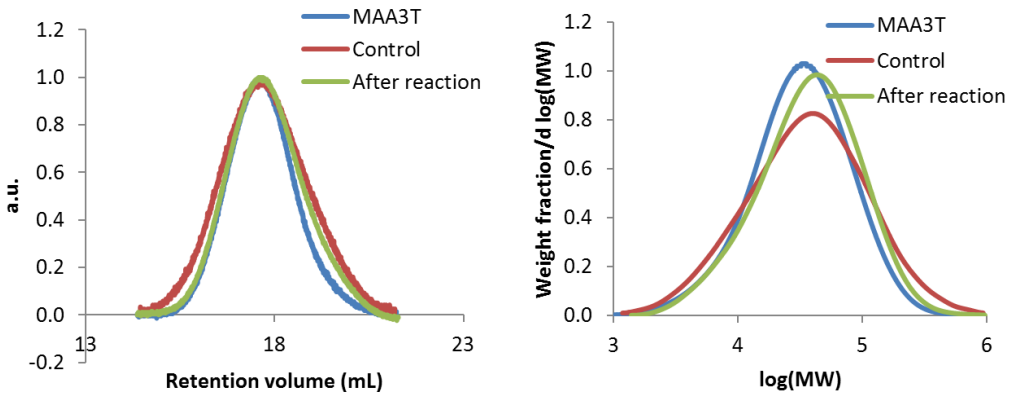

Figure 5.15: Elution profiles (left) and molecular weight distributions (right) of model reactions of CA-MAA with thiophenol. There were no changes after the reaction, indicating no combination or degradation occurring during the reaction.

5.3.2.3 Model thiol-ene addition with Cell-AcO$_{2.02}$-GMA$_{0.98}$ and dodecanethiol

The addition reaction was also attempted with dodecanethiol and the cellulosic material Cell-AcO$_{2.02}$-GMA$_{0.98}$ from Chapter 3. This reaction was done using a 0.12 M TEA in DMSO solution at 50^{O}C for 24 hours. Even at these non-optimized conditions the reaction proceeded

quantitatively, as can be seen from the complete disappearance of the alkene signal in Figure 5.16. The signals from dodecanethiol are clearly present in the final spectrum as well, showing that the dodecanethiol remained covalently bonded after purification. DMSO has been found not to oxidize dodecanethiol at room temperature [42] and so the addition reaction proceeded quickly enough that disulfide formation was not an issue.

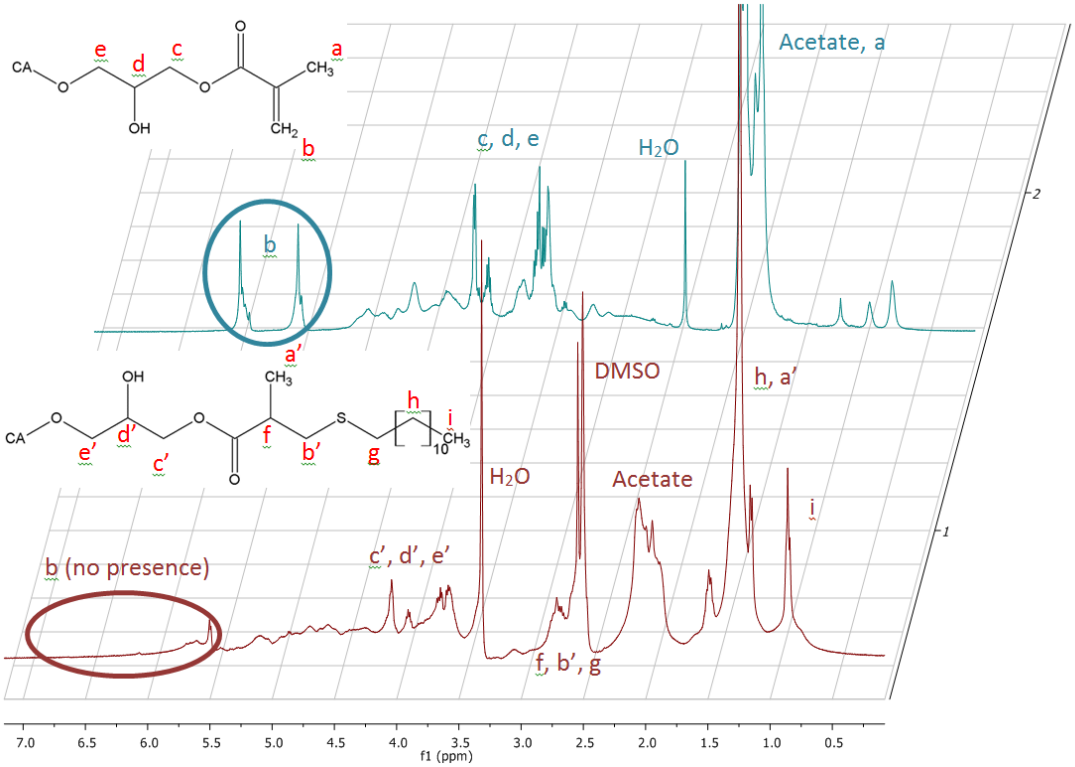

Figure 5.16: Addition of dodecanethiol to Cell-AcO-GMA in 0.12 M TEA/DMSO. After the reaction the alkene signal has disappeared and signals attributed to dodecanethiol have appeared. The product was not soluble in acetone so the spectrum was recorded in DMSO-d_6.

5.3.2.4 Grafting of synthetic chains onto $CA_{2.77}$-$MAA_{0.13}$

Samples PMMA6-R1 and PMA8-R1 (reduced using DTT in DMF) were reacted with $CA_{2.77}$-$MAA_{0.13}$ (sample MAA3T) in an attempt to graft the synthetic polymers onto the cellulose acetate. The PMMA sample was measured to be 39% functional by oxidation of the thiols using

DMSO, but the PMA had no measurable functionality. Nonetheless, the reaction was attempted with both samples. Elution profiles of the samples were recorded on the Viscotek GPC (Figure 5.17) and are compared to the starting $CA_{2.77}$-$MAA_{0.13}$. No attempts were made to separate the grafted and ungrafted polymer samples and so both appear in the profile. The tallest peaks appear in the high retention volume (low molecular weight) region of the scale; these peaks correspond to ungrafted synthetic polymer. It is obvious that there was a large quantity of ungrafted polymer present after the reaction, but it can also be seen that the peak retention volume (Vr_p) of the cellulose acetate had decreased (marked with vertical lines in Figure 5.17). This decrease in retention volume indicated an increase in the size of the cellulose; as there was no change in Vr_p in the control reaction, this led to the conclusion that grafting had successfully ocurred. The Vr_p of $CA_{2.77}$-$MAA_{0.13}$ occured at 17.6 mL; this showed a moderate decrease to 17.2 mL after the PMA grafting, and a much greater decrease to 16.2 mL after the PMMA grafting. There were only marginal changes in the elution profiles when increasing the reaction time from 24 hours to 48 hours, indicating that the reaction was complete within the first day.

The PMMA reaction resulted in a signifcantly broader distribution of the CA-g-PMMA than that of the original CA. This may indicate an uneven distribution of grafts. As the ratio of sulfide to alkene was low (0.1), it is reasonable to conclude that there remained cellulose acetate without any grafted chains in the mixture. It was not expected that the PMA reaction would show a change in retention volume as there was no sulfide functionality measured by oxidation of the reduced polymer. The decrease observed may indicate that there was in fact a low quantity of sulfide-terminated polymers present that was not detectable by oxidation.

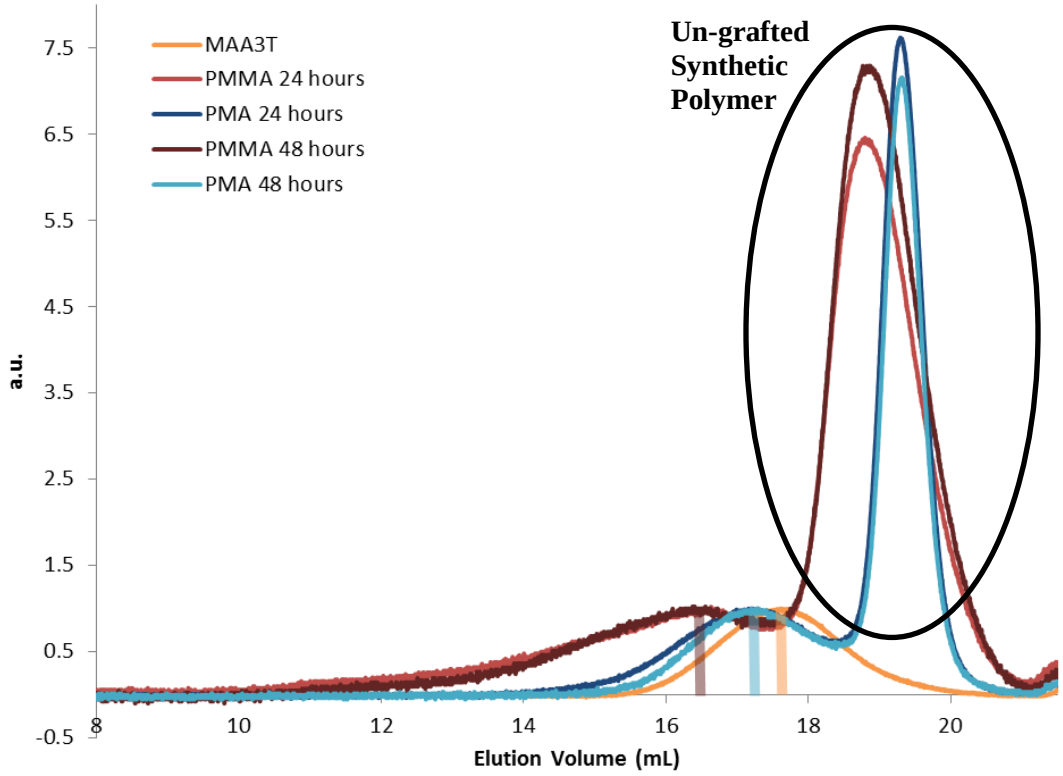

Figure 5.17: Elution profiles of grafted cellulose samples. The un-grafted synthetic polymer (Vr_p = 18.7 mL, 19.2 mL) has a large presence after the reaction, but the peak retention volume of the cellulose acetate clearly increases: from 17.6 mL to 17.2 mL for PMA grafting, and from 17.6 mL to 16.2 mL for PMMA grafting. The increase in Vr_p indicates that grafting has occurred.

5.3.2.5 In-situ reduction and grafting of synthetic chains onto $CA_{2.77}$-$MAA_{0.13}$

The addition reaction was attempted by cleaving the disulfide bond in the reaction mixture without subsequent separation and purification of the reduced polymer. Sodium borohydride was used for this as both DTT and ME contain sulfides and would therefore react preferentially with the methacrylate groups over the sulfides on the polymer chains. Reduction of disulfide with $NaBH_4$ generates thiolates which can then be protonated to form sulfides; since the Michael addition reaction requires de-protonation of the sulfide, the generation of thiolates was not seen to be an issue. It has been reported in the literature that RAFT-terminated polymers can be reduced in-situ to thiolates using $NaBH_4$; the thiolates were then successfully bonded to gold

nanoparticles [43]. However, solubility of the cellulose in the work presented here was a problem. The first reaction was done at a concentration of CA-MAA of only 17 mg/mL, but addition of the $NaBH_4$ to the DMF/polymer solution caused the CA-MAA to form a gel. After 45 minutes stirring had ceased (due to gelation) and so the reaction was stopped. All samples were completely soluble in THF and were analyzed by GPC, with the results presented in Figure 5.18. The reaction with PMA had no significant change, but the reaction with PMMA showed a small decrease in Vr_p from 17.5 mL to 17.2 mL which may indicate some grafting occurred despite the short reaction time, poor mixing, and poor cellulose acetate solubility.

In an attempt to improve the cellulose acetate solubility, the volume of solvent was doubled and dioxane was tried in addition to the DMF. However, in each case the cellulose acetate formed a gel. These mixtures were still capable of being stirred so they were left for 24 hours. The resulting polymer was largely insoluble; the control sample was insoluble in all solvents tried, while small portions of the other samples were THF-soluble. GPC analysis of these THF-soluble fractions revealed the presence of only the synthetic polymer peak and no cellulose acetate peak.

While these reactions were not successful, the small change in the PMMA sample in Figure 5.18 suggests that the reaction could work provided the right reducing agent is found. Sodium borohydride caused the cellulose acetate to gel in solution. It also reacted with the cellulose acetate, as evidenced by the complete insolubility of the cellulose acetate after the reaction and subsequent purification. Other, milder reducing agents should be considered.

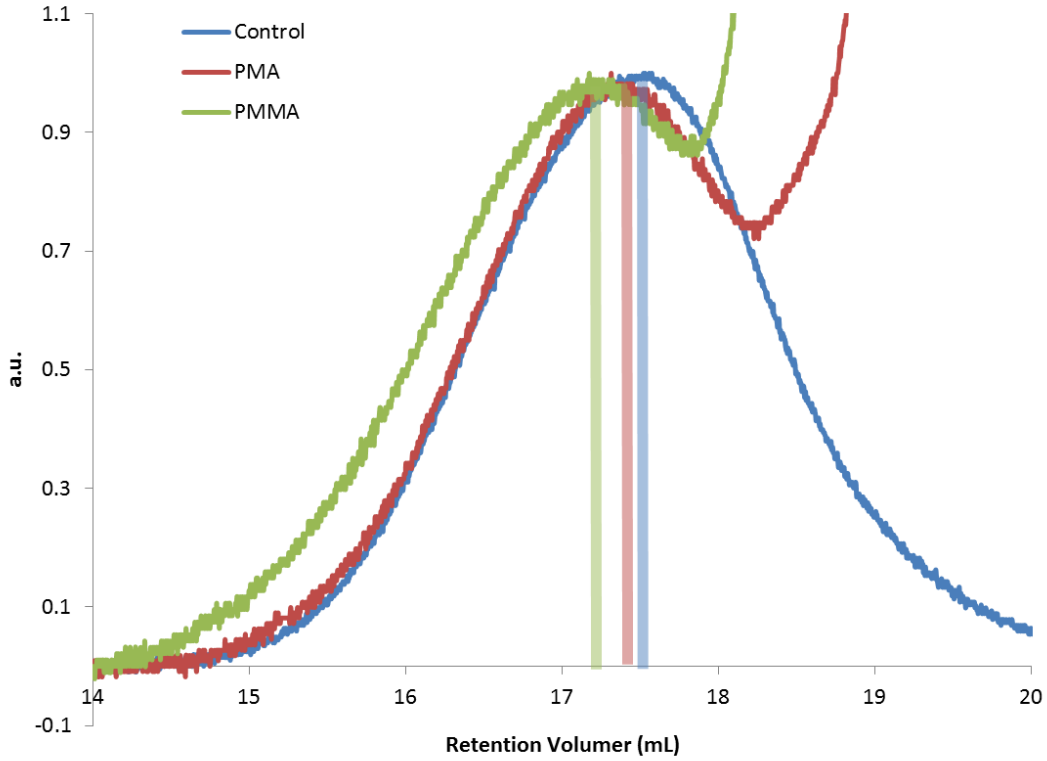

Figure 5.18: Elution profiles for in-situ reduction of disulfide and addition to CA-MAA. Samples PMA8 and PMMA5 used. The reaction with PMMA shows a small decrease in retention volume of the CA-MAA peak which may indicate grafting has occurred. Sodium borohydride was used for the in-situ reduction but caused the solution to turn heterogeneous, thereby hindering the reaction.

5.4 Conclusions and recommendations

5.4.1 Conclusions

Polymerization of MA from the disulfide containing initiator $[(BrBE)_2S_2]$ resulted in an extremely fast polymerization, low polydispersity, and complete initiation efficiency. Thus, molecular weights of the cleaved chains could be easily controlled. The disulfide bond appears to be capable of cleaving during the polymerization process and this may affect the polymerization kinetics; this would need to be studied in more detail. Polymerization of MMA was not as fast as MA and resulted in higher polydispersities of the cleaved chains. More problematic was the fact

that initiation efficiency was very low (22% on average) and decreased as shorter chains were targeted. This created difficulties in controlling the molecular weight of PMMA, particularly when shorter chains were desired.

Reduction of the disulfide bond in the PMA samples proceeded easily and quickly, with monomodal and symmetrical molecular weight distributions obtained. The reduced molecular weights agreed with the predicted values and had low polydispersities, as small as 1.07. Reduction of PMMA resulted in only minor changes in molecular weight, which was expected as the initiation efficiencies were very low and so few bi-initiated species were expected. However, the bimodal nature observed in some of the reduced samples as well as the large range of polydispersities (1.43 - 1.74) encountered would qualitatively suggest that the PMMA samples are being incompletely reduced.

Oxidation of the reduced samples resulted in a wide range of sulfide functionalities being measured. However, PMA samples showed a much lower change in molecular weight upon oxidation than the PMMA samples did. Reductions performed in DMF resulted in a lower measured sulfide functionality than reductions performed in THF, and reductions using $NaBH_4$ were found to have a lower sulfide functionality than the other reducing agents studied. Further study is required to determine the cause of these trends.

The addition of thiophenol and dodecanethiol to cellulose acetate functionalized with methacrylate groups proceeded quantitatively, with complete disappearance of the alkene signal observed by NMR. This reaction scheme could be used to impart cellulose acetate with a wide variety of functional groups. The addition of sulfide-terminated polymers resulted in a low grafting yield, which was not unexpected due to the low functionality of sulfide measured. However, significant changes in retention volume of the cellulose acetate were observed, confirming that grafting of synthetic chains onto cellulose acetate had occurred. The grafting concept illustrated here can be successfully employed for any controlled polymerization that

contains a disulfide bond or other group that can be converted to a sulfide, but it requires optimization. The end-group functionality of sulfide-terminated polymers can be conveniently monitored through redox reactions and molecular weight measurements, which is the prime advantage of using thiol-ene chemistry over other 'click' reactions.

5.4.2 Recommendations and future work

- Sulfide functionality of the synthetic polymer appears to be the limiting feature of this reaction. The loss of sulfide functionality needs to be examined in greater detail and corrected to ensure an efficient reaction. Acetone was one solvent that was found to decrease sulfide functionality.
- Loss of sulfide functionality may potentially be occurring during the purification stage. As such, an in-situ formation of sulfides could be a solution to the problem. The reducing agents employed in this study could not be used to that end, as DTT and ME both have thiol functionality that would react with the alkene groups and $NaBH_4$ caused gel formation of the cellulose acetate solution, so other reducing agents would be needed. Since the PMMA has low initiation efficiency, a large number of low molecular weight thiols would be produced and as such the alkene would need to be present in a large enough excess to account for this.
- A quantitative method for measuring grafting yield needs to be determined. If sulfide functionality of the polymer can be increased this should increase the grafting yield and may eliminate the need for separating the polymers, but barring that a higher molecular weight cellulosic material could be used to increase the separation of peaks in the GPC elution profile, or a selective solvent extraction of the un-grafted polymer could be attempted (this also may be easier with a higher molecular weight cellulose).

5.5 Acknowledgements

The author would like to thank the financial support provided by the Ontario Ministry of Research Innovation (Early Researcher Award Program, Dr. Pascale Champagne), by the Government of Ontario (Ontario Research Chair in Green Chemistry and Engineering, Dr. Michael F. Cunningham), and by Queen's University.

5.6 References

[1] E. Sjoholm, "12 Size Exclusion Chromatography of Cellulose and Cellulose Derivatives," in *Handbook of Size Exclusion Chromatography and Related Techniques 2nd Ed.*, New York, Marcel Dekker, 2004, pp. 311-354.

[2] T. Heinze and T. Liebert, "Unconventional methods in cellulose functionaliztion," *Progress in Polymer Science*, vol. 26, no. 9, pp. 1689-1762, 2001.

[3] H. Kamitakahara and F. Nakatsubo, "Synthesis of diblock copolymers with cellulose derivatives. 1. Model study with azidoalkyl carboxylic acid and cellobiosylamine derivative," *Cellulose*, vol. 12, no. 2, pp. 209-219, 2005.

[4] H. Kamitakahara, Y. Enomoto, C. Hasegawa and F. Nakatsubo, "Synthesis of diblock copolymers with cellulose derivatives. 2. Characterization and thermal properties of cellulose triacetate-block-oligoamide," *Cellulose*, vol. 12, no. 5, pp. 527-541, 2005.

[5] M. Tizzotti, A. Charlot, E. Fleury, M. Stenzel and J. Bernard, "Modification of polysaccharides through controlled/living radical polymerization grafting - towards the generation of high performace hybrids," *Macromolecular Rapid Communications*, vol. 31, no. 20, pp. 1751-1772, 2010.

[6] D. Roy, M. Semsarilar, J. T. Guthrie and S. Perrier, "Cellulose modification by polymer grafting: a review," *Chemical Society Reviews*, vol. 38, no. 7, pp. 2046-2064, 2008.

[7] O. Fichet, F. Vidal, J. Laskar and D. Teyssie, "Polydimethylsiloxane-cellulose acetate butyrate interpenetrating polymer networks synthesis and kinetic study. Part 1," *Polymer*, no. 46, no. 1, pp. 37-47, 2005.

[8] F. Vidal, O. Fichet, J. Laskar and D. Teyssie, "Polysiloxane-cellulose acetate butyrate cellulose interpenetrating polymers networks close to true IPNs on a large composition range. Part II," *Polymer*, no. 47, no. 11, pp. 3747-3753, 2006.

[9] D. Aoki, Y. Teramoto and Y. Nishio, "SH-containing cellulose acetate derivatives: preapration and charachterization as a shape memory-recovery material," *Biomacromolecules*, vol. 8, no. 12, pp. 3749-3757, 2007.

[10] E. Malmstrom and A. Carlmark, "Controlled grafting of cellulose fibres - an outlook beyond paper and cardboard," *Polymer Chemistry*, vol. 3, no. 7, pp. 1702-1713, 2012.

[11] Y. Habibi, L. A. Lucia and O. J. Rojas, "Cellulose nanocrystals: chemistry, self-assembly, and applications," *Chemical Reviews,* vol. 110, no. 6, pp. 3479-3500, 2010.

[12] E. Bianchi, E. Marsano, L. Ricco and S. Russo, "Free radical grafting onto cellulose in homogeneous conditions 1. Modified cellulose-acrylonitrile system," *Carbohydrate Polymers,* vol. 36, no. 4, pp. 313-318, 1998.

[13] Y. A. Aggour and E. Abdel-Razik, "Graft copolymerization of end allenoxy polyoxyethylene macromonomer onto ethyl cellulose in a homogeneous system," *European Polymer Journal,* vol. 35, no. 12, pp. 2225-2228, 1999.

[14] V. Raus, M. Stepanek, M. Uchman, M. Slouf, P. Latalova, E. Cadova, M. Netopilik, J. Kriz, J. Dybal and P. Vleck, "Cellulose-based graft copolymers with controlled architecture prepared in a homogeneous phase," *Polymer Chemistry,* vol. 49, no. 20, pp. 4353-4367, 2011.

[15] P. Vlcek, M. Janata, P. Latalova, J. Kriz, E. Cadova and L. Toman, "Controlled grafting of cellulose diacetate," *Polymer,* vol. 47, no. 8, pp. 2587-2595, 2006.

[16] E. Ostmark, S. Harrisson, K. L. Wooley and E. E. Malmstrom, "Comb polymers prepared by ATRP from hydroxypropyl cellulose," *Biomacromolecules,* vol. 8, no. 4, pp. 1138-1148, 2007.

[17] X. Sui, J. Yuan, M. Zhou, J. Zhang, H. Yang, W. Yuan, Y. Wei and C. Pan, "Synthesis of cellulose-graft-poly(N,N-dimethylamino-2-ethyl methacryalte copolymers via homogeneous ATRP and their aggregates in homogeneous media," *Biomacromolecules,* vol. 9, no. 10, pp. 2615-2620, 2008.

[18] M. Hiltunen, J. Siirila and S. L. M. Maunu, "Effect of catalyst systems and reaction conditions on the synthesis of cellulose-g-PDMAam copolymers by controlled radical polymerization," *Polymer Chemistry,* vol. 50, no. 15, pp. 3067-3076, 2012.

[19] M. S. Hiltunen, J. Raula and S. L. Maunu, "Tailoring of water-soluble cellulose-g-copolymers in homogeneous medium using single-electron-transfer living radical polymerization," *Polymer International,* vol. 60, no. 9, pp. 1370-1379, 2011.

[20] P. Mansson and L. Westfelt, "Grafting of monodisperse low-molecular-molecular weight polystyrene onto cellulose acetate," *Journal of Polymer Science: Polymer Chemistry Edition,* vol. 19, no. 6, pp. 1509-1515, 1981.

[21] C. J. Biermann, J. B. Chung and R. Narayan, "Grafting of polystyrene onto cellulose acetate by nucleophilic displacement of mesylate groups using the polystyrylcarboxylate anion," *Macromolecules,* vol. 20, no. 5, pp. 954-957, 1987.

[22] Y. Enomoto-Rogers, H. Kamitakahara, A. Yoshinaga and T. Takano, "Comb-shaped graft copolymers with cellulose side-chains prepared via click chemistry," *Carbohydrate Polymers,* vol. 87, no.3, pp. 2237-2245, 2012.

[23] P. Tingaut, R. Hauert and T. Zimmermann, "Highly efficient and straightforward functionalization of cellulose films with thiol-ene click chemistry," *Journal of Materials Chemistry,* vol. 21, no. 40, pp. 16066-16076, 2011.

[24] J. W. Chan, B. Yu, C. E. Hoyle and A. B. Lowe, "The nucleophilic, phosphine-catalyzed thiol-ene click reaction and convergent star synthesis with RAFT prepared homopolymers," *Polymer,* vol. 50, no. 14, pp. 3158-3168, 2009.

[25] D. J. Krasznai, T. F. L. McKenna, M. F. Cunningham, P. Champagne and N. M. B. Smeets, "Polysaccharide-stabilized core cross-linked polymer micelle analogues," *Polymers,* vol. 3, no. 4, pp. 992-1001, 2012.

[26] A. B. Lowe, "Thiol-ene 'click' reactions and recent applications in polymer and materials synthesis," *Polymer Chemistry,* vol. 1, no. 1, pp. 17-36, 2010.

[27] N. V. Tsarezsky and K. Matyjaszewski, "Reversible redox cleavage/coupling of polystyrene with disulfide or thiol groups prepared by Atom Transfer Radical Polymerization," *Macromolecules,* vol. 35, no. 24, pp. 9009-9014, 2002.

[28] N. V. Tsarevsky and K. Matyjaszewski, "Combining Atom Transfer Radical Polymerization and disulfide/thiol redox chemistry: a route to well-defined (bio)degradable polymeric materials," *Macromolecules* , vol. 38, no. 8, pp. 3087-3092, 2005.

[29] P. Y. Bruice, Organic Chemistry, 5th ed., Toronto: Pearson Education Canada, Inc., 2007.

[30] R. M. Silverstein, F. X. Webster and D. J. Kiemle, Spectrometric Identification of Organic Compounds, 7th ed., Hoboken, NJ: John Wiley & Sons, Inc., 2005.

[31] L. Patiny, "nmrdb.org: Database of NMR Spectra," Ecole Polytechnique Fédérale de Lausanne, [Online]. Available: http://www.nmrdb.org/. [Accessed January 2013].

[32] S. Beuermann, D. Paquet, J. McMinn and R. Hutchinson, "Determination of free-radical propagation rate coefficients of butyl, 2-ethylhexyl, and dodecyl acrylates by pulsed-laser polymerization," *Macromolecules,* vol. 29, no. 12, pp. 4206-4215, 1996.

[33] T. Gruendling, T. Junkers, M. Guilhaus and C. Barner-Kowollik, "Mark-Houwink parameters for the universal calibration of acrylate, methacrylate, and vinyl acetate polymers determined by online size-exclusion chromatography - mass spectrometry," *Macromolecular Chemistry and Physics,* vol. 211, no. 5, pp. 520-528, 2010.

[34] R. A. Hutchinson, J. H. McMinn, D. A. J. Paquet, S. Beuermann and C. Jackson, "A pulsed-laser study of penultimate copolymerization propagation kinetics for methyl methacrylate/n-butyl acrylate," *Industrial & Engieering Chemistry Research,* vol. 36, no. 4, pp. 1103-1113, 1997.

[35] V. Percec, T. Guliashvili, J. S. Ladislaw, A. Wistrand, A. Stjerndahl, M. J. Sienkowska, M. J. Monteiro and S. Sahoo, "Ultrafast synthesis of ultrahigh molar mass polymers by metal-catalyzed living radical polymerization of acrylates, methacrylates, and vinyl chloride mediated by SET at 25^{O}C," *Journal of the American Chemical Society,* vol. 128, no. 43, pp. 14156-14165, 2006.

[36] S. Fleischmann and V. Percec, "SET-LRP of methyl methacrylate initiated with sulfonyl halides," *Journal of Polymer Science: Part A: Polymer Chemistry,* vol. 48, no. 10, pp. 2236-2242, 2010.

[37] B. M. Rosen, G. Lligadas, C. Hahn and V. Percec, "Synthesis of dendrimers through divergent iterative thio-bromo 'click' chemistry," *Journal of Polymer Science: Part A: Polymer Chemistry,* vol. 47, no. 15, pp. 3931-3939, 2009.

[38] D. R. Lide, Ed., CRC Handbook of Chemistry and Physics, 88th Edition, 2007-2008 ed., Boca Raton, Florida: CRC Press, 2008.

[39] W. Cleland, "Dithiothreitol, a new protective reagent for SH groups," *Biochemistry,* vol. 3, no. 4, pp. 480-482, 1964.

[40] J. Butler, S. P. Spielberg and J. D. Schulman, "Reduction of disulfide-containing amines, amino acids, and small peptides," *Analytical Biochemistry,* vol. 75, no. 2, pp. 674-675, 1976.

[41] C. Stahl and S. Siggia, "Determination of organic disulfides by reduction with sodium borohydride," *Analytical Chemistry,* vol. 29, no. 1, pp. 154-155, 1957.

[42] T. J. Wallace, "Reactions of thiols with sulfoxides. I. Scope of the reactions and synthetic applications," *Journal of the American Chemical Society,* vol. 86, no. 10, pp. 2018-2021, 1964.

[43] A. B. Lowe, B. S. Sumerlin, M. S. Donovan and C. L. McCormick, "Facile preparation of transition metal nanoparticles stabilized by well-defined (co)polymers synthesized via aqueous Reversible Addition-Fragmentation Chain Transfer Polymerization," *Journal of the American Chemical Society,* vol. 124, no. 39, pp. 11562-11563, 2002.

Chapter 6

Conclusions and Recommendations for Future Work

6.1 Conclusions

This thesis investigated the synthesis of cellulose graft copolymers using Cu(0)-mediated polymerization in homogeneous media using both 'grafting-from' and 'grafting-to' approaches. As 'grafting-from' is well established in the literature, this thesis sought to clarify the extent to which graft copolymerizations behaved like more widely studied linear homopolymerizations. This information was currently lacking but is required to enable better design of the grafting reaction. 'Grafting-to' has received a more limited treatment, and so this thesis demonstrated the feasibility of a novel 'grafting-to' method with thiol-ene addition that can be used with controlled radical polymerization techniques.

Cellulose was reacted with α-bromoisobutyryl bromide in the ionic liquid 1-butyl-3-methylimidazolium chloride (BMIM Cl) to synthesize an Atom Transfer Radical Polymerization (ATRP) macroinitiator (Cell-BiB). The degree of substitution (DS) of the BiB groups was 1.13 as measured by ion chromatography; this was less that the DS_{BiB} of 1.75 predicted by NMR. The discrepancy was attributed to the substitution of bromine groups occurring during the reaction due to the elevated temperature ($50^{O}C$) required for the solvent. The elevated temperature, high viscosity, and highly hygroscopic nature of BMIM Cl are obstacles to its use as a reaction medium for cellulose, both on a laboratory and industrial scale. The acylation of cellulose was also attempted in the ionic liquid 1-ethyl-3-methylimidzaolium acetate (EMIM AcO), but this resulted primarily in acetylation from the solvent rather than the desired acylation, as evidenced by NMR, ion chromatography, and the polymerization rate of the macroinitiator. EMIM AcO is therefore unsuitable for esterification reactions. The synthesis of cellulose acetate with methacrylate functionality (CA-MAA) via Steglich esterification with methacrylic acid in

tetrahydrofuran (THF) was found to be a good route that allowed control over the reaction without degradation of the cellulose occurring. Ring-opening of glycidyl methacrylate was also attempted as an alternative route for obtaining methacrylate functionality using the solvents EMIM AcO and THF, but the reaction was difficult to control, had difficulties with autopolymerization, and degraded the cellulose.

Polymerization of methyl acrylate from Cell-BiB proceeded at a slower but comparable rate to EBiB (a commonly used ATRP initiator that is analogous in structure to Cell-BiB) under the same conditions, but the initiation efficiency was lower for Cell-BiB than for EBiB. Polymerization of methyl methacrylate (MMA) from EBiB demonstrated that the system suffered from slow initiation; this limited the graft density as a non-uniform initiation meant that un-initiated BiB groups became buried in the growing polymer brush and inaccessible. This reason for the limited graft efficiency could not have been easily determined by studying the graft copolymerization alone and demonstrated the usefulness of modelling the grafting reaction with linear homopolymers. Graft density for poly(methyl acrylate) (PMA) was higher than poly(methyl methacrylate) (PMMA) (average DS_{graft} of 0.71 as opposed to 0.15). The grafted chains were successfully cleaved from the cellulose using acid-catalyzed transesterification with methanol, but the reaction was sensitive to the solvent conditions used, which is suspected to be related to the solvation of the grafted chains. Base-promoted transesterification was not successful as it resulted in irreversible hydrolysis of the pendant methyl ester groups in the PMA and PMMA grafts. Chain extension experiments conducted on the Cell-g-PMA demonstrated the living behaviour of the system and the retention of bromine functionality.

Thiol-ene Michael addition of thiophenol and dodecanethiol to CA-MAA proceeded quantitatively at room temperature without any loss in the integrity of the cellulose acetate, demonstrating the usefulness of this reaction for attaching functional groups to cellulose acetate. Chains of PMA and PMMA with end-group sulfide functionality were synthesized using a

bifunctional ATRP initiator containing an internal disulfide bond. The disulfide bond was reduced to cleave the chains and form the sulfide groups. The redox of the disulfide was monitored by molecular weight changes in the polymers; this convenient method of calculating end-group functionality is the primary advantage of thiol-ene chemistry over other 'click' reactions. The reduction step proceeded quickly and quantitatively under a range of conditions. Subsequent oxidation of the reduced polymers resulted in an increase in molecular weight demonstrating the presence of sulfide groups, but the increase was less than expected, indicating the sulfide functionality was less than complete. The sulfide-terminated polymers were then added to the methacrylate groups on the CA-MAA to form a graft copolymer. This was determined to be successful by measuring a decrease in retention volume of the cellulose acetate during chromatographic separation, indicating an increase in size of the molecule. The grafting efficiency appeared to be limited by the sulfide functionality of the synthetic polymers. The low sulfide functionality is something that further research should be able to overcome, allowing much higher grafting efficiencies. Thus, the 'grafting-to' approach has great potential for the synthesis of cellulose graft copolymers as the synthesis of the grafts separate from the cellulose avoids many of the difficulties encountered when using a 'grafting-from' scheme. In addition, if a large cellulose content is desired in the copolymer the low graft densities obtained using 'grafting-to' are desirable.

6.2 Recommendations and future work

The following sections list the recommendations produced from this thesis, organized by chapter. There are recommendations for future work that still needs to be examined, for procedures to be used when carrying out this research, and for procedures to be avoided when carrying out this research.

6.2.1 Functionalization of cellulose

Chapter 3 described methods for functionalizing cellulose with groups required for the grafting reactions in Chapters 4 and 5. The lessons are applicable to other functional groups and other cellulose derivatives synthesized in a similar fashion.

- The use of non-ionic liquid solvent systems such as dimethylacetamide (DMAc)/LiCl should be examined for the functionalization of cellulose. The difficulties encountered in this work with ionic liquids suggest other solvents may be more effective. EMIM AcO should be avoided as it can react with the cellulose, while BMIM Cl is inappropriate for reactions requiring low temperatures and its highly hygroscopic nature makes it unsuitable for moisture-sensitive reactions.

- Steglich esterification using cellulose acetate was an effective method of functionalization and could be applied to other functional groups. Cellulose acetate with a lower DS_{AcO} than that used here (~2.8) should be examined in order to obtain higher degrees of substitution of the desired functional group.

- The acylation of virgin cellulose with methacryloyl chloride in DMAc/LiCl for use in thiol-ene addition reactions should be furthered investigated to eliminate the need for protection of the cellulose. The reaction was attempted in BMIM Cl unsuccessfully, which was attributed to the high moisture content of the solvent (5690±50 ppm) and the elevated temperatures required by the solvent (50^{O}C).

6.2.2 Synthesis of cellulose graft copolymers using a 'grafting-from' approach

Chapter 4 investigated the similarity of graft copolymerization kinetics to linear homopolymerization kinetics in order to improve the design of the grafting reactions. Accurate characterization of the copolymer grafts was crucial for this analysis.

- EBiB is useful for modelling the grafting reaction from Cell-BiB and should be used to optimize the grafting conditions, in particular to overcome the problems experienced with intermolecular combination and limited graft density. Researchers using polysaccharides with ATRP initiating groups other than BiB should find an analogous non-polymeric initiator to use for their homopolymerizations.

- Cell-BiB with a higher DS_{BiB} should be synthesized in order to examine the limits of graft density. It is not clear from the work in this thesis whether the maximum possible graft density (due to steric considerations) had been reached as the highest density obtained (DS_{graft} 1.0) was similar to the density of initiating sites (DS_{BiB} 1.13).

- It is recommended that acidic conditions be used for the transesterification reaction and not the basic conditions common in the literature. Using hydroxide causes irreversible hydrolysis of ester groups in PMA and PMMA, creating inaccuracies in molecular weight measurements and affecting the efficiency of the reaction.

- The effect of solvation on the transesterification needs to be understood better in order to properly design the reaction. The transesterification was found to be very sensitive to solvent conditions, and cleaving the grafted chains is extremely important for proper characterization of the copolymer and understanding of the polymerization.

- THF may not be the most appropriate solvent choice for studying the molecular weights of the copolymer and other solvents should be examined. Measurement of Mark-Houwink parameters and intrinsic viscosity indicate the polymer is poorly solvated by THF with the chains being minimally extended.

6.2.3 Synthesis of graft copolymers using a 'grafting-to' approach

Chapter 5 developed a method for grafting synthetic polymers to cellulose acetate using thiol-ene Michael addition. Cu(0)-mediated polymerization was used in this chapter to synthesize the grafts, but this method of grafting could be easily transposed to any controlled polymerization technique that can incorporate a sulfide group in the initiator.

- Sulfide functionality of the synthetic polymer appears to be the limiting feature of this grafting approach. The loss of sulfide functionality needs to be examined in greater detail and corrected to ensure an efficient reaction. Acetone was one solvent that was found to decrease sulfide functionality.

- An in-situ formation of sulfides should be examined in order to avoid any potential loss of functionality during the purification process of the sulfide-terminated polymers. The reducing agents employed in this study could not be used to that end, as dithiothreitol and mercaptoethanol both have thiol functionality that would react with the alkene groups and sodium borohydride caused gel formation of the cellulose acetate solution, so other reducing agents would be needed. Since the PMMA had low initiation efficiency, a large number of low molecular weight thiols would be produced and as such the alkene would need to be present in a large enough excess to account for this.

- A quantitative method for measuring grafting yield needs to be determined. If sulfide functionality of the polymer can be increased this should increase the grafting yield and may eliminate the need for separating the polymers, but barring that a higher molecular weight cellulosic material could be used to increase the separation of peaks in the GPC elution profile, or a selective solvent extraction of the un-grafted polymer could be attempted (this also may be easier with a higher molecular weight cellulose).